Spray-drying of biopharmaceutical drug products

Carla Barcelo

Université Fédérale
Toulouse Midi-Pyrénées

THÈSE

IMT Mines Albi-Carmaux
École Mines-Télécom

En vue de l'obtention du

DOCTORAT DE L'UNIVERSITÉ DE TOULOUSE

délivré par

IMT – École Nationale Supérieure des Mines d'Albi-Carmaux

présentée et soutenue par

Carla María BARCELO CHONG

le 10 mars 2023

Titre :

Spray-drying of biopharmaceutical drug products

École doctorale et discipline ou spécialité :

MEGEP : Génie des procédés et de l'environnement

Unité de recherche :

Centre RAPSODEE, UMR CNRS 5302, IMT Mines Albi

Directeur et Directrice de thèse :

Maria Inês RÉ, Professeure, IMT Mines Albi

Mostafa NAKACH, Global head of process engineering, Sanofi Vitry sur Seine

Autres membres du jury :

Stéphane DESOBRY, Professeur, Université de Lorraine, Vandoeuvre-lès-Nancy (Rapporteur)

Helen HUGHES, Professeur, Waterford Institute of Technology, Ireland (Rapporteure)

Roman PECZALSKI, Professeur, Université Claude Bernard Lyon 1 (Président)

Vasco FILIPE, Department head – Biologics Drug Product Development France, Sanofi, Vitry-sur-Seine (Examinateur)

Acknowledgments

I would like to express my gratitude to everyone who has accompanied and supported me throughout this adventure called a PhD.

First and foremost, I want to thank my supervisors, Maria-Inês, Mostafa, and Vasco, for their guidance, encouragement, and tremendous support during my research. Thank you also for allowing me to participate in such an interesting project. Your experience and knowledge have guided me in the best possible way, and I am truly grateful for your mentorship.

I would also like to thank the teams at RAPSODEE and SANOFI for all the support provided throughout the experiments (both professionally and emotionally, as we know how tough this process can be). I appreciate it wholeheartedly.

When spirits are low, the support of friends is what helps us move forward. I am infinitely grateful for all the love and support I received from each one of you. From crying together, laughing, stressing out, dancing, singing, and reflecting, thank you for always being there with words of encouragement… and food.

Last but not least, I want to thank my family, who have always been present in every important moment of my life, supporting me and cheering me on. Even though they are not physically close to me, I know they have always been by my side in every step I have taken, and they have always put their trust in me, which has been invaluable. I love you all.

Por último, pero no menos importante, quiero agredecer a mi familia que siempre ha estado presente en todos los momentos importantes de mi vida apoyandome y echandome porras. Aunque no esten cerca de mi fìsicamente, sé que siempre han estado a mi lado en cada paso que he dado y siempre han puesto su confianza en mi y eso ha sido invaluable para mi. Especialmente quiero agradecer a mis papàs por todos los esfuerzos, sacrificios y el amor que han tenido hacia mi, ya que todo eso me ha permitido llegar tan lejos. Los amo.

Table of Contents

Chapter 1

This introductory chapter presents the general introduction to the work, the objectives of the thesis and a summary description of all chapters of the manuscript (thesis outline)

Biopharmaceuticals, also known as biologic drugs, are all molecules that are obtained through biotechnological techniques. They comprise of nucleic acids, living cells, tissues and proteins. They are used in many areas of medicine and have become the most effective clinical treatments for a variety of diseases, including cancers and metabolic disorders (Kesik-Brodacka, 2018; Yeh *et al.*, 2018). From a manufacturing, formulation, and quality control standpoint, therapeutic proteins pose many challenges compared to low molecular weight molecules because of their complexity (Staub *et al.*, 2011).

Interest in some protein biopharmaceuticals, such as monoclonal antibodies, which are large heterodimeric proteins, has grown recently because they possess highly specific targeting properties approved for the treatment of diverse chronic and life-threatening diseases (Castelli *et al.*, 2019; Ramezani *et al.*, 2014). Monoclonal antibodies are the largest group of recombinant proteins used for both, human therapy and *in vivo* imaging of different types of diseases (Kunert *et al.*, 2016). There are several mAb classes, of which IgGs are the only ones currently in clinical use due to their prolonged circulating half-life and relative ease of production (Kaplon *et al.*, 2022; Ramezani *et al.*, 2014).

During the year 2021 alone 11 different monoclonal antibodies were granted first approvals in either the United States or Europe, and globally 27 novel antibody therapeutics are undergoing review by regulatory agencies. This shows a growth of 30% in the late-stage commercial clinical pipeline of monoclonal antibodies therapeutics (Kaplon *et al.*, 2022). One of the major challenges for the development of monoclonal antibodies is their inherent instability and the consequent need to develop stable formulations. Most commercial formulations of monoclonal antibodies are available as liquid dosage forms that provide patient-convenient administration options, with subcutaneous administration being the most common according to many authors (Batens *et al.*, 2018; Jackisch *et al.*, 2014; Le Basle *et al.*, 2020; Viola *et al.*, 2018). Nevertheless, a liquid formulation presents several challenges from a stability standpoint (Ramezani *et al.*, 2014; SINGH *et al.*, 2017; Walters *et al.*, 2014). Compared to other dosage forms, liquid formulations of monoclonal antibodies favour monomer-monomer interactions and several chemical changes, which can impact several critical quality attributes (CQAs), such as aggregation, fragmentation and loss of biologic activity (Le Basle *et al.*, 2020).

Water removal grants the formulation with different benefits, such as a reduction in transportation costs, ease of handling and storage, and most importantly a higher molecular stability (Ramezani *et al.*, 2014). As well, it can eliminate disadvantages linked with the freezing step of the drug substance before its conversion into drug product, such as the protein denaturation caused by cryoconcentration and pH shifts, and the heterogeneity of freezing rate, that can result in substantial changes in the composition of the frozen solution (Langford *et al.*, 2020). The advantages of water removal can be obtained with

the production of a powdered formulation from a drying process such as freeze-drying, spray freeze-drying and spray-drying.

The spray-drying process involves the nebulization, through a nozzle of a liquid formulation, into a heated gas phase where the solvent evaporates. The droplet formation and the further solvent evaporation happen at a very fast rate (< 2s from droplet formation to dried particles) (Bögelein *et al.*, 2010; Bowen *et al.*, 2013; Ousset *et al.*, 2018; Schaefer *et al.*, 2015; Ziaee *et al.*, 2019). Advantages of spray-drying as a powder manufacturing process includes process scalability and particle engineering capacity.

In the last 15 years, some protein pharmaceuticals have been successfully spray-dried (Ajmera, 2014; Devahastin *et al.*, 2020; Emami *et al.*, 2018; Pinto *et al.*, 2021). Nevertheless, spray-drying of a pure protein-containing solutions leads to substantial worries about degradation and inactivation, as a result of damage to its structured elements (Ajmera, 2014; Emami *et al.*, 2018; Keshani *et al.*, 2015). Possible stress factors that the protein experiences during spray-drying occur at the atomization step, where the protein, which is sensitive to the air-water interface, is subjected to shear stress applied by the spraying device. Another source of stress is found at the conversion of the protein into dry solid state (Ajmera, 2014; Grasmeijer *et al.*, 2019; Mensink *et al.*, 2017). Any activity loss during spray-drying means a reduction in the quality of the final product.

To minimize the impact of the process on the protein structure and improve stability during the process and then during storage, stabilization mechanisms can be adapted to retain the entire activity after rehydration of the spray-dried powder. In this context, excipients are then of great help for stabilizing pharmaceutical proteins, such as monoclonal antibodies, against the stress generated by spray-drying, given that they provide different protective mechanisms (water replacement, vitrification and competitive adsorption, and preferential exclusion) against denaturation (Grasmeijer *et al.*, 2013; Chiu *et al.*, 2011; Mensink *et al.*, 2017; Sudrik *et al.*, 2017).

Another critical point is that the response of the formulation stability to spray-drying can vary from device to device and within process parameters. The analysis of operating and formulation parameters on the integrity of the proteins is a complex task as the different stresses are present (mechanical, thermal, dehydration…) during this very fast drying process. Understanding the individual effects of some of these stresses (mechanical, thermal/dehydration) on pharmaceutical protein denaturation might be an interesting strategy to help screening of the drying process conditions, as well as stabilizing excipients. Obviously, this strategy of screening and understanding the effects of the operation and formulation parameters does not replace the study of the spray-drying process which must be carried out for optimization of operating conditions and formulation (type and level of excipients, protein concentration) in order to obtain a final composition of a spray-dried powder with high-quality for reconstitution.

1.1 Thesis objectives

This thesis aims to provide a better understanding of the factors affecting the stability of a spray- dried powder containing a specific antibody, mAb-A, using the following working method:

1. Decoupling some sources of stress (mechanical, thermal/dehydration) to which a pharmaceutical protein is subjected to during a spray-drying process, using different experimental set-ups. This approach was applied to different proteins: a non-formulated model protein (BSA) solution and a formulated mAb solution (mAb-A).
2. Spray-drying of the mAb-A formulation and investigation of the effect of operating parameters and formulation composition (protein concentration, excipients) on the integrity (aggregation level) of the protein after reconstitution.

1.2 Thesis outline

The outline of the thesis is shown on Figure 1.1

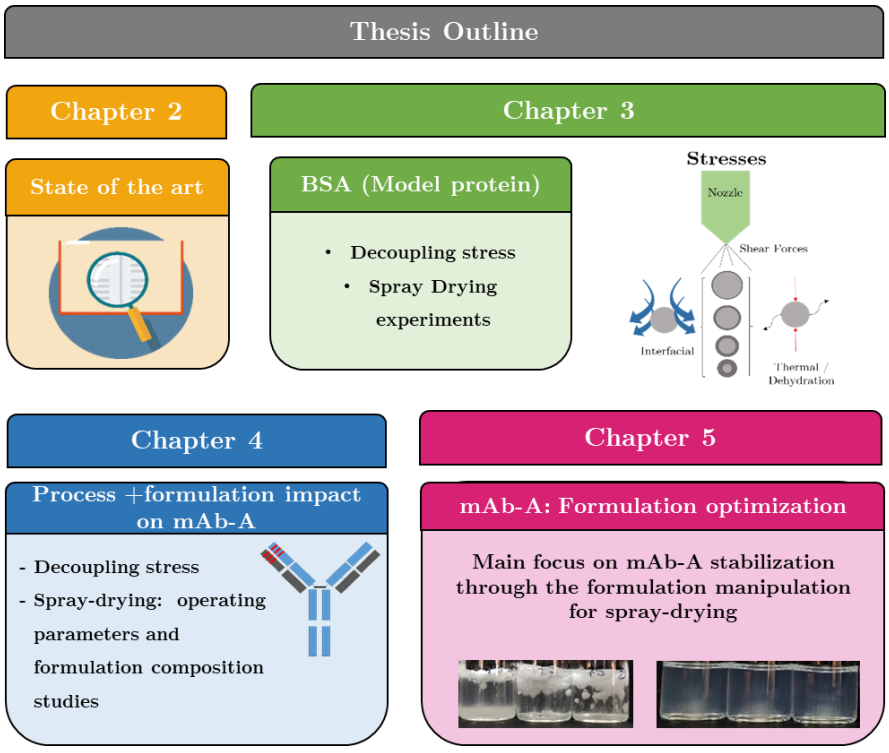

Figure 1.1. Outline of the thesis chapters

Chapter 1. Introductory chapter of the thesis.

Chapter 2. Provides background information and is divided into five different Sections, as follows: 1) introduction to biopharmaceuticals and proteins, 2) description of monoclonal antibodies, 3) instabilities of liquid formulations and introduction to the relevance of powder formulations, 4) drying techniques for biopharmaceuticals, 5) spray-drying.

Chapter 3. Includes the presentation of the model protein (bovine serum albumin) and the studies performed for the first approach of decoupled stresses techniques on a non-formulated protein solution.

Chapter 4. This chapter introduces the target protein of this thesis, the mAb-A, and it encompasses three main Sections:

1) Study of the decoupled stresses on mAb-A formulation.
2) Study of the spray-drying parameters on the final powder and reconstituted solution characteristics.
3) Impact of the protein and excipients concentration on mAb-A stability during spray-drying.

Chapter 5. The final chapter encompasses a more in depth study of the impact of each excipient on the mAb-A stability at fixed spray-drying operating conditions. It was divided into three main parts:

1) Study of the impact of the mAb-A concentration on the aggregation phenomena
2) Study of effect of excipients type and concentration on mAb-A formulation.

Conclusion and future perspectives. Through all the different chapters, a final work conclusion was built, which also opened the path for future perspectives to enrich the results obtained in this thesis.

Chapter 2

Background

This chapter provides an introduction to biopharmaceutical proteins and the problems they face in liquid formulation. It is shown that the transition from a liquid to a powder formulation through drying processes is a very interesting option for pharmaceutical companies. Different drying techniques are introduced, to finally focus on spray-drying which is the one used in this thesis. Finally, monoclonal antibodies are introduced which are the biopharmaceutical molecules of our interest.

2.1 Proteins

Proteins are macromolecules that given their variety and complexity can perform different biological functions such as catalysis, carriers, storage, transmission/reception of information and immune protection. They are categorized as polymers, formed by the combination of 20 amino-acids, whose side chains confers proteins their known versatility and diversity (Deng *et al.*, 2014). The functionality of proteins depends on their spatial configuration. There are four levels of structural organization, primary, secondary tertiary and quaternary structures, detailed in Table 2.1 and represented in Figure 2.1 (Antony *et al.*, 2022).

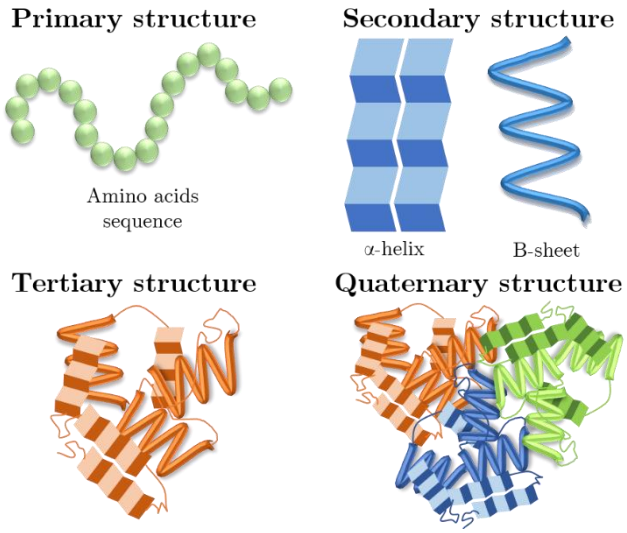

Figure 2.1. General diagram of the primary, secondary, tertiary and quaternary structure of proteins (adapted from Antony et al., 2022).

Proteins are very sensitive molecules that can be affected by a wide range of external stresses, such as pH shifts, high temperatures, mechanical forces, among others. It has been reported that protein aggregation is mainly linked to hydrophobic interaction (non-covalent process) and to disulphide-bond interchange (covalent process) (Ramezani *et al.*, 2014, Wang *et al.*, 2007).

In recent years the production of protein-based pharmaceutical products for human use has increased, given the valuable contributions of biological proteins, among which we have a wide spectrum of action, high efficacy, safety and selectivity to target (Agyei *et al.*, 2017). Some examples of these well-known therapeutic proteins are cytokines (i.e. TNF-α), fusion proteins, hormones (i.e. insulin) and monoclonal antibodies (i.e. IgG1) (Conner *et al.*, 2014).

Table 2.1. Detailed conformation of each protein structure level and the destabilization mechanism of each one (Antony et al., 2022, Das et al., 2020; Deller et al., 2016).

Level	Characteristics	Source of destabilization	Examples of types of destabilization
Primary Structure	Sequence of up to 20 amino acids combination forming a polypeptide chain. The linear structure is held up by covalent peptide bonds, which make it more stable upon degradation.	Change in the amino acid sequence or modification in the structure of the amino acids	- Postranslational modifications - Proteolysis - Protein splicing
Secondary Structure	Hydrogen bonding interactions between adjacent amino acid residues belonging to peptide groups of the main chain groups. They can form substructures known as regular structures and described as helical or pleated segments, known as α-helix, β-sheet.	Change of the α-helix, β-sheet content	- Secondary structure formation - Racemization - Aromatic side chain interactions
Tertiary Structure	It refers to the three-dimensional structure of the protein. The folding of the polypeptide chains becomes more compact and gives the protein a globular shape.	Change in the overall fold or protein conformation	- Hydrogen bonding - Hydrophobic interactions - Conformational changes - Disulfide bonding
Quaternary Structure	The majority of the proteins are comprised of two or more tertiary structures joined by their polypeptide chains.	Change in oligomeric state	- Protein-protein interaction - Oligomerization

2.1.1 Protein degradation

A protein is considered to be denatured when it loses its higher-order structure. At this point the protein is no longer functional, even though its primary sequence remains intact. Before arriving to a complete denaturation, the protein can undergo two main categories of instabilities, physical and chemical. It should be kept in mind that certain chemical instabilities, like deamination and disulphide bond cleavage, can lead to physical instabilities, and vice-versa (Manning *et al.*, 1989).

A summary of the different instabilities, physical and chemical, will now be discussed.

2.1.1.4 Physical degradation of proteins

The physical instabilities refer to all protein modifications that do not involve any covalent modification of the protein. It mainly consists of changes in the higher order structure (beyond the secondary protein structure). These instabilities are classified as unfolding, adsorption, denaturation, aggregation, fragmentation, and precipitation (Ramezani *et al.*, 2014).

Denaturation

Denaturation is related to the perturbation of the secondary or tertiary structure, which can lead to the exposure of hidden amino acids. As a result, the molecules are more prone to chemically react and to lose their native state (Jacob *et al.*, 2016; Manning *et al.*, 2010).

Aggregation

When proteins self-associate they can form multimers and in drastic cases, aggregates, and precipitates (Jacob *et al.*, 2016). A reportedly common mechanism for protein aggregation involves the protein denaturation and non-covalent association via hydrophobic interfaces (Jacob *et al.*, 2016).

According to Manning *et al.* (2010), there are five main mechanisms of aggregation: 1) Association of native monomers, 2) Aggregation of conformationally altered monomers, 3) Aggregation of chemically-modified monomers, 4) Nucleation-controlled aggregation and 5) Surface-induced aggregation.

Non-ionic surfactants are usually added to the protein solutions to avoid these protein-protein interactions (Jacob *et al.*, 2016).

Adsorption to the surfaces

During production, therapeutic proteins are in contact with a wide diversity of surfaces (air-liquid interface, solid-solid interface, liquid-solid interface), which can induce interfacial stresses on the protein by changing its solid state.

The surface-induced protein instability starts with the adsorption of either the native or partially unfolded protein to a certain surface. This interaction is known to be more energetically favourable when a protein is partially unfolded due to a greater exposure of hydrophobic amino acid side chains (Jacob *et al.*, 2016, Manning *et al.*, 2010).

After the initial adsorption of the protein, surface tension forces direct the aggregation process by structurally impacting the neighbour proteins, which can lead to nucleation and growth of aggregates in the bulk solution (Jacob *et al.*, 2016; Manning *et al.*, 1989).

2.1.1.5 Chemical degradation of proteins

Chemical instabilities refer to the formation or destruction of covalent bonds in the protein structure. Some of the common causes for this are deamination, oxidation and cysteine destruction/disulfide exchange, racemisation, proteolysis, hydrolysis (Manning *et al.*, 1989). They are considered as irreversible chemical degradations for biopharmaceuticals (Ramezani *et al.*, 2014). Some of these instabilities are described below.

a) Deamination

Deamination is one of the most common chemical degradation mechanism, and it involves the hydrolysis of asparagine and glutamine side chain amides. The control of pH is the most effective way to control the deamination rate. It is also possible to avoid deamination by changing the protein conformation (Manning *et al.*, 2010)

b) Hydrolysis

Protein hydrolysis, also known as proteolysis, is generally a mechanism of cleavage of the protein into smaller components (fragments) (Manning *et al.*, 2010). This could be avoided by reducing the final water content present in the protein formulation (Ramezzani *et al.*, 2013).

c) Oxidation

Different amino acids, like methionine, cysteine, tryptophan, and tyrosine, are susceptible to oxidation. It can be caused by different agents, such as air, residual peroxide content, intense fluorescent light. What happens is that these agents transform the thioether component to sulfoxide and then sulfone (Ramezzani *et al.*, 2013). It is normally avoided by keeping the desired pH of the protein in solution and avoiding reducing agents in the formulation (Jacob *et al.*, 2016).

e) Disulfide exchange

Cysteine residues can form disulfide bonds, which can play a major role in aggregation through covalent cross-linking (Manning *et al.*, 2010). As well, they can change the protein structure by a rearrangement of the disulfide bonds within the same protein structure.

2.1.2 Biopharmaceutical proteins

The term "biopharmaceutical" was first introduced in the 80s, when recombinant insulin started to be commercially manufactured. This term refers to pharmaceuticals manufactured from organisms, or their functional components, by using biotechnological techniques. Recombinant proteins, monoclonal antibodies (mAbs), vaccines, blood/plasma-derived products, non-recombinant culture-derived proteins and cultured cells, nucleic acids and tissues (animal and human origin) are considered as biopharmaceuticals (Eibl & Eibl, 2019). They are complex molecules whose order of magnitude can be larger compared to the synthetic ones. They are normally produced through culture technology by using living cells, such as microbial and mammalian, as well as other organisms. The product recovered follows a set of purification steps to ensure the quality and efficiency of the final therapeutic protein. Throughout the process of purification, the proteins can undergo different stresses that can lead to denaturation. These aggregates may vary from dimers to micron-sized visible particles, in lower

quantities they may not affect the efficacy of the product but can affect its safety, since some of these aggregates can be immunogenic (Das *et al.*, 2020; Walsh *et al.* 2015)

2.1.3 **Monoclonal Antibodies**

Monoclonal antibodies (mAbs) are monovalent antibodies, which are large heterodimeric protein molecules, which use offers the advantage of a targeted activity with fewer side effects and it can be used as a delivery agent for a conjugated therapeutic component. They are mainly used in the medical areas such as oncology, immunology and hematology (Lu *et al.*, 2020; Chan *et al.*, 2009; Ryman et Meibohm, 2017; Liu, 2014).

The mAbs have an approximate molecular weight of 150 kDa, where 50 kDa represents the heavy chains and 25 kDa corresponds to the light chains and are produced by the B-cells as part of the humoral response (Lu *et al.*, 2020; Ryman & Meibohm, 2017).

The *Y*-shaped structural arrangement of mAbs includes four polypeptide chains, two pairs of heavy and light chains bonded by a disulphide bridge (Figure 2.2). Each arm of the upper part, known as the hyper-variable region (Fb), counts with six complementarity-determining regions (CDRs), three from the heavy and three light chains. This region will bind to a specific antigen, giving the mAbs their specificity (Lu *et al.*, 2020).

The tail Section is referred to as the fragment crystallisable region (Fc), all the antibodies of the same group will have the same Fc. This region is in charge of producing a signal that will unchain a certain response depending on the type of mAb (Chan *et al.*, 2009). According to this, there are five different classes of mAbs - IgA, IgD, IgE, IgM, IgG. At the present time all the clinical used therapeutic antibodies are from the class IgG. (Wang *et al.*, 2007).

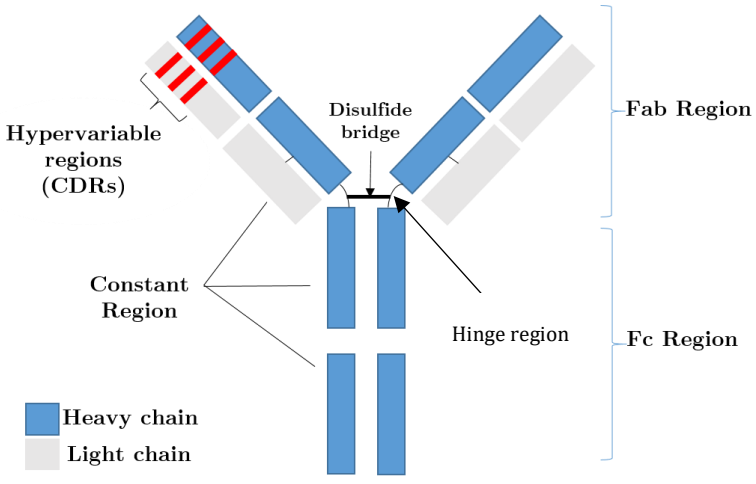

Figure 2.2. Monoclonal Antibody structure. (Adapted from Moorthy et al., 2015)

Their stability depends on their hydrophobicity, pI, individual sequence and carbohydrate content, they are as well very labile molecules. When a mAb generates degradation products, its activity is reduced

and their immunogenicity is increased. The majority of the mAb instabilities can be observed in liquid, frozen and lyophilized states, with a variable extent of degradation (Wang *et al.*, 2007).

Many of the drug products involving the mAbs are envisioned for a subcutaneous delivery, given that it allows the administration of a high-dose of mAbs (several mg per kg), which is preferred for the treatment of chronic diseases (Batens *et al.*, 2018; Bowen *et al.*, 2012). To achieve a high-dose, a high mAb concentration formulation is then required.

One of the many challenges encountered when formulating high concentration drug-products, is that protein-protein interactions tend to increase while in solution.

2.2 The challenges of moving from a liquid to a solid formulation containing biopharmaceuticals

As previously discussed in Section 2.1, proteins have an intrinsic instability that creates a challenge for their formulation and processing. During the manipulation of a protein-containing drug product, the protein can start degradation processes when encountering some environmental stresses, like extreme pH, high temperature, freezing, light, agitation, shear stress, organic solvents and others (Emami *et al.*, 2018, Horn *et al.*, 2012).

Another disadvantage of proteins in aqueous formulations is the cold chain, -40°C to -20°C for the drug substance and 5°C for the drug product, which they have to follow during storage and transportation to assure a proper stability (Langford *et al.*, 2018).

While in liquid state, the proteins are characterized by a melting temperature (T_m), above which they undergo unfolding and lose their functionality (Rajagopal *et al.*, 2013). For formulations in the solid state the glass transition temperature (T_g) characterizes the threshold that, when surpassed, the degradation rate increases rapidly. (Grasmeijer *et al.*, 2013; Olsson *et al.*, 2016).

In comparison, the degradation after surpassing the value of T_g (kinetic parameter) is not as drastic as the one when surpassing the T_m (thermodynamic parameter) (Mensink *et al.* 2017). Protein degradation can, of course, happen at lower temperatures than T_g and T_m but at a much slower rate that does not necessarily leads to protein unfolding/denaturation (Mensink *et al.*, 2017).

The previous information suggests that reducing the moisture content in the protein formulation will increase its stability. Dried biopharmaceuticals powders have been shown to be stable at storage temperatures of <25°C (Emami *et al.*, 2018). To achieve this, different drying strategies have been proposed, which will be described in the next Section (2.3).

2.3 Drying biopharmaceuticals

A drying process involves passing from a solution or suspension into a dry powder or cake using heat in the form of convection, conduction and/or radiation.

As described by Emami *et al.* (2018) a general drying process encompass three main stages:

In the first stage the energy is transferred from the heat source to the dispersion medium, which in a second stage undergoes a change of phase from liquid to vapour or solid phase. Finally, the third step is the isolation of the dried particles from the vapour generated. There are different drying mechanisms that remove water such as evaporation (vacuum drying, foam drying), evaporation and atomization (spray-drying), and sublimation (freeze drying, spray freeze drying), among others.

The drying method is selected according to the desired final output of the dried powder as well as the type of molecule which is being used. In Table 2.2 some examples of drying processes currently used in the pharmaceutical industry are given.

Freeze-drying (FD), spray-freeze drying (SFD) and spray-drying (SD) are the drying techniques most used in the pharmaceutical industry, and they will be described now.

Table 2.2. Drying technologies and molecules normally dried (Emami et al., 2018; Ishwarya et al., 2015; Bohr et al., 2014; Mutukuri et al., 2021; Sharma et al., 2021; Bhambhani et al., 2021).

Drying technology	**Principle**	**Molecules**
Freeze Drying	Ice sublimation process at low pressure conditions	- IgG - Lyzozyme - BSA
Spray-Freeze Drying	Atomization process in cryogenic medium to achieve sublimation of ice in small size droplets	- IgG - BSA - Calcitonin - Influeza Vaccine
Spray-drying	Atomization of a solution/suspension into a heated gas phase where the solvent evaporates	- IgG - Catalase - Erythropoietin
Electrospray-drying	Liquid atomization using electrostatic charges through a high potential capillary nozzle, which attracts the solvent to the droplet surface and optimizes the drying process at lower temperatures..	- Whey protein - Maltodextrin - Anti IgE antibody - Influenza vaccine
Drum Drying	Conductive drying by rolling a solution / suspension through a heated surface on a horizontal metal cylinder	- Vitamin A - Antiretrovirals

Table 2.3. (Continuation) Drying technologies and molecules normally dried (Emami et al., 2018; Ishwarya et al., 2015; Bohr et al., 2014; Mutukuri et al., 2021; Sharma et al., 2021; Bhambhani et al., 2021).

Drying technology	Principle	Molecules
Supercritical drying	SCF (CO_2) used as an anti-solvent (drying gas) during SD, or as an aerosolization aid	- IgG - Lyzozyme - Insulin
Foam-drying	Foaming formation under reduced vapour pressure followed by rapid evaporation	- rhumAb - bacterias
Microwave vacuum drying	Vibrations generated by microwaves which create intermolecular heat resulting in evaporation under vacuum conditions	- Haemoglobin - Catalase - Virus

Among these drying techniques the freeze-drying, spray-freeze drying and spray-drying, are the most used in the pharmaceutical industry (Walter *et al.*, 2014). These methods will be described below.

2.3.1 Freeze Drying

The freeze-drying (FD) technique is one of the most common processes for the solid production of biopharmaceuticals in a powdered form (Emami *et al.*, 2018; Depreter *et al.*, 2013; Walters *et al.*, 2014).

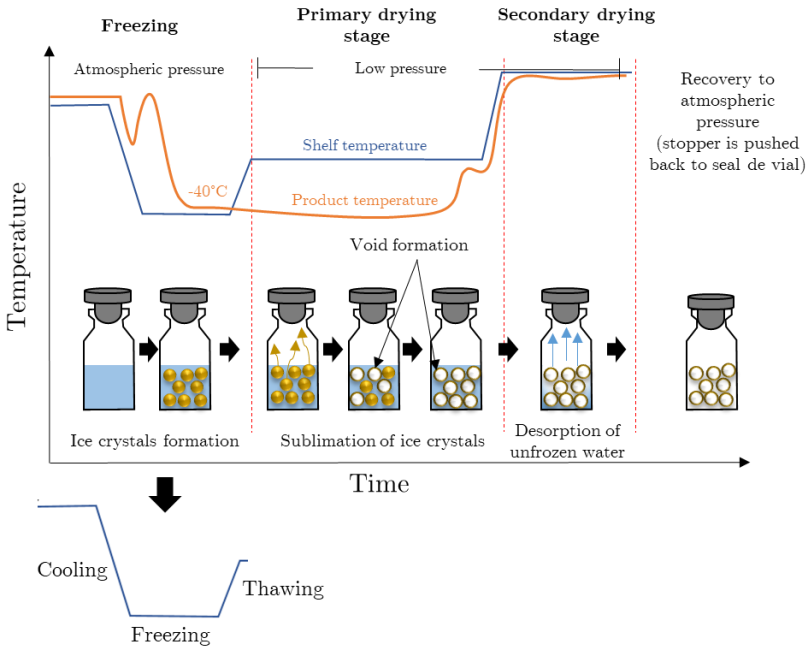

Figure 2.3. Scheme of the different stages of a freeze-drying process. The blue and orange curves represent the shelf temperature and product temperature, respectively (Adapted from Kawasaki et al., 2019).

The process itself can be divided into three stages, as illustrated in in the previous diagram (Figure 2.3) (Bhatnagar *et al.*, 2007; Kawasaki *et al.*, 2019; Langford *et al.*, 2020).

1) **First stage -** Freezing
    a. **Cooling** is the first step of the freeze-thaw cycle, it can be done at different rates, ranging from slow (<1°C/min), intermediate (1-10°C) to high (10-900°C)
    b. The second step refers to the post-nucleation ice crystal growth, also known as **freezing**. Given that the ice crystallization is an exothermic event, an increase in temperature is observed during the freezing stage. Two of the parameters that control the freezing are the degree of super-cooling and the rate of ice crystallization. Sometimes some freezing phenomena can occur at the cooling step.
    c. **Thawing** is the final step of the freezing process, and it involves the elevation of the temperature of the frozen sample. It could, as well, be done at different rates: slow (1-5°C/min), fast (>5°C/min).
    d.
2) **Second stage** - Primary drying

    Also known as the sublimation drying stage, at this point the chamber pressure is lowered below the equilibrium vapour pressure of ice. On the other hand, the shelf temperature is increased to favour the heat transfer from the shelf surface to the product, inducing the sublimation of the ice crystals generated during the first stage.

3) **Third stage** – Secondary drying

    The secondary drying consists of increasing the temperature higher than in the second stage, so the bound-water, trapped inside the drying particles and that was not transformed into ice during the freezing phase, could be evaporated.

- Stresses in the FD process for proteins

Some of the stresses are the dehydration stress, solid-liquid interfacial stress due to the ice formation. When the water is evaporated the concentration of solutes and proteins change in the formulation, which also affect protein stability during the freezing process. Mainly, ionic strength increases during ice formation and can generate pH changes that could destabilise the protein (Emami *et al.*, 2018; Depreter *et al.*, 2013; Bhatnagar *et al.*, 2007). Nevertheless, the extent of the impact of these stresses on the protein aggregation has not been fully understood (Bhatanagar *et al.*, 2007).

2.3.2 Spray Freeze Drying

In general, the spray-freeze drying (SFD) technique consists of a liquid solution that is sprayed into a a cryogenic fluid via a nozzle device. It is normally divided as a three-step process that includes: 1) droplet formation by spraying, 2) droplet solidification when in contact with a cryogenic fluid and 3) sublimation

at low pressure and temperature (Emami *et al.*, 2018; Anandharamakrishnan & Ishwarya, 2015; Walters *et al.*, 2014).

SFD process broadly is composed of three processes (spraying, freezing and sublimation), they can be performed by using different methodologies and equipments. The technique used for each process can be permutated to obtained multiple types of SFD.

One of the most common types of spraying processes is the Spray Freezing into Vapour, which refers to the solution that is sprayed into a cold dry gas. Spray Freezing into Liquid, is when the solution is sprayed directly into a cryogenic liquid. Spray Freezing into Vapour over Liquid, is when the formulation is sprayed into a cryogenic liquid but with the atomisation occurring in a gaseous region above the liquid (Ishwarya *et al.*, 2015; Wanning *et al.*, 2015).

For the freeze-drying process the following techniques are proposed: vacuum, atmospheric pressure, sub-atmospheric pressure, fluidized bed (at atmospheric or sub-atmospheric pressure) (Dutta *et al.*, 2018).

- Stresses in the SFD process for proteins

The stresses present in the SFD process will depend on the type of spraying and drying that is being used. Some of them can be shear stress, thermal stresses (freezing, dehydration), and interfacial stresses (solid-liquid interface, air-liquid interface).

2.3.3 Spray-Drying

Spray-drying, being the process of our interest in this work, it will be described in more detail.

2.3.3.4 General principles of the process

Spray-drying is a popular method used for particle production and known for its particle engineering capacity. It consists of the transformation of a liquid solution into dried particles (powder) by using a gaseous hot drying medium (Ameri & Maa, 2007; Santos *et al.*, 2017; Anandharamakrishnan & Ishwarya, 2015, Ohtake & Wang, 2013)

The spray-drying process consists of four main phases:

1) spraying of the liquid solution through the nozzle,
2) contact of sprayed-generated droplets with the hot gas phase (drying chamber),
3) evaporation of moisture (droplet-to-particle transformation) in the drying chamber, and
4) particle collection by using a cyclone, as described in Figure 2.4 .

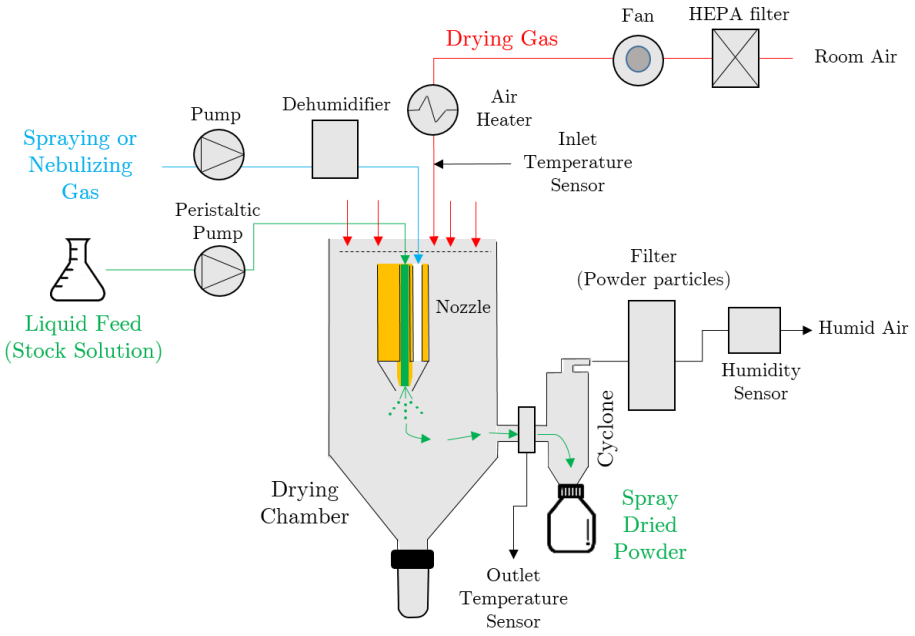

Figure 2.4. Spray-drying process diagram

Phase 1: Droplet formation of the liquid feed

The spraying step is critical in the production of droplets of a specific size or morphology. It influences the physical properties of the final product which includes the particle size, drying chamber residence time and product morphology. The process consists of breaking the feed flow into many individual droplets by making it pass through a nozzle at a determined rate and pressure. The product of this liquid disintegration is defined as spray, mist or aerosol. (Dalmoro *et al.*; 2013) (Singh & Van den Mooter.; 2016).

During the spraying, the cohesive forces (surface tension, viscosity) on the liquid surface compete against the forces (aerodynamic, centrifugal and electrostatic forces) exerted by the nozzle, creating fluctuations and disturbances in the liquid, that leads to its dispersion. The surface tension keeps the liquid in its lowest surface energy state and the viscosity prevents any variation in liquid geometry. (Dalmoro *et al.*; 2013).

There are different types of nozzles depending on the atomization force, pressure, centrifugal, electrostatic or ultrasonic energy. The main types of nozzles are: rotary, hydraulic(pressure), pneumatic or ultrasonic nozzle. Its use depends on the desired product characteristics, such as shape, size and structure (Santos *et al.* 2017) (Singh & Van den Mooter; 2015).

Hydraulic or pressure nozzle

The hydraulic nozzle, also known as one-fluid nozzle, consists of passing the feed solution through a pipe with a gradually reducing diameter. The outlet of the pipe is usually between 0.4 to 4 mm in diameter, and the fluid emerges at high velocity with a simultaneous loss in pressure, which generates

the disintegration of the fluid into small droplets. The final droplet distribution is narrow ranging between 10 to 400 μm (Ziaee *et al.*, 2019; Santos *et al.* 2017).

Pneumatic or multi-fluid

This type of nozzle uses the pressure energy and the kinetic energy of the spray-drying gas is transferred to the feed flow in the central collision point when going out of the nozzle, this will cause the droplet formation (Santos *et al.* 2017) The droplet size is controlled by the feed rate, atomizing gas rate and pressure (Dalmoro *et al.*, 2013). The droplets are very fine, ranging from 10 to 100 μm (Ziaee *et al.*, 2019).

This type of atomization can be classified into three categories (Hede *et al.*, 2008):

1) internal mixing (contact of air and liquid jets within the nozzle head),
2) external mixing (contact of air and liquid jets outside the nozzle head), and
3) pneumatic cup atomiser (contact OF air and liquid at the rim of a rotating nozzle head).

Rotary

This type of atomization is based on centrifugal forces generated by the atomizer motor when the liquid passes through the nozzle which can be a wheel or a disk. The centrifugal force accelerates the feed solution to the periphery which forms the spray of droplets (Santos *et al.* 2017) (Singh & Van den Mooter, 2015). The particle size that is possible to obtain with this nozzle is in a range of 10-500 μm (Ziaee *et al.*, 2019).

Ultrasonic

The droplets are formed when a vibrational energy is generated, formed by a high frequency electric signal applied to two electrodes placed between two piezoelectric transducers which vibrate. This vibration is transferred and amplified by a titanium nozzle (Santos *et al.* 2017). A wide droplet size range can be obtained with the ultrasonic nozzle, varying from 5 μm to 100 μm.

Stage 2. Spray-gas contact (mixing and flow)

The spray-gas contact mode can be classified according to the airflow pattern generated in the drying chamber. The most used airflow configurations are the mixed flow, counter current and co-current (Figure 2.5).

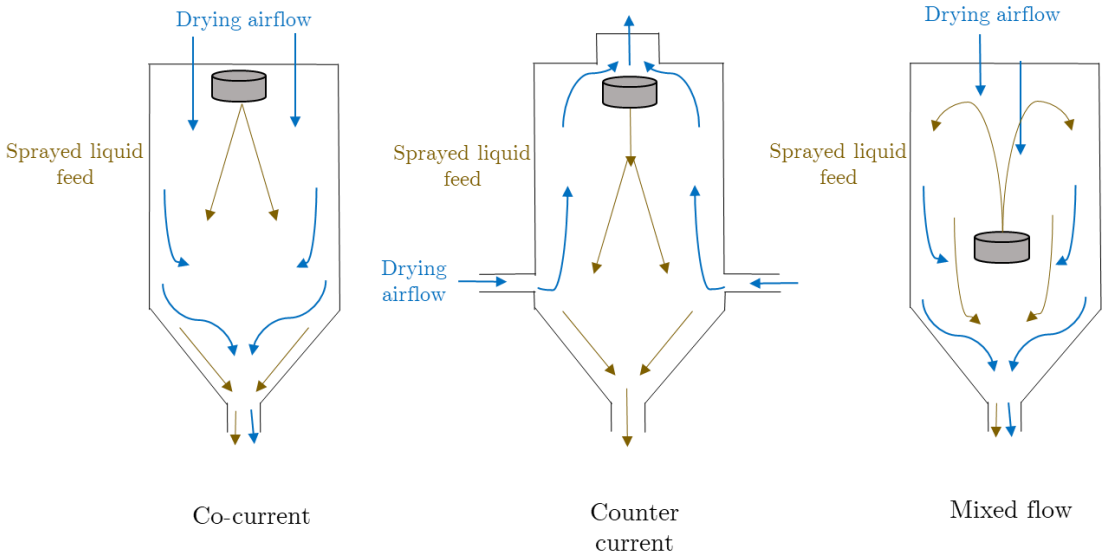

Figure 2.5. Types of airflow in a spray-dryer, generated by the liquid flow rate/atomization gas and the drying gas flow rates (adapted from Ziaee et al., 2019).

In the co-current arrangement, the sprayed liquid and the drying airflow in the same direction, from the upper part of the spray-dryer to the bottom. When going out of the nozzle, the feed flow gets in contact with the drying air at the higher temperature regime, but the droplets still have a high liquid content. Therefore, the sprayed drug product will be protected from the high temperatures by an evaporating cooling effect. This phenomenon, in addition to a high evaporation rate, reduces the exposure of the proteins to thermal/dehydration driven degradations, consequently it is suitable for heat sensitive materials (Ziaee *et al.*, 2019). In co-current the overall temperature of the droplet, during the most intense stage of drying, is lower compared with counter-current and mix flow regimes (Ortega-Rivas *et al.*; 2005)

Meanwhile in the counter-current configuration the feed flow (top) and the drying gas (bottom) follow opposite directions. In this way, droplets get in contact with the higher temperature regimes at the bottom of the drying chamber. At this moment the droplets might be in the final stage of drying and the cooling evaporation effect is no longer present. Therefore, this is not the best configuration for heat sensitive materials. Although it is suitable for molecules that need longer drying cycles, given its higher drying efficacy (Ortega-Rivas *et al.*, 2005; Ziaee *et al.*, 2019)

The Mixed Flow configuration is a combination of the co-current and counter-current airflow patterns. A nozzle is placed in the bottom half of the chamber, which forces the atomized feed flow to go upward, or downward, until it is overcome by gravity and the drying air is coming from the top of the drying chamber. When both flows (liquid and gas) encounter each other, the gas flow is going to force the liquid trajectory to the bottom of the drying camber The mixed flow configuration is a flexible option for materials with different ranges of thermal stability. Upward spraying is recommended for thermally sensitive materials, while the downward spraying set up will be used to decrease the air-droplet interactions (Ziaee *et al.*, 2019).

When using air as a drying medium the preferred choice will be using an open cycle, where the air will go directly to the exhaust. On the other hand, when working with flammable solvents, toxic products or oxygen sensitive products it is necessary to use an inert gas as a drying medium (Ziaee *et al.*, 2019).

Stage 3. Drying of the spray liquid feed

The drying kinetics of a droplet can be divided in to two main stages according to Mezhericher & Borde (2007), where the first stage comprises the 'initial period' and the 'constant drying rate period', and the second stage comprises the 'falling rate period'.

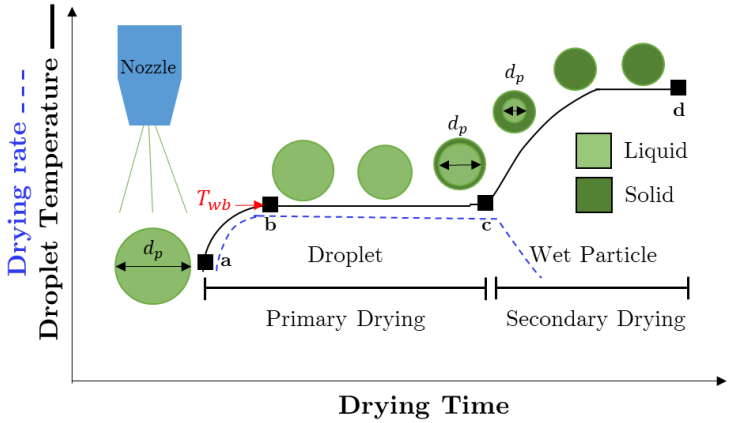

Figure 2.6. Graphical representation of the drying kinetics of a droplet during spray-drying (Adapted from Mezhericher et al.,2008, Boel et al., 2020).

A graphical representation of the drying kinetics of a droplet during spray-drying is given in **Erreur ! Source du renvoi introuvable.**. In the first stage, a droplet of initial diameter $\mathbf{d_p}$, gets in contact with the drying medium, at this point the droplet has the greatest amount of liquid. When passing through the drying medium the droplet gains sensible heat, and the evaporation of the liquid phase starts at the particle surface (path a – b).

At path (**a-b**) the particle has reached the Wet Bulb Temperature (T_{wb}), up to this point it is known as the "initial period". The solvent evaporation at this step is driven by the relative humidity, temperature, and velocity of the drying gas. Now the droplet enters the 'constant drying rate period' where it is assumed to have a constant evaporation rate, that leads to the particle diameter shrinking (path **b-c**). At this point a concentration gradient has formed within the droplet due to solvent evaporation. As the drying process continues, the viscosity of the droplet increases, the solvent content decreases, and a thin layer of a dry solid crust is formed at the outer surface of the droplet (**point c**).

At point **c**, the droplet moisture content reaches a critical value and the droplet has reached now the dry-bulb temperature. At this point the second drying stage begins, also known as "falling rate period". Now the moisture transfer is limited by internal diffusive mass transfer. Therefore, the droplet is considered a wet particle with a constant outer diameter (path **c-d**). This wet particle is comprised of two regions: solid crust (porous structure) and a wet core (solids and liquids) (Eijkelboom *et al.*, 2023).

At this point the heat transfer to the wet particle and mass transfer to the drying agent is simultaneous and the solid crust stars to continuously increase, while the diameter of the wet core (d) shrinks until it reaches a desired value, previously determined by the drying parameters. The final particle shape and moisture content will depend on the drying rate and diffusion coefficient of the solutes, as well as their permeability. The drying rate will be dependent on the energy required to evaporate the solvent and therefore the heat transport towards the surface of the droplet (Boel et al., 2020)

Stage 4. Separation of dried product from the gas

In traditional spray-drying a cyclone separator is often included in a succeeding separation step, after a spray-drying chamber. A gas-solid cyclone separator is a separation device that separates solid particles from a gas phase using a centrifugal force field.

Operating conditions

The spray-drying process operating conditions are influenced by different factors, as noted in Figure 2.7, which are finally correlated to the dried powder end characteristics, as well as the process outlet parameters (outlet temperature, absolute humidity of drying air, etc) (Re, 2016). In this Section, these operating conditions will be further discussed.

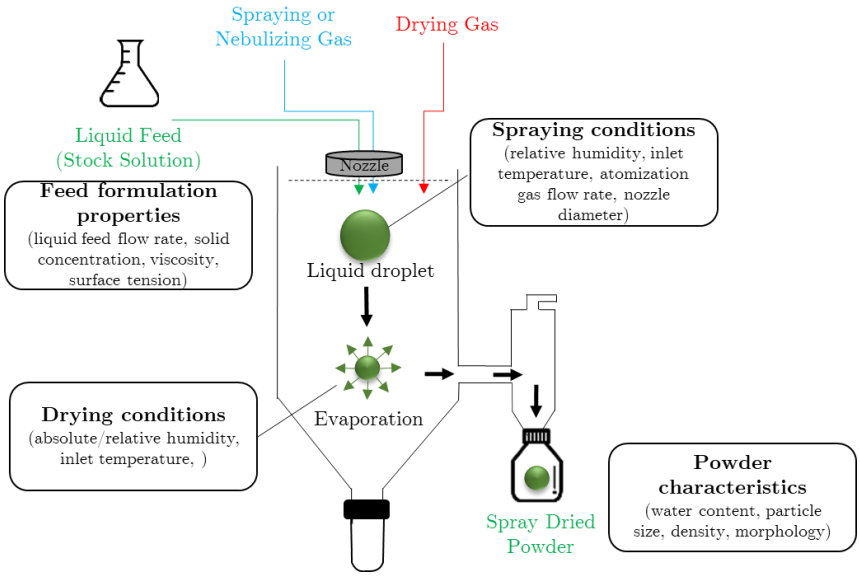

Figure 2.7. Parameters affecting the solid particle formation by spray-drying.

Liquid Feed

The liquid feed flow rate controls the amount of solvent and solid content that enter the drying chamber. This parameter influences the droplet size, particle size, particle morphology/surface/density and protein stability, among other physicochemical properties such as solvent evaporation rate (Ziaee *et al.*; 2019).

An increase in feed flow rate will cause a decrease in particle size, as a result of higher energy supplied for breaking the droplets. If the ratio of feed flow rate to atomizing gas flow rate is higher than 1, the droplets tend to be larger, due to lower spraying energies.

The outlet temperature and the cycle duration will depend on the feed flow rate. As the feed rate is increased, the outlet temperature decreases which is relevant for protein stability (Singh & Van den Mooter, 2016). On the other hand, an increase in the liquid feed flow rate can result in an increase in final moisture content in the spray-dried powder.

Also the process yield can be impacted by the liquid feed flow rate. As example, when drying at the same inlet temperature, processes with lower feed flow rates reported higher process yield, when compared to higher liquid feed flow rates (Ziaee *et al.*, 2019).

Another important parameter is the feed concentration. Higher feed concentrations mean less solvent in each droplet, which is related to shorter evaporation times, as well as an increase on the agglomeration or formation of multimers between polymer chains of API molecules. All this can result in the formation of porous particles with lower density and a rougher surface (Littringer *et al.*, 2012; Kim *et al.*, 2003).

Drying gas

The drying gas flow rate supplied into the drying chamber will impact the interaction of the sprayed droplets. At higher flow rates, the air-droplet interactions are minimized by increasing the particle movements inside the chamber (Santos *et al.*, 2017)

The type of gas used also plays an important role for heat and mass transfer processes. The mass flowrate and specific heat of the drying gas determine the energy lost in the evaporation. For example, CO_2 gives a better heat and mass transfer than air and N_2, but if we are spray-drying a product that is sensible to oxidation, the selected gas will be N_2. Thus, the final selection of the drying gas will depend more on the solvents and molecules present in the liquid feed (Singh & Van den Mooter, 2016).

Inlet/outlet temperature

Phenomena such as heat and mass transfer is affected by the selected inlet temperature. At higher inlet temperatures it is expected to impact the particle morphology, due to high rate of solvent evaporation. Elevated temperatures can, as well, lead to the rapid formation of a solid skin on the outer surface of the droplet which entraps solvent vapours, which may collapse the particle, generating a porous surface (Ziaee *et al.*, 2019).

In combination with the liquid feed flow rate, an appropriate selection of an inlet temperature plays an important role on the outlet parameters, powder moisture content and outlet temperature. The latter have a big impact on the protein stability, lower moisture contents results in an increase in the protein stability in the spray-dried powder (Santos *et al.*, 2017). However, a compromise must be found between achieving a lower moisture content and the protein thermal stability.

The temperature that a spray dried particle reaches is between the outlet air temperature and the wet-bulb temperature of the outlet air. This means that the temperature at the which the protein is submitted is 10-20°C below the outlet temperature (Raimundo da Silva *et al.* 2017).

Output process parameters

Yield. The yield is primary controlled by cyclone efficiency, which is dependent on atomization gas and liquid feed flow rate, and solid content in the liquid feed. A higher yield is achieved at higher concentrations of solids in the liquid feed, higher temperatures and lower liquid feed flow rates (Ziaee *et al.*, 2019).

As a result of the different process parameters above mentioned the powder will have certain final properties. These are briefly discussed as follows, and will be summarized in Table 2.4.

Powder properties

- *Particle size distribution***.** It is highly dependent on the solid content in the liquid feed, nozzle size and liquid feed to atomizing gas ratio.
- *Morphology.* The morphology is influenced mainly by the evaporation rate and the composition of the formulation.
- *Moisture content.* The solid content present in the liquid feed, the liquid feed flow rate and the temperature are the main driving factors to manipulate the spray-dried powder moisture content.

Table 2.4. Explanation of the impact of certain spray-drying parameters on some outlet process parameters and powder characteristics, where (+) means an increasing value and (-) a decreasing value on both inlet and outlet parameters. The particle size and the powder moisture content are parameters that can be previously targeted for a desired value. (Vasconcelos, 2016; H.S. Lee et al., 2011; Jalalipour et al., 2007; Wilson et al., 2020; Ziaee et al., 2019)

	Powder			**Process**		**Reconstituted solution from spray dried powder**
Outlet Parameter / **Inlet parameter**	*Particle size*	*Particle porosity*	*Particle smoothness*	*Powder moisture content*	*Powder yield*	*Monomer Loss*
(+) Inlet temperature	+	-	-	-	+	+
(+) Drying Gas Flow Rate	-	+	+	-	+	+
(+) Liquid Feed Flow Rate	-	-	+	+	-	+
(+) Solid content in feed	+	-	-	-	+	+
(+) Solution viscosity	+	-	-	+	+	+
(+) Protein concentration	+	-	+	-	+	+
(+) Humidity	+	+	-	+	+	+
(+) Nozzle diameter	+	+	-	+	+	+

For a protein to arrive to the dried particle state, through the use of the different operating conditions previously mentioned, it will have to be submitted to different stresses. These stresses can generate destabilizations in its structure and make it non-functional. That is why many of the protein formulations are supplemented with stabilizers that have specific mechanisms against one or more stresses.

In the next Section these stresses and protection mechanisms will be discussed.

2.3.3.5 Stresses present during drying of a liquid formulation containing a protein

During the spray-drying process, the drying product undergoes different stresses such as shear, thermal/dehydration, and interfacial stresses (Figure 2.8) (Grasmeijer *et al.*, 2019). These stresses can disrupt the tertiary structure of a protein and unfold it, then the hydrophobically buried sites are exposed and are free to interact with other solvent components, proteins, or the air interface (Haque *et al.*, 2015).

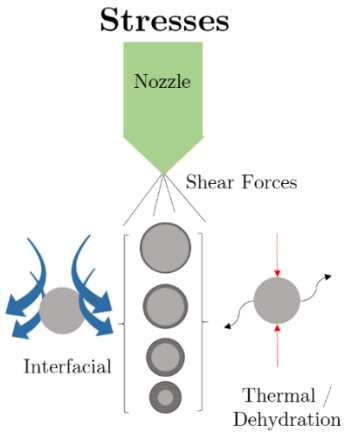

Figure 2.8. Stresses present during spray-drying, as shear forces at the spraying step in the nozzle, interfacial stresses at the droplet air-liquid interface, and thermal/dehydration stresses induced by the evaporation caused by the drying air.

Shear Stress

Proteins encounter shear forces during the spraying phase. Normally, these forces are not harmful to the protein, but in combination with the large air/liquid interfaces it may lead to protein degradation. It can as well create an unstable organisation of the protein that will make it more susceptible to further stresses (Duerkop *et al.* 2018, Arsiccio *et al.* 2020, Ajmera, 2014; Ghandi *et al.*, 2012)

This process will be further discussed in Chapter 3, Section 3.4.2.1(a).

Interfacial stress

The interfacial stress, that can lead to protein aggregation, is caused by changes in conformation, as proteins modify their higher order structure in response to interfacial stresses such as hydrophobicity, charge, and mechanical stress (Li *et al.*, 2019).

Thermal/Dehydration

When temperature increases beyond a certain level (depending on the protein) during spray-drying, the tertiary structure of the protein starts to break due to thermal motion and other factors, gradually altering the secondary structure (Haque *et al.*, 2017).

As the temperature increases the dehydration rate increases as well, and the removal of water molecules causes insufficiency of hydrogen bonds needed to stabilize the different levels of the protein structure. For example, the secondary structure of a protein (α-helices and β-sheets), tertiary structure (polar side chains) and quaternary structure (subunits bonding) (Ameri *et al.*, 2007; Haque *et al.*, 2017).

2.3.3.6 Stabilization mechanisms against protein degradation during spray-drying

Various mechanisms have been proposed to explain the role of excipients in protecting proteins from denaturation. Some of the more prevalent theories are illustrated below.

Vitrification theory

The protein mobility leads to its degradation over time, as a result of the interactions it has with other proteins or with other molecules when in solution. Therefore, the entrapment of the protein onto a rigid, amorphous glassy matrix will slow down its degradation by reducing the protein mobility (Ajmera, 2014; Mensink *et al.*, 2017) (Figure 2.9).

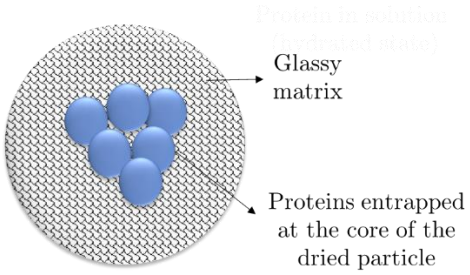

Figure 2.9. Vitrification theory diagram

This stabilization theory is used to reduce the mobility of proteins in the medium when in liquid state and as well to avoid thermal stresses.

Excipients used as a glassy matrix

Amino acids have been proven to give a more rigid matrix to the protein when transforming into the solid state (Ajmera, 2014).

Sugars are known for stabilizing the molecule through the principle of the vitrification theory (Pinto *et al.*, 2021). Trehalose is one of the most common sugars used in the improvement of protein stability (i.e. Human immunoglobulin G, L-lactic dehydrogenase, Polyclonal human IgG, Alkaline phosphatase, Humanised IgG4). Some attributes of trehalose are its high glass transition temperature (T_g) (~106°C) (Roe & Labuza, 2007), and its ability to form an hydrogen bond with the proteins (Maury *et al.*, 2005;

Grasmeijer *et al.*, 2019; Grasmeijer *et al.*, 2016; Batens *et al.*, 2018; Emami *et al.*, 2018; Dani *et al.*, 2007; Ziaee *et al.*, 2019).

The mobility of the protein will be secured by the difference between the sugar T_g and the storage room temperature. The T_g should be, at least, 50°C above the storage temperature (Grasmeijer *et al.*, 2013, Ajmera,2014)

Water replacement

In solution proteins are usually bound to many water molecules, and they are considered to be in a hydrated state. When proteins go through a drying process, those bonds break.

There are certain excipients, like sugars and amino acids, that can form hydrogen bonds with proteins during the water removal process, creating a water-like environment for them, which helps to protect and strengthen its tertiary structure (Ziaee *et al.*, 2019). It is known that the hydroxyl groups of the stabilizer molecule form hydrogen bonds with the protein (Figure 2.10) (Mensink *et al.*, 2017; Ajmera,2014; Tscheliessnig *et al.*, 2012).

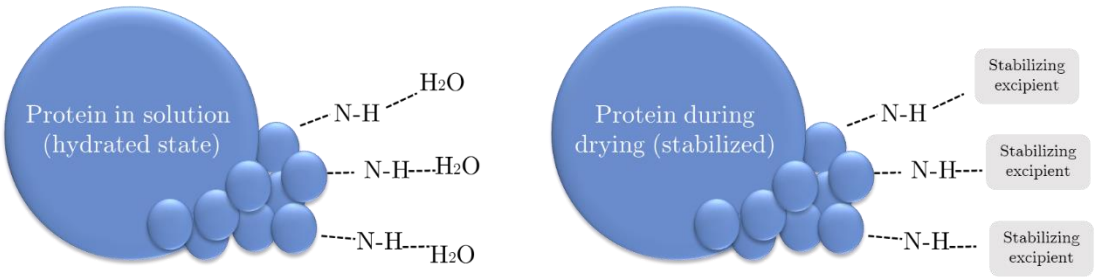

Figure 2.10. Water replacement theory mechanism on a protein in liquid state (left) bonded to water molecules, during a drying process where it is by bonding with the excipients acting as stabilizers (right) (adapted from Tscheliessnig et al., 2012)..

This protection mechanism is used to stabilize the proteins against thermal/dehydration stresses.

(a)Excipients used for water replacement

Sugars are known to thermodynamically stabilize proteins by replacing these hydrogen bonds, and thus, allow the biomolecules to maintain their native conformation (Pinto *et al.*, 2021).

For instance, sucrose and trehalose, and polyols could function according to the water-replacement theory. (Ziaee *et al.*, 2019, Maury *et al.*, 2005; Emami *et al.*, 2018). Sugar molecules should have a close fit to the protein surface and should thus be in the amorphous state (not crystalline) to maximize the hydrogen bonding with the protein (Grasmeijer *et al.*, 2013; Ajmera,2014).

Some amino acids seem to also replace the hydrogen bonds between the water and the protein molecules (Ajmera, 2014).

Competitive adsorption

The surface activity of the stabilizers acting as surfactants reduce the protein concentration at the surface, which prevents its denaturation at the air/water interface (Figure 2.11) (Maa *et al.*, 1998; Maa & Steven, 2000; Ajmera 2014).

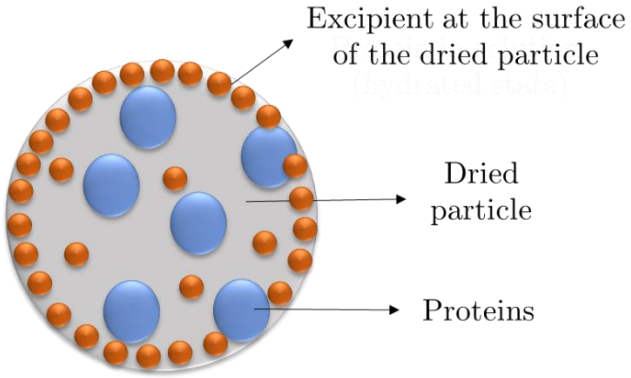

Figure 2.11. Diagram of the competitive adsorption theory.

This protection mechanism is directed towards the protection of the protein against the interfacial stresses.

(a)Excipients used against competitive adsorption

As an example, the surfactants Tween 80 (polysorbate 80) and SDS (sodium dodecyl sulfate) (Adler *et al.*, 2000), can occupy the surface of the droplets and protect proteins from air-liquid interface tension (Ziaee *et al.* 2019, Emami *et al.*, 2018).

Surfactants are believed to bind to the hydrophobic surfaces of the proteins, which are potential unfolding sites, at the same time they prevent that other proteins binding to those sites (Ajmera,2014).

Other excipients, such as small amino acid molecules (arginine), are prone to display this type of protection mechanism during a protein spray-drying process (Ajmera, 2014).

Preferential Exclusion

In solution, the surface of a protein molecule must be in contact with a solvent component, where the protein is defined as in the hydrated state. There are certain components in the solvent that are preferentially excluded from the surface of proteins, which increases protein chemical potential creating repulsion forces between the proteins (Timasheff *et al.*, 2002; Sudrik *et al.* 2017).

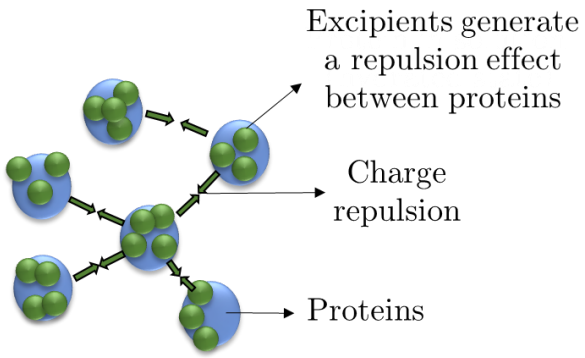

Figure 2.12. Diagram of the preferential exclusion theory.

Given that this protection mechanism avoids the interaction of the denatured proteins with each other, avoiding the aggregation phenomena, it could reduce the protein destabilization by shear, thermal and interfacial stresses.

(a)Excipients that generate a preferential exclusion

Sugars like trehalose and sucrose are known to have preferential exclusion towards mAbs in solution, meaning that the sugar molecules are excluded from the surface of the mAb, creating a repulsion effect and therefore avoiding the interaction between mAbs (Sudrik *et al.*, 2017; Kendrick *et al.*, 1997)

2.4 Synthesis chapter 2

The stabilization of proteins in liquid formulation is a challenge that the pharmaceutical industry faces nowadays. One of the proposed solutions to overcome this, is to pass from a liquid to a solid formulation through the help of a drying process.

There are different types of drying processes (spray-freeze drying, freeze-drying, spray-drying, electrospray-drying, etc.), each one with a different set of operating parameters which will generate different kind of stresses.

A technique, such as freeze-drying presents solid-liquid interfacial stress, dehydration stress and pH changes, among others. Spray-freeze drying presents formulation changes (pH, concentration of components), shear stress, and dehydration stress.

One of the drying techniques, with a growing relevance in the manufacturing of protein based biopharmaceuticals, is the spray-drying process. However, this technique also presents certain stresses, where the main three are: thermal/dehydration stress, shear stress, and interfacial stress.

To lower the impact of the stresses during spray-drying, the selection of good operating parameters conditions is key. The spray-drying airflow in the configuration of co-current process seems to be the most appropriate for thermolabile materials such as proteins. The liquid feed flow rate and the spraying-gas flow rate ratios play an important role in the control of the generated spray-dried powder, and the final protein stability. The inlet temperature will define the stability of the protein through the control of the thermal stress exerted during the drying and the final moisture content in the powder.

Besides the operating conditions of the spray-drying process, the formulation is another critical factor in the stabilization of protein biopharmaceuticals. Different stabilizers can be added to the formulation to avoid or reduce the impact of the stresses present in the spray-drying process. However, it is important to keep in mind that the selection of the stabilizer will be related to the protection mechanism that it offers.

In this thesis our interest is the generation of dry stable forms of mAbs. In the following chapters we will explore the impact of a spray-drying process and formulation on a protein based formulation stability, by the characterization of the spray-dried powders and the reconstituted solutions generated from them.

Chapter 3

Bovine Serum Albumin as model for protein spray-drying study

Although many drying processes can be used to prepare protein powders, choosing an appropriate process for each specific product remains a challenge. Here we focus on spray-drying. Chapter 3 presents the first part of our study which was devoted to a rational investigation of the resistance of a protein to the different stresses it will undergo by this drying technique, without any protective formulating factor against denaturation (aggregation). Bovine Serum Albumin (BSA) was chosen as the model protein since its characteristics such as purity, water solubility, economical and easy accessibility make it a commonly used protein model in pharmaceutical industries and scientific research for process and formulation studies.

3.1 Introduction

Different proteins have been used as models for studies of the protein resistance to the inherent stresses of the drying techniques. The most common models are enzymes such as Alcohol Dehydrogenase (Shiga *et al.* 2014), Lactic Dehydrogenase (Grasmeijer *et al.* 2019), Lysozyme (Ajmera 2014), or a family of globular proteins (Albumins) such as bovine gamma globulin BGG (Heng & Yeates, 2018), ovoalbumin OVA (Ajmera 2014), and Bovine Serum Albumin BSA (Hackl et al, 2018.I, Hackl *et al.*, 2018.II). The molecular weights of these most common model proteins are in the range 14 to 240 kDa.

Many studies have been conducted with BSA and different excipients using spray-drying as the chosen process (Jalalipour *et al.* 2007, Rajagopal *et al.* 2013, Constantino *et al.* 2000, Prinn *et al.* 2002, Grasmeijer *et al.* 2016, Wilson *et al.* 2020) and it is the model protein of choice in the initial phase of our study. The following Section (3.2) will focus on gathering the main information found in the literature from these studies.

3.2 Bovine Serum Albumin

Bovine Serum Albumin (BSA) proteins are formed by three domains (Figure 3.1), containing 6 helices and 9 loops, which are stabilized by an internal networking of disulphide bridges (Pattnayak *et al.*, 2010).

Figure 3.1. 3D model of Bovine Serum Albumin (Retrieved from Majorek et al., 2012)

In total BSA has 17 intramolecular disulphide bridges, also known as thiols (SH), that assist in keeping its tight structure. It also has a set of hydrophobic residues on its surface. Free sulfhydryl amino residue and tryptophan residues, which have been used as internal indicators of tertiary structure changes, are also BSA proteins characteristic components (Babcock *et al.*, 2014; Bogahawaththa & Vasiljevic, 2022).

Some of the BSA physiochemical (Table 3.1) and structural properties, coupled with its availability and inexpensiveness, makes it an ideal model for research. (De Maria *et al.*, 2015)

Table 3.1. BSA physicochemical properties (Babcock et al., 2014 ; Pattnayak et al., 2010 ; De Maria et al., 2015)

Parameter	Value
Molecular weight (kDa)	66
pI in water (25 °C)	4.5 - 5.0
pH (higher stability)	7
Intrinsic Viscosity	0.0413
Optic absorbance of 1gm/L A279nm	0.667
α-helix (%)	54
β- helix (%)	18

Having a pI range of 4.5-5.0, at neutral pH the BSA molecule is negatively charged and at acidic conditions it is positively charged. In a neutral pH environment, the disulphide bridges will be buried in the protein molecule and consequently they are not exposed to the solvent in a liquid formulation. (Phan *et al.*, 2015; Borzova *et al.*, 2015).

On the other hand, when an external stress is applied to BSA, such as temperature or pressure, it modifies its conformational structure exposing the thiol groups, which can be used as a protein denaturation or protein unfolding factor (Boland *et al.*, 2011) (Aramwit & Agren, 2016) (De Maria *et al.*, 2016).

3.3 Spray-drying of Bovine Serum Albumin

Table 3.2 details a number of studies carried out on spray-drying of solutions containing BSA. The objective, the study parameters, the type of equipment used, and the main results of the research studies are summarized and will be discussed. For spray-drying, the inlet temperature and the flow rate of the drying air, the flow rate and the solids concentration in the liquid feed, and the spraying conditions are important parameters whose influence is often investigated, as shown in more detail in Table 3.3 for the research mentioned in Table 3.2. The combined effect of these inlet parameters results in a certain outlet condition that should be suitable for the desired product, such as chemical integrity and physical characteristics like moisture content and particle size.

Table 3.2. Research work on spray-drying of Bovine Serum Albumin.

Reference	Objective	Studied parameters	Findings
Adler *et al.*, 2000	Demonstrate that addition of a surfactant reduces the protein adsorption at the droplet surface, increasing the protein stability during spray-drying	**a) Formulation:** - Surfactant concentration (Tween 80*, SDS*) **Spray dryer used**: Büchi B-190	Polysorbate 80 was proven to protect protein at the droplet surface during spray-drying. The protection was found to be directly proportional to its concentration in the liquid formulation.
Prinn *et al.*, 2001	Statistical analysis of the impact of formulation and process parameters on particle size, yield and outlet temperature	**a) Formulation:** - Protein concentration - Zinc:protein ratio **b) Process:** - Inlet temperature - Liquid feed rate - Drying airflow rate - Atomizing nitrogen pressure **Spray dryer used**: Büchi B-191	Inlet temperature showed clear correlation with monomer loss %. The solid-particle morphology was clearly influenced by the formulation, specifically by the protein concentration
Jalalipur *et al.*, 2007	Study of effect of stabilizers on protein physical state and aerodynamic behaviour of spray-dried BSA	**a) Formulation:** - Stabilizer concentration (Zinc, Tween 80) - Zinc:protein ratio **Spray dryer used**: Büchi B-191	The use of surfactant and zinc chloride as excipients for BSA helped in its stabilization during spray-drying. Tween 80 having the higher impact.
H.S. Lee *et al.* 2011	Study of the formulation and process parameters impact on the particle size and morphology of spray-dried powders, and process yield	**a) Formulation:** - Surfactant concentration - BSA concentration **b) Process:** - Nozzle diameter - Drying air-flow rate -Inlet temperature **Spray dryer used**: Büchi Nano Spray Dryer B-90	The nozzle diameter and the surfactant concentration had an effect on the morphology and size of the spray-dried BSA powder.
Rajagopal *et al.*, 2013	Assessment of viability of spray-drying of proteins at high temperatures, and investigation of the effect of trehalose and histidine-HCl buffer on BSA second structure stability after spray-drying	**a) Formulation:** -Stabilizer concentration - Presence of buffer **b) Process:** - Inlet temperature **Spray dryer used**: Büchi B-191	An optimal formulation containing trehalose and histidine-HCl buffer has been found to significantly limit the aggregation of BSA in spray-dried particles at 100°C. Trehalose had a greater contribution

*Tween 80 = Polysorbate 80; SDS = sodium dodecyl sulfate

Table 3.3. (Continuation) Research work on spray-drying of Bovine Serum Albumin.

Reference	Objective	Studied parameters	Findings
Wilson *et al.*, 2020	Study the impact of saccharide-containing excipients on surface composition and matrix heterogeneity of spray dried BSA powder.	**a) Formulation:** - Sugar concentration (sucrose, trehalose, dextran) **Spray dryer used**: Büchi Mini Spray-Dryer B-290	Saccharides shown to be good stabilizers for BSA against spray-drying stresses, trehalose being the better option given the final T_g of the produced powder, which was 40°C higher than the one of dextrane
Reslan *et al.*, 2016	Study of the improvement of BSA physical stability during spray-drying by the use of two synergistic amino acids: arginine and glutamic acid	**a) Formulation:** - impact of amino acids (arginine and glutamic acid) on BSA aggregation **Spray dryer used**: : Büchi Mini Spray-Dryer B-290	Arginine was found to improve BSA stability after spray-drying. While the synergistic effect of arginine and glutamic acid showed no improvement in BSA physical stability during spray-drying at the concentrations used in the study.

*Tween 80 = Polysorbate 80; SDS = sodium dodecyl sulfate

Table 3.4. Operating conditions used in spray-drying of BSA in the works presented in Table 3.2

Author	Temperature [°C]	Nozzle [mm]	Feed Flow Rate [ml/min]	Atomizing Airflow Rate [L/h]
Adler *et al.*, 2000	Tin=150 Tout=95	0.7	4	700
Prinn *et al.*, 2002	Tin= 110-120 Tout=36-125	Not reported	3-20	500-900
Jalalipur *et al.*, 2007	Tin= 100 Tout=70	Not reported	2.5	600
H.S. Lee *et al.* 2011 *	Tin= 80-120 Tout=36-45	4 µm, 5.5 µm, 7 µm	Not reported	(Nitrogen) 5400, 7200, 9000
Rajagopal *et al.*, 2013	Tin= 87 Tout=57	Not reported	2	600
Wilson *et al.*, 2020	Tin=100 Tout=50-55	Not reported	2	600
Reslan *et al.*,2016	Tin= 60°C Tout= 39°C	Not reported	2.2	742

*Nano-spray-drying

Tin= inlet temperature, Tout= outlet temperature

3.3.1 **Protein Stability**

When BSA is in solution without excipients, the process parameter of spray-drying noticed as having the higher impact on the monomer loss % is the inlet temperature, but this impact can be reduced by the presence of stabilizers such as polysaccharides and zinc ions (Prinn *et al.*, 2002, Costantino *et al.*, 2000). Secondly, the formulation has been showed to have a high impact on the reduction of BSA aggregation during spray-drying.

Jalalipour *et al.* (2007) found, that the addition of surfactants and zinc ions decreased the monomer loss % during spray-drying, using different mechanisms and to different extents. The monomer loss corresponding to the addition of zinc ions was around 4%, while for the formulation containing Tween 80 no monomer loss was detected. These results showed a clear improvement In the formulation stability in comparison to the BSA formulation with no added excipients, which had a monomer loss around 12%.

Different authors reported that the use of surfactants and polysaccharides in BSA formulations decrease the monomer loss percentage. By using electron spectroscopy for chemical analysis (ESCA), Adler *et al.* (2000) proved that surfactants (Tween 80, SDS) were efficient in the reduction of monomer loss % by protecting the protein at the droplet surface.

Rajagopal *et al.* (2013) showed that the combination of other excipients (histidine and trehalose) reduced aggregation phenomena in BSA, with a greater contribution from trehalose. Another literature source (Wilson *et al.*, 2020) demonstrated that the use of excipients with higher molecular weights (like dextran) resulted in a higher protein concentration at the particle surface, compared to lower molecular weight excipients (sucrose, trehalose).

Regarding another category of excipients, the presence of amino acids such as glutamic acid could reduce protein-protein interaction by increasing electrostatic repulsion (by increasing the net negative surface charge of BSA) in the drying droplets, during the spray-drying (Reslan *et al.*, 2016). This effect was found to be dependent on the concentration of amino acids added to the BSA solution.

Intrinsic properties of the spray-dried powder, such as the glass transition temperature (T_g) and of the liquid formulation such as the melting temperature (T_m), are directly related to protein stability and can be modified to give the protein formulation a higher stability. The higher the T_g, the lower the aggregation present in the dried powder, which is typically attributed to the vitrification stabilization theory (Grasmeijer *et al.* 2013). The T_g values can be increased, by the addition of sugars to the formulation (Jalalipour *et al.*, 2017). This was well demonstrated by Wilson *et al.* (2020) and Jajalipour *et al.* (2017), in that the presence of trehalose in the BSA formulation increased the Tg values of spray dried powders. The T_m of a protein corresponds to the temperature at which the protein in solution denatures. When in solution, BSA T_m is lower due to a higher backbone mobility. By passing from a liquid to a powder formulation the T_m. increases from 70°C to 150°C according to Rajagopal *et al.* (2013).

3.3.2 Particle Size and morphology

The particle size is heavily impacted by the formulation composition, by the ratio of atomization gas flow rate to liquid feed flow rate (Prinn *et al.*, 2002) and the nozzle size diameter (H.S. Lee *et al.*, 2011). Costantino *et al.* (2020) and Prinn *et al.* (2002) reported that an increase in the ratio of atomization gas flow rate to liquid feed flow rate decreased the droplet size, and therefore the spray-dried particle size.

Regarding the formulation composition, the use of certain excipients can impact the particle size or morphology of the spray dried BSA particles. For example, Adler *et al.* (2000) found that the addition of only trehalose (a high molecular weight excipient) to the BSA solution created wrinkled particles due to changes in the balance of surface-to-viscous forces in the drying droplet. On the other side, the addition of a surfactant (PS80) created round smooth particles. This was also found by H.S. Lee *et al.*, (2011), who reported that smooth particles were generated using Tween 80 (0.05% w/v) in the formulation. Smooth particles when adding surfactants was also reported by (Prinn *et al.* 2002). Other excipients such as glutamic acid also led to a reduction in the particle size of the spray-dried powder (Reslan *et al.* 2016).

The concentration of BSA in the liquid formulation can also affect the particle size and shape of spray-dried powders (Prinn *et al.*, 2002, Jalalipour *et al.*, 2007). As an example, without excipients, the pure BSA powder particle showed a dimpled structure (Jalalipour *et al.*, 2007).

3.3.3 Yield

The yield was reported to be highly dependent on the composition and concentration of the solution containing BSA, as well as on the temperature and the liquid feed flow rate (Prinn *et al.*, 2002, Costantino *et al.*, 2000). The higher the concentration of dissolved solids in the formulation, the higher the yield in powder production.

3.3.4 Moisture Content

Certain excipients can increase the final moisture content of the sample given their hygroscopic characteristics. For example, when zinc chloride was added to the BSA solution, the moisture content in the spray-dried powder increased from 4.2% (without zinc chloride) to 6.4%(with zinc chloride), under the same operating conditions.

Rajagopal *et al.* (2013) showed that the moisture content is also dependent on the solid concentration in solution. Moisture content also impacts the T_g values of the dried powders (Wilson *et al.*, 2020).

3.3.5 Literature summary

In summary, from these works on spray-drying of BSA, it can be concluded that BSA is usually dried in the presence of a combination of excipients, such as surfactants and sugars, amino acids or others

such as zinc ions. Besides the protective effect on protein stability, the presence of excipients impacts the particle characteristics such as particle size and shape, moisture content and process yield.

Despite all this technical information about spray-drying of BSA, we were interested in knowing the effect of the spray-drying process on the pure protein in the absence of a protectant, considering that the literature does not present enough information on its denaturation relative to the different stresses imposed by a spray-drying process. Therefore, the drying of a pure BSA solution became the object of this first study. Results obtained from this study were an important departure point for the selection of the spray-drying operating parameters that were more suitable for protein drying, that were then used on the protein of interest, the mAb-A.

3.4 Materials and Methods

3.4.1 Materials

BSA Mw ≈ 66 kDa, heat shock fraction, approx. 98% purity, was purchased from Sigma-Aldrich (St. Louis, MO) and was used to prepared the formulation FB1.

Formulation FB1. Formulation FB1 consisted of reconstituded BSA powder in Milli-Q water at two different protein concentrations: 100 mg/ml (FB1.100) and 200 mg/ml (FB1.200) (pH=7).

These formulations were filtered (hydrophilic polyethersulfone (PES) 0.22 µm) right before being spray-dried.

3.4.2 Methods

3.4.2.1 Decoupling of spray-drying stresses

As already mentioned, during a spray-drying process, proteins can undergo degradation due to shear, thermal and dehydration stresses. Difficulty relies on recognizing the real contribution of each of the stress sources on protein denaturation, during spray-drying. Therefore, we propose to separate the study of the stresses into two tests: Shear Stress Test (SST) and Dehydration and Thermal Stresses Test (TDST) as shown in diagram on Figure 3.2.

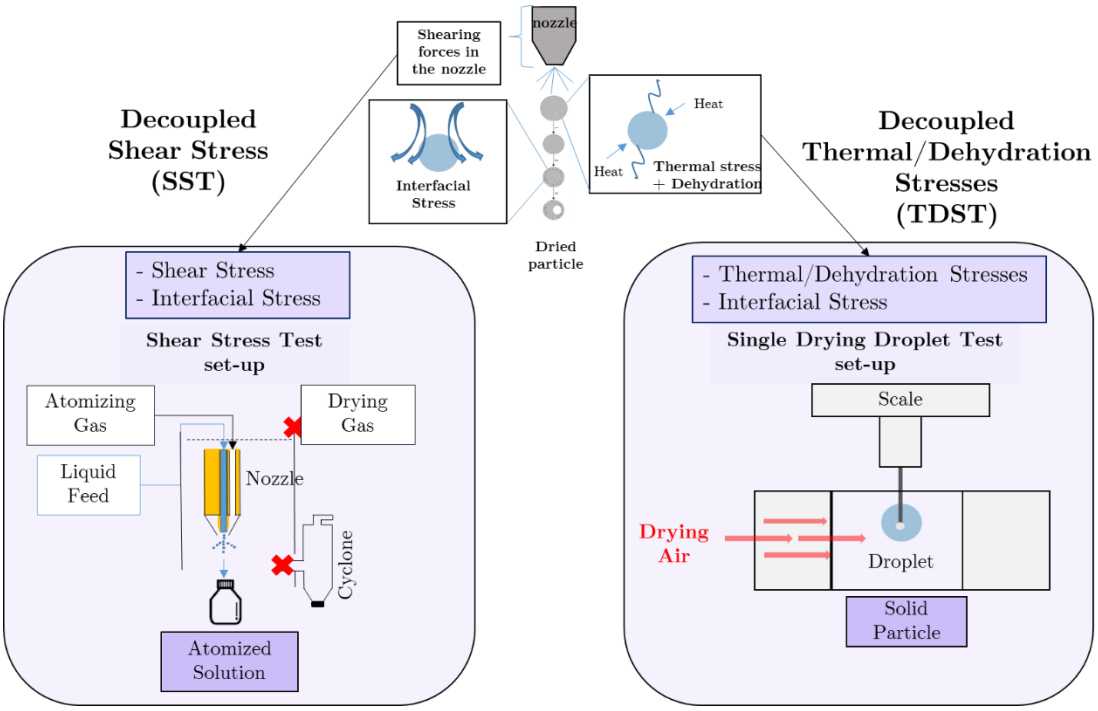

Figure 3.2. Diagram of decoupling of spray-drying shear and thermal/dehydration stresses

Shear Stress Test (SST)

The final properties and functionality of proteins can be modified by shearing forces alone. Shear-induced modifications affect mainly the secondary structure of the protein, leading to protein unfolding, thus exposing the hidden reactive sites of the globular structure of BSA (Quevedo *et al.*, 2021). This can lead to new protein-protein interactions, which results in aggregation of the protein, through disulfide bonding involving the free sulfhydryl residue, as reported by Bogahawaththa *et al.*, (2022). The aggregates play a very important role in the functionality of the protein (Huppertz *et al.*, 2019; Bogahawaththa *et al.*, 2022). Quevedo *et al.*, (2021) reported that some stresses, like shear and thermal, can reduce the activation energy of the denaturation reaction.

In this part of the study, shear stress was first decoupled from thermal and dehydration stresses, by carrying out in a laboratory spray dryer (Büchi Mini Spray Dryer B-290), a spraying process of the BSA formulations (FB1.100 and FB1.200) through the spray nozzle, without drying. The sprayed solution was recovered and analysed with respect to protein aggregation, as shown in Figure 3.2.

(a) Shear rate, shear stress and shear strain calculation

In order to study the effect of shear forces on BSA stability, it was necessary to obtain a physical value that would allow comparison between shear forces generated by different operating conditions. Therefore, three different parameters were measured: shear rate, shear strain, and shear stress. The shear strain and the shear stress show the stress experienced by a protein during a certain exposure time and the stress related to the viscosity of the solution, respectively.

When reporting hydrodynamic flow phenomena of proteins, the term shear stress (σ) has been described as a better indicator of actual denaturing forces acting on the protein (Jaspe & Hagen *et al.*, 2006). The shear stress (σ) corresponds to the force acting on the fluid at certain shear rate , expressed in Pa (Safaric, 2020; Duerkop *et al.*, 2018), and is calculated by the relationship between the fluid viscosity (η) and the shear rate ($\dot{\gamma}$) (Equation 3.1)

$$\sigma = \dot{\gamma} \times \eta \qquad (3.1)$$

The shear rate ($\dot{\gamma}$) provides information about the mechanical stress to which the fluid is subjected during the spraying process. It can be calculated by the fluid velocity gradient perpendicular to the flow direction $(v_z)\dot{\gamma} = \frac{dvz}{dx}$, expressed in terms of average velocity (v_{av}), of the liquid feed and nebulizing gas flow velocities, liquid feed velocity (v_{liq}), and the nozzle diameter (D_{in}) (Equation 3.2) (Safaric, 2020; Duerkop *et al.*, 2018).

$$\dot{\gamma} = \frac{2(v_{av} - v_{liq})}{D_{in}} \qquad (3.2)$$

At this point, if momentum exchange with the surroundings is neglected, and just momentum transfer between the liquid and the gas flows is assumed at the mixing zone, it can be considered that both flows will leave the spraying zone at constant velocity, which is known as the average velocity (v_a), and it can be calculated as indicated in Equation 3.3.

$$v_{av} = \frac{v_g \dot{m}_g + v_l \dot{m}_L}{\dot{m}_g + \dot{m}_L} \quad (3.3)$$

Where $\dot{m}_g$ and $\dot{m}_L$are the mass feed flow rates of gas and liquid respectively, also the velocities, v_L and v_g, are calculated at the point of fluid disintegration by using the cross-Sectional area of the nozzle. For this, the nozzle cross-Sectional area corresponding to the liquid feed (A_{liq}) and atomization gas (A_{gas}) flows, were considered to have a circular area and were calculated using the diameters D_l and D_g respectively, showed in Figure 3.3a-b and given in equations shown on Figure 3.3b.

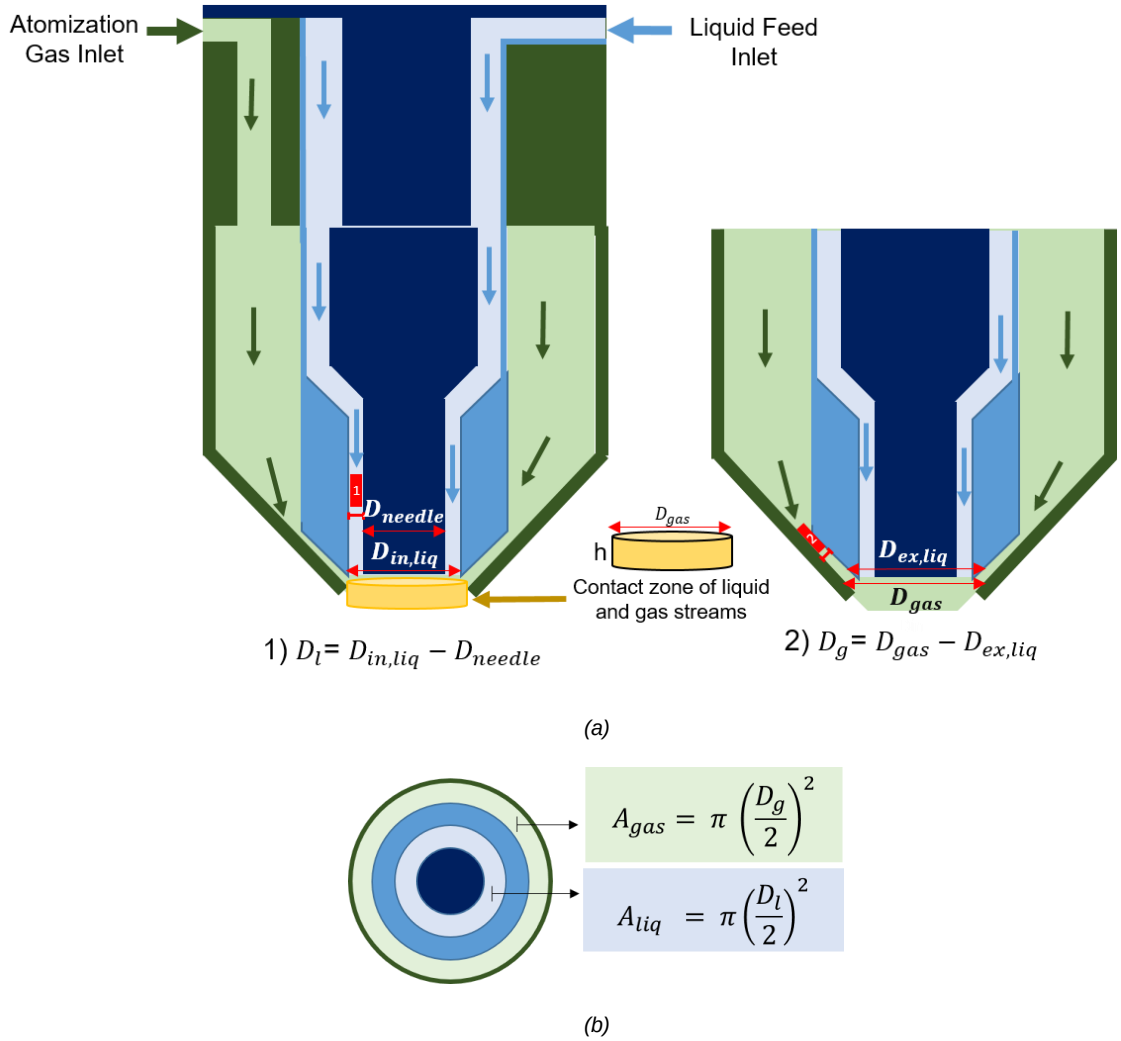

Figure 3.3. Diagram of the two-fuid nozzle indicating the a) diameters and the b) cross-Sectional areas used for the calculations of shear rate, shear strain and shear stress

The other parameter, used to assess the stress followed by a protein submitted to shear forces is the shear strain or shear deformation (γ). It is a dimensionless measure of the time (t_{res}) that a protein has been exposed to a shear rate ($\dot{\gamma}$) generating a velocity gradient (Equation 3.4). The residence time (t_{res}) corresponds to the ratio of the volume of the contact zone (V_{cz}), corresponding to the spraying nozzle, and the liquid flow rate ($\dot{Q}_L$).

$$\gamma = \dot{\gamma} \times t_{res} \quad (3.4)$$

The Vcz is calculated as the volume of a cylinder; $V_{cz} = \pi(\frac{D_{gas}}{2})^2 h$, h, where h is the height of the contact zone, and D_{gas} is its diameter (Table 3.5). As well as for the rate and shear stress, the contact zone used for the calculation of the shear strain (γ) is considered at the point of impact of the liquid and gas streams at the tip of the nozzle, which correspond to the yellow cylinder in Figure 3.3a.

Table 3.5. Two-fluid nozzle dimensions used in the Shear Stress Test on the Büchi Mini Spray Dryer B-290

Nozzle Diameter (Din, liq) [m]	Nozzle Diameter (Dgas) [m]	Height of contact area [m]	Volume of Contact Zone [m3]
0.0005	0.0015	0.0003	5.40E-10
0.0007	0.0015	0.0003	5.30E-10
0.002	0.0026	0.0003	1.60E-09

The shear tests were performed on formulations FB1.100 and FB1.200, which were sprayed at room temperature (20°C), using the operating conditions given in Table 3.5. The nozzle diameter and the liquid feed flow rate were varied to produce different values of shear stress and shear strain during spraying. Before each spraying test all solutions were filtered (PES 0.22 µm). The three parameters shear rate, shear stress and shear strain could be calculated from the experimental results, their detailed calculations are given in Table 3.14 and Table 3.15 in Section 3.7 (APPENDIX). An ANOVA two-factor analysis was performed (with triplicate data), where the impact of the variables of concentration and the nozzle/liquid feed flow rate on the protein aggregation was analysed. If $p<0.05$, for a variable it means that it has an impact on the aggregation output.

In Table 3.6 the conditions used to study shear forces impact on BSA using the Büchi Mini Spray Dryer B-290 are detailed.

Table 3.6. Shear Stress Test (SST) conditions for Formulation FB1.100 and FB1.200, at ≈ 25°C. The variations observed for the feed flow rate are inherent to the equipment set-up used in this study.

Condition	**Feed Flow Rate [ml/min]**		**Nozzle Diameter [mm]**		**Shear Strain**		**Shear Stress (10^3) [Pa]**	
BSA conc.[mg/ml] / Condition	100	200	100 l	200	100	200	100	200
SST 1	3.50	4.48	0.7	0.7	4.47	3.3	3.12	2.92
SST 2	4.45	4.47	1.4	1.4	5.65	5.6	2.89	2.89
SST 3	4.51	4.51	0.7	0.7	3.25	3.3	2.92	2.92
SST 4	3.85	4.56	1.4	1.4	6.80	5.5	3.01	2.87
SST 5	4.34	4.57	0.7	0.7	3.42	3.2	2.95	2.91
SST 6	3.52	4.59	1.4	1.4	7.60	5.4	3.07	2.86
Stock solution	NA	NA	NA	NA	0	0	0	0

BSA conc.= BSA concentration

(b)Reynolds number calculation

For the Reynolds number calculation, given the physical form of the nozzle, the velocity profile $v(r)$ resembles a parabola wrapped around in a circle to form a split doughnut (Figure 3.4). Therefore, a system of annular flow is considered and the Reynolds number calculated for this system is known as Re_{Dh} (liquid stream Equation 3.5) (gas stream Equation 3.6).

$$Re_{Dh,liq} = \frac{\rho_{liq} v_{liq} D_{h,liq}}{\mu_{liq}} \quad (3.5)$$

$$Re_{D_{h,gas}} = \frac{\rho_{gas} v_g D_{h,gas}}{\mu_{liq}} \quad (3.6)$$

Where the diameter was used, called the hydraulic diameter, $D_{h,liq}$ for the liquid stream and $D_{h,gas}$ for the gas stream in the nozzle, were calculated as indicated in Figure 3.4

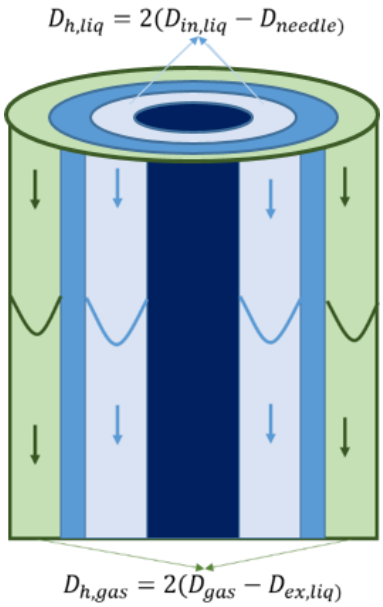

Figure 3.4. Diameter identification for the Reynolds calculation at the nozzle of the Büchi Mini Spray Dryer B-290.

A correction factor (1/ζ) for the hydraulic diameter used for calculating Re_{Dh} is introduced as shown in Equations 3.7 and 3.8, for the liquid and gas streams respectively. This correction factor corresponds to the Reynolds calculation of a system containing two concentric cylinders as the two-fluid nozzle in this study. It is calculated from the ratio of the outer radius, and the inner radius corresponding to the Section of each flow rate. For the two-fluid nozzle the values for ζ_{liq} and ζ_{gas} were both 0.67 (White, 2011) .

$$Re_{liq} = \frac{1}{\zeta} Re_{Dh,liq} \quad (3.7)$$

$$Re_{gas} = \frac{1}{\zeta} Re_{Dh,gas} \quad (3.8)$$

All the information required for the calculation of the Reynolds number for the liquid and gas stream is detailed from Table 3.20 to Table 3.23. In Section 3.7 (APPENDIX).

Thermal and dehydration stresses test (TDST) with a single drying droplet set-up

As previously mentioned, the thermal stresses are also reported to reduce the activation energy of the denaturation reaction (Quevedo *et al.*, 2021). Dynamic scanning calorimetry (DSC) has been used to determine the BSA denaturation temperature, which was found to be around 64°C (Giancola *et al.*, 1997, Yamasaki & Yano, 1990; Matsarkaia *et al.*, 2020). The thermal-induced modifications are more likely to affect the tertiary structure of the BSA and they are also highly dependent on the pH of the solution. Heating BSA at higher net charges lead to the formation of small B-sheet-type aggregates, while heating at lower net charges seems to lead to more polydisperse aggregates (Matsarkaia *et al.*, 2020)

In order to evaluate the impact of the thermal/dehydration stress, avoiding the shear stress generated in spraying step during spray-drying, different techniques can be used to approximate a similar drying behavior such as the single droplet drying (SDD) technique (Boel *et al.*, 2020). This technique is regularly divided in two categories: 1) levitation methods, which immobilize the droplet through contact levitation (suspended on a filament or deposed on a flat surface), 2) and non-contact levitation (acoustic levitator, free-fall technique) (Schutyser *et al.*, 2019).

For the development of the TDST, it was decided to use the single droplet drying method that involved suspending a droplet of pure BSA solution, from a glass filament. To our knowledge, the measurement of the effect of thermal stress on protein aggregation using a suspended single droplet drying technique at high BSA concentrations without excipients has not been yet reported in the literature.

The set-up used in the present work, was previously conceived for the experimental study of a single drying droplet by R. Souza (2020) aiming for the acquisition of drying kinetics from a suspended droplet under well controlled drying conditions. In this study, the same set-up was used for drying a droplet of the formulations FB1.100 and FB1.200 suspended at the tip of a glass filament.

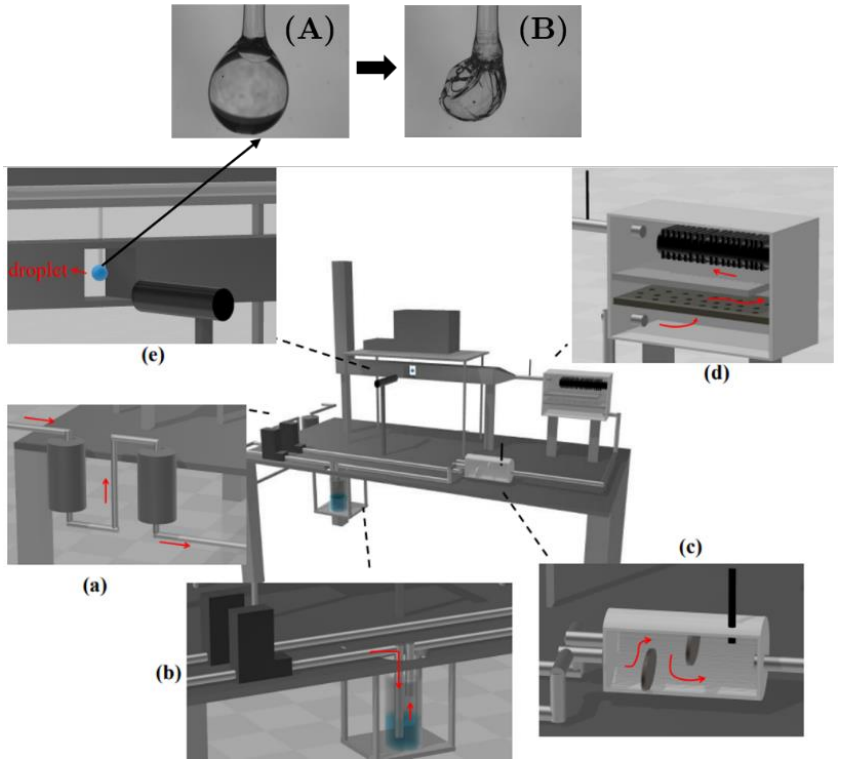

The set-up, shown in Figure *3.5*, encompasses five principal elements, designed to regulate the airflow rate, absolute humidity, and temperature. The drying airflow rate passes along the system as follows: a) First it will flow through a pressure regulator and dehydration column containing silicon hydroxide to reduce the pressure to 2 bars, as well as the initial humidity (Figure 3.a). b) the dried air is then divided into two streams whose volumetric flows are controlled by two flow meters (model SLA5860, Serv' Instrumentation, Ivigny, France), one of the two streams is sent to a glass column filled with distilled water for saturation of the air stream with water vapour (Figure 3.b). One of the two streams was sent to a glass column (10 cm in height and 6 cm in diameter) filled with distilled water for saturation of the

air stream with water vapour. c) At the end of this element the saturated and dry air streams, with controlled volumetric flow rates, are mixed inside a horizontal cylinder with the help of a series of baffles (Figure 3.c). d) At the exit, the temperature and relative humidity of the humid air are measured by a hygrometer (model HC2-SM stainless steel, Michell Instruments, France). Following this, the humid air stream passed through a heating zone containing a heating element (model ASI, Chromalox, Pennsylvania, U.S.A.) with a thermocouple (Type K), placed at the end of this zone, used for the temperature control. The humid air was sent to a flow straightener (i.e. honeycomb) at the entrance of the rectangular wind tunnel (4 cm × 4 cm), which minimized any swirling motion in the air stream caused by passage through the set-up (Figure 3.d). e) Finally the droplet suspension zone (

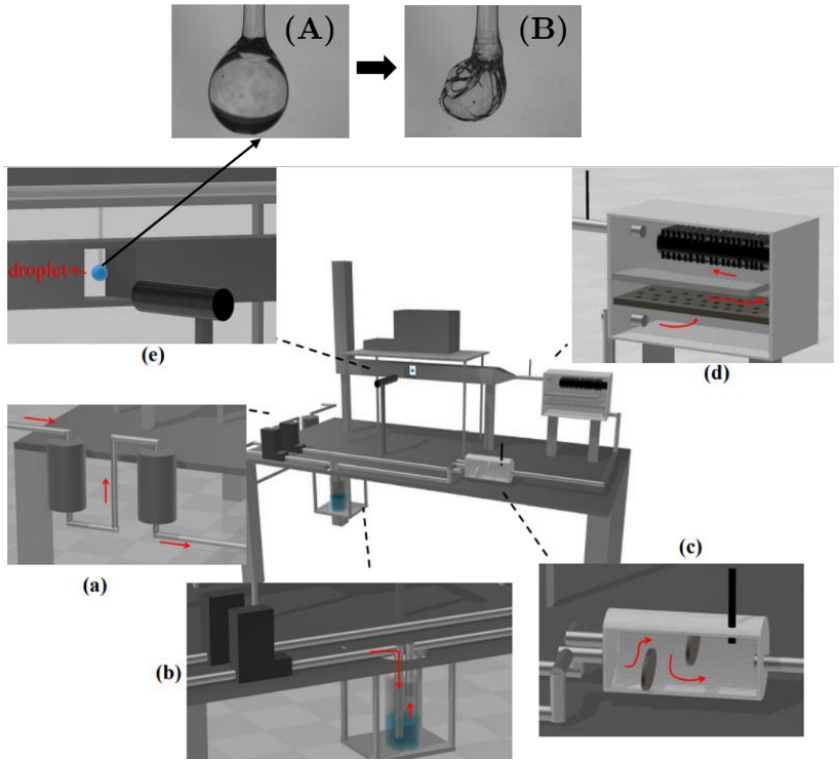

Figure *3.5*) consists of a thin glass filament (approximately 5 cm in length and 200 µm in diameter) suspended under a precision balance (Sartorius Genius Series ME215S, Goettingen, Germany) with the help of a pressure disk on a rectangular device. One droplet could then be placed at the filament knob with the use of a micropipette.

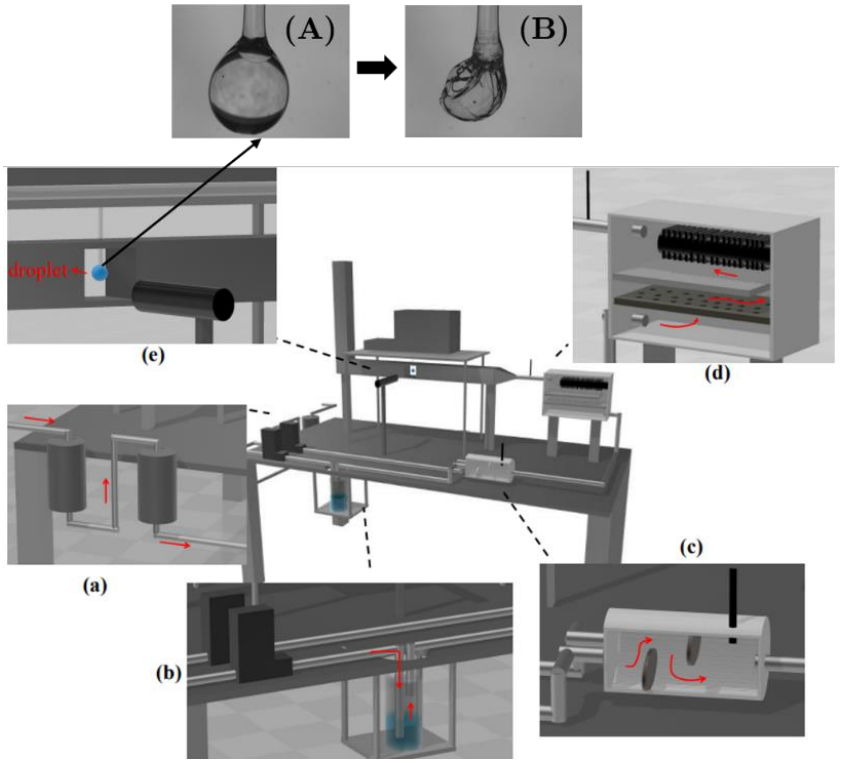

Figure 3.5. Set-up for drying of a single liquid droplet adapted from Souza (2020). Drying of a single droplet of FB1.100 and FB1.200 and in suspension (A) at T0; (B) at the end of the drying cycle.

The droplet image could be acquired with a monochrome camera (MB133USB, Sentech America, U.S.A.) with a resolution of 1290×960 pixels and attached to a zero-distortion macro lens (MC100, Sentech America, U.S.A.). The resulting association provides a field of vision of 4.8 mm ×3.6 mm, where each pixel has a dimension of 3.75 µm ×3.75 µm. All images and mass information are stored in software conceived for this experimental set-up.

The drying conditions kept for the TDST test were the following:

- Drying airflow rate of 4 L/min.
- Drying cycle of 1 hour. A volume of 6 μl of formulation FB1.100 and FB1.200 (100 mg/ml and 200 mg/ml of BSA respectively) was foreseen for each of the three replications per drying time. Before each drying test the solution was filtered (PES 0.22 μm).
- Drying temperature of 72°C with an absolute humidity of 3 g/kg

From experimental data previously obtained by SANOFI (data not shown) the mAb-A showed to be stable up to 65°C. As previously mentioned in Section 2.3.3.4, the temperature that the protein is submitted to during drying is found to be in between the outlet and the wet-bulb temperatures of the outlet drying air, which means 10–20°C below the outlet air temperature. During spray-drying this temperature was in the range of 20-30°C. The reason of the selection of a temperature of 72°C for the single droplet drying was that its wet bulb temperature, at an absolute humidity of 3g/kg, was around 28°C which was in the range of the conditions obtained in the spray-drying process.

At the end of the test, the dried drop was recovered from the stem of the glass filament and reconstituted as the powders produced by spray-drying.

An ANOVA single-factor analysis was performed (in triplicate), where the impact of the concentration variation on the protein aggregation was analysed. If $p<0.05$, for a variable it means that it has an impact on the aggregation output.

3.4.2.2 Spray-drying experiments

The lab scale spray drier model used was the Büchi Mini spray drier B-290 in a co-current configuration, using a two-fluid nozzle and an open loop configuration that used the air present in the room. A dehumidifier (Dehumidifier B-296, Büchi) was placed at the inlet of the drying and atomization gas tubes. The equipment was as well equipped with a HEPA filter

For these spray-drying tests, the formulation FB1 at different BSA concentrations, formulations FB1.100 and FB1.200, at 100 mg/ml and 200 mg/ml respectively, were spray-dried using two different nozzle diameters: 0.7 and 1.4 mm, which as a consequence represents a variation in the shear rate as shown on Table 3.7. All other parameters remained constant:

- liquid feed flow rate (LFFR) (4.5 ml/min),
- drying air temperature (T_{in}) of 105°C,
- relative humidity (RH) in a range of 20-27%
- drying airflow rate (22 m^3/h),
- spraying airflow rate (571 L/h).

Some relevant characteristics of the solution to be spray-dried such as the dissolved solid content, viscosity and density were measured. This information was used for the calculation of the pertinent measurements of shear stress and Reynolds number.

The methods used to measure dissolved solid content and viscosity were the same as those that will be described later for reconstituted solutions from spray-dried powders.

The solution density before spray-drying and after reconstitution was measured with a Mettler Toledo DM-40 densimeter, at 20°C. Use of 3 ml of a water standard with a density of 0.9982g/cm^3 at 20°c The operating principle is based on the oscillation of a U-shaped borosilicate glass tube (volume = 1mL) whose resulting frequency is directly proportional to the density of the liquid or gas injected. It has an integrated electronically controlled thermostat. The density is the physical quantity that characterizes the mass of a body per unit of volume. It was expressed in g/cm^3 in the international system.

The three main outlet parameters of interest from the spray drying process were moisture content of the powder, process yield and level of protein aggregation in the reconstituted BSA solutions.

Table 3.7.Spray-drying conditions used for drying formulations FB1.100 and FB1.200

		Inlet parameters			*Outlet parameters*	
Protein concentration [mg/ml]	**Condition**	**Nozzle diameter [mm]**	**Shear Strain**	**Shear Stress [mPa]**	**Tout [°C]**	**Twb [°C]**
100	SD 01	0.7	4.5	3.1	59	24
	SD 02	1.4	5.7	2.9	59	22
	SD 03	0.7	3.3	3.0	59	22
	SD 04	1.4	5.6	2.9	56	20
	SD 05	0.7	3.3	3.0	58	21
	SD 06	1.4	5.5	2.9	61	18
200	SD 01	0.7	2.7	2.8	48	24
	SD 02	1.4	4.6	2.8	51	23
	SD 03	0.7	2.7	2.8	53	23
	SD 04	1.4	4.7	2.8	52	17
	SD 05	0.7	2.6	2.8	50	22
	SD 06	1.4	4.6	2.8	50	17

3.4.2.3 Powder Characterization

(a)Moisture content

Karl Fischer was used to determine the residual water content in the spray-dried powder using a dry method. The Karl Fischer oven titration principle is based on the Karl Fischer reaction, which in the first step causes the methanol, sulfur dioxide and imidazole to react and provide imidazolium methyl sulphite. In the second step, the latter reacts with the water from the powder sample which is then evaporated using the oven and carried to the measurement cell using a nitrogen gas flow, and iodine, providing imidazolium methyl sulfate and imidazolium iodide (Popescu *et al.*, 2020; Aro *et al.*, 2020) (Figure 3.6). Each iodide molecule consumed corresponds to a molecule of water. The iodide is generated within the measurement cell, and quantified using a generator electrode via integration of electric current over time. A constant alternating current is maintained between these electrodes, the excess of iodine is indicated by a decrease in the measured voltage required for maintaining the current (Aro *et al.*, 2020). Equation 3.9 was used for the calculation of the final moisture content on the powder sample:

$$Moisture\ content\ [\%] = \frac{Reagent\ consumed \times Water\ per\ ml\ in\ the\ reagent}{mass\ of\ powder\ sample} \times 100 \qquad (3.9)$$

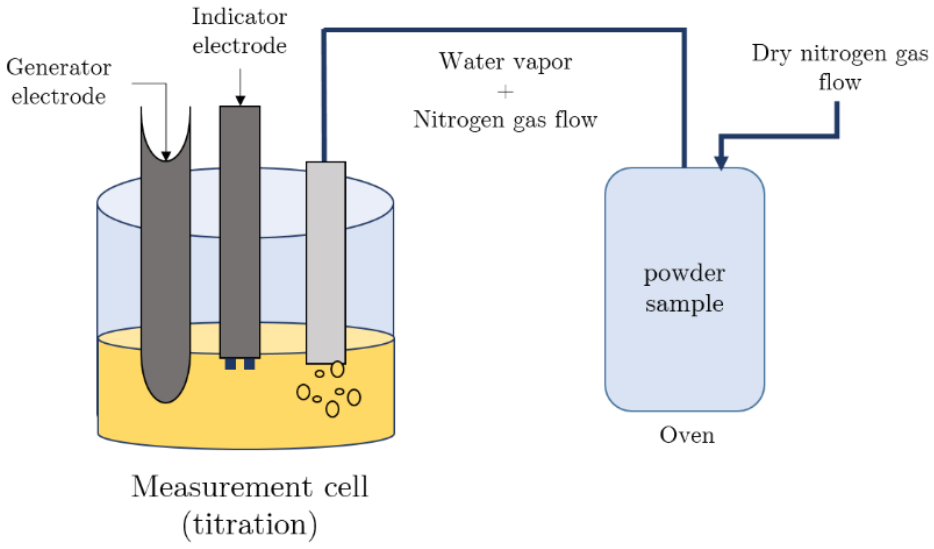

Figure 3.6. Karl Fischer oven titration set-up diagram for the measurement of the moisture content present in a powder sample with the use of an oven (Adapted from Aro et al., 2020).

The equipment used was an 851 Titrando from Metrohm. The oven temperature was set to 120°C and airflow was set to 80 mL/min. The drift needed to be below 20 µg of water/minute to start the measurement. The stop criterion was to have a relative drift near 15 µg of water/minute. Water content results were considered significantly different for differences equal to or more than 0.3\%. The reactants used were the HYDRANAL ™-Coulomat AG-OVEN (as the anolyte) and HYDRANAL ™ - Coulomat CG (as the catholyte). The equipment accuracy was verified at the beginning of the measurements with an HYDRANAL ™ Water Standard KF-OVEN (220-230°C).

(b)Particle Size Distribution

The particle size of the spray-dried powders was measured in a Mastersizer-3000 laser granulometer (Malvern Panalytical). A pre-dispersion of powder in isopropyl was prepared to have a final ratio of powder:isopropyl 5mg:3ml in the dispersion phase (isopropyl) of the equipment.

The detection of the sizes of particles, using laser diffraction, relies on Fraunhofer diffraction or the Mie scattering theory, which uses the scattered intensity of a particle measured at different angles to approximate a particle size (or distribution) ((Figure 3.7).

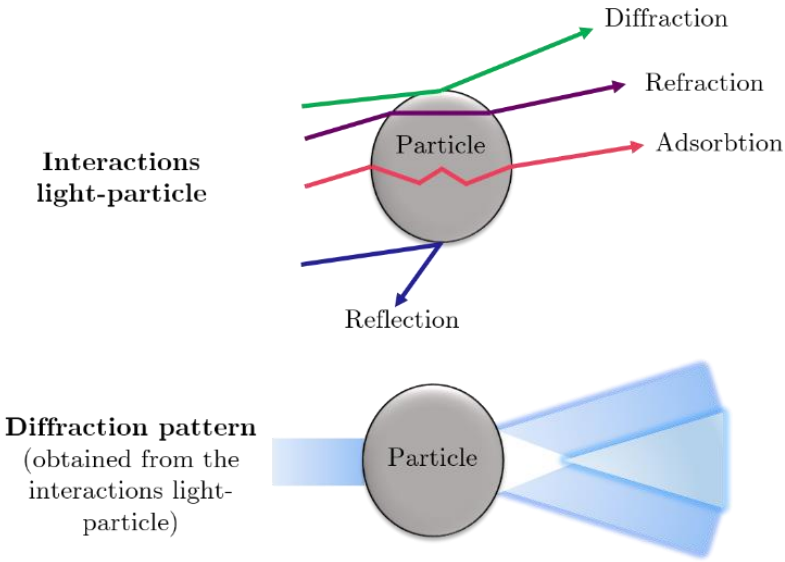

Figure 3.7. (top) Theoretical light interactions observed in laser diffraction, and (bottom) diffraction patterns of a plane wave scattering of a particle (adapted from H. Li et al., 2019).

(c)Scanning Electron Microscopy

Images from the spray-dried powder were taken with a scanning electron microscopy (SEM). This technique uses high-energy primary electrons beam on an electrically conductive sample, to avoid overcharging on the surface and thus a poor image outcome (Akhtar *et al.*, 2018). Then the sample release the secondary electrons (SEs) and an image can be formed by collecting these secondary electrons from each point of the specimen (Figure 3.8.). One of the requirements of SEM is to be done in a vacuum environment, given that any interactions of the primary electron beam with gas molecules will lower the image resolution (Zhou *et al.*, 2007).

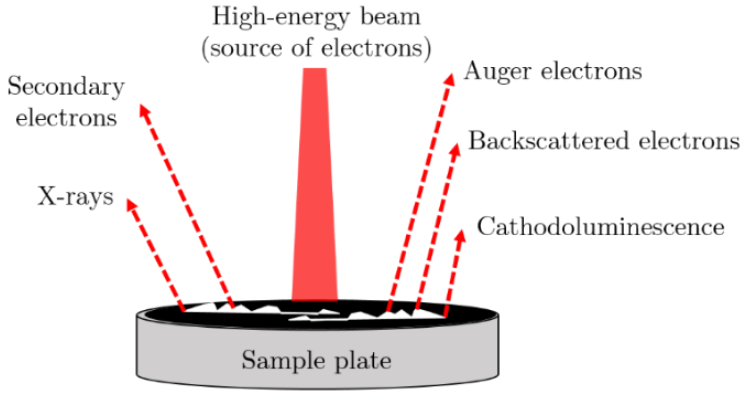

Figure 3.8. The interaction of the electron beam with the specimen and the signal emitted from the sample (adapted from Akhtar et al., 2018)

The non-conductive samples are usually sputter coated with a thin layer of carbon or metal (i.e. gold, platinum) that is able to reflect electrons (Akhtar *et al.*, 2018). Therefore, our powder samples were

previously coated with two layers of platinum using the Sputter Coater Polaron SC7640, using argon gas, a current of 19 mA and a vacuum of 8.6 x 10^{-2} mbar. The coated powder images were then captured using a SEM Nova NanoSEM 450 from ThermoFisher (FEI),a high-resolution SEM with FEG tip with field emission. Samples were observed with a resolution of x5000.

(d)RAMAN Spectroscopy

Raman mapping was done using using a Raman confocal microscope Alpha 300 AR (WITec, Germany) Surface and depth analyses were performed, using the 532 nm wavelength laser and integration times of 0.05 seconds, and tests were conducted at room temperature. The operating parameters for each scan are detailed in Table 3.8.

Raman spectroscopy is one of the vibrational spectroscopic analyses that allows the determination of molecular structure. The vibrational properties of molecules induced changes in the wavelength of the light scattered in the sample (Jones *et al.*, 2019; Bumbrah et Sharma, 2016)

This technique is able to qualitatively detect the presence of a component by measuring the frequency of scattered radiations, while quantitative analysis can be performed by measuring the intensity of scattered radiations (Bumbrah et Sharma, 2016).

Its principle (shown in Figure 3.9) is as follows:

The sample is illuminated with a monochromatic laser beam that interacts with the sample and produces a scattered light, which has a different frequency from the incident light. This new scattered light is used to build the Raman spectrum based on the principle of the Rayleigh scattering (Jones *et al.*, 2019).

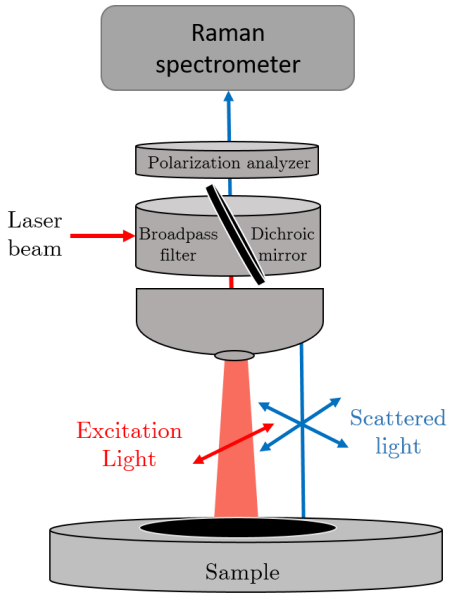

Figure 3.9. Set-up diagram of the RAMAN spectrometer for the detection of components on solid samples (powder, dried particles) (adapted from Jones et al., 2019)

Table 3.8. Operating data resulting from Raman spectroscopy on spray-dried powder (SD) and particles generated from the TDST samples

	Powder sample (SD)	Particle (TDST)
Scan Surface image	1 scan de 12*12 µm (001) 1 scan de 6*6 µm (004)	Numerous analyses taken with WiTec Alpha 300AR and Alpha 300R, 532 nm and 785 nm laser but no spectra obtained
No. of points/line and no. of lines/image	001: 72 et 72 004: 36 et 36	
Scan Image in depth	1 scan de 12*10 µm (002) 1 scan de 4,3*6 µm (005)	
No. of points/line and no. of lines/image	002: 72 et 60 005: 24 et 36	

3.4.2.4 Reconstituted solution from spray-dried powders

(a) Reconstitution protocol

Reconstitution of the powders can be affected by different properties such as wettability, dispersibility and solubility (Fournaise *et al.*, 2020).

To reconstitute the spray dried sample a volume of milli-Q water was added to achieve the initial solution concentration for protein and excipients. Then the suspension was placed in an orbital shaker UniShaker 25 (LLG Labware) for 90 min at 70 rpm. The characterization of the produced powder consisted of moisture content measurement and particle size distribution.

Our work was not oriented to the optimization of the reconstitution characteristics, therefore the protocol selected was mainly based on the previous SANOFI selected parameters (Orbital shaker, 70 rpm), the reconstitution time corresponded to the time that the reconstituted solution reached a homogeneous state.

(b) Protein Concentration

Proteins are known to have a characteristic ultraviolet (UV) absorption spectrum around 280 nm, due to the aromatic amino acids tyrosine and tryptophan. The concentration of a protein can be estimated from a linear concentration plot using the absorbance, but if its molar extinction coefficient is known then the Beer–Lambert law can be used to accurately quantify the amount of protein (Noble, 2014; Mckechnie *et al.*, 2018).

A spectrophotometer (Agilent Cary 8454) was used to measure the protein concentration at 280 nm using in a quartz cell, using an extinction coefficient of 1.55 $ml.\ mg^{-1}cm^{-1}$. The blank used was milli-Q water.

(c) Viscosity

Solution viscosity was measured using a Brookfield AMETEK Low-Range Viscometer, 100 to 240 VAC (spindle 61) at a temperature of 22°C in a range of 50 to 100 rpm, using a volume of solution of 60 ml.

The rotational viscometer used measures the torque (M) when the spindle rotates in the sample solution at a constant speed, shearing the fluid. In our case, the spindle system is a concentric cylindrical system (Kurkin *et al.*, 2020).

When in motion the equipment measures the torque, product of a force and the perpendicular distance, known as moment arm, to the axis of rotation. Where R_b corresponds to the radius of the inner cylinder (spindle), and R_c corresponds to the radius of the outer cylinder container (Figure 3.10) (Melito and Daubert, 2017).

The calculation of the shear stress (σ_b) generated at the inner cylinder surface is shown in Equation 3.10. One important assumption for this calculation is that the inner cylinder surface is the boundary of the fluid, thus assuming that a thin layer immediately adjacent is moving at the same velocity (Melito and Daubert, 2017; Kurkin *et al.*, 2020).

$$\sigma_b = \frac{M}{2\pi R_b^2} \qquad (3.10)$$

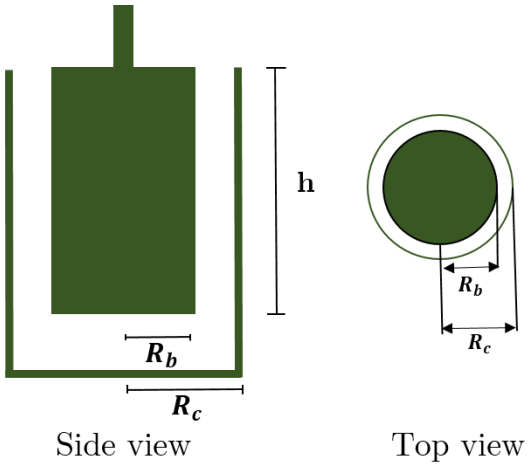

Figure 3.10. Set-up of a rotational viscometer, where the Rb corresponds to the radius of the spindle (inner cylinder) and Rc corresponds to the radius of the outer cylinder container (Adapted from Melito and Dauber, 2017)

(d) Assessment of the presence of aggregation in a protein solution

For the study of the types of aggregate populations (as a result from the stresses generated by spray-drying) in the reconstituted solution, there are many orthogonal techniques that can be applied, as will be further discussed in Chapter 5. However, for an initial assessment of the presence of aggregation in

a protein solution, techniques such as turbidity and dynamic light scattering which are straight forward and accessible, were the two techniques used in this study.

(d.1) Turbidity

The turbidity, described as an opalescence of the solution, is an optical manifestation of light scattering, and it has been correlated with undesirable outcomes of biopharmaceutical solutions, among which, protein aggregation is included (Barros *et al.*, 2021). The causes of turbidity are complex protein-protein interactions, due to changes in pH, temperature, protein concentration and stresses.

The turbidity assessment is usually accompanied by the optical inspection of the formulation. Nevertheless, the optical inspection is usually user dependent which is not a quantitative assessment of the opalescence of a solution. A common technique used to measure turbidity quantitatively is by measuring the absorbance with a spectrophotometer at wavelengths at which the attenuation of the light beam is essentially due to scattering and adsorption is negligible (Figure 3.11) (Ndoye *et al.*, 2013, Giroux *et al.*, 2010)

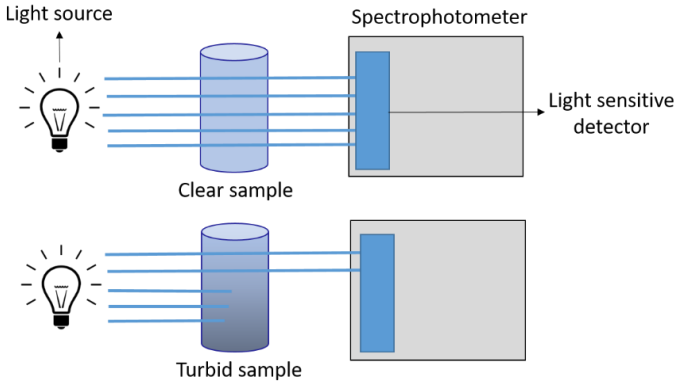

Figure 3.11. Diagram of turbidity measurement by the use of a spectrophotometer

After measuring the absorbance of the samples using the spectrophotometer, the values obtained can be transformed into nephelometric turbidity units (NTU). The NTU are based on the turbidity of a primary reference standard of formazin, which is a polymer that precipitates after mixing aqueous solutions of hydrazine sulphate and hexamethylenetetramine, and they are used to report opalescence (Barros *et al.*, 2021; Münzberg *et al.*, 2016). The absorbance of the formazine standards, already linked to an NTU value, is linearized to obtain an equation that allows for the conversion of the measured absorbance of the samples into NTU.

The turbidity of the samples was quantified by measuring the absorbance at 600 nm using a Varioskan LUX Multimode Microplate Reader from Thermo Fisher Scientific. A calibration curve was obtained using calibrated formazin standards. Reference suspensions I, II, III and IV have values of 0.1 NTU, 3 NTU, 6 NTU, 18 NTU and 30 NTU respectively. Pharmacopoeia opalescence degrees are denoted as I (until 3 NTU), II (from 3 to 6 NTU), III (from 6 to 18 NTU), IV (from 18 to 30 NTU). For each sample, two wells filled with 200 µL were analysed (n = 2). The turbidity of each sample was calculated from the calibration curve and given in nephelometric turbidity units (NTU).

(d.2) Dynamic Light Scattering (DLS)

The principle of measurement is as follows: in solution, particles (i.e., aggregates), micelles and molecules present a phenomena known as Brownian motion, which refers to the arbitrary zig-zag motion caused by collisions with solvent molecules, which are arbitrarily moving as well. The velocity of particles, undergoing Brownian motions, is proportional to the particle mass, and it can be represented as the product of size and density. (Uskokovic, 2012). The set-up of the DLS equipment is given in Figure 3.12.

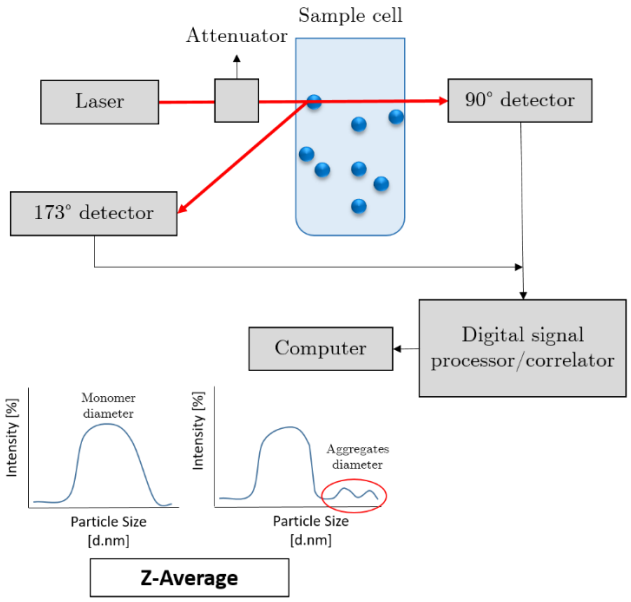

Figure 3.12. Dynamic Scattering set-up diagram for the detection of aggregates using laser scattering techniques (Adapted from Maguire et al., (2018)).

The basis of Dynamic Light Scattering (DLS) relies on the principle of retrieving information on the diffusion and size properties of dispersed particles in suspension in Brownian motion (Uskokovic, 2012). An analysis of the intensity fluctuations that result from the Doppler effect when particles undergo Brownian motion retrieves the particles velocities and, thus, the particle size from the Stokes-Einstein relationship. Through this equation it is possible to calculate the hydrodynamic radius of the particle, it is also known as Z-average and can be expressed as the radius or diameter. It corresponds to a sphere that diffused at the same rate as the molecules in suspension (Uskokovic, 2012). Changes in the Z-average value indicate the presence of aggregates in the formulation, usually at larger values than the ones corresponding to the stable molecule Z-average.

In the reconstituted protein solution. DLS was performed on a Zetasizer Nano (Malvern, Herrenberg Germany) as follows: 60 µl of the BSA solutions, diluted at 1 mg/ml, were analysed in plastic cuvettes at 25°C using the automatic mode for identifying the best number of sub-runs and measurement time (n=3). The z-average diameter (Z-Ave) was calculated from the correlation function using the Dispersion Technology Software version 6.01 (Malvern, Herrenberg, Germany).

3.5 Results and Discussion

3.5.1 Decoupling of spray-drying stresses

3.5.1.1 Shear Stress Test (SST)

Usually, the hydrodynamic diameter of BSA is dependent on the protein concentration in solution (Borzova *et al.*, 2014). For our two working concentrations, the values of Z-average (hydrodynamic diameter, d.nm, measured by DLS) before spraying were in fact slightly different, 4.5 d.nm for FB1.100 and 5.5 d.nm for FB1.200 (Figure 3.13).

After spraying the Z-average values showed that at 100 mg/ml the protein seems to not be really affected by the shear forces, while for a concentration of 200 mg/ml a slight increase in hydrodynamic diameter is observed (Figure 3.13). A higher presence of proteins in the solution at the moment of spraying is more prone to lead to a higher interaction phenomena leading an increase of the protein aggregation, as observed in our results.

From the ANOVA two-factor analysis the concentration was showed to have an impact on aggregation during the shear stress test ($p<0.05$), while the nozzle size showed no correlation to the aggregation phenomena ($p>0.05$).(data shown in graph Table 3.24 in Section 3.7 – APPENDIX) The shear stresses conditions, generated at the same liquid feed flow rate (4.5 ml/min) but with different nozzle diameters, in the order of 10^3 [Pa], were close enough to not generate a different response on aggregation within the same BSA concentration.

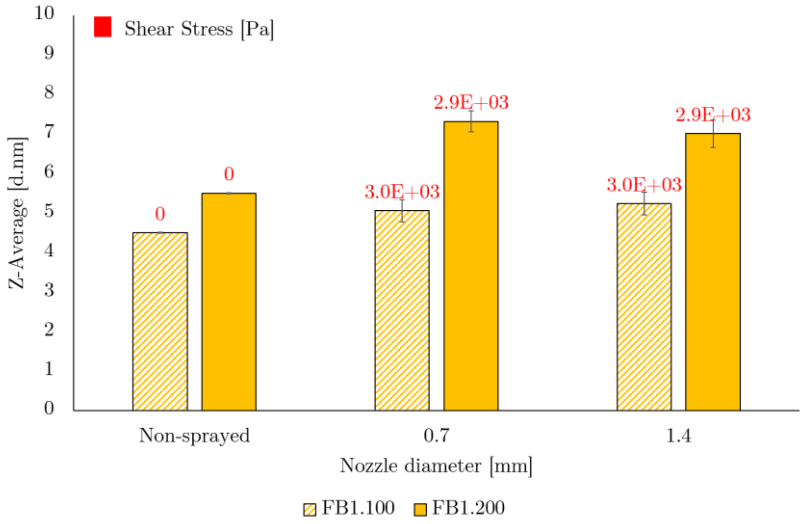

Figure 3.13. Effect of shear stress (where the non-sprayed have a shear stress of 0) on the aggregation level (Z-average, measured by DLS), in the formulation FB1.100 and FB1.200 sprayed through the nozzle device of the Büchi Mini Spray Dryer B-290 (n=3)

A study conducted by Dobson *et al.*, (2017), where they tested the impact of the shear forces generated in a capillary set-up on BSA aggregation, reported that different shear rates (order of 10^4 [s^{-1}]) did not generate significant changes in protein aggregation, when at lower than 50 passages on the capillary

system. On the other hand, when increasing the passages after the first 50, the aggregation increased proportionally. This phenomenon was explained as a result of the shear strain, which is the time of exposure of the protein to a certain shear rate. This suggested that the protein must be exposed to the shear forces for a certain time in order to achieve a certain level of damage before starting unfolding.

In the case of a lab-scale spray-dryer, the shear strain, is a parameter that is not often variated given that it was linked to the specific geometry of the nozzle used. The residence time in the nozzle was short and multiple passages might be required to generate a real impact on the protein denaturation at shear rates generated in the operating conditions used.

The protein might have sufficient time to denature while flowing at lower shear rates given that the shear strain is higher, while at higher shear rates exposure time may not be enough (Jaspe & Hagen, 2006).

3.5.1.2 Thermal and Dehydration Stress Test (TDST) with a single drying droplet set-up

The drying kinetics observed for the droplets correspond to two different formulations FB1.100 and FB1.200 is shown on Figure 3.14. To assure a higher reproducibility of the single drying droplet technique, both droplets had similar weights, 0.0065 gr for FB1.100 and 0.0064 gr for FB1.200. The drying curves have a similar drying kinetics rate behavior by looking at the period under 250s. From the initial volume used, the theoretical final dried particle corresponding to FB1.100 should be at a mass of 0.00053 gr, while for FB1.200 the dried particle should be at 0.0014, which corresponds to the value of the final drying curve plateau.

The formulation with the higher solid content (x_{sol}=0.2), which is FB1.200, had the first solid appearance at t=21s and reached the theoretical dried particle value around t=300s, while for FB1.100 the first solid appeared at t=57s and reached the theoretical dried particle value at around t=500-600s, which corresponded to the difference in water percentage present in the droplet, higher for FB1.100. with a value of 90%, while for FB1.200 a value of 80% was achieved.

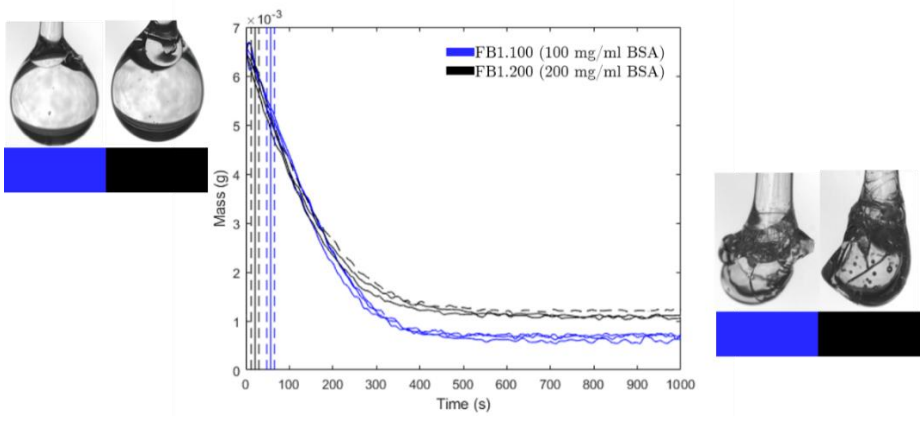

Figure 3.14. Evolution of the droplet mass during droplet drying (drying cycle of 1h): - the vertical lines indicate the time the first solid appeared for FB1.100 (blue, at 57s) and FB1.200 (black, at=21s) (n=3).

Results reported in Figure 3.15, indicate that the thermal stress induced during the TDST led to protein aggregation. This extent of denaturation at both BSA concentrations, was higher than the one encountered in spray-drying, as expected due to exposure time to the thermal stress of BSA.

During the TDST, the exposure time is considerably longer than the ones experienced during spray-drying, while the wet bulb temperature, associated to the temperature that the protein is really exposed to during drying is similar between both methods at around 30°C. The denaturation temperature of BSA has been reported to be approximately 55°C (Taha *et al.*, 2015). The conditions proposed here were selected to observe the behavior of the BSA in denaturation conditions under drastic thermal stress. Furthermore, the single ANOVA factor analysis ($p>0.05$) showed that concentration did not have an impact on the aggregation during these drying conditions (Table 3.25 in Section 3.7)

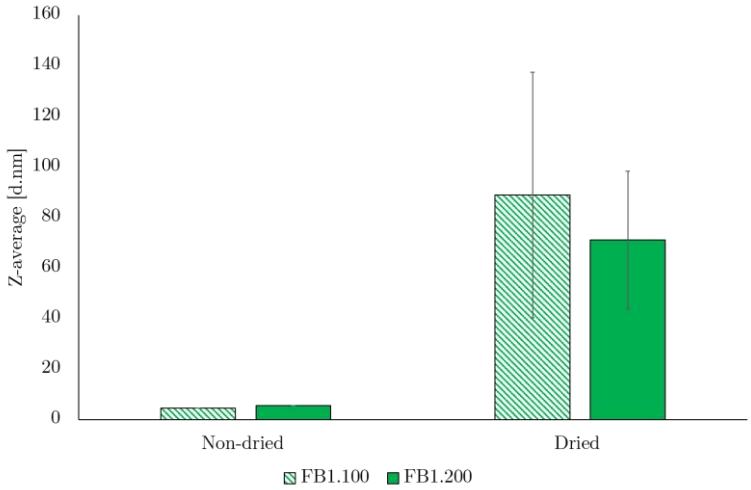

Figure 3.15. Effect of drying conditions on the aggregation level (Z-average measured by DLS) of dried droplets (TDST) of BSA formulation FB1.100 and FB1.200 (n=3)

When retrieving the dried particles from the glass filament they can be broken, as shown on Figure 3.16a. However, independently from the BSA concentration, the particles had similar morphologies (as shown in Figure 3.14 at the right side of the figure). A full view of the droplet morphology and surface texture is found in Figure 3.16b.

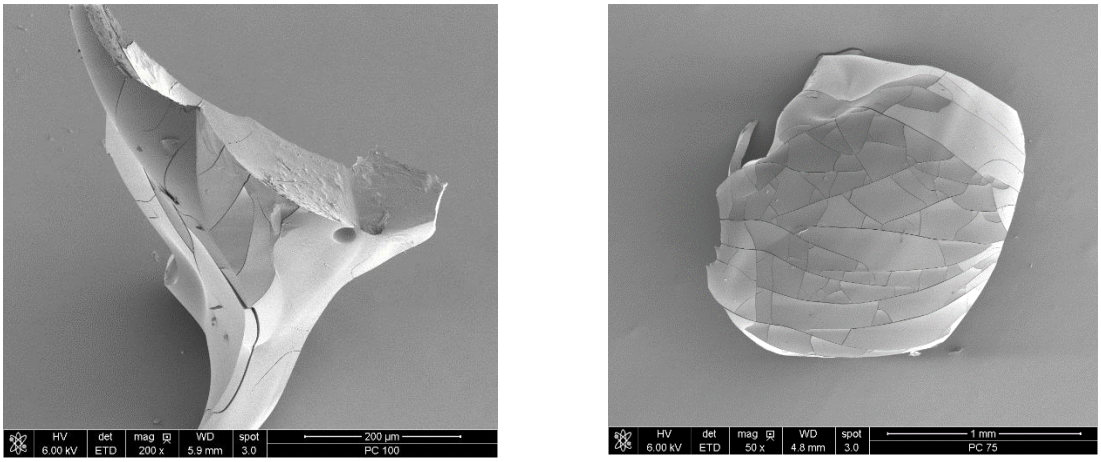

(a)

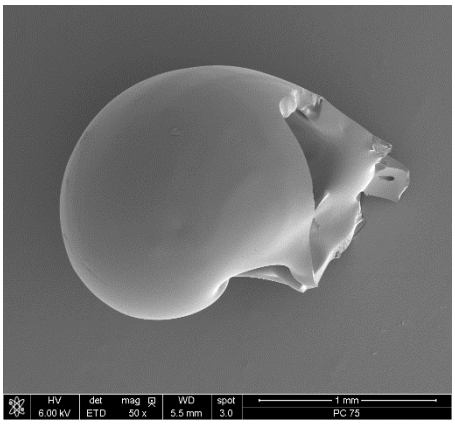

(b)

Figure 3.16. SEM Image of the dry particles produced in the TDST through the single drying droplet technique for formulations (a) FB1.100, all samples were broken upon recovery, and (b) FB1.200.

3.5.2 Coupling of shear and thermal/dehydration stresses during spray-drying: effect on FB1.100 and FB1.200

3.5.2.1 Spray-drying tests

An initial screening of different spray-drying inlet operating conditions, including: inlet temperatures (90-180 °C), liquid feed flow rates (2.5, 3.6, 5.0 ml/min) and nozzle diameters (0.5, 1.4, 2.0 mm) was performed at different concentrations of BSA (100, 150, 200, 250 mg/ml). The results (not shown here) did not present a clear correlation of the impact of the inlet parameters on the measured outlet parameters (moisture content, yield and aggregation). Nevertheless, the conditions that seemed to yield the best results were selected for the spray-drying of this section. The fixed conditions were the inlet temperature (105°C), the liquid feed flow rate (4.5ml/min), the atomization gas flow rate (571 L/h) and the drying gas flow rate (22 m^3/h), while the variating parameters were the nozzle diameters (0.7 mm and 1.4 mm). The two nozzle sizes were selected to observe if the change of the droplet size at a fixed

temperature and liquid feed flow rate, was relevant enough to allow a selection of better outlet conditions of the process and the spray-dried powder (yield, moisture content and protein aggregation.

From the results obtained from the SST, the TDST and the spray-drying (SD) process, it was possible to observe again that the shear stress alone, in the SST, was not sufficient to create a high instability on the non-formulated BSA and therefore an increase in aggregation, compared to when it is coupled with the thermal/dehydration stresses during spray-drying (Figure 3.17). The thermal stress (more drastic in TDST) mainly showed that at two different protein concentrations the aggregation is high and very similar.

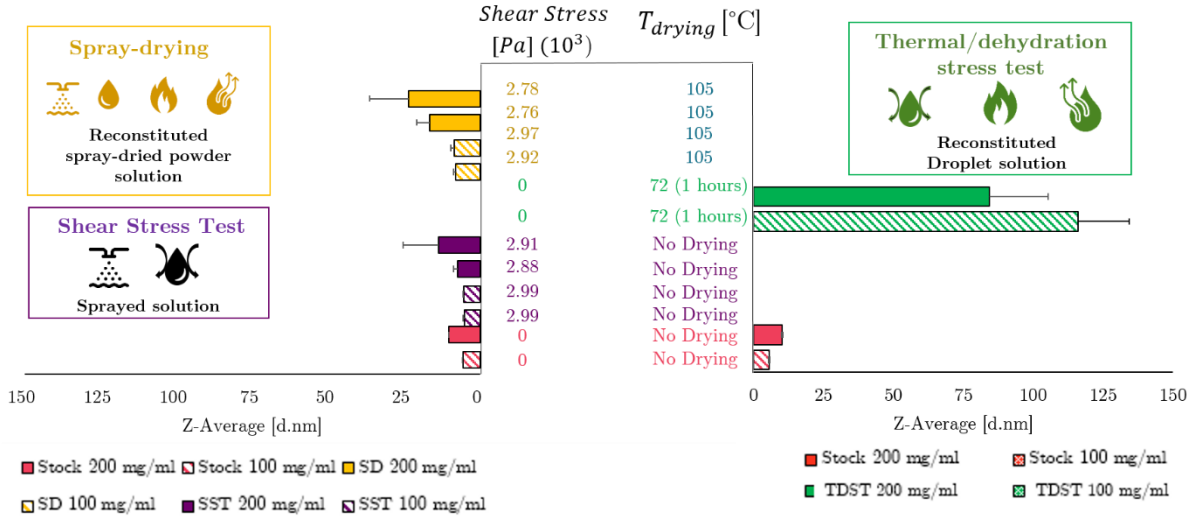

Figure 3.17. Aggregation resulting from the decoupling of shear (SST) and thermal/dehydration (TDST) stresses on BSA formulation FB1.100 and FB1.200 The yellow bars (left top side of the graph) correspond to the results of coupled stresses of the spray-drying process, which can be compared to the decoupled stresses: purple bars corresponding to shear stress (left bottom side of the graph) and green bars corresponding to the TDST (right side of the graph). The red bars on the left and right side of the graph corresponds to the stock solution, which was not exposed to any stress (n=3).

The moisture content % of the powder right after spray-drying (Figure 3.18) showed very similar values for both BSA formulations (FB1.100 and FB1.200) at the two nozzle sizes. This study intended to study the presence of water immediately after the spray-drying process, as well as the protein aggregation at that point, therefore no further secondary drying was performed. As verification, the ANOVA two-factor analysis indicated that the moisture content was not influenced by the protein concentration or the nozzle diameter ($p>0.05$).

As mentioned in Section 3.3.3, the process yield depends highly on the temperature and the liquid feed flow rate, as well as the solid fraction of the solution to be spray-dried. In our case, the only parameter among those impacting the yield % was the protein concentration. Higher yields were obtained for the lower protein concentration (100 mg/ml – FB1.100) (Figure 3.19). Further tests, using a larger protein concentration range, will be required to verify the cause behind this behavior.

In addition, the ANOVA two factor results showed that for the process yield, nozzle diameter does not seem to have a statistical impact ($p>0.05$), while the protein concentration seems to have a statistical impact on this output variable ($p<0.05$) (Table 3.26 in Section 3.7 – APPENDIX)

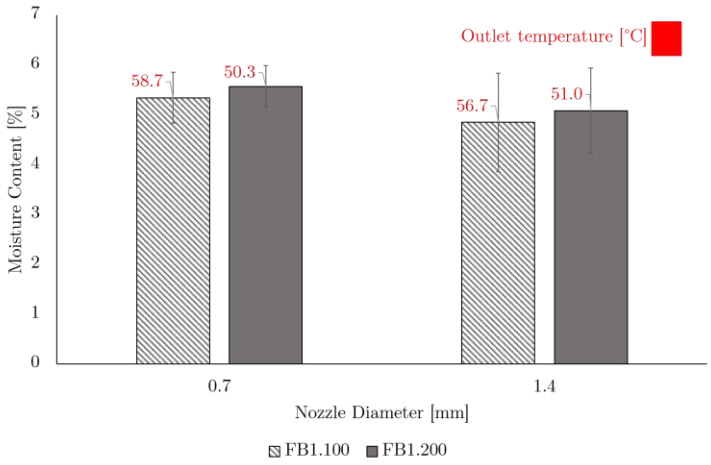

Figure 3.18. Results of moisture content % on the powder obtained by spray-drying in a Büchi Mini Spray-Dryer B-290 for samples FB1.100 and FB1.200 from the spray-drying process, at an inlet temperature of 105°C (n=3).

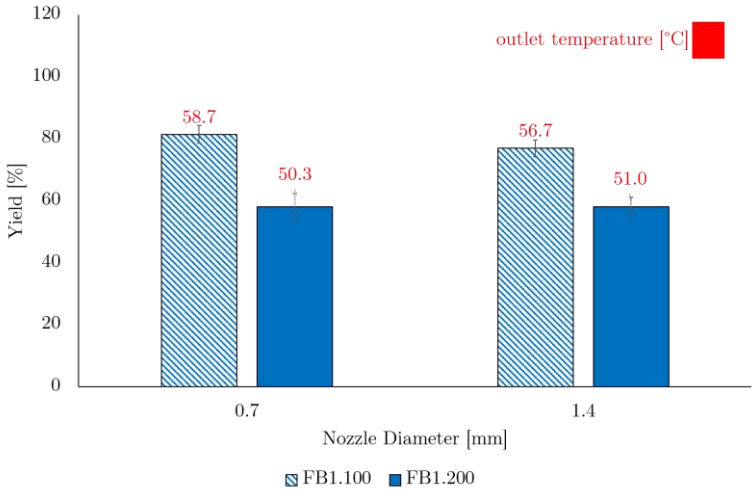

Figure 3.19. Spray-drying process yield [%], in a Büchi Mini Spray-Dryer B-290, for formulations FB1.100 and FB1.200, at an inlet temperature of 105°C (n=3).

Finally, the concentration of the protein seems to have an impact on the aggregation given by Z-average ($p>0.05$). On the other hand, nozzle diameter/liquid feed flow rate do not appear to impact the aggregation of the protein ($p>0.05$). The protein interactions without any excipients are more prone to exist, given that there are no electrostatic repulsion forces that avoid their interactions. This is seen more at higher protein concentrations, which is the case observed in Figure 3.20

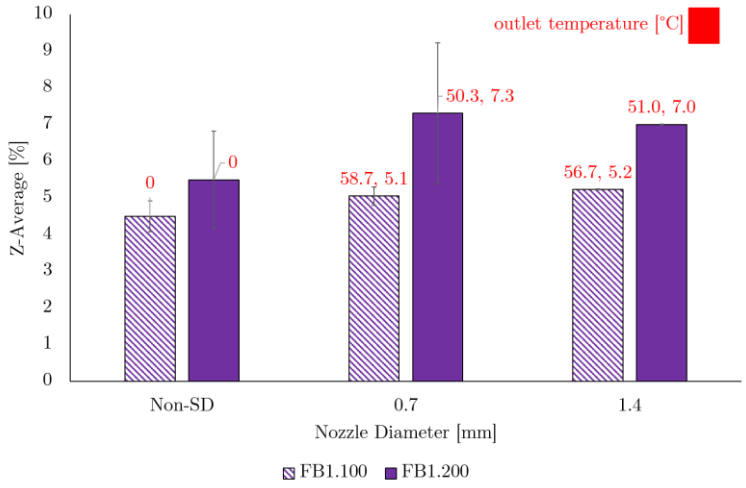

Figure 3.20. Z-average value as a measurement of aggregation of a protein during spray-drying, measured in the reconstituted solution from the spray-dried powder of FB1.100 and FB1.200 (n=3).

One of the major advantages associated with DLS is the high sensitivity towards small quantities of aggregates (Bansal *et al.*, 2019), which was very useful to detect the presence of aggregation at the different stress conditions. On the other hand, the DLS is unable to determine the amount of each of the different aggregated species individually. At higher molecular weights, the sensitivity of the technique increases, and thus can help in detecting even tiny quantities of very large aggregate molecules (Maguire *et al.*, 2018; Bansal *et al.*, 2019). Therefore, orthogonal techniques are proposed for a further study of the different populations of aggregates present in the reconstituted solution from spray-dried powder.

Raman analysis of the spray-dried powder:

The interest in applying Raman spectrometry was to detect if there was degradation of the BSA structure at the surface of the spray-dried particles, corresponding to the solution fraction that is in contact with the drying-air.

Two spray-dried powders produced from the liquid formulations, FB1.100 and FB1.200, were analysed using surface and depth scanning, for which the only difference was the BSA concentration, of 100 mg/ml and 200 mg/ml respectively. As a reference, a non-spray-dried (non-SD) BSA spectrum, previously retrieved, was used to compare the degradation present in the spray-dried powders.

For formulation FB1.100, the corresponding clusters images (left) and spectra (right) for the (a) surface and (b) depth scanning analysis can be seen in Figure 3.21 and Table 3.218. The clusters 1 and 2 obtained from the surface scan 007 have a very similar spectra, corresponding to the presence of BSA molecules (Figure 3.21a). However, due to background noise on cluster 2 (blue line), generated by the sample positioning, only cluster 1 (red line) was considered for comparison to the reference spectrum of the non-SD BSA, for which results are shown in Table 3.9. For the depth scan 008 (Figure 3.21b) just cluster 1 was recovered.

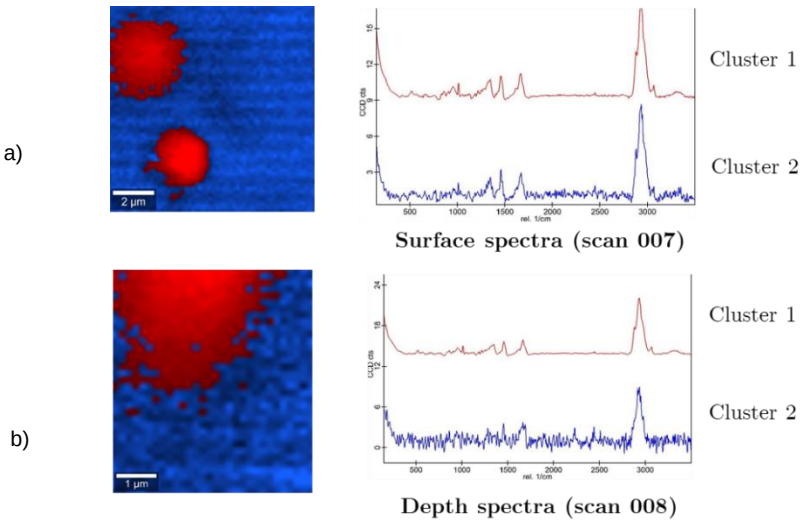

Figure 3.21. . Raman spectroscopy results for formulation FB1.100, expressed as a relationship between CCD (charge-coupled device counts) and Raman shift in wavenumbers (rel. 1/cm) corresponding to a) scan 007, surface cluster image (left), and surface spectrum (right), b) scan 008, depth cluster image not available (left) and depth spectrum (right). The cluster 1 (red line) in the surface and depth spectra corresponds to the red zones in both corresponding images, same for the blue line in the spectra, corresponding to cluster 2.

Table 3.9. Data on the correspondence of the spectra of the samples FB1.100 to the non-SD BSA from the reference database.

Scan	***Analysis***	***Cluster***	**SD FB1.100 correspondence to spectra of non-SD BSA [%]**
007	Surface	1	98
008	Depth	1	96

Figure 3.22 presents the comparison between the spectrum of surface scan 007, corresponding to the spray-dried formulation FB1.100, and the scan of non-SD BSA, having a correspondence of about 98%. In the depth scan 008, the correspondence % between the spray-dried and non-SD BSA is high as well.

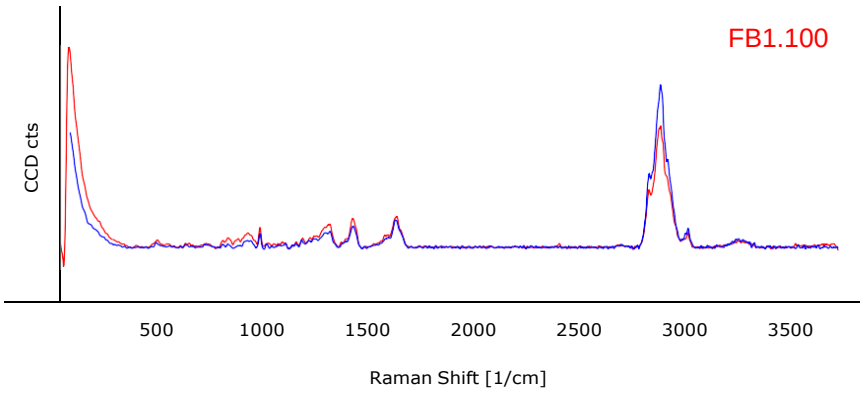

Figure 3.22. . Comparison of the spectra of non-SD BSA (blue line) against the spray-dried BSA of FB1.100 (red line), expressed as a relationship between CCD (charge-coupled device counts) and Raman shift in wavenumbers (rel. 1/cm)

Figure 3.23 corresponding to Table 3.21 FB1.200, shows the corresponding clusters images (left) and spectra (right) for the (a) surface and (b) depth scanning analysis. For the surface scan 004 just the cluster 1 (Figure 3.23a) was compared to the non-SD BSA (due to high background noise on cluster 2). While in Figure 3.23b, both clusters of depth scan 005 were viable to be compared to the non-SD BSA, observable in the homogeneity of the cluster zones (1 and 2) . The correspondence % of the spectra of FB1.200 from the surface and depth scanning is shown in **Erreur ! Source du renvoi introuvable.**.

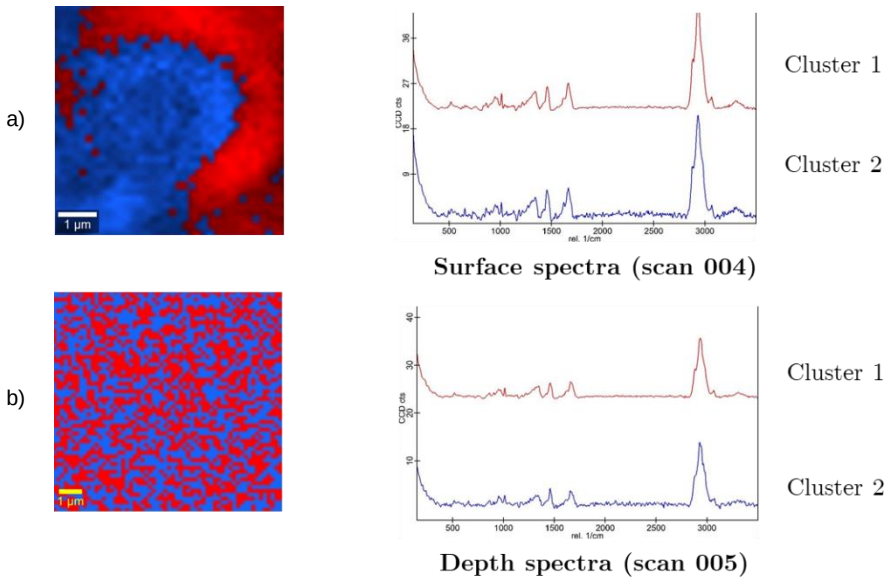

Figure 3.23. Raman spectroscopy results for formulation FB1.200, expressed as a relationship between CCD (charge-coupled device counts) and Raman shift in wavenumbers (rel. 1/cm). Corresponding to a) scan 004, surface cluster image (left), and surface spectrum (right), b) scan 005, depth cluster image (left) and depth spectrum (left). The cluster 1 (red line) in the surface and depth spectra corresponds to the red zones in both corresponding images, same for the blue line in the spectra corresponding to cluster 2.

In Figure 3.24 we can observe the comparison between the spectrum of scan 004 to the scan of non-SD BSA, with a correspondence of about 98% on the particle surface.

Table 3.10. Data on the correspondence of the spectra of the samples FB1.200 to the non-SD BSA from the reference database.

Scan	***Analysis***	***Cluster***	**SD FB1.100 correspondence to spectrum of non-SD BSA [%]**
004	Surface	1	98
005	Depth	2	95
		1	96

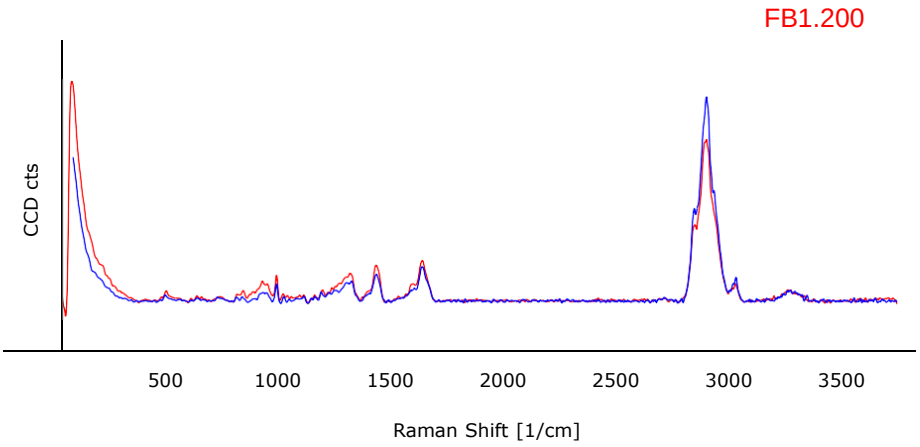

Figure 3.24. Comparison of the spectra of non-SD BSA (blue line) against the spray-dried BSA of FB1.200 (red line). Expressed as a relationship between CCD (charge-coupled device counts) and Raman shift in wavenumbers (rel. 1/cm)

Both formulations (FB1.100 and FB1.200) have very similar spectra and a high spectrum correspondence to the non-SD BSA, of around 95.5% and 95.0% for a concentration of 100 mg/ml and 200 mg/ml respectively (**Erreur ! Source du renvoi introuvable.** and Table 3.9). Nevertheless, there are small molecular changes detected which are also in the same proportion for both formulations,

The changes are suggested to belong to side chains modifications, among these changes we find:

- Shift in Amide I (1665 cm^{-1} and 1665 cm^{-1}), corresponding to α-helix.
- Shift in peaks 1672 cm^{-1} et 1674 cm^{-1}, corresponds to β-sheets
- Presence of a peak at 1348 cm^{-1}, from the deformation of C-C_{alpha}-H and stretching of C_{alpha}-C.
- Presence of double peaks at 1270 cm^{-1} and 1280 cm^{-1}, corresponding to the Amide III for the alpha-helix.

The presence of the changes detected by Raman might be an indicator of the reason for the aggregation detected in the Z-average measurement. Nevertheless, it is important to note that these modifications are just measured in the exterior of the particle and at a certain depth (4-10 µm), which means there can be other molecules of BSA with modifications throughout the dried powder particle. Therefore, Z-average values may vary from the results of the Raman spectroscopy analysis.

Powder physical characteristics

Powder granulometry (Table 3.11), is dependent on the nozzle sizes and concentration used. The bigger the diameter of the nozzle the bigger the particle size, and the same for the concentrations of BSA. However, these differences with respect to particle size are not outstanding.

Table 3.11. Particle size distribution for the spray-dried powders belonging to formulations FB1.100 and FB1.200 at two different nozzle sizes.

		Particle Size Distribution [µm]		
	Nozzle Diameter [mm]	*Dx (10)*	*Dx (50)*	*Dx (90)*
FB1.100	0.7	1.0	4.5	11.1
	1.4	1.1	6.3	15.7
FB1.200	0.7	1.0	4.5	11.1
	1.4	1.3	7.3	17.2

The morphology of BSA is very similar for both formulations, with surfaces that look smooth, and some dimpled particles as well (Figure 3.25).

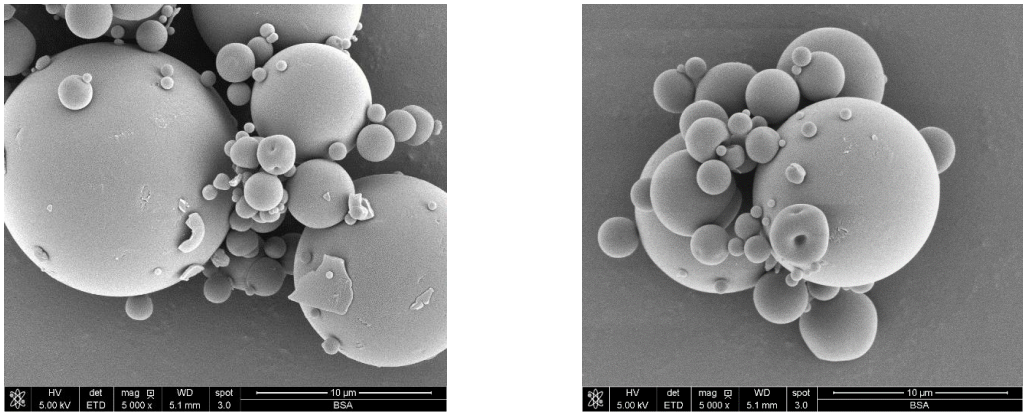

Figure 3.25. SEM images of the spray-dried powder obtained for formulations FB1.100 (left) and FB1.200 (right), observed at a focus of 5000x.

3.6 Synthesis Chapter 3

From the results obtained in this chapter on the decoupling of shear and thermal/dehydration stresses, we observed that the shear stress generated using the conditions of a lab-scale spray-dryer does not create high levels of aggregation on BSA. In addition, the BSA formulation did not contain any stabilizer in, hence, even without any protection the shear stress seems not to be relevant on the protein denaturation phenomena.

The reconstituted spray dried non-formulated BSA showed a slightly higher aggregation, at both concentrations, than the one obtained in the shear stress test, indicating that a possible synergistic effect on the protein denaturation activation is occurring when both stresses (shear and thermal/dehydration) are present.

When the BSA was exposed to a drastic thermal stress, which means that is not the typical thermal stress that will be generated during a spray-drying process, it showed a higher aggregation status for both concentrations of BSA. A lack of protection mechanisms against thermal/dehydration stresses in this formulation, where no excipients were present, might be the suspected cause for this behavior.

The results from this study have confirmed that high temperatures and lack of excipients were responsible for an increase in aggregation. From the literature review it seems that the addition of certain stabilizers will allow a better control (reduction) of the level of protein aggregation in the conditions used in a lab-scale spray dryer.

The following studies will start from formulations containing excipients to better protect the protein of our interest from the coupled stresses found in the spray-drying process.

3.7 APPENDIX Chapter 3

Shear rate, shear stress and shear strain from Shear Stress Test (SST) (FB1.100 and FB1.200)

Table 3.12. Data used for the calculation of the shear rate values of the shear stress test at different operating conditions in a Büchi Mini Spray Dryer B-290 of formulation FB1.100.

		Ml	**Mg**	**d**	**d**	**QL**	**QG**	**Dneedle**	**Din,liq**	**Dex,liq**	**Dgas**	**Aliq**	**Agas**	**VL**	**VG**	**Vav**	**gamma**
		[kg/s]	[kg/s]	[kg/m3]	[kg/m3]	[m3/s]	[m3/s]	[m]	[m]	[m]	[m]	[m2]	[m2]	[m/s]	[m/s]	[m/s]	[1/s]
Condition	Nozzle [mm]	*mass flow liquid*	*mass flow gas*	*density*	*density*	*volumetric flow liquid*	*volumetric flow gas*	*Diameter center needle*	*Inner Diameter liquid*	*External diameter liquid*	*Inner diameter gas*	*Cross-Sectional area liquid*	*Cross-Sectional area gas*	*liquid velocity*	*gas velocity*	*average velocity*	*Shear Rate*
SST 01	0.70	5.8E-05	1.9E-04	1000.00	1.20	5.8E-08	1.6E-04	6.3E-04	7.0E-04	1.2E-03	1.5E-03	7.3E-08	7.2E-07	0.80	220	169	4.79E+05
SST 02	1.40	7.4E-05	1.9E-04	1000.00	*1.20*	7.4E-08	1.6E-04	1.4E-03	1.4E-03	1.9E-03	2.0E-03	8.7E-08	3.7E-07	0.86	434	312	4.45E+05
SST 03	0.70	7.5E-05	1.9E-04	1000.00	1.20	7.5E-08	1.6E-04	6.3E-04	7.0E-04	1.2E-03	1.5E-03	7.3E-08	7.2E-07	1.03	220	158	4.49E+05
SST 04	1.40	6.4E-05	1.9E-04	1000.00	*1.20*	6.4E-08	1.6E-04	1.4E-03	1.4E-03	1.9E-03	2.0E-03	8.7E-08	3.7E-07	0.74	434	325	4.63E+05
SST 05	0.70	7.2E-05	1.9E-04	1000.00	1.20	7.2E-08	1.6E-04	6.3E-04	7.0E-04	1.2E-03	1.5E-03	7.3E-08	7.2E-07	0.99	220	160	4.53E+05
SST 06	1.40	5.9E-05	1.9E-04	1000.00	*1.20*	5.9E-08	1.6E-04	1.4E-03	1.4E-03	1.9E-03	2.0E-03	8.7E-08	3.7E-07	0.68	434	332	4.73E+05

Table 3.13. Data used for the calculation of the shear rate values of the shear stress test at different operating conditions in a Büchi Mini Spray Dryer B-290 of formulation FB1.200.

		Ml	**Mg**	**d**	**d**	**QL**	**QG**	**Dneedle**	**Din,liq**	**Dex,liq**	**Dgas**	**Aliq**	**Agas**	**VL**	**VG**	**Vav**	**gamma**
		[kg/s]	[kg/s]	[kg/m3]	[kg/m3]	[m3/s]	[m3/s]	[m]	[m]	[m]	[m]	[m2]	[m2]	[m/s]	[m/s]	[m/s]	[1/s]
Condition	Nozzle [mm]	*mass flow liquid*	*mass flow gas*	*density*	*density*	*volumetric flow liquid*	*volumetric flow gas*	*Diameter center needle*	*Inner Diameter liquid*	*External diameter liquid*	*Inner diameter gas*	*Cross-Sectional area liquid*	*Cross-Sectional area gas*	*liquid velocity*	*gas velocity*	*average velocity*	*Shear Rate*
SST 01	0.7	7.1E-05	1.9E-04	1000	1.2	7.1E-08	1.6E-04	6.3E-04	7.0E-04	1.2E-03	1.5E-03	7.3E-08	7.2E-07	0.97	220	161	4.6E+05
SST 02	1.4	7.2E-05	1.9E-04	1000	*1.2*	7.2E-08	1.6E-04	1.4E-03	1.4E-03	1.9E-03	2.0E-03	8.7E-08	3.7E-07	0.83	434	315	4.5E+05
SST 03	0.7	7.0E-05	1.9E-04	1000	1.2	7.0E-08	1.6E-04	6.3E-04	7.0E-04	1.2E-03	1.5E-03	7.3E-08	7.2E-07	0.96	220	161	4.6E+05
SST 04	1.4	7.1E-05	1.9E-04	1000	*1.2*	7.1E-08	1.6E-04	1.4E-03	1.4E-03	1.9E-03	2.0E-03	8.7E-08	3.7E-07	0.82	434	316	4.5E+05
SST 05	0.7	7.1E-05	1.9E-04	1000	1.2	7.1E-08	1.6E-04	6.3E-04	7.0E-04	1.2E-03	1.5E-03	7.3E-08	7.2E-07	0.97	220	161	4.6E+05
SST 06	1.4	7.2E-05	1.9E-04	1000	*1.2*	7.2E-08	1.6E-04	1.4E-03	1.4E-03	1.9E-03	2.0E-03	8.7E-08	3.7E-07	0.83	434	315	4.5E+05

Table 3.14. Data used for the calculation of the shear strain and shear stress values of Shear Stress Test (SST) using previous calculated shear rate in Table 3.9 in a Büchi Mini Spray Dryer B-290 for formulation FB1.100.

Condition	Feed Flow Rate [ml/min]*	Nozzle [mm]	Shear Rate [1/s]	Volume of nozzle device [m3]	Liquid Flow Rate [m3/s]	Residence Time [s]	Shear Strain	Shear Stress [mPa]
SST 01	3.50	0.7	4.8E+05	5.4E-10	5.8E-08	9.3E-03	4.5E+03	3.1E+03
SST 02	4.45	1.4	4.4E+05	9.4E-10	7.4E-08	1.3E-02	5.7E+03	2.9E+03
SST 03	4.51	0.7	4.5E+05	5.4E-10	7.5E-08	7.2E-03	3.2E+03	2.9E+03
SST 04	3.85	1.4	4.6E+05	9.4E-10	6.4E-08	1.5E-02	6.8E+03	3.0E+03
SST 05	4.34	0.7	4.5E+05	5.4E-10	7.2E-08	7.5E-03	3.4E+03	2.9E+03
SST 06	3.52	1.4	4.7E+05	9.4E-10	5.9E-08	1.6E-02	7.6E+03	3.1E+03

Table 3.15. Data used for the calculation of the shear strain and shear stress values of Shear Stress Test (SST) using previous calculated shear rate in Table 3.10 in a Büchi Mini Spray Dryer B-290 for formulation FB1.200.

Run	Feed Flow Rate [ml/min]*	Nozzle [mm]	Shear Rate [1/s]	Volume of nozzle device [m3]	Liquid Flow Rate [m3/s]	Residence Time [s]	Shear Strain	Shear Stress [mPa]
SST 01	4.48	0.7	4.5E+05	5.4E-10	7.5E-08	7.3E-03	3.3E+03	2.9E+03
SST 02	4.47	1.4	4.4E+05	9.4E-10	7.5E-08	1.3E-02	5.6E+03	2.9E+03
SST 03	4.51	0.7	4.5E+05	5.4E-10	7.5E-08	7.2E-03	3.3E+03	2.9E+03
SST 04	4.56	1.4	4.4E+05	9.4E-10	7.6E-08	1.2E-02	5.5E+03	2.9E+03
SST 05	4.57	0.7	4.5E+05	5.4E-10	7.6E-08	7.2E-03	3.2E+03	2.9E+03
SST 06	4.59	1.4	4.4E+05	9.4E-10	7.7E-08	1.2E-02	5.4E+03	2.9E+03

Shear rate, shear stress and shear strain from spray-drying (SD) (FB1.100 and FB1.200)

Table 3.16. Data used for the calculation of the Shear Rate values of spray-drying at different operating conditions in a Büchi Mini Spray Dryer B-290 for formulation FB1.100

		Ml	**Mg**	**d**	**d**	**QL**	**QG**	**Dneedle**	**Din,liq**	**Dex,liq**	**Dgas**	**Aliq**	**Agas**	**VL**	**VG**	**Vav**	**gamma**
		[kg/s]	[kg/s]	[kg/m3]	[kg/m3]	[m3/s]	[m3/s]	[m]	[m]	[m]	[m]	[m2]	[m2]	[m/s]	[m/s]	[m/s]	[1/s]
Conditions	Nozzle [mm]	*mass flow liquid*	*mass flow gas*	*density*	*density*	*volumetric flow liquid*	*volumetric flow gas*	*Diameter center needle*	*Inner Diameter liquid*	*External diameter liquid*	*Inner diameter gas*	*Cross-Sectional area liquid*	*Cross-Sectional area gas*	*liquid velocity*	*gas velocity*	*average velocity*	*Shear Rate*
SD 01	0.7	7.1E-05	1.9E-04	1000	1.2	7.1E-08	1.6E-04	6.3E-04	7.0E-04	1.2E-03	1.5E-03	7.3E-08	7.2E-07	0.97	220	161	4.6E+05
SD 02	1.4	7.2E-05	1.9E-04	1000	*1.2*	7.2E-08	1.6E-04	1.4E-03	1.4E-03	1.9E-03	2.0E-03	8.7E-08	3.7E-07	0.83	434	315	4.5E+05
SD 03	0.7	7.0E-05	1.9E-04	1000	1.2	7.0E-08	1.6E-04	6.3E-04	7.0E-04	1.2E-03	1.5E-03	7.3E-08	7.2E-07	0.96	220	161	4.6E+05
SD 04	1.4	7.1E-05	1.9E-04	1000	*1.2*	7.1E-08	1.6E-04	1.4E-03	1.4E-03	1.9E-03	2.0E-03	8.7E-08	3.7E-07	0.82	434	316	4.5E+05
SD 05	0.7	7.1E-05	1.9E-04	1000	1.2	7.1E-08	1.6E-04	6.3E-04	7.0E-04	1.2E-03	1.5E-03	7.3E-08	7.2E-07	0.97	220	161	4.6E+05
SD 06	1.4	7.2E-05	1.9E-04	1000	*1.2*	7.2E-08	1.6E-04	1.4E-03	1.4E-03	1.9E-03	2.0E-03	8.7E-08	3.7E-07	0.83	434	315	4.5E+05

Table 3.17. Data used for the calculation of the Shear Rate values of spray-drying at different operating conditions in a Büchi Mini Spray Dryer B-290 for formulation FB1.200

		Ml	**Mg**	**d**	**d**	**QL**	**QG**	**Dneedle**	**Din,liq**	**Dex,liq**	**Dgas**	**Aliq**	**Agas**	**VL**	**VG**	**Vav**	**gamma**
		[kg/s]	[kg/s]	[kg/m3]	[kg/m3]	[m3/s]	[m3/s]	[m]	[m]	[m]	[m]	[m2]	[m2]	[m/s]	[m/s]	[m/s]	[1/s]
Conditions	Nozzle [mm]	*mass flow liquid*	*mass flow gas*	*density*	*density*	*volumetric flow liquid*	*volumetric flow gas*	*Diameter center needle*	*Inner Diameter liquid*	*External diameter liquid*	*Inner diameter gas*	*Cross-Sectional area liquid*	*Cross-Sectional area gas*	*liquid velocity*	*gas velocity*	*average velocity*	*Shear Rate*
SD 01	0.7	8.78E-05	1.9E-04	1000	1.2	8.78E-08	1.6E-04	6.3E-04	7.0E-04	1.2E-03	1.5E-03	7.3E-08	7.2E-07	1.20	219.99	150.92	4.3E+05
SD 02	1.4	8.70E-05	1.9E-04	1000	*1.2*	8.70E-08	1.6E-04	1.4E-03	1.4E-03	1.9E-03	2.0E-03	8.7E-08	3.7E-07	1.00	433.74	298.04	4.2E+05
SD 03	0.7	8.75E-05	1.9E-04	1000	1.2	8.75E-08	1.6E-04	6.3E-04	7.0E-04	1.2E-03	1.5E-03	7.3E-08	7.2E-07	1.20	219.99	151.06	4.3E+05
SD 04	1.4	8.60E-05	1.9E-04	1000	*1.2*	8.60E-08	1.6E-04	1.4E-03	1.4E-03	1.9E-03	2.0E-03	8.7E-08	3.7E-07	0.99	433.74	299.06	4.3E+05
SD 05	0.7	8.80E-05	1.9E-04	1000	1.2	8.80E-08	1.6E-04	6.3E-04	7.0E-04	1.2E-03	1.5E-03	7.3E-08	7.2E-07	1.20	219.99	150.84	4.3E+05
SD 06	1.4	8.75E-05	1.9E-04	1000	*1.2*	8.75E-08	1.6E-04	1.4E-03	1.4E-03	1.9E-03	2.0E-03	8.7E-08	3.7E-07	1.01	433.74	297.42	4.2E+05

Table 3.18. . Data used for the calculation of the shear strain and shear stress values of spray-drying using previous calculated shear rate in Table 3.13 in a Büchi Mini Spray Dryer B-290 for formulation FB1.100

Conditions	Feed Flow Rate [ml/min]*	Nozzle [mm]	Shear Rate [1/s]	Volume of nozzle device [m3]	Liquid Flow Rate [m3/s]	Residence Time [s]	Shear Strain	Shear Stress [mPa]
SD 01	4.24	0.7	4.6E+05	5.4E-10	7.1E-08	7.7E-03	3.5E+03	3.0E+03
SD 02	4.30	1.4	4.5E+05	9.4E-10	7.2E-08	1.3E-02	5.9E+03	2.9E+03
SD 03	4.23	0.7	4.6E+05	5.4E-10	7.0E-08	7.7E-03	3.5E+03	3.0E+03
SD 04	4.26	1.4	4.5E+05	9.4E-10	7.1E-08	1.3E-02	6.0E+03	2.9E+03
SD 05	4.25	0.7	4.6E+05	5.4E-10	7.1E-08	7.7E-03	3.5E+03	3.0E+03
SD 06	4.31	1.4	4.5E+05	9.4E-10	7.2E-08	1.3E-02	5.9E+03	2.9E+03

Table 3.19. . Data used for the calculation of the shear strain and shear stress values of spray-drying using previous calculated shear rate in Table 3.14 in a Büchi Mini Spray Dryer B-290 for formulation FB1.200

Conditions	Feed Flow Rate [ml/min]*	Nozzle [mm]	Shear Rate [1/s]	Volume of nozzle device [m3]	Liquid Flow Rate [m3/s]	Residence Time [s]	Shear Stress	Shear Stress [mPa]
SD 01	5.27	0.7	4.3E+05	5.4E-10	8.8E-08	6.2E-03	2.7E+03	2.8E+03
SD 02	5.22	1.4	4.2E+05	9.4E-10	8.7E-08	1.1E-02	4.6E+03	2.8E+03
SD 03	5.25	0.7	4.3E+05	5.4E-10	8.8E-08	6.2E-03	2.7E+03	2.8E+03
SD 04	5.16	1.4	4.3E+05	9.4E-10	8.6E-08	1.1E-02	4.7E+03	2.8E+03
SD 05	5.28	0.7	4.3E+05	5.4E-10	8.8E-08	6.2E-03	2.6E+03	2.8E+03
SD 06	5.25	1.4	4.2E+05	9.4E-10	8.8E-08	1.1E-02	4.6E+03	2.8E+03

Reynolds number calculation for the Shear Stress Test of FB1.100 and FB1.200

Table 3.20. Data required for the calculation of the Reynolds number for the liquid feed stream on the shear stress test for FB1.100 liquid solution.

	Fluid Dynamic Viscosity	Fluid density	Fluid Velocity	a	b	Hydraulic Diameter	Hydraulic Reynold	Laminar Friction Factors		Reynolds
Conditions	*μ [kg/m.s]*	*ρ [kg/m3]*	*v [m/s]*	*Din,liq [m]*	*Dneedle [m]*	*Dh*	Re(Dh,liq)	*b/a*	*1/ζ*	*Re*
SD 01	0.0038	1000	0.80	7.0E-04	6.3E-04	1.4E-04	29.4	0.90	0.67	19.6
SD 02	0.0038	1000	0.86	1.4E-03	1.4E-03	8.0E-05	18.0	0.97	0.67	12.0
SD 03	0.0038	1000	1.03	7.0E-04	6.3E-04	1.4E-04	37.9	0.90	0.67	25.3
SD 04	0.0038	1000	0.74	1.4E-03	1.4E-03	8.0E-05	15.6	0.97	0.67	10.4
SD 05	0.0038	1000	0.99	7.0E-04	6.3E-04	1.4E-04	36.4	0.90	0.67	24.3
SD 06	0.0038	1000	0.68	1.4E-03	1.4E-03	8.0E-05	14.2	0.97	0.67	9.5

Table 3.21. Data required for the calculation of the Reynolds number for the atomization gas stream on the shear stress test for FB1.100

	Fluid Dynamic Viscosity	Fluid density	Fluid Velocity	a	b	Hydraulic Diameter	Hydraulic Reynold	Laminar Friction Factors		Reynolds
Conditions	*μ [kg/m.s]*	*ρ [kg/m3]*	*v [m/s]*	*Din,liq [m]*	*Dneedle [m]*	*Dh*	Re(Dh,liq)	*b/a*	*1/ζ*	*Re*
SD 01	1.83E-05	118	220	7.0E-04	6.3E-04	1.4E-04	2.00E+05	0.90	0.67	1.3E+05
SD 02	1.83E-05	118	434	1.4E-03	1.4E-03	8.0E-05	2.25E+05	0.97	0.67	1.5E+05
SD 03	1.83E-05	118	220	7.0E-04	6.3E-04	1.4E-04	2.00E+05	0.90	0.67	1.3E+05
SD 04	1.83E-05	118	434	1.4E-03	1.4E-03	8.0E-05	2.25E+05	0.97	0.67	1.5E+05
SD 05	1.83E-05	118	220	7.0E-04	6.3E-04	1.4E-04	2.00E+05	0.90	0.67	1.3E+05
SD 06	1.83E-05	118	434	1.4E-03	1.4E-03	8.0E-05	2.25E+05	0.97	0.67	1.5E+05

Table 3.22. Data required for the calculation of the Reynolds number for the liquid feed stream on the shear stress test for FB1.200 liquid solution.

	Fluid Dynamic Viscosity	**Fluid density**	**Fluid Velocity**	**a**	**b**	**Hydraulic Diameter**	**Hydraulic Reynold**	**Laminar Friction Factors**		**Reynolds**
Conditions	*μ [kg/m.s]*	*ρ [kg/m3]*	*v [m/s]*	*Din,liq [m]*	*Dneedle [m]*	*Dh*	Re(Dh,liq)	*b/a*	*1/ζ*	*Re*
SD 01	0.0065	1000	1.02	7.0E-04	6.3E-04	1.4E-04	22.0	0.90	0.67	14.7
SD 02	0.0065	1000	0.86	1.4E-03	1.4E-03	8.0E-05	10.6	0.97	0.67	7.1
SD 03	0.0065	1000	1.03	7.0E-04	6.3E-04	1.4E-04	22.1	0.90	0.67	14.8
SD 04	0.0065	1000	0.88	1.4E-03	1.4E-03	8.0E-05	10.8	0.97	0.67	7.2
SD 05	0.0065	1000	1.04	7.0E-04	6.3E-04	1.4E-04	22.4	0.90	0.67	14.9
SD 06	0.0065	1000	0.88	1.4E-03	1.4E-03	8.0E-05	10.9	0.97	0.67	7.2

Table 3.23. Data required for the calculation of the Reynolds number for the atomizing gas stream on the shear stress test for FB1.200 liquid solution.

	Fluid Dynamic Viscosity	**Fluid density**	**Fluid Velocity**	**a**	**b**	**Hydraulic Diameter**	**Hydraulic Reynold**	**Laminar Friction Factors**		**Reynolds**
Conditions	*μ [kg/m.s]*	*ρ [kg/m3]*	*v [m/s]*	*Din,liq [m]*	*Dneedle [m]*	*Dh*	Re(Dh,liq)	*b/a*	*1/ζ*	*Re*
SD 01	1.83E-05	118	219.99	7.0E-04	6.3E-04	1.4E-04	199810.3	0.90	0.67	1.3E+05
SD 02	1.83E-05	118	433.74	1.4E-03	1.4E-03	8.0E-05	225117.7	0.97	0.67	1.5E+05
SD 03	1.83E-05	118	219.99	7.0E-04	6.3E-04	1.4E-04	199810.3	0.90	0.67	1.3E+05
SD 04	1.83E-05	118	433.74	1.4E-03	1.4E-03	8.0E-05	225117.7	0.97	0.67	1.5E+05
SD 05	1.83E-05	118	219.99	7.0E-04	6.3E-04	1.4E-04	199810.3	0.90	0.67	1.3E+05
SD 06	1.83E-05	118	433.74	1.4E-03	1.4E-03	8.0E-05	225117.7	0.97	0.67	1.5E+05

Table 3.24 ANOVA two-factor analysis with replication (n=3) of the impact of concentration (100 mg/ml and 200 mg/ml) and the nozzle diameter (0.7 mm and 1.4 mm) on the protein aggregation, indicated by the Z-average value, during the Shear Stress Test (SST).

Source of Variation	***SS***	***df***	***MS***	***F***	***P-value***	***F crit***
Nozzle Size [mm]	0.03	1	0.03	0.03	0.87	5.32
BSA concentration [mg/ml]	14.29	1	14.29	13.70	0.01	5.32
Interaction	0.02	1	0.02	0.02	0.90	5.32
Within	8.35	8	1.04			
Total	22.69	11				

Table 3.25 ANOVA single-factor analysis with replication (n=3) for the impact of the BSA concentration (100 mg/ml and 200 mg/ml) on aggregation phenomena during the Thermal/Dehydration Stress Test (TDST) by using a single droplet drying technique.

Source of Variation	***SS***	***df***	***MS***	***F***	***P-value***	***F crit***
Between Groups (BSA concentration)	1157.95	1	1157.95	4.86	0.09	7.71
Within Groups (BSA concentration)	953.68	4	238.42			
Total	2111.64	5				

Table 3.26 ANOVA two-factor analysis with replication (n=3) of the impact of concentration (100 mg/ml and 200 mg/ml) and the nozzle diameter (0.7 mm and 1.4 mm) on the protein aggregation, indicated by the Z-average value, during the spray-drying process (SD).

Source of Variation	***SS***	***df***	***MS***	***F***	***P-value***	***F crit***
Nozzle diameter [mm]	9.33	1.00	9.33	0.26	0.63	5.32
Protein concentration [mg/ml]	289.01	1.00	289.01	7.91	0.02	5.32
Interaction	5.19	1.00	5.19	0.14	0.72	5.32
Within	292.15	8.00	36.52			
Total	595.67	11.00				

Chapter 4

Spray-drying of monoclonal antibodies: the impact of various stresses factors encountered by a protein formulation undergoing spray-drying

This chapter focuses on the drying of proteins of our interest, which are monoclonal antibodies.

4.1 Introduction

Among the different studies conducted on spray-drying of biopharmaceutical proteins, the ones with monoclonal antibodies (mAbs) have gained popularity in the last years (Batens *et al.*, 2018; Bowen *et al.*, 2013; Gikanga *et al.*, 2015; Maury *et al.*, 2005; Ramezani *et al.*, 2014). Spray-drying of mAbs corresponds to the topics discussed in Chapters 4 and 5 of this thesis.

As already stated in the previous chapters, spray-drying brings together different stresses for proteins, such as shear/interfacial and thermal/dehydration, that depends on the operating parameters and the type of equipment used.

It is already known that certain levels of shear stress can induce molecular rearrangements in the protein bringing it to a state of instability, which can make it more susceptible to other stresses (Morgan *et al.*, 2020). Studies of shear stress isolation using high pressure homogenizers, capillarity, and spraying nozzles, have been reported on different proteins, such as human growth hormone, caseinate, lactoferrine and mAbs (IgG) (Dao *et al.*, 2022; Duerkop *et al.*, 2018; Maa *et al.*, 1998b; Wang *et al.*, 2019). Nevertheless, to the best of our knowledge, the study of shear stress on mAbs has not been reported on a spraying nozzle set-up.

On the other hand, the highest contribution to instability of biomolecules during spray-drying is considered to occur mainly in the drying stage due to thermal and dehydration stresses, which will mainly affect the secondary and tertiary structures (Bhambhani *et al.*, 2020; Ghandi *et al.*, 2012). Different experimental techniques have been used to evaluate protein thermal stress by heating solutions containing proteins in water baths or oven environments (Alsaddique *et al.*, 2016; Hawe *et al.*, 2009). A suspended single-droplet drying technique, which has been mainly used to study the kinetics of drying (Boel *et al.*, 2020; Sadek *et al.*, 2015; Souza Lima *et al.*, 2020) could be interesting to investigate the thermal/dehydration impact of a drying operation on a single droplet containing the protein, as demonstrated by Haque *et al.* (2013), with whey protein isolate (Haque *et al.*, 2013).

In this chapter the study carried out on a solution of mAb (mAb-A) is divided in three parts:

1. A first study in which the shear stress due to the atomization step and the thermal/dehydration stresses during the drying step were decoupled, as previously done in chapter 3 with a model protein. No study of decoupling of mechanical and thermal/dehydration stresses like the one carried out on BSA seems to have been previously performed on mAb formulations. The impact of decoupling these sources of stress was compared to that observed on the mAb aggregation level in a mAb solution (F1) reconstituted from a powder produced by spray-drying.
2. A second study of spray-drying at varying conditions of liquid feed flow rate and inlet temperature was carried out in mAb-A.
3. A final study of spray-drying of mAb solutions (F1, F2), where the study parameter was the composition of the formulation. This was achieved by manipulating the protein concentration and the type and concentration of stabilizers (surfactants, aminoacids, sugars).

4.2 Materials and Methods

4.2.1 Materials

Initial Solution of antibodies (mAb-A). An initial antibody solution (mAb-A) provided by SANOFI (Paris, France), was previously concentrated by tangential flow filtration to obtain a range of 113-120 mg/ml of mAb-A and formulated in trehalose 2% w/w and Histidine 5 mM (pH=6). All excipients used for the formulation screening were provided by SANOFI (Paris, France).

F1 formulation. Formulation F1 has a target protein concentration of 100 mg/ml (then named F1.100), and it was formulated by adding to the initial solution of mAb-A the buffer containing the following excipients: Histidine 5mM (pH=6), Arginine 25mM, Trehalose 4% w/w and Polysorbate-80 (PS80) 0.02% w/v, until the desired protein concentration was reached.

F2 formulation. Formulation F2 was formulated at two different mAb-A concentrations (75 and 100 mg/ml), now named F2.75 and F2.100, by adding a buffer solution of Histidine 5 mM (pH=6), Arginine 53mM, Trehalose 8.6% w/w, and Tween-80 0.075% w/v, to the initial solution of mAb-A.

The main difference between formulation F1 and F2 was the increase in the excipients concentration and the reduction of the mAb-A concentration.

Placebo formulation. A placebo formulation is introduced to be able to use assess the impact of the presence of the protein on the formulation. The Placebo Formulation does not contain the mAb-A and it was prepared as follows: a buffer solution of Histidine 5mM (pH=6), Arginine 25mM, Trehalose 4% w/w and Polysorbate-80 (PS80) 0.02% w/v.

4.2.2 Methods

4.2.2.1 Decoupling of Spray-Drying Stresses

Shear Stress Test

The apparatus and the experimental method used for this study have been presented in detail in Chapter 3 in Section 3.4.2.1. These tests were performed on formulation F1.100, which was sprayed at the operating conditions given in Table 4.1, at room temperature ≈20°C. The nozzle diameter and the liquid feed flow rate were varied to produce different values of shear rate/shear stress during spraying (Table 4.1). Before each spraying test all solutions were filtered (hydrophilic polyethersulfone (PES) 0.22 µm).

Table 4.1. Shear Stress Test conditions for formulation F1.100 at ≈ 20°C.

Condition	Feed Flow Rate [ml/min]	Nozzle [mm]	Shear Strain	Shear Stress [Pa]
SST 1	2.90	0.5	2.2	6.72
SST 2	9.25	0.5	2.2	4.48
SST 3	23.31	0.5	2.3	2.82
SST 4	21.64	0.7	7.9	1.91
SST 5	2.88	2.0	8.1	2.07
SST 6	9.16	2.0	39.6	1.39
SST 7	22.03	2.0	43.8	0.87
Stock solution	NA	NA	0	0

Thermal and dehydration stresses test (TDST) with a single drying droplet set-up

This test was performed using a suspended single droplet drying set-up. The apparatus and the experimental method used for this study have also been presented in detail in Chapter 3 in Section 3.4.2.1.

The drying conditions kept for this test were the following: drying temperature of 72°C with an absolute humidity of 3.09 g/kg, and a drying airflow rate of 4 L/min. These set-up conditions were used for two different Mab formulations: F1.100 and F2.75 and two different drying times (2h, 3h).

A volume of 6 µl of formulation F1.100 and F2.75 was used for each of the three replications per drying time (2 and 3 hours). Before each drying test the solution was filtered (PES 0.22 μm). At the end of the test, the dried drop was recovered from the stem of the glass filament and reconstituted as the powders produced by spray-drying (methodology described below in Section 4.2.3.7). The reconstituted solutions were further analysed for the presence of aggregates. Given the small volume reconstituted, turbidity analysis could be not performed.

4.2.2.2 Spray-Drying Experiments

The apparatus and the experimental method used for this study have also been presented in detail in Chapter 3 in Section 3.4.2.2. The tests were conducted in two different series:

First series

In a first series of tests, the formulation F1.100 (100 mg/ml of mAb-A) was spray-dried under different operating conditions regrouping liquid feed flow rate (LFFR) and drying air temperature (Tin) as variable parameters and, drying airflow rate (22 m^3/h) spraying airflow rate (571 L/h) and nozzle diameter (0.7 mm) as fixed parameters (Table 4.2). The experiments were performed in triplicate, under the conditions

given in Table 4.2. After recovery, the spray-dried powder was placed in a sealed vial and stocked at 4°C. The powders were stored from 24 – 48 h at 4°C before being reconstituted in milli-Q water, protocol previously mentioned on Chapter 3 in Section 3.4.2.2.

The three main outlet parameters of interest in our study were moisture content of the powder, process yield and level of protein aggregation in the reconstituted mAb-A solution.

Table 4.2. Operating parameters for the first series of spray-drying experiments performed with formulation F1.100.

	Inlet Parameters				***Outlet Parameters***	
Condition	**Tin**	**LFFR**	**Shear Strain (10^3)**	**Shear Stress [Pa]**	**Tout**	**Twb**
	°C	**[ml/min]**		**[Pa]**	**°C**	**°C**
C1	70	3.6	4.4	4.33	36 ±3	21 ± 6
C2	80	3.6	4.3	4.33	39 ± 3	22 ± 5
C3	90	3.6	4.3	4.33	44 ± 5	21 ± 2
C4	100	3.5	4.6	4.38	47 ± 2	20 ± 1
C5	110	3.6	4.3	4.34	52 ± 2	21 ± 1
C6	120	3.6	4.3	4.35	54 ± 0	22 ± 1
C7	70	3.8	1.9	3.56	29 ± 1	21 ± 6
C8	80	6.6	2	3.60	34 ± 4	22 ± 4
C9	90	6.5	2.4	4.35	35 ± 2	21 ± 1
C10	100	6.7	1.9	3.60	38 ± 1	22 ± 1
C11	110	6.8	1.9	3.56	44 ± 1	22 ± 1
C12	120	6.9	1.8	3.54	47 ± 4	23 ± 1
C13	105	4.9	3.1	4.05	47 ± 2	20 ± 2

Second series

This new series of spray-drying tests with mAb-A formulations F1.100, F2.100 and F2.75, were performed under fixed operating conditions as follows: inlet drying air temperature (Tin) 105°C, drying airflow rate 22 m^3/h, spraying airflow rate 571 L/h and liquid feed flow rate 4.5 ml/min. After recovery the spray-dried powder was placed in a sealed vial and stocked at 4°C before analysis. Three replicates were performed per formulation. The same conditions were kept for the spray-drying of the placebo formulation.

A two-way analysis of variance (ANOVA) was applied to experimental data for analysis of the influence of studied process parameters on the response settings. The three replicates were considered for the analysis, where if p-value <0.05 the selected parameter does have an impact on the response setting studied.

4.2.2.3 Powder Characterization

(a) Moisture Content

The Karl Fischer technique was used to determine the residual water content in the spray-dried powder, using the 851 Titrando from Metrohm. The oven temperature was set to 120°C and airflow was set to 80 mL/min. The drift needed to be below 20 µg of water/minute to start the measurement. The stop criterion was to have a relative drift near 15 µg of water/minute. Water content results were considered significantly different for differences equal or more than 0.3%. The reactants used were the HYDRANAL ™-Coulomat AG-OVEN (as the anolyte) and HYDRANAL ™ - Coulomat CG (as the catholyte). The equipment accuracy was verified at the beginning of the measurements with an HYDRANAL ™ Water Standard KF-OVEN (220-230°C)

(b) Particle Size Distribution

The particle size distribution of the spray-dried powders was measured using a laser diffraction granulometer (Mastersizer-3000, Malvern Panalytical). A pre-dispersion of powder in isopropyl was prepared to have a final ratio of powder:isopropyl of 5 mg:3 ml in the dispersion phase (isopropyl) of the equipment.

(c)Scanning Electron Microscopy (SEM)

Scanning electron microscopy analysis was done using a SEM Nova NanoSEM 450 from ThermoFisher (FEI), high-resolution SEM with FEG tip with field emission. Samples were observed with a resolution of × 5000. In this case the SEM was used to measure the size of the dried droplets of the TDST. Powder samples were previously coated with two layers of platinum using the Sputter Coater Polaron SC7640, using argon gas, a current of 19 mA and a vacuum of $(8 - 6) \times 10^{-2}$ mbar.

(d) Density

The principle of liquid pycnometry relies on the displacement of a liquid from the powder, within a container with a certain volume (10 cm^3), generated by the addition of a powder material in an immiscible liquid, in this case soybean oil, with a density of 9800 g/cm^3. This technique allows the measurement of the true density of a powder, which means that it will also consider the air bubbles inside the power in the density calculation.

Firstly, the oil system was introduced in the pycnometer and weighted, it was then emptied and cleaned. Secondly, the powder mass was added to the pycnometer, (2 gr) and weighted. Finally, the oil was added to the pycnometer with the powder mass and weighted. Since the volume of the pycnometer is constant, it is possible to calculate the volume of oil that was displaced by the powder, as we know the

density and mass of the oil. This volume allows for the final calculation of the powder density using the weighted mass.

To assess the real volume of the pycnometer, it is filled to the top with water (mass is known) and then the volume of the container is measured using water density.

4.2.2.4 Reconstituted Solution from Powder

(a)Reconstitution Methods

Since the final drug product (mAb-A formulation) is searched to be administered in a liquid form, it is important to perform a reconstitution step of the spray-dried powder, which consists of suspending the powder in the desired solvent, which in this case is water for injection (WFI). The resulting suspension (powder from formulation F1.100 dispersed in WFI) is then stirred until a homogeneous solution is formed, which is at the same initial concentration as that of the solution before SD. Three different reconstitution protocols were tested:

The first protocol, named OS, consisted of stirring the suspension on an orbital shaker UniShaker 25 (LLG Labware) at 70 rpm and at room temperature. Given that this is the classic reconstitution method used for this type of formulation, the recovery of samples for analysis was carried out at a previously selected time of homogenization 90 min.

For the second reconstitution protocol, named OS-WB, the orbital shaker was placed inside a water bath at 40°C, and the third one, named OS-WB-V, added to the second protocol a final vortex step at 1200 rpm for 30 s. For the second and third protocols, different samples were recovered at different times during a period of 390 min and were then analysed by DLS and spectrometry (UV-Vis).

From the results, which will be shown in Section 2.3.1, the first protocol was adopted for the reconstitution tests with a reconstitution time of 90 min. After reconstitution, the resulting solution was characterized with respect to protein concentration, turbidity and presence of aggregates as follows:

(b)Protein Concentration

A spectrophotometer (Agilent Cary 8454) was used to measure the protein concentration at 280 nm using in a quartz cell, and an extinction coefficient of 1.55 $ml.\ mg^{-1}cm^{-1}$. The blank used was milli-Q water.

(c)Density

The solution density before spray-drying and after reconstitution was measured with a Mettler Toledo DM-40 densimeter, at 20°C. A water standard with a volume of 3 ml and a density of 0.9982g/cm3 at 20°C was also used. The operating principle is based on the oscillation of a U-shaped borosilicate glass tube (volume = 1mL) whose resulting frequency is directly proportional to the density of the liquid or gas injected. It has an integrated electronically controlled thermostat. The density is the physical quantity

that characterizes the mass of a body per unit of volume. It was expressed in g/cm^3 in the international system.

(d)pH measurement

The pH of the solution was measured before SD and after SD by a 902 Titrando Metrohm (swiss mode) OMNIS Ready.

(e)Visual inspection

Observation and count of visible particles in the agitated solution placed in front of two different panels (black and white) in a standard bench for manual inspection was carried out.

The used code was as follows: (++) for more than 5 particles visible to the naked eye, (+) 1-5 particles visible to the naked eye, (-) particles only visible when inspecting under light, (--) no visible particles in any observation condition

(f)Turbidity

The turbidity of the samples was quantified by measuring the absorbance at 600 nm using a Varioskan LUX Multimode Microplate Reader from Thermo Fisher Scientific. A calibration curve was obtained using calibrated formazin standards. For each sample, two wells filled with 200 µL were analysed (n = 2). The turbidity of each sample was calculated from the calibration curve and given in nephelometric turbidity units (NTU).

(g)Dynamic Light Scattering (DLS)

Dynamic Light Scattering performed on a Zetasizer Nano (Malvern, Herrenberg Germany) as follows: 60 µl of the mAb-A solutions, diluted to 1 mg/ml, were analysed in plastic cuvettes at 25°C using the automatic mode for identifying the best number of sub-runs and measurement time (n=3). The z-average diameter (Z-Ave) was calculated from the correlation function using the Dispersion Technology Software version 6.01 (Malvern, Herrenberg, Germany).

4.3 Results and Discussion

4.3.1 Implementation of the reconstitution method for mAb-A

As mentioned, three different protocols were tested for reconstitution of the dry Mab formulations. The first method consisted of using solely the orbital shaker (OS) for F1.100 and optical inspection at different times of reconstitution (30-120 min) to identify the reconstitution time in which visual homogeneity was achieved. It was identified at 90 min, and this time was the starting condition for the

second method using the orbital shaker and the water bath (OS-WB) and the third method using the orbital shaker, water bath and vortex (OS-WB-V). With these different techniques a variation of temperature and/or mixing conditions and reconstitution times were tested.

Figure 4.1.a displays the values of Z-average measured using the OS-WB and OS-WB-V protocols in the reconstituted solutions (reconstitution times from 90 to 390 min) in comparison to OS protocol (reconstitution time 90 min). Both second and third protocols showed a similar starting point of aggregation and turbidity as the first protocol (OS). As it can be seen, increasing the reconstitution time beyond 90 min did not improve the dispersion and, on the contrary, even led, mainly for the second protocol, to an increase in the values of aggregation (Figure 4.1a) and turbidity (Figure 4.1b). For that reason, the protocol for reconstitution was fixed using the OS method at 70 rpm for 90 min.

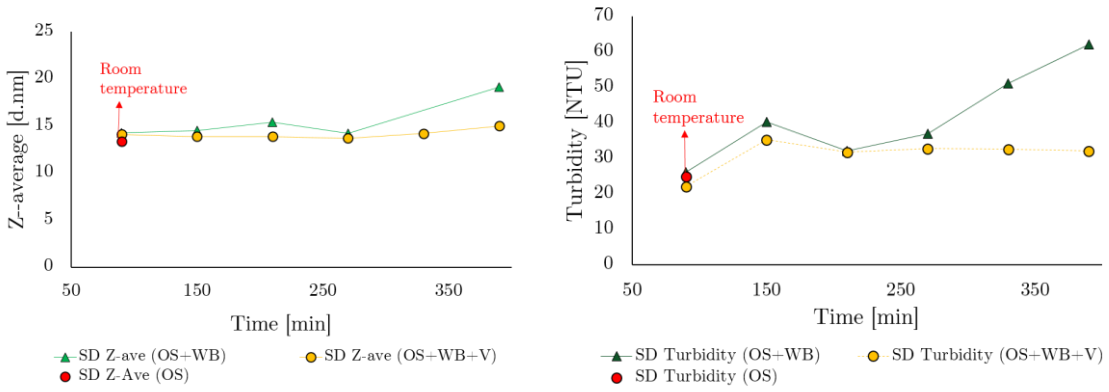

(a) (b)

Figure 4.1. Comparison of a) Aggregation results (Z-average) and b) Turbidity (NTU) levels measured on reconstituted solutions from spray-dried F1.100 powder, through three different reconstitution protocols (n=3).

4.3.2 Decoupling of spray-drying stresses

This Section presents the individual results of the decoupling stress tests, before comparing them to the SD results in the following Section.

Shear Stress Test (SST)

The conditions used for these tests are shown in Table 4.1 in Section 4.2.2.1 As described in Chapter 3, Section (a), the values of shear rate, shear strain and shear stress are used to investigate and compare protein aggregation levels at different operating conditions. All data necessary to calculate these parameters are given in Table 4.6 Table 4.7, Table 4.8 and Table 4.9 in Section 4.5 (APPENDIX). During spraying of a liquid the Reynolds number (Re), which in spray-drying processes is calculated for both gas and liquid streams, is used to assess the regime of the flow and the liquid jet breakup capability (Prigent *et al.*, 2022). When spraying the liquid stream is surrounded by a gas with greater momentum flux, thus the breakup of the jet is generated by the transfer of kinetic energy from the high-speed gas to the liquid, process known as air-blast atomization. (Lasheras *et al.*, 2020). The spraying is generated

at Reynolds in the order of 10^5 (turbulent), owing to short wavelength shear instabilities, indicating that at higher Reynolds numbers higher shear forces were present in the spraying step. In the Büchi Mini Spray Dryer B290 used in this thesis the Reynolds numbers obtained for the liquid and gas streams were Re<100 (laminar) and $3 \times 10^5 > Re > 6 \times 10^5$ (turbulent), respectively (Table 4.10 and Table 4.11 in Section **Erreur ! Source du renvoi introuvable.** -APPENDIX).

Figure 4.2 shows the aggregation level measured by DLS (Z-average) in F1.100 solution sprayed under different spraying conditions, represented by shear stress values. During these tests, the shear stresses ranged between 0.9×10^3 and 6.7×10^3 Pa. The red line in the figure corresponds to the level of protein aggregation in the stock (non-sprayed) solution, allowing us to see that no noticeable effect on aggregation was in fact observed under these conditions.

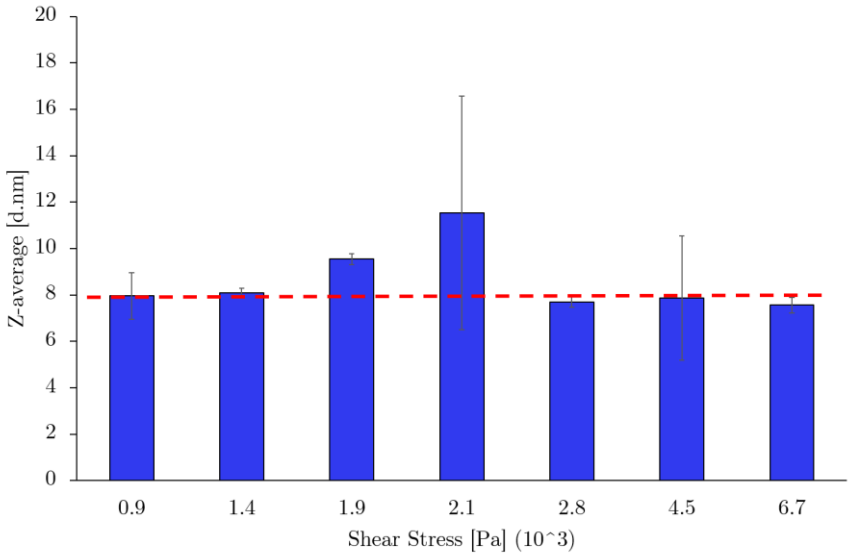

Figure 4.2. Effect of shear stress on the aggregation level (Z-average, measured by DLS), in the formulation F1.100 sprayed through the nozzle device of the Büchi Mini Spray Dryer B-290 (n=3).

We considered that the use of the shear stress [Pa] parameters was more pertinent to observe the impact on aggregation that the time of exposure during spray-drying had on the mAb-A. Meanwhile, in the literature this stress generated by the nozzle it is usually expressed in shear rate [s^1], the values we obtained for the shear rate are found in Section 4.5 – APPENDIX.

Results of aggregation, like those obtained for F1.100 (Z-average < 15 d.nm), were also observed with recombinant human growth hormone (rgGH) in a high pressure homogenizer (Maa *et al.*, 1998b), and sodium caseinate (Wang *et al.*, 2019) during similar tests of nozzle spraying, both within shear rates of $10^5 - 10^6$ [s^{-1}]. In these studies, no effect on aggregation was observed either. More, Jaspe *et al.* (2006) studied the impact of the shear stress on a protein flowing through a capillary system, going up to shear rates of 10^5 [s^{-1}]. finding no impact of this order of magnitude of shear rate on protein stability. A stress decoupling performed directly on the spray dryer (spraying step) has not yet been reported for monoclonal antibodies, although, similar experiments have been conducted on proteins like lactoferrin and caseinate (Dao *et al.*, 2022; Wang *et al.*, 2019).

The first results obtained from similar tests with BSA (Chapter 3, Section 3.5.1.1), showed Z-average ≈ 8 d.nm and 6-11 d.nm, at a concentration of 100 mg/ml and 200 mg/ml respectively, with the corresponding stock solution (non-treated) of 6 d.nm and 8 d.nm. For formulation F1.100 the results of the Z-average were around 8-12 d.nm and the stock solution Z-average value was around 8 d.nm. For both solutions, BSA (pure solution) and F1.100 (mAb-A formulated with excipients such as surfactants, amino acids and sugars), the shear forces generated in the tested conditions seem to have a mild impact on the aggregation phenomena.

It is true that in spray-drying, as well as in other drying processes, the stresses that can be imposed on proteins are often very dependent on the design of the equipment. We have tried to obtain during SST the widest range of stresses that can be undergone by proteins in terms of shear stresses, in the possible variation of the process parameters at the scale of the equipment available for this study. In terms of shear rate, the highest values achieved in our study were of 10^5 [s^{-1}] which remained in the same magnitude of value as the shear rate obtained with other bench scale spraying processes as we have just discussed. Using a mathematical model, it was found that apparently a shear rate of 10^7 [s^{-1}] will be necessary to denature a globular protein (Bee *et al.*, 2009; Jaspe *et al.*, 2006). Thus, considering this literature information, a shear rate of grater than 10^7 [s^{-1}] would have a degradation effect on proteins could be expected during the atomization step. This threshold might be a first consideration when setting the choice of atomization conditions for a larger scale operation.

Thermal and dehydration stresses (TDST) test with a single drying droplet set-up

The objective of the TDST test was to study the effect of thermal and dehydration stresses on mAb stability, dissociated from the disintegration step of the liquid formulation into droplets where the shear stress is involved.

Besides generating a heating environment for the droplet drying, the TDST test allows the follow-up of the evolution of drying kinetics of each droplet, both mAb-A formulations, F1.100 and F2.75, as represented in Figure 4.3. The initial and final droplets images as well as the mass evolution during TDST, can be observed in Figure 4.3. Given that both formulations have a very similar composition and total solid contents were quite close (14.6%wt for F1.100 and 17.3%wt for F2.75), both drying curves are very alike. In this figure the horizontal red lines, the solid (F2.75) and dotted (F1.100) respectively, indicated that the final mass expected at 100% water evaporation for the corresponding solid content are 1.04×10^{-3} gr and 0.87×10^{-3} gr, respectively for the volume used (6 µl). The vertical lines indicate the first appearance of the solid during drying, F2.75 (blue) and F1.100 (black), at 89 s for F1.100 and 48 s for F2.75.

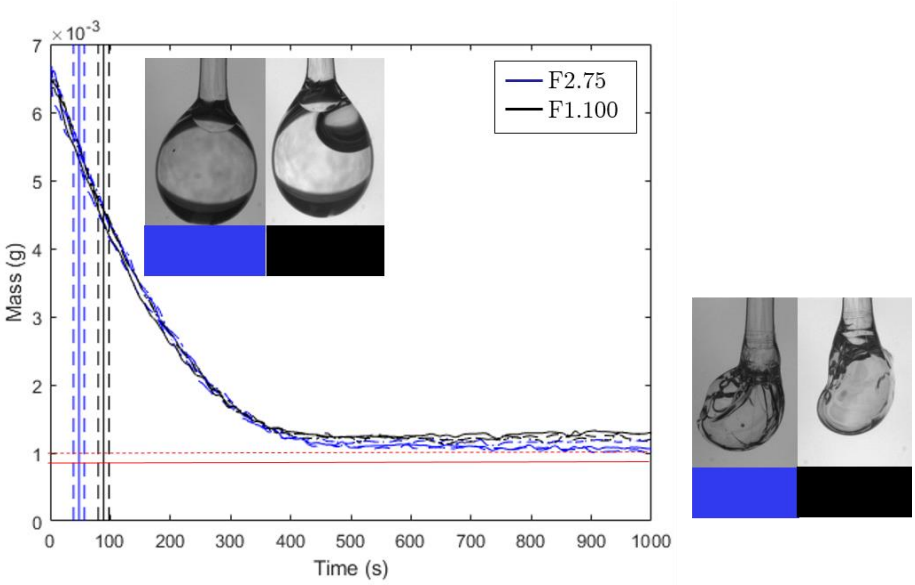

Figure 4.3. Evolution of the droplet mass during droplet drying (drying cycle of 2h): - the vertical lines indicate the time of first solid appearance for F2.75 (blue) and F1.100 (black); - the red horizontal lines indicate the theoretical mass of a final pure solid with a moisture content of 0% (solid red line for F2.75 and dotted red line for F1.100) (n=3)

At the end of experiments, as already explained, the dry droplet was detached from the filament and analysed by DLS for Z-average measurements. Figure 4.4 shows the values of Z-average measured for mAb-A formulations at the end of the cycle after, 2 and 3 hours: 8.8 d.nm (2h) and 9.5 d.nm (3h) for F1.100 and 9.6 d.nm (2h) and 10.4 d.nm (3h) for F2.75. This indicated a slight tendency of aggregation increase for longer drying periods, but the effect remained very weak.

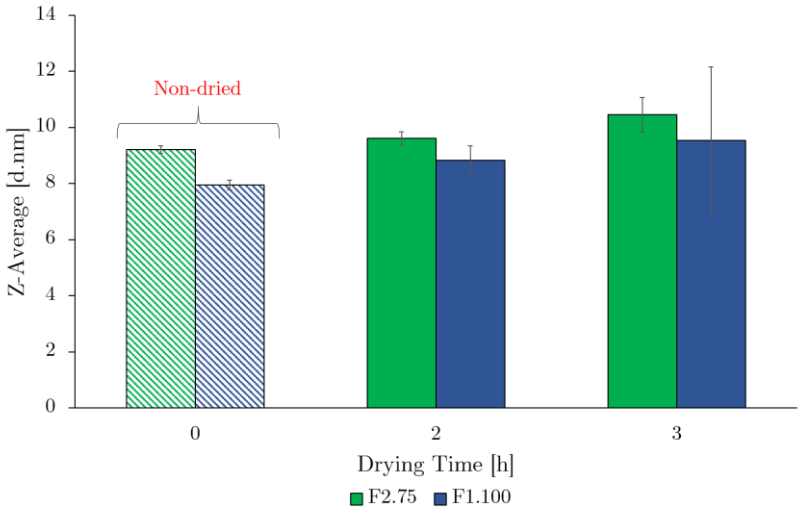

Figure 4.4. Effect of drying time on the aggregation level (Z-average measured by DLS) of dried droplets.(TDST) of mAb-A formulation F1.100 (n=3).

The pure solution of BSA (Chapter 3, Section 3.5.1.2) was more sensitive to aggregation during droplet drying (Z-Average of ≈ 75-100 d.nm), very likely due to the absence of stabilizers against dehydration/thermal stresses, which in the case of F1.100 and F2.75 were present.

Between F1.100 and F2.75 there seems to be a slight tendency of F1.100 to have a higher increase of aggregation with drying time (3 h), but overall, they seem to have excipients (trehalose, arginine, histidine and PS80) that can stabilize, under the studied drying conditions, the protein against thermal/dehydration stresses.

4.3.3 **Coupling of shear and thermal/dehydration stresses during spray-drying: effect on F1**

After investigating the effect of decoupled stresses in the previous Section (4.3.3), the F1.100 formulations were spray-dried and the aggregation levels of the reconstituted solutions were then measured by DLS.

The operating conditions for spray-drying of F1.100 was those coded C13 in Table 4.2 in Section Methods 4.2.2. They are as follows: nozzle diameter (0.7 mm), inlet temperature 105°C, liquid feed flow rate 4.5 ml/min drying airflow rate (22 m^3/h) and, atomization airflow rate (571 L/h) and shear stress of 3 × 10^3 Pa and an outlet temperature of 49°C.

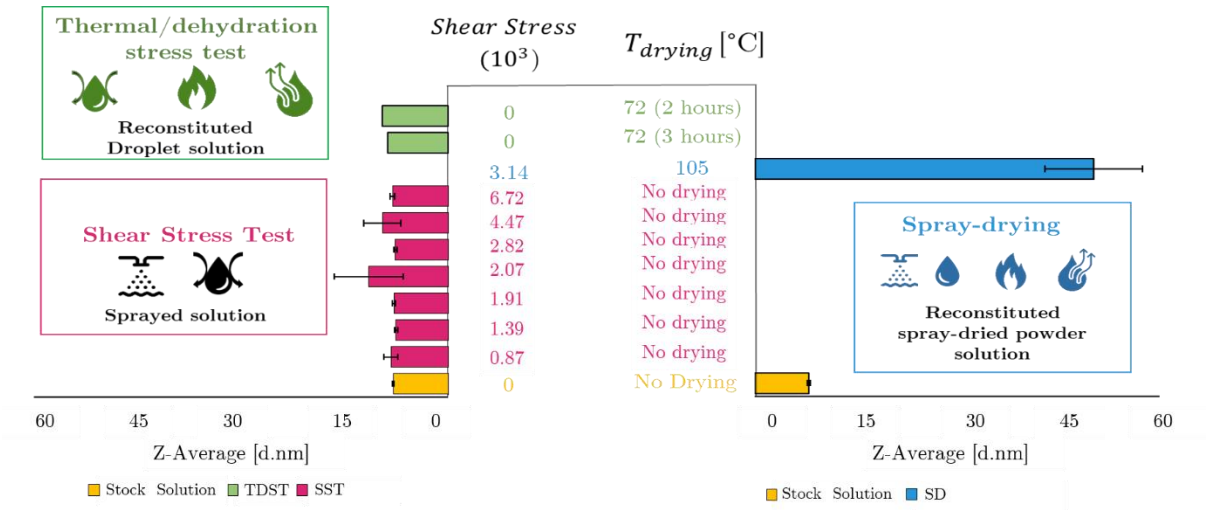

Figure 4.5. Aggregation resulting from the decoupling of shear (SST-pink bars) and thermal/dehydration (TDST- green bars) stresses on the (left side of the graph), compared to its coupling in the spray-drying process (blue bar) (right side of the graph). While the yellow bars correspond to the stock solution (n=3).

During spray-drying, in the drying chamber, right after being sprayed, the proteins are exposed to higher temperatures induced by the drying airflow rate. Given the low retention time in the drying chamber (<2 s) (Ousset *et al.*, 2018), it is unlikely that the drying air caused degradation since, at the early stage

of drying, where the droplet surface remains moisture saturated, the droplet surface temperature is maintained at the wet-bulb temperature (Table 4.2).

It is important to note that the droplet surface in contact with the drying air during the TDST is a lot smaller than the surface available for drying generated in the spraying step of the SD process. In fact, as it is not possible to measure experimentally the size distribution of the nebulized solution, we could estimate the mean size of a nebulized droplet from the dried particle, starting from the experimentally measured mean particle size of the spray-dried powder, using the mass conservation balance on the droplet during drying (Figure 4.6), as described below from Equation 4.1 to Equation 4.5.

$$V_{droplet}\rho_{droplet} = m_{droplet}$$

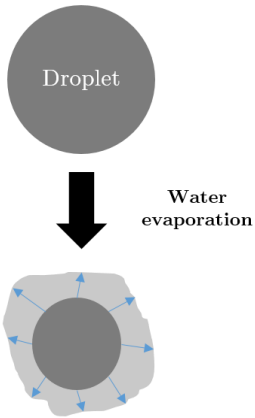

$$V_{particle}\rho_{particle} = V_{droplet}\rho_{droplet} - V_{droplet}\rho_{droplet}(1 - Solid\ Fraction)$$

Figure 4.6. Mass balance on the droplet generated during spraying for the dry particle generation.

$$m_{pa}x_{pa} = m_{dr} - m_{dr}(1 - x_{dr}) \quad (4.1)$$

$$V_{pa}\rho_{pa}x_{pa} = V_{dr}\rho_{dr} - V_{dr}\rho_{dr}(1 - x_{dr}) \quad (4.2)$$

$$V_{pa}\rho_{pa}x_{pa} = x_{dr}V_{dr}\rho_{dr} \quad (4.3)$$

$$\frac{V_{pa}}{V_{dr}} = \frac{\rho_{dr}x_{dr}}{\rho_{pa}x_{pa}} \quad (4.4)$$

$$\frac{D50_{pa}}{D50_{dr}} = \left(\frac{\rho_{dr}x_{dr}}{\rho_{pa}x_{pa}}\right)^{1/3} \quad (4.5)$$

Where $D50_{pa}$ is the particle diameter and $D50_{dr}$ is the droplet diameter, x_{dr} is the solid fraction in the droplet, x_{pa} is the solid fraction after spray-drying, which considers the final moisture content, ρ_{dr} is the droplet density and ρ_{pa} is the particle density, which is the mass of the particle divided by the volume of a sphere of diameter D_{pa}, it will include the internal and external voids. This apparent density can be calculated with a gas pycnometer using helium. All data required to perform the calculation of the droplet size ($D50_{dr}$) is presented in Table 4.3. The particle $D50_{pa}$ was obtained by laser granulometry, while the $D50_{dr}$ was obtained from the SEM observations (Figure 4.7 a-b).

Table 4.3. Data used for the calculation of the droplet size from the particle size of the dried powder of F1.100 and F2.75.

Formulation	Powder density ρ_{pa} [g/cm3]	MC [%]	Powder mass fraction x_{pa}	Liquid density ρ_{dr} [g/cm3]	Liquid mass fraction x_{dr}	D50 of particle [µm]
F2.75	1.1	5.24	0.9476	1.03	0.173	5.5
	1.21*	15**	0.8482	1.03	0.173	1632***
F1.100	1.18	5.14	0.95	1.03	0.15	5.45
	1.29*	20**	0.80	1.03	0.15	1720***

	$D50_{dr}$ Droplet [µm]	
Formulation	**SD**	**TDST**
F2.75	29.0	69773.0
F1.100	36	7563

*The density used for the particle was approximated by assuming its volume as a sphere, using the $D50_{dr}$, and using the mass of the dried particle.
** Moisture content was calculated from the initial solid content in the droplet and the final weight of the droplet.
***Approximated by SEM technique.

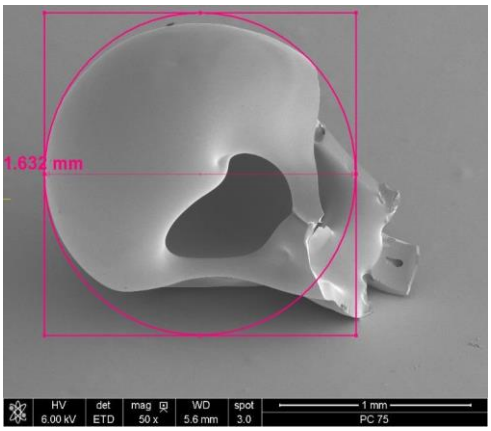

(a)

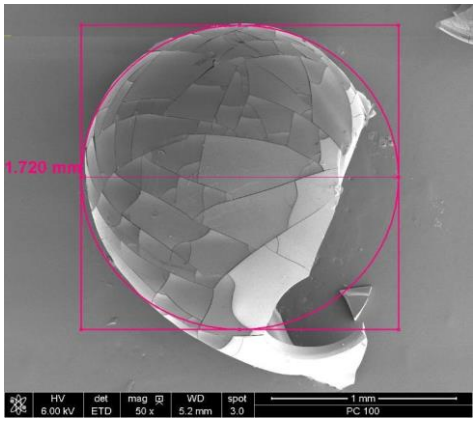

(b)

Figure 4.7. SEM Image of the dry particles produced in the TDST through the single drying droplet technique for formulations a) F2.75 and b) F1.100.

Starting with a dried particle size of about 5 μm and returning to the size of a droplet a value of about 29.3 μm and 35.6 μm for formulation F2.75 and F1.100 (Table 4.3), whereas when starting with diameters of dried particles of about 1632 μm (F2.75) and 1720 μm (F1.100) the diameters of the suspended single droplet were of approximately 6973 μm and 7563 respectively. Assuming that the droplets produced by spraying do not show high polydispersity, the available hanging droplet surface for drying is roughly about 250 times smaller than the one of the droplets produced during spray-drying.

In Figure 4.8 the turbidity of mAb-A after SST and SD can be visualized, which is linked to aggregation phenomena. This confirms the aggregation results measured by DLS and allows visualization of the impact of the coupling of mechanical, and thermal/dehydration on protein aggregation in the SD process. The volume of the solution corresponding to the reconstituted solid obtained from the drying droplet test (TDST) was too low to allow an image collection.

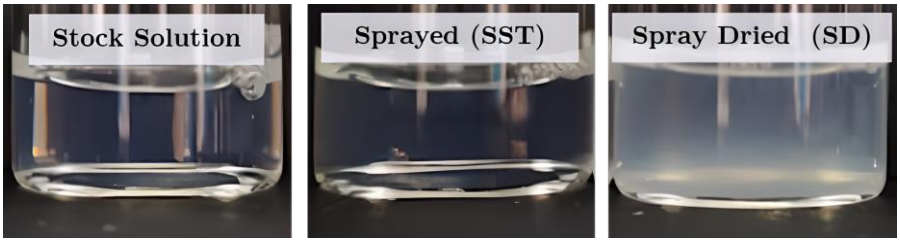

Figure 4.8. Pictures from formulation F1.100 a) Stock solution b) sprayed solution (from SST, non-dried), c) reconstituted solution from spray-dried powder

The results of stresses decoupling shows that each individual stress cannot account for the degradation of the mAb-A formulation, observed after spray-drying. It seems to be the combination of the different stresses that destabilize mAb-A, increasing its aggregation and consequently the turbidity in the reconstituted solution. Therefore, the next study focuses on a complementary study on spray-drying of mAb-A formulation where the operating conditions or the formulation composition (level of excipients and mAb-A concentration) are modified.

4.3.4 Spray-drying of mAb-A formulation: experimental studies

A first series of drying experiments was carried out aiming to investigate the impact of the operating conditions on the characteristics of the spray-dried powders (particle size, moisture content, protein aggregation level on reconstituted solutions) and process yield.

Then in a second series, the formulation composition was the studied parameter. The level of excipients and the mAb-A concentration were modified in comparison with F1.100.

4.3.4.1 First series: spray-drying of formulation F1.100 under varying operating conditions

The operating parameters for the first series of spray-drying experiments with formulation F1.100 were presented in Table 4.2 (Section 4.2.2.2). They correspond to 13 different experimental conditions, coded C1 to C13.

Table 4.4 presents some characteristics of the spray-dried powders (particle size and moisture content) obtained from experiments C1 to C13. The mean particle size is around 7-9 µm, within a particle size distribution from 2 μm (D10) to 26 μm (D90). These powders presented a moisture content from 5 to 7% w/w, within expected values for a lab-scale spray-dryer in the conditions used in this Section (Cabral-Marques *et al.*, 2009; Maa *et al.*, 1998a; Maury *et al.*, 2005; Wilson *et al.*, 2020; Ziaee *et al.*, 2019).

From the two-way ANOVA anaysis (p-values < 0.05), both moisture content (MC) and yield of the spray-dried powders was affected by both inlet air temperature (T) and liquid feed flow rate (LFFR) (Table 4.12 and

Table 4.13 in Section 4.5 – APPENDIX).

Figure 4.9 shows, for the two liquid feed flow rates (LFFR), the relationship between MC (Figure 4.9a) and process yield (Figure 4.9b) and the outlet air temperature (which was defined by the set of inlet operating conditions such as air inlet temperature, liquid feed flow rate, drying gas flow rate and nozzle size). For outlet temperatures ranging from 29°C and 54°C, the MC values are fairly close, with a lower moisture content seemingly corresponding to the lower LFFR value. Regarding the process yield, it increased when increasing the outlet temperature and it is possible to observe an improvement at LFFR of 3 ml/min.

Table 4.4. Physical characteristics from the spray-dried powders of F1.100 (first series) in terms of particle size distribution and moisture content. The particle size distribution of some tests was not retrieved.

	PSD [µm]			
Condition	**D10**	**D50**	**D90**	**Moisture Content [%]**
C1	-	-	-	6
C2	-	-	-	6
C3	2	7	15	5
C4	2	8	19	6
C5	2	9	19	7
C6	2	8	26	6
C7	-	-	-	6
C8	-	-	-	6
C9	2	8	18	6
C10	2	9	20	7
C11	2	8	16	6
C12	2	8	17	7
C13	2	9	23	7

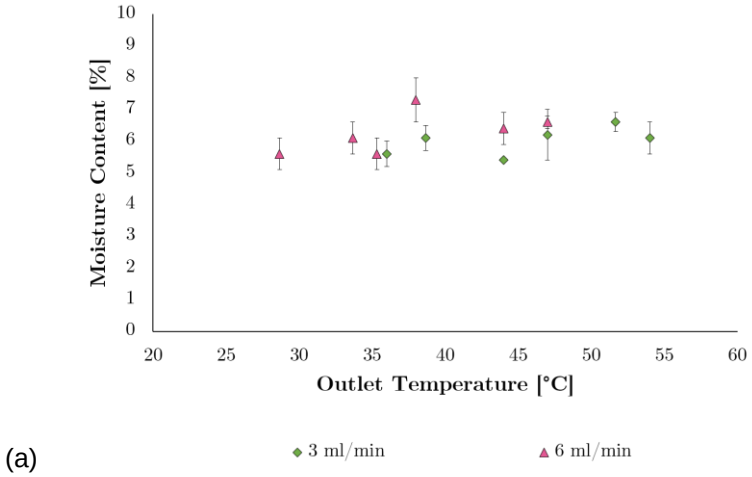

(a)

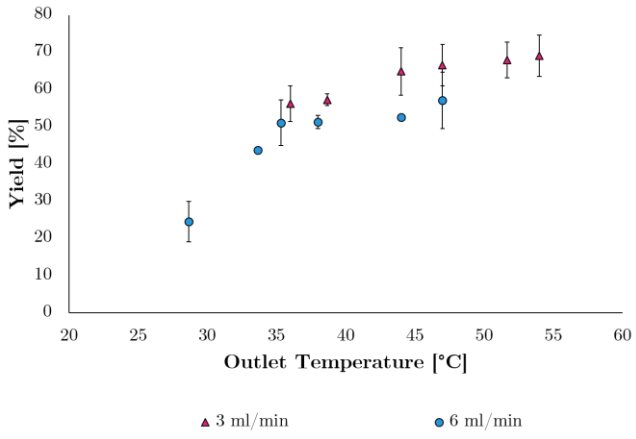

(b)

Figure 4.9. Impact of the outlet temperature on: a) spray-dried powder moisture content; b) process yield (n=3).

Figure 4.10 presents the effect of two parameters, the outlet air temperature and LFFR, on the aggregation protein level (Z-average from DLS) in reconstituted solutions. The shear stress values related to the LFFR of 3 ml/min and 6 ml/min represented in Figure 4.3.10 are on average 1.8×10^3 and 4.6×10^3 Pa , respectively (Table 4.8 and Table 4.9 – Section 4.5 APPENDIX) Accordingly, the two-way ANOVA test (p-values > 0.05) (Table 4.14 in Section 4.5 - APPENDIX), the inlet (LFFR) and outlet (T_{out}), set up by the inlet temperature, variables did not determine the level of protein aggregation (Z-average value). In fact, it can be observed in Figure 4.10 that $T_{out}$and LFFR do not have a direct correlation with the aggregation level.

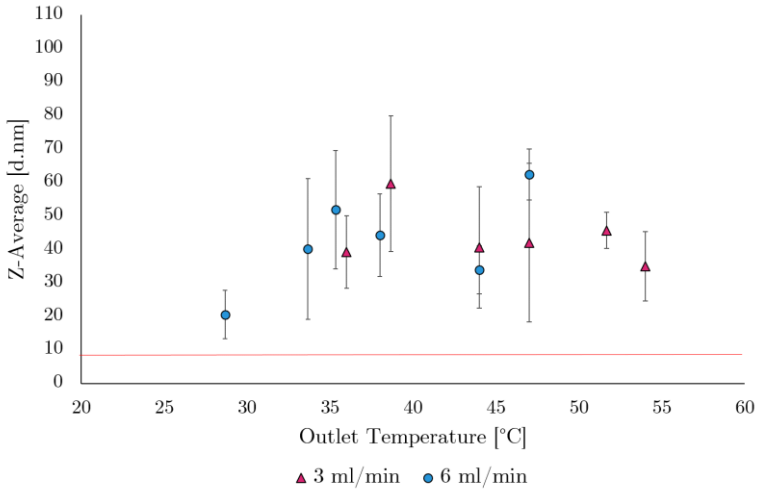

Figure 4.10. Aggregation (Z-average, measured by DLS) on spray-dried F1.100 powder as a function of the outlet temperature (the red line indicates Z-average of the stock solution of F1.100) (n=3).

The objective of this first series was to investigate the effect of some spray-drying process parameters on relevant powder properties such as the residual water content and on technical feasibility parameters such as the yield. From the results obtained, and according to the previous discussion on T_{out} and LFFR impact, the following values were the chosen conditions for further investigation concerning formulation parameters:

- Intermediate value of LFFR 4.5 ml/min.
- Inlet air temperature T_{in} of 105°C to reduce aggregation values and MC, while increasing the yield.
- The other operating conditions are nozzle diameter 0.7 mm, drying airflow rate 22 m^3/h and atomization airflow rate 571 L/h.

4.3.4.2 Second Series: Spray-drying of MAb-A formulations F1.100, F2.100 and F2.75 under selected operating conditions in First Series.

In this series, the mAb-A aggregation was studied as a function of the formulation composition. The level of excipients and the mAb-A concentration were modified in comparison with F1.100.

Placebo effect (F1.100)

Before proceeding to the variation of the mAb-A formulation, the effect of the SD process on the F1.100 formulation without mAb (named Placebo) was tested under the selected spray-drying conditions described at the end of the first series of experiments.

Figure 4.11 compares the level of aggregation, given in NTU, measured in reconstituted Placebo solution and in the same stock solution (non-dried). As expected, the SD processing did not modify the turbidity after reconstitution, which points to the presence of the mAb-A as the principal factor for the

previously observed turbidity in the reconstituted F1.100 solutions (76-105 NTU). This overrules the possibility of excipients having any undesired interactions during spray-drying and reconstitution processes.

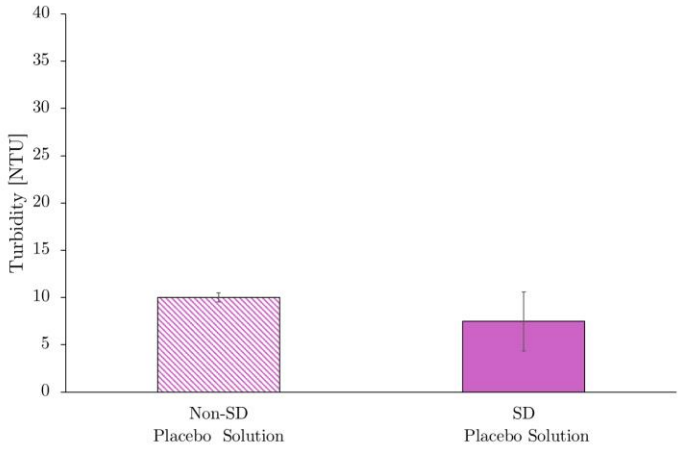

Figure 4.11. Comparison between turbidity measurements of the Placebo formulation (did NOT contain mAb-A) before and after spray-drying processing (n=3).

A new formulation for testing F2

To understand the influence that excipients may have on the aggregation phenomenon observed for the spray-dried powders, a new formulation was tested: F2.100.

The formulation F2.100 contains the same concentration of mAb-A (100 mg/ml), and a higher concentration of the same excipients: Arginine 53mM, Trehalose 8.6% w/w, and Tween-80 0.075% w/v for F2.100 against L-Arginine 25mM, Trehalose 4% w/w and Polysorbate-80 (PS80) 0.02% w/v for F1.100, Histidine is at 5 mM for both formulations.

Another important formulation parameter studied was the concentration of mAb-A in the liquid formulation. For this purpose, the concentration of mAb in the formulation F2 was reduced from 100 mg/ml to 75 mg/ml, resulting in a formulation called F2.75.

F2.100 and F2.75 were then spray dried and reconstituted solutions from the spray-dried powders were analysed by DLS in order to identify and compare protein aggregation. The Z-average results after SD and reconstituted to the same initial protein and excipients concentration can be seen in Figure 4.12.

The reconstituted solutions presented a real concentration of 93.4 mg/ml for F1.100, 95.3 mg/ml for F2.100 and of 72.3 mg/ml for formulation F2.75, measured by UV visible spectroscopy.

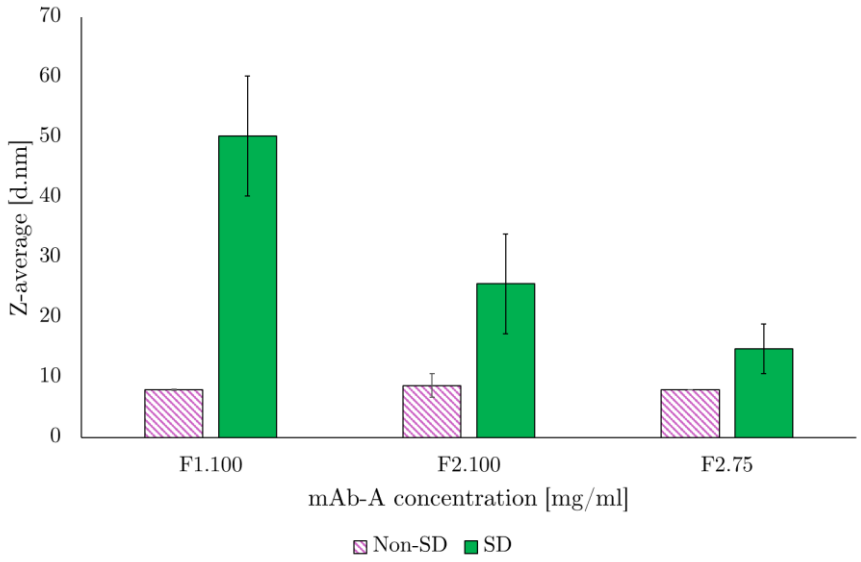

Figure 4.12. Z-average for stock solutions (non-spray-dried) and solutions reconstituted for spray-dried powders of F2 and F1 formulations (n=3).

The results shown in Figure 4.12 revealed that both excipient and protein concentrations, have a significant impact on the aggregation level of the reconstituted solution. The Z-average measured for reconstituted solutions for spray-dried F1.100 and F2.100 powders demonstrated that an increase in excipients concentration led to a reduction in protein aggregation.

Regarding the composition, the formulation F2.100 contains the same concentration of mAb-A (100 mg/ml) as F1.100, however a higher concentration of the same excipients: L-Arginine 53mM, Trehalose 8.6% w/w, and Tween-80 0.075% w/v for F2.100 against L-Arginine 25mM, Trehalose 4% w/w and Polysorbate-80 (PS80) 0.02% w/v for F1.100. In addition, the optical inspection (Figure 4.13) confirmed the difference in turbidity between the three reconstituted solutions, F1.100, F2.100 and F2.75.

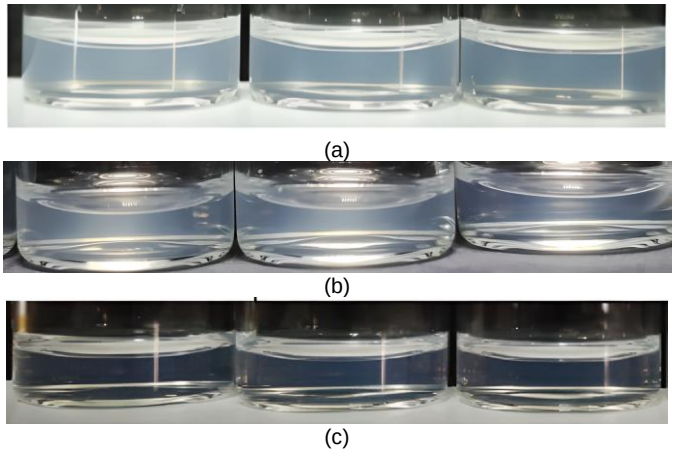

Figure 4.13. Optical inspection of reconstituted solutions from spray-dried powders a) F1.100, b) F2.100, c) F2.75.

Both stock solutions, F1.100 and F2.100, showed Z-average values of 8.3 d.nm and 9.6 d.nm, which upon spray-drying increased drastically for F1.100, compared to F2.100 (Figure 4.12). As the Z-average

measures the size distribution of the sample, the presence of higher aggregate conglomerates in the sample will increase the Z-average value. Zhou *et al.* (2015) also showed that when mAbs are exposed to the same thermal stress conditions, their Z-average will be higher for those formulations with higher mAb concentration (Zhou *et al.*, 2015), which is consistent with the results presented here.

The comparison between F2.100 and F2.75 revealed a decrease in Z-average (Figure 2.11), confirmed by turbidity measurements (103±2 and 50±1), which is directly related to the protein concentration. Both changes, an increase in the excipient concentration and the reduction of the mAb-A concentration, provided the formulation with a higher stability, which is F2.75. The images of the optical inspection in Figure 2.12 confirmed the difference in turbidity between the two reconstituted solutions, F1.100 and F2.75.

The increase of mAb-A aggregation at higher protein concentrations is prone to occur given the high potential of protein-protein interactions and the macromolecular crowding in solution that mAbs have, which was avoided by the use of excipients such as sugars and surfactants (Baek *et al.*, 2017; Jordan *et al.*, 1994; Kannan *et al.*, 2019). In addition, compared to F1.100 formulation, the increase of the concentration of excipients in the F2 formulations ensures a better protection of mAb-A from the several sources of stress required by spray-drying.

Some physical properties of the spray dried powders from F1.100, F2.100 and F2.75 formulations are grouped in Table 4.5.

Table 4.5. Physical characteristics form the powder obtained at fixed SD configuration for three different formulation compositions (F1.100, F2.100, F2.75).

		PSD [µm]			
Formulation	**Mass fraction**	**D10**	**D50**	**D90**	**Average Moisture Content [%]**
F1.100	0.146	2±0.1	7.7±1.7	17±1.7	6.8±0.3
F2.100	0.198	2.2±0.2	6.9±1.1	17.2±1.7	4.9±0.1
F2.75	0.173	2.3±0.9	8.2±0.6	15.7±1.5	5.1±0.1

These powders presented a moisture content (MC) ranging from 4.9 to 6.8% w/w. As shown in Table 4.5, the powder MC is mostly affected by the dry weight content in formulations, where the higher the dry weight content the lower will be the MC.

Regarding powder granulometry, the mean particle size is around 6.9-8.5 µm, within a particle size distribution from 2 µm (D10) to 17.2 µm (D90).

Process yield, on the other hand, showed no direct correlation to the change of the concentration of excipients in the formulation with slight variations around 70%.

4.4 Synthesis Chapter 4

It was important for us to study, in an individual way, the effect of different sources of stress on the protein stability found in the spray-drying process. Therefore, this chapter revisited the decoupling of stresses techniques used in the previous chapter with the model protein (BSA) and applied them to a mAb-A formulation, which has not been studied with this approach.

Results showed that decoupled thermal/dehydration and shear stresses are not as detrimental for mAb-A formulation F1.100, as when coupled in the spray-drying process.

As well, the formulation composition (protein and excipient concentration) had a bigger impact on the mAb-A stabilization than the process operating parameters, indicated by a decrease in the protein concentration (100 mg/ml to 75 mg/ml) and increasing the excipients concentration.

We could observe that the change in the formulation composition was more effective in improving the formulation stability than the process parameters of spray-drying. This finding opened the possibility to explore the level of protection that every excipient offers to mAb-A, which was performed in the next study presented in Chapter 5.

4.5 APPENDIX

Shear rate, shear stress and shear strain from Shear Stress Test (SST) (F1.100)

Table 4.6. Data used for the calculation of the Shear Rate values of the shear stress test at different operating conditions in a Büchi Mini Spray Dryer B-290.

		Ml	**Mg**	**dl**	**dg**	**QL**	**QG**	**Dneedle**	**Din,liq**	**Dex,liq**	**Dgas**	**Aliq**	**Agas**	**VL**	**VG**	**Vav**	**gamma**
		[kg/s]	*[kg/s]*	*[kg/m3]*	*[kg/m3]*	*[m3/s]*	*[m3/s]*	*[m]*	*[m]*	*[m]*	*[m]*	*[m2]*	*[m2]*	*[m/s]*	*[m/s]*	*[m/s]*	*[1/s]*
Condition	*Nozzle [mm]*	*mass flow liquid*	*mass flow gas*	*density*	*density*	*volumetric flow liquid*	*volumetric flow gas*	*Diameter center needle*	*Inner Diameter liquid*	*External diameter liquid*	*Inner diameter gas*	*Cross-Sectional area liquid*	*Cross-Sectional area gas*	*liquid velocity*	*gas velocity*	*average velocity*	*Shear Rate*
SST 1	0.5	5E-05	2E-04	1000	1.2	5.0E-08	1.6E-04	4.5E-04	5.0E-04	1.2E-03	1.5E-03	3.7E-08	6.8E-07	1.3E+00	2.3E+02	1.8E+02	7.3E+05
SST 2	0.5	2E-04	2E-04	1000	1.2	1.7E-07	1.6E-04	4.5E-04	5.0E-04	1.2E-03	1.5E-03	3.7E-08	6.8E-07	4.5E+00	2.3E+02	1.3E+02	4.9E+05
SST 3	0.5	3E-04	2E-04	1000	1.2	3.4E-07	1.6E-04	4.5E-04	5.0E-04	1.2E-03	1.5E-03	3.7E-08	6.8E-07	9.1E+00	2.3E+02	8.9E+01	3.2E+05
SST 4	0.7	4E-04	2E-04	1000	1.2	3.9E-07	1.6E-04	6.3E-04	7.0E-04	1.2E-03	1.5E-03	7.3E-08	7.2E-07	5.3E+00	2.2E+02	7.6E+01	2.0E+05
SST 5	2	4E-05	2E-04	1000	1.2	3.9E-08	1.6E-04	1.9E-03	2.0E-03	2.5E-03	2.6E-03	2.5E-07	5.7E-07	1.6E-01	2.8E+02	2.3E+02	2.3E+05
SST 6	2	2E-04	2E-04	1000	1.2	1.6E-07	1.6E-04	1.9E-03	2.0E-03	2.5E-03	2.6E-03	2.5E-07	5.7E-07	6.5E-01	2.8E+02	1.5E+02	1.5E+05
SST 7	2	4E-04	2E-04	1000	1.2	3.7E-07	1.6E-04	1.9E-03	2.0E-03	2.5E-03	2.6E-03	2.5E-07	5.7E-07	1.5E+00	2.8E+02	9.6E+01	9.4E+04
SST 8	0.5	5E-05	2E-04	1000	1.2	4.7E-08	1.6E-04	4.5E-04	5.0E-04	1.2E-03	1.5E-03	3.7E-08	6.8E-07	1.3E+00	2.3E+02	1.9E+02	7.4E+05
SST 9	0.5	2E-04	2E-04	1000	1.2	1.6E-07	1.6E-04	4.5E-04	5.0E-04	1.2E-03	1.5E-03	3.7E-08	6.8E-07	4.3E+00	2.3E+02	1.3E+02	4.9E+05
SST 10	0.5	4E-04	2E-04	1000	1.2	3.7E-07	1.6E-04	4.5E-04	5.0E-04	1.2E-03	1.5E-03	3.7E-08	6.8E-07	9.8E+00	2.3E+02	8.6E+01	3.0E+05
SST 11	0.7	4E-04	2E-04	1000	1.2	3.6E-07	1.6E-04	6.3E-04	7.0E-04	1.2E-03	1.5E-03	7.3E-08	7.2E-07	4.9E+00	2.2E+02	7.9E+01	2.1E+05
SST 12	2	5E-05	2E-04	1000	1.2	4.7E-08	1.6E-04	1.9E-03	2.0E-03	2.5E-03	2.6E-03	2.5E-07	5.7E-07	1.9E-01	2.8E+02	2.2E+02	2.2E+05
SST 13	2	2E-04	2E-04	1000	1.2	1.6E-07	1.6E-04	1.9E-03	2.0E-03	2.5E-03	2.6E-03	2.5E-07	5.7E-07	6.4E-01	2.8E+02	1.5E+02	1.5E+05
SST 14	2	4E-04	2E-04	1000	1.2	3.5E-07	1.6E-04	1.9E-03	2.0E-03	2.5E-03	2.6E-03	2.5E-07	5.7E-07	1.4E+00	2.8E+02	1.0E+02	9.8E+04
SST 15	0.5	5E-05	2E-04	1000	1.2	4.8E-08	1.6E-04	4.5E-04	5.0E-04	1.2E-03	1.5E-03	3.7E-08	6.8E-07	1.3E+00	2.3E+02	1.9E+02	7.4E+05
SST 16	0.5	2E-04	2E-04	1000	1.2	1.6E-07	1.6E-04	4.5E-04	5.0E-04	1.2E-03	1.5E-03	3.7E-08	6.8E-07	4.3E+00	2.3E+02	1.3E+02	4.9E+05
SST 17	0.5	4E-04	2E-04	1000	1.2	3.7E-07	1.6E-04	4.5E-04	5.0E-04	1.2E-03	1.5E-03	3.7E-08	6.8E-07	9.9E+00	2.3E+02	8.5E+01	3.0E+05
SST 18	0.7	4E-04	2E-04	1000	1.2	3.6E-07	1.6E-04	6.3E-04	7.0E-04	1.2E-03	1.5E-03	7.3E-08	7.2E-07	4.9E+00	2.2E+02	7.9E+01	2.1E+05
SST 19	2	5E-05	2E-04	1000	1.2	4.9E-08	1.6E-04	1.9E-03	2.0E-03	2.5E-03	2.6E-03	2.5E-07	5.7E-07	2.0E-01	2.8E+02	2.2E+02	2.2E+05
SST 20	2	2E-04	2E-04	1000	1.2	1.6E-07	1.6E-04	1.9E-03	2.0E-03	2.5E-03	2.6E-03	2.5E-07	5.7E-07	6.5E-01	2.8E+02	1.5E+02	1.5E+05
SST 21	2	4E-04	2E-04	1000	1.2	3.7E-07	1.6E-04	1.9E-03	2.0E-03	2.5E-03	2.6E-03	2.5E-07	5.7E-07	1.5E+00	2.8E+02	9.6E+01	9.5E+04

Table 4.7. Data used for the calculation of the shear strain and shear stress values of shear stress test using previous calculated shear rate in Table 4.6 in a Büchi Mini Spray Dryer B-290.

Condition	Feed Flow Rate [ml/min]	Nozzle [mm]	Shear Rate [1/s]	Volume of nozzle device [m3]	Liquid Flow Rate [m3/s]	Residence Time [s]	Shear Strain (γ)	Shear Stress [Pa]
SST 1	3.0E+00	5.0E-01	7.3E+05	5.3E-10	5.0E-08	1.1E-02	7.8E+03	6.7E+03
SST 2	1.0E+01	5.0E-01	4.9E+05	5.3E-10	1.7E-07	3.2E-03	1.5E+03	4.4E+03
SST 3	2.0E+01	5.0E-01	3.2E+05	5.3E-10	3.4E-07	1.6E-03	5.0E+02	2.9E+03
SST 4	2.3E+01	7.0E-01	2.0E+05	5.4E-10	3.9E-07	1.4E-03	2.8E+02	1.8E+03
SST 5	2.3E+00	2.0E+00	2.3E+05	1.6E-09	3.9E-08	4.3E-02	9.9E+03	2.1E+03
SST 6	9.6E+00	2.0E+00	1.5E+05	1.6E-09	1.6E-07	1.0E-02	1.6E+03	1.4E+03
SST 7	2.2E+01	2.0E+00	9.4E+04	1.6E-09	3.7E-07	4.4E-03	4.2E+02	8.6E+02
SST 8	2.8E+00	5.0E-01	7.4E+05	5.3E-10	4.7E-08	1.1E-02	8.4E+03	6.8E+03
SST 9	9.7E+00	5.0E-01	4.9E+05	5.3E-10	1.6E-07	3.3E-03	1.6E+03	4.5E+03
SST 10	2.2E+01	5.0E-01	3.0E+05	5.3E-10	3.7E-07	1.5E-03	4.4E+02	2.8E+03
SST 11	2.2E+01	7.0E-01	2.1E+05	5.4E-10	3.6E-07	1.5E-03	3.2E+02	1.9E+03
SST 12	2.8E+00	2.0E+00	2.2E+05	1.6E-09	4.7E-08	3.5E-02	7.8E+03	2.0E+03
SST 13	9.5E+00	2.0E+00	1.5E+05	1.6E-09	1.6E-07	1.0E-02	1.6E+03	1.4E+03
SST 14	2.1E+01	2.0E+00	9.8E+04	1.6E-09	3.5E-07	4.7E-03	4.6E+02	8.9E+02
SST 15	2.9E+00	5.0E-01	7.4E+05	5.3E-10	4.8E-08	1.1E-02	1.6E-04	6.7E+03
SST 16	9.7E+00	5.0E-01	4.9E+05	5.3E-10	1.6E-07	3.3E-03	1.6E+03	4.5E+03
SST 17	2.2E+01	5.0E-01	3.0E+05	5.3E-10	3.7E-07	1.4E-03	4.3E+02	2.8E+03
SST 18	2.2E+01	7.0E-01	2.1E+05	5.4E-10	3.6E-07	1.5E-03	3.2E+02	1.9E+03
SST 19	2.9E+00	2.0E+00	2.2E+05	1.6E-09	4.9E-08	3.3E-02	7.4E+03	2.0E+03
SST 20	9.7E+00	2.0E+00	1.5E+05	1.6E-09	1.6E-07	1.0E-02	1.5E+03	1.4E+03
SST 21	2.2E+01	2.0E+00	9.5E+04	1.6E-09	3.7E-07	4.4E-03	4.2E+02	8.6E+02

Spray-drying (F1.100)

Table 4.8. Data used for the calculation of the Shear Rate values of spray-drying at different operating conditions in a Büchi Mini Spray Dryer B-290.

		Ml	**Mg**	**dl**	**dg**	**QL**	**QG**	**Dneedle**	**Din,liq**	**Dex,liq**	**Dgas**	**Aliq**	**Agas**	**VL**	**VG**	**Vav**	**gamma**
		[kg/s]	*[kg/s]*	*[kg/m3]*	*[kg/m3]*	*[m3/s]*	*[m3/s]*	*[m]*	*[m]*	*[m]*	*[m]*	*[m2]*	*[m2]*	*[m/s]*	*[m/s]*	*[m/s]*	*[1/s]*
Condition	*Nozzle [mm]*	*mass flow liquid*	*mass flow gas*	*density*	*density*	*volumetric flow liquid*	*volumetric flow gas*	*Diameter center needle*	*Inner Diameter liquid*	*External diameter liquid*	*Inner diameter gas*	*Cross-Sectional area liquid*	*Cross-Sectional area gas*	*liquid velocity*	*gas velocity*	*average velocity*	*Shear Rate*
SD 1	0.7	1.67E-05	1.90E-04	1000	1.2	1.67E-08	1.59E-04	6.30E-04	7.00E-04	1.18E-03	1.52E-03	7.31E-08	7.21E-07	2.28E-01	2.20E+02	2.02E+02	5.77E+05
SD 2	0.7	3.33E-05	1.90E-04	1000	1.2	3.33E-08	1.59E-04	6.30E-04	7.00E-04	1.18E-03	1.52E-03	7.31E-08	7.21E-07	4.56E-01	2.20E+02	1.87E+02	5.34E+05
SD 3	0.7	5.00E-05	1.90E-04	1000	1.2	5.00E-08	1.59E-04	6.30E-04	7.00E-04	1.18E-03	1.52E-03	7.31E-08	7.21E-07	6.84E-01	2.20E+02	1.74E+02	4.96E+05
SD 4	0.7	6.67E-05	1.90E-04	1000	1.2	6.67E-08	1.59E-04	6.30E-04	7.00E-04	1.18E-03	1.52E-03	7.31E-08	7.21E-07	9.12E-01	2.20E+02	1.63E+02	4.64E+05
SD 5	0.7	8.33E-05	1.90E-04	1000	1.2	8.33E-08	1.59E-04	6.30E-04	7.00E-04	1.18E-03	1.52E-03	7.31E-08	7.21E-07	1.14E+00	2.20E+02	1.53E+02	4.35E+05
SD 6	0.7	1.00E-04	1.90E-04	1000	1.2	1.00E-07	1.59E-04	6.30E-04	7.00E-04	1.18E-03	1.52E-03	7.31E-08	7.21E-07	1.37E+00	2.20E+02	1.45E+02	4.09E+05
SD 7	0.7	1.17E-04	1.90E-04	1000	1.2	1.17E-07	1.59E-04	6.30E-04	7.00E-04	1.18E-03	1.52E-03	7.31E-08	7.21E-07	1.60E+00	2.20E+02	1.37E+02	3.87E+05
SD 8	0.7	1.33E-04	1.90E-04	1000	1.2	1.33E-07	1.59E-04	6.30E-04	7.00E-04	1.18E-03	1.52E-03	7.31E-08	7.21E-07	1.82E+00	2.20E+02	1.30E+02	3.67E+05
SD 9	0.7	1.50E-04	1.90E-04	1000	1.2	1.50E-07	1.59E-04	6.30E-04	7.00E-04	1.18E-03	1.52E-03	7.31E-08	7.21E-07	2.05E+00	2.20E+02	1.24E+02	3.48E+05
SD 10	0.7	1.67E-04	1.90E-04	1000	1.2	1.67E-07	1.59E-04	6.30E-04	7.00E-04	1.18E-03	1.52E-03	7.31E-08	7.21E-07	2.28E+00	2.20E+02	1.18E+02	3.32E+05
SD 11	0.7	1.83E-04	1.90E-04	1000	1.2	1.83E-07	1.59E-04	6.30E-04	7.00E-04	1.18E-03	1.52E-03	7.31E-08	7.21E-07	2.51E+00	2.20E+02	1.13E+02	3.17E+05
SD 12	0.7	2.00E-04	1.90E-04	1000	1.2	2.00E-07	1.59E-04	6.30E-04	7.00E-04	1.18E-03	1.52E-03	7.31E-08	7.21E-07	2.74E+00	2.20E+02	1.09E+02	3.03E+05
SD 13	0.7		1.90E-04	1000	1.2	2.17E-07	1.59E-04	6.30E-04	7.00E-04	1.18E-03	1.52E-03	7.31E-08	7.21E-07	2.96E+00	2.20E+02	2.20E+02	6.20E+05
SD 14	0.7	2.33E-04	1.90E-04	1000	1.2	2.33E-07	1.59E-04	6.30E-04	7.00E-04	1.18E-03	1.52E-03	7.31E-08	7.21E-07	3.19E+00	2.20E+02	1.01E+02	2.78E+05
SD 15	0.7	2.50E-04	1.90E-04	1000	1.2	2.50E-07	1.59E-04	6.30E-04	7.00E-04	1.18E-03	1.52E-03	7.31E-08	7.21E-07	3.42E+00	2.20E+02	9.70E+01	2.67E+05
SD 16	0.7	2.67E-04	1.90E-04	1000	1.2	2.67E-07	1.59E-04	6.30E-04	7.00E-04	1.18E-03	1.52E-03	7.31E-08	7.21E-07	3.65E+00	2.20E+02	9.38E+01	2.57E+05
SD 17	0.7	2.83E-04	1.90E-04	1000	1.2	2.83E-07	1.59E-04	6.30E-04	7.00E-04	1.18E-03	1.52E-03	7.31E-08	7.21E-07	3.87E+00	2.20E+02	9.07E+01	2.48E+05
SD 18	0.7	3.00E-04	1.90E-04	1000	1.2	3.00E-07	1.59E-04	6.30E-04	7.00E-04	1.18E-03	1.52E-03	7.31E-08	7.21E-07	4.10E+00	2.20E+02	8.79E+01	2.39E+05
SD 19	0.7	3.17E-04	1.90E-04	1000	1.2	3.17E-07	1.59E-04	6.30E-04	7.00E-04	1.18E-03	1.52E-03	7.31E-08	7.21E-07	4.33E+00	2.20E+02	8.53E+01	2.31E+05
SD 20	0.7	3.33E-04	1.90E-04	1000	1.2	3.33E-07	1.59E-04	6.30E-04	7.00E-04	1.18E-03	1.52E-03	7.31E-08	7.21E-07	4.56E+00	2.20E+02	8.29E+01	2.24E+05

SD 21	0.7	3.50E-04	1.90E-04	1000	1.2	3.50E-07	1.59E-04	6.30E-04	7.00E-04	1.18E-03	1.52E-03	7.31E-08	7.21E-07	4.79E+00	2.20E+02	8.06E+01	2.17E+05
SD 22	0.7	3.67E-04	1.90E-04	1000	1.2	3.67E-07	1.59E-04	6.30E-04	7.00E-04	1.18E-03	1.52E-03	7.31E-08	7.21E-07	5.01E+00	2.20E+02	7.85E+01	2.10E+05
SD 23	0.7	3.83E-04	1.90E-04	1000	1.2	3.83E-07	1.59E-04	6.30E-04	7.00E-04	1.18E-03	1.52E-03	7.31E-08	7.21E-07	5.24E+00	2.20E+02	7.65E+01	2.04E+05
SD 24	0.7	4.00E-04	1.90E-04	1000	1.2	4.00E-07	1.59E-04	6.30E-04	7.00E-04	1.18E-03	1.52E-03	7.31E-08	7.21E-07	5.47E+00	2.20E+02	7.46E+01	1.98E+05
SD 25	0.7	4.17E-04	1.90E-04	1000	1.2	4.17E-07	1.59E-04	6.30E-04	7.00E-04	1.18E-03	1.52E-03	7.31E-08	7.21E-07	5.70E+00	2.20E+02	7.29E+01	1.92E+05
SD 26	0.7	4.33E-04	1.90E-04	1000	1.2	4.33E-07	1.59E-04	6.30E-04	7.00E-04	1.18E-03	1.52E-03	7.31E-08	7.21E-07	5.93E+00	2.20E+02	7.13E+01	1.87E+05

Table 4.9. Data used for the calculation of the shear strain and shear stress values of spray-drying using previous calculated shear rate in Table 4.8 in a Büchi Mini Spray Dryer B-290.

Condition	Feed Flow Rate [ml/min]	Nozzle [mm]	Shear Rate [1/s]	Volume of nozzle device [m3]	Liquid Flow Rate [m3/s]	Residence Time [s]	Shear Strain (γ)	Shear Stress [Pa]
1	3.52	0.7	4.79E+05	5.44E-10	5.863E-08	9.29E-03	4.4E+03	4.37E+03
2	3.45	0.7	4.81E+05	5.44E-10	5.755E-08	9.459E-03	4.5E+03	4.39E+03
3	3.43	0.7	4.82E+05	5.44E-10	5.711E-08	9.531E-03	4.6E+03	4.39E+03
4	3.43	0.7	4.82E+05	5.44E-10	5.711E-08	9.531E-03	4.6E+03	4.39E+03
5	5.62	0.7	4.19E+05	5.44E-10	9.372E-08	5.809E-03	2.4E+03	3.82E+03
6	6.51	0.7	3.98E+05	5.44E-10	1.084E-07	5.020E-03	2.0E+03	3.63E+03
7	6.43	0.7	4.00E+05	5.44E-10	1.071E-07	5.083E-03	2.0E+03	3.64E+03
8	6.52	0.7	3.97E+05	5.44E-10	1.086E-07	5.012E-03	2.0E+03	3.62E+03
9	3.68	0.7	4.74E+05	5.44E-10	6.135E-08	8.873E-03	4.2E+03	4.32E+03
10	3.23	0.7	4.88E+05	5.44E-10	5.391E-08	1.010E-02	4.9E+03	4.45E+03
11	3.71	0.7	4.73E+05	5.44E-10	6.177E-08	8.813E-03	4.2E+03	4.31E+03
12	3.73	0.7	4.72E+05	5.44E-10	6.220E-08	8.752E-03	4.1E+03	4.30E+03
13	6.88	0.7	6.24E+05	5.44E-10	1.146E-07	4.749E-03	3.0E+03	5.69E+03
14	6.32	0.7	4.02E+05	5.44E-10	1.053E-07	5.168E-03	2.1E+03	3.67E+03
15	7.04	0.7	3.86E+05	5.44E-10	1.173E-07	4.640E-03	1.8E+03	3.52E+03
16	7.21	0.7	3.83E+05	5.44E-10	1.201E-07	4.533E-03	1.7E+03	3.49E+03
17	3.70	0.7	4.73E+05	5.44E-10	6.170E-08	8.823E-03	4.2E+03	4.31E+03
18	3.69	0.7	4.73E+05	5.44E-10	6.152E-08	8.848E-03	4.2E+03	4.32E+03
19	3.68	0.7	4.74E+05	5.44E-10	6.132E-08	8.878E-03	4.2E+03	4.32E+03
20	3.60	0.7	4.76E+05	5.44E-10	5.995E-08	9.080E-03	4.3E+03	4.34E+03
21	7.01	0.7	3.87E+05	5.44E-10	1.169E-07	4.656E-03	1.8E+03	3.53E+03
22	7.18	0.7	3.83E+05	5.44E-10	1.196E-07	4.551E-03	1.7E+03	3.49E+03
23	7.00	0.7	3.87E+05	5.44E-10	1.166E-07	4.669E-03	1.8E+03	3.53E+03
24	7.13	0.7	3.84E+05	5.44E-10	1.188E-07	4.584E-03	1.8E+03	3.50E+03
25	4.14	0.7	4.59E+05	5.44E-10	6.900E-08	7.889E-03	3.6E+03	4.19E+03
26	5.24	0.7	4.29E+05	5.44E-10	8.731E-08	6.235E-03	2.7E+03	3.91E+03

Reynolds of shear stress test (F1.100)

The Reynolds number calculation is described in Chapter 3 Section 3.4.2.1(b).

Table 4.10. Data required for the calculation of the Reynolds number for the liquid feed stream on the shear stress test.

Fluid Dynamic Viscosity	**Fluid density**	**Fluid Velocity**	**a**	**b**	**Hydraulic Diameter**	**Hydraulic Reynold**	**Laminar Friction Factors**		**Reynolds**
μ [kg/m.s]	*ρ [kg/m3]*	*v [m/s]*	*Din,liq [m]*	*Dneedle [m]*	*Dh*	Re(Dh,liq)	*b/a*	*1/ζ*	*Re*
0.009	1030	1.3	5.0E-04	4.5E-04	1.0E-04	15.2	9E-01	6.7E-01	10.2
0.009	1030	4.5	5.0E-04	4.5E-04	1.0E-04	51.0	9E-01	6.7E-01	34.0
0.009	1030	9.1	5.0E-04	4.5E-04	1.0E-04	103.7	9E-01	6.7E-01	69.2
0.009	1030	5.3	7.0E-04	6.3E-04	1.4E-04	84.7	9E-01	6.7E-01	56.5
0.009	1030	0.2	2.0E-03	1.9E-03	1.6E-04	2.9	1E+00	6.7E-01	1.9
0.009	1030	0.7	2.0E-03	1.9E-03	1.6E-04	11.9	1E+00	6.7E-01	8.0
0.009	1030	1.5	2.0E-03	1.9E-03	1.6E-04	27.7	1E+00	6.7E-01	18.5
0.009	1030	1.3	5.0E-04	4.5E-04	1.0E-04	14.3	9E-01	6.7E-01	9.5
0.009	1030	4.3	5.0E-04	4.5E-04	1.0E-04	49.4	9E-01	6.7E-01	33.0
0.009	1030	9.8	5.0E-04	4.5E-04	1.0E-04	112.0	9E-01	6.7E-01	74.7
0.009	1030	4.9	7.0E-04	6.3E-04	1.4E-04	79.2	9E-01	6.7E-01	52.8
0.009	1030	0.2	2.0E-03	1.9E-03	1.6E-04	3.5	1E+00	6.7E-01	2.3
0.009	1030	0.6	2.0E-03	1.9E-03	1.6E-04	11.8	1E+00	6.7E-01	7.9
0.009	1030	1.4	2.0E-03	1.9E-03	1.6E-04	26.1	1E+00	6.7E-01	17.4
0.009	1030	1.3	5.0E-04	4.5E-04	1.0E-04	14.7	9E-01	6.7E-01	9.8
0.009	1030	4.3	5.0E-04	4.5E-04	1.0E-04	49.4	9E-01	6.7E-01	33.0
0.009	1030	9.9	5.0E-04	4.5E-04	1.0E-04	113.3	9E-01	6.7E-01	75.6
0.009	1030	4.9	7.0E-04	6.3E-04	1.4E-04	78.5	9E-01	6.7E-01	52.4
0.009	1030	0.2	2.0E-03	1.9E-03	1.6E-04	3.7	1E+00	6.7E-01	2.4
0.009	1030	0.7	2.0E-03	1.9E-03	1.6E-04	12.0	1E+00	6.7E-01	8.0
0.009	1030	1.5	2.0E-03	1.9E-03	1.6E-04	27.5	1E+00	6.7E-01	18.3

Table 4.11. Data required for the calculation of the Reynolds number for the liquid feed stream on the shear stress test.

Fluid Dynamic Viscosity	**Fluid density**	**Fluid Velocity**	**a**	**b**	**Hydraulic Diameter**	**Hydraulic Reynold**	**Laminar Factors**	**Friction**	**Reynolds**
μ [kg/m.s]	*ρ [kg/m3]*	*v [m/s]*	*Din,liq [m]*	*Dneedle [m]*	*Dh*	Re(Dh,liq)	*b/a*	*1/ζ*	*Re*
1.83E-05	118.40	232.02	1.5E-03	1.2E-03	6.4E-04	9.6E+05	8E-01	6.7E-01	6.4E+05
1.83E-05	118.40	232.02	1.5E-03	1.2E-03	6.4E-04	9.6E+05	8E-01	6.7E-01	6.4E+05
1.83E-05	118.40	232.02	1.5E-03	1.2E-03	6.4E-04	9.6E+05	8E-01	6.7E-01	6.4E+05
1.83E-05	118.40	219.99	1.5E-03	1.2E-03	6.8E-04	9.7E+05	8E-01	6.7E-01	6.5E+05
1.83E-05	118.40	280.64	2.6E-03	2.5E-03	2.8E-04	5.1E+05	9E-01	6.7E-01	3.4E+05
1.83E-05	118.40	280.64	2.6E-03	2.5E-03	2.8E-04	5.1E+05	9E-01	6.7E-01	3.4E+05
1.83E-05	118.40	280.64	2.6E-03	2.5E-03	2.8E-04	5.1E+05	9E-01	6.7E-01	3.4E+05
1.83E-05	118.40	232.02	1.5E-03	1.2E-03	6.4E-04	9.6E+05	8E-01	6.7E-01	6.4E+05
1.83E-05	118.40	232.02	1.5E-03	1.2E-03	6.4E-04	9.6E+05	8E-01	6.7E-01	6.4E+05
1.83E-05	118.40	232.02	1.5E-03	1.2E-03	6.4E-04	9.6E+05	8E-01	6.7E-01	6.4E+05
1.83E-05	118.40	219.99	1.5E-03	1.2E-03	6.8E-04	9.7E+05	8E-01	6.7E-01	6.5E+05
1.83E-05	118.40	280.64	2.6E-03	2.5E-03	2.8E-04	5.1E+05	9E-01	6.7E-01	3.4E+05
1.83E-05	118.40	280.64	2.6E-03	2.5E-03	2.8E-04	5.1E+05	9E-01	6.7E-01	3.4E+05
1.83E-05	118.40	280.64	2.6E-03	2.5E-03	2.8E-04	5.1E+05	9E-01	6.7E-01	3.4E+05
1.83E-05	118.40	232.02	1.5E-03	1.2E-03	6.4E-04	9.6E+05	8E-01	6.7E-01	6.4E+05
1.83E-05	118.40	232.02	1.5E-03	1.2E-03	6.4E-04	9.6E+05	8E-01	6.7E-01	6.4E+05
1.83E-05	118.40	232.02	1.5E-03	1.2E-03	6.4E-04	9.6E+05	8E-01	6.7E-01	6.4E+05
1.83E-05	118.40	219.99	1.5E-03	1.2E-03	6.8E-04	9.7E+05	8E-01	6.7E-01	6.5E+05
1.83E-05	118.40	280.64	2.6E-03	2.5E-03	2.8E-04	5.1E+05	9E-01	6.7E-01	3.4E+05
1.83E-05	118.40	280.64	2.6E-03	2.5E-03	2.8E-04	5.1E+05	9E-01	6.7E-01	3.4E+05
1.83E-05	118.40	280.64	2.6E-03	2.5E-03	2.8E-04	5.1E+05	9E-01	6.7E-01	3.4E+05

Table 4.12 ANOVA Two-factor with replication (n=3), on the correlation of the liquid feed flow rate and the outlet temperature on the spray-drying process yield..

Source of Variation	***SS***	***df***	***MS***	***F***	***P-value***	***F crit***
Liquid Feed Flow Rate [ml/min]	1058.06	1.00	1058.06	26.73	0.00	4.26
Outlet Temperature [°C]	560.08	5.00	112.02	2.83	0.04	2.62
Interaction	915.31	5.00	183.06	4.62	0.00	2.62
Within	949.95	24.00	39.58			
Total	3483.40	35.00				

Table 4.13 ANOVA Two-factor with replication (n=3), on the correlation of the liquid feed flow rate and the outlet temperature on the spray-dried powder moisture content.

Source of Variation	SS	df	MS	F	P-value	F crit
Liquid Feed Flow Rate [ml/min]	0.81	1.00	0.81	5.36	0.03	4.26
Inlet Temperature [°C]	7.09	5.00	1.42	9.39	0.00	2.62
Interaction	2.28	5.00	0.46	3.02	0.03	2.62
Within	3.63	24.00	0.15			
Total	13.81	35.00				

Table 4.14 ANOVA Two-factor with replication (n=3), on the correlation of the liquid feed flow rate and the outlet temperature on the aggregation levels of the mAb-A in the reconstituted solution from the spray-dried power. .

Source of Variation	***SS***	***df***	***MS***	***F***	***P-value***	***F crit***
Liquid Feed Flow Rate [ml/min]	372.38	1.00	372.38	0.83	0.37	4.26
Inlet Temperature [°C]	1638.92	5.00	327.78	0.73	0.61	2.62
Interaction	1843.97	5.00	368.79	0.82	0.55	2.62
Within	10830.54	24.00	451.27			
Total	14685.80	35.00				

Chapter 5

Spray-drying of monoclonal antibodies: mAb-A formulation studies

This chapter is structured in three parts, for each one a formulation parameter is chosen: Part I is dedicated to the variation of mAb-A concentration in the formulation to be spray-dried; Part 2 is devoted to the variation of the concentration of the individual excipients, and finally Part 3 gathers the information recovered from Parts 1 and 2 to generate an improved formulation for mAb-A that is spray-dried and characterized more in depth for a better understanding of the aggregation phenomena.

5.1 Introduction

In Part 1 of this chapter, we have investigated the threshold concentration of mAb-A required to prepare relatively high concentration protein solutions for spray-drying, leading to reconstituted solutions with little or no aggregates.

Once the threshold protein concentration was identified, Part 2 consisted of studying the impact of excipients, at said mAb-A concentration, on the aggregation of the reconstituted solution from the spray-dried powder. As discussed in Chapter 2, a wide range of excipients can be added to protein solutions to provide overall stability and protection against different type of stresses (Chiu *et al.*, 2011; Emami *et al.*, 2018; Grasmeijer *et al.*, 2013; Maury *et al.*, 2005; Mensink *et al.*, 2017; Pinto *et al.*, 2021; Sudrik *et al.*, 2017). Sugars, surfactants and amino acids are among the excipients selected for this study: trehalose, sucrose, arginine, lysine, histidine, citrate, polysorbate-80 (PS80), polysorbate-20 (PS20) and poloxamer-188 (Pol-188).

Four different cycles of drying were carried out, each one corresponding to one excipient, which was studied at different concentrations, while the others remained constant. The analysis of each individual excipient helped to have a better perspective to the possible protection mechanisms that have taken place during the spray-drying process.

Finally, from the selection of the more appropriate mAb-A and excipients concentration, a new mAb-A formulation is proposed and the resulting spray-dried powder is subject to further characterization studies, using orthogonal techniques, which are detailed in Part 3 of this chapter.

The three parts will be presented sequentially in the following Sections.

5.2 PART 1

Search for a protein concentration threshold

5.2.1 Materials and Methods

5.2.1.1 Materials

Initial solution of antibodies (mAb-A).

An initial mAb solution (mAb-A) was provided by SANOFI (Paris, France), at 113-120 mg/ml of mAb-A, verified by UV-Vis Spectroscopy at 280 nm, extinction coefficient of 1.55 $ml.\ mg^{-1}cm^{-1}$, and stabilized with trehalose 2% w/w and histidine at 5 mM to achieve a pH of 6. This formulation was used as the starting point to produce the different formulations used throughout this chapter. The excipients were formulated in a separated solution that diluted the initial solution of antibodies to the desired mAb-A concentrations, while the target excipient concentration was reached. All excipients used for the formulation screening were provided by SANOFI (Paris, France).

Formulation FA

Formulation FA was prepared from the initial solution of mAb-A and diluted to different protein targets, from 100 to 20 mg/ml, by adding a buffer solution of histidine 5 mM (pH=6) arginine 53 mM, trehalose 8.6% w/w, and PS80 0.075% w/v, to the initial solution of mAb-A.

5.2.1.2 Methods

Spray-drying experiments

A previous presentation of the set-up and the experimental method used for this study has been presented in detail in Chapter 3, Section 3.4.2.1.

Operating conditions were fixed as indicated in Chapter 4, Section 4.3.4: nozzle diameter of 0.7 mm, inlet temperature 105°C, liquid feed flow rate 4.5 ml/min, drying airflow rate 22 m^3/h and, atomization airflow rate 571 L/h.

All spray-drying tests were performed in triplicate. Before each drying test, all liquid formulations (stock solution) were filtered (hydrofilic polyethersulfone (PES) 0.22 μm). No secondary drying was performed on the spray-dried powders. The powders were filled in glass neck pillbox vials (SODIPRO), sealed with a butyl stopper (Merck) and finally closed with an aluminium crimped cap (Merck).

Powder characterization

(a) Moisture Content

Karl Fischer was used to determine the residual water content in the spray-dried powders. The device used was the 851 Titrando from Metrohm. The oven temperature was set to 100°C and airflow was set to 80 mL/min. The drift needed to be below 20 µg of water/minute to start the measurement. The stop criterion was to have a relative drift near 15 µg of water/minute. Water content results were considered significantly different for differences equal to or more than 0.3%. The reactants used were the HYDRANAL ™-Coulomat AG-OVEN (as the anolyte) and HYDRANAL ™ - Coulomat CG (as the catholyte). The equipment accuracy was verified at the beginning of the measurements with an HYDRANAL ™ Water Standard KF-OVEN (220-230°C)

Reconstituted Solution from Powder

To reconstitute the spray dried sample a volume of milli-Q water was added to achieve the same initial solution concentration for protein and excipients of the stock solution. Then the suspension was placed in an orbital shaker UniShaker 25 (LLG Labware) for 90 min at 70 rpm. The characterization of the produced powder consisted of moisture content measurement and particle size distribution. After reconstitution, the resulting solutions were characterized with respect to protein concentration, turbidity and presence of aggregates, as described in Chapter 3, Section 3.4.2.4.

(a)Protein Concentration

A spectrophotometer (Agilent Cary 8454) was used to measure the protein concentration at 280 nm using in a quartz cell and an extinction coefficient of 1.55 $.ml.\ mg^{-1}cm^{-1}$. The blank used was milli-Q water.

(b) pH measurement

The pH of the solution was measured before and after SD by a 902 titrando Metrohm (swiss mode) OMNIS Ready.

(c) Visual inspection

Observation and count of visible particles in the agitated solution was carried out by placing them in front of two different panels (black and white) on a standard bench for manual inspection.

The used code used is as follows: (++) more than 5 particles visible to the naked eye, (+) 1-5 particles visible to the naked eye, (-) particles only visible when inspecting under light, (--) no visible particles in any observation condition

(d) Turbidity

The turbidity of the samples was quantified by measuring the absorbance at 600 nm using a Varioskan LUX Multimode Microplate Reader from Thermo Fisher Scientific. For each sample, two wells filled with 200 µL were analysed (n = 2). The turbidity of each sample was calculated from the calibration curve and given in nephelometric turbidity units (NTU).

(e) Dynamic Light Scattering (DLS)

DLS was performed on a Zetasizer Nano (Malvern, Herrenberg Germany) as follows: 60 µl of the mAb-A solutions, diluted to 1 mg/ml, were analysed in plastic cuvettes at 25°C using the automatic mode for identifying the best number of sub-runs and measurement time (n=3). The z-average diameter was calculated from the correlation function using the Dispersion Technology Software version 6.01 (Malvern, Herrenberg, Germany).

5.2.2 **Results and Discussion**

One of the main challenges in the formulation of mAb drug products is achieving high- concentration solutions while avoiding aggregation produced by protein-protein associations during processing, transport, storage, and administration (Gikanga *et al.*, 2015). Nowadays, protein solutions with a mAb concentration higher than 30 mg/ml, around 50-150 mg/ml, are considered to be in the range of high-concentration formulations, particularly for subcutaneous delivery (Garidel *et al.*, 2017). Thus, finding the highest protein concentration in solution, at which protein-protein self-interactions and resulting aggregation are reduced, has become a relevant subject. With this in mind, in Part 1 (Section 5.2) we studied the behaviour of mAb-A at different concentrations in order to select the most suitable protein concentration for the next part of the formulation study.

We had previously demonstrated in Chapter 4 that a decrease in the mAb-A concentration from 100 mg/ml to 75 mg/ml caused a reduction in the presence of aggregates in the reconstituted solution. Then, we decided to further investigate the protein behaviour during spray-drying at lower mAb-A concentrations within the additional range of 20 to 60 mg/ml and the same operating drying conditions fixed for these previous experiments. The presence of aggregation phenomena was followed by optical inspection, DLS (Z-average) and turbidity (NTU). The results are shown in Table 5.1 for optical inspection and Figure 5.1.1a-b for DLS and turbidity results.

Matching results were obtained from DLS and turbidimetry measurements, as shown in Figure 5.1a and Figure 5.1b respectively. Since the concentration of the excipient was kept constant while that of the protein was varied, it is expected that the higher ratio of excipients to protein in solution would avoid direct interaction between the mAb-A molecules (Ziaee et al., 2019).

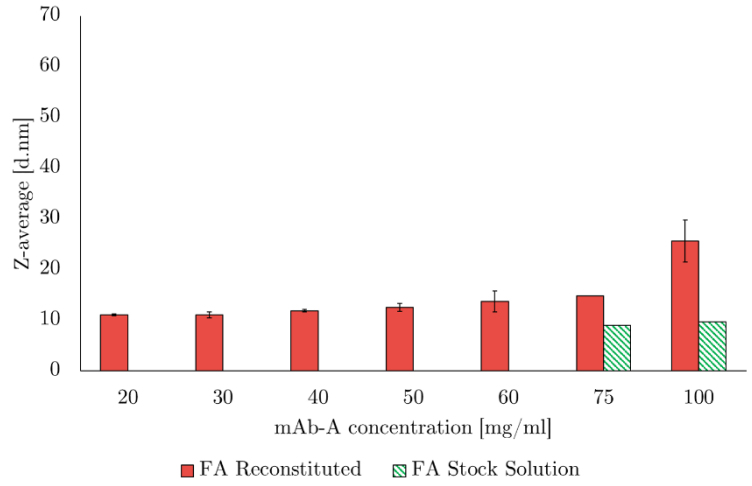

(a)

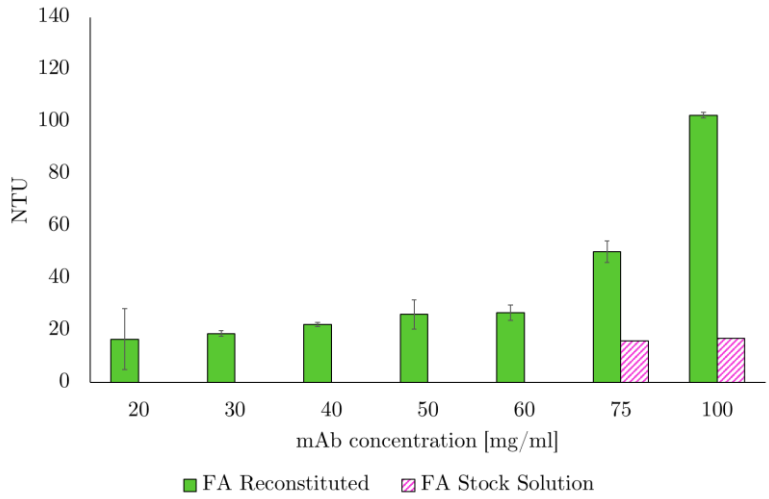

(b)

Figure 5.1. Reconstituted solutions from spray-dried powder (powder moisture content of 1) Formulation FA at different concentrations a) Z-average, obtained by DLS b) Turbidity measured by UV-Vis. For all formulations pH=5.9-6.3 after reconstitution (n=3).

The optical inspection (Table 5.1) revealed a reduction of turbidity in spray-dried reconstituted solutions by lowering the mAb-A concentration, and particularly below 60 mg/ml. The measured moisture content of the powder after SD (Table 5.1) does not seem to have a direct correlation with the turbidity in the sample nor the aggregation results. It will be expected that a lower protein concentration there will be a higher presence of moisture in the spray-dried powders which could impact on the protein mobility in the sample, leading to aggregation.

Table 5.1. Optical Inspection of formulation FA, at different mAb-A concentrations, where the values of present particles are represented as follows: (++) more than 5 particles visible at the naked eye, (+) 1-5 particles visible at the naked eye, (-) particles only visible when inspecting under light, (--) no visible particles in any observation condition.

Formulation	Visual Inspection
FA.20	--
FA.30	--
FA.40	--
FA.50	-
FA.60	+
FA.75	+
FA.100	++

In fact, below a mAb-A concentration of 40 mg/ml there was no observable increase in aggregation. From 40 mg/ml a slight and proportional increase in protein turbidity and aggregation was perceptible, and increasing beyond 75 mg/ml (FA.75) seems to have a significant negative impact on the aggregation. Using a lower concentration to reduce the aggregation to the minimum seems plausible, but the interest in the antibodies formulations nowadays is to aim for reconstitution at the highest possible concentration to be able to reduce the dose volume or the dose number, when aiming for a subcutaneous administration. Results obtained here led to the selection of 75 mg/ml as the recommended protein concentration of mAb-A for SD at the drying conditions used.

5.3 PART 2

Study of the influence of the level of excipients

5.3.1 Materials and Methods

5.3.1.1 Materials

Formulation FB

Formulation FB, also prepared from the initial solution of mAb-A, targeted the mAb-A concentration of 75 mg/ml. It was used for four cycles, as described in the methodology, where each excipient changed for each cycle, while maintaining a pH of 6.

5.3.1.2 Methods

Spray-Drying (SD)

The same conditions used for spray-drying of FA (Section 5.2.1.2) was used now with FB .

As already explained, it was in the interest of the present study to fix a protein concentration at the highest level that did not generate as many aggregates after spray-drying. Once working concentration was set to 75 mg/ml, as shown in Part 1 (Section 5.1), the role of different excipients was then further evaluated.

Four different cycles (Table 5.2) were carried out, each one corresponding to one of the excipients present in the formulation (sugars, surfactants, amino acid 1 - arginine, amino acid 2 -histidine).

Table 5.2. Excipients cycles and their corresponding concentration levels for formulation FB. Alternative excipients were proposed at a concentration equivalent to the medium level of the initial excipients in the previous formulations (FA in Section 5.1)

			Level				
Excipient Cycle	**Excipient**	**C. units**	**Absence**	**Low**	**Medium**	**High**	**Alternative Excipient**
Amino acids	Arginine	mM	0	5	53	100	Lysine (53 mM)
	Histidine (pH)	mM	NA	NA	5	10	Sodium Citrate (5 mM)
Surfactants	PS80	% w/v	0	0.02	0.075	0.15	Pol-188 (0.4 % w/v)
Sugar	Trehalose	%w/v	0	4	8.6	14	Sucrose (8.6%)

C. units= concentration units

At every cycle all excipient concentrations were fixed, except for the one excipient being studied. The concentrations were set at four different levels: high, medium, low and absence. The medium level

corresponds to values used in formulation FA.75, which already had less aggregation when reconstituted after spray-drying.

For the absence level the excipient is not present in the formulation. The two amino acids used in this study (arginine and histidine) are used mainly for protein stabilization support through bonding-interactions and as well as for pH control in the case of histidine.

To eliminate the trehalose for the sugar cycle, the initial solution of antibodies was dialyzed by using a Slide-A-Lyzer cassette of MWCO of 10kDa (Thermo Scientific) which was placed in a buffer of histidine 5mM (pH=6) under agitation for 12 h with an intermediate change of buffer.

Powder Characterization

The spray-dried powders of FB were characterized in terms of particle size and moisture content using the same methods already described in Part 1. An additional characterization was added in this Section, the density measurement as described in Chapter 4, Section 4.2.2.3.

Reconstituted solution from powder

The reconstituted solutions from spray-dried powders of FB were characterized in terms of concentration, aggregation and turbidity, using the same methods already described in Chapter 4, Section 4.2.2.4).

5.3.2 Results and Discussion

When formulating a protein drug-product solution certain parameters, such as protein concentration, ionic strength/osmolality, pH among others, must be attained in the final product according to the type of delivery chosen. In terms of protein stability, pH is a critical parameter that is directly linked to protein conformation stabilization (Zheng *et al.*, 2017). For the specific formulation of the mAb-A, the optimal pH was reported as pH=6 ±0.3.

It has been widely reported that radical change of pH could lead to non-covalently linked soluble aggregates (Mason *et al.*, 2012), as well as to protein fragmentation. That said, the variation of the excipients in this chapter did not intend to study the effect of pH changes on the aggregation formation.

The first test to assess the possible presence of aggregates, was the optical test. The results shown in Table 5.3 are a good indicator of the formulations that might present problems, because it immediately showed if the formulation presented a high turbidity and/or visible aggregates (higher than 100 μm (Joubert *et al.*, 2011)). The results obtained by aggregation and turbidity analysis corresponded to what was observed in the optical inspection for the aggregation present at different levels of concentration of excipients.

Table 5.3. Optical Inspection of formulation FB, where the values of present particles are represented as follows: (++) more than 5 particles visible to the naked eye, (+) 1-5 particles visible to the naked eye, (-) particles only visible when inspecting under light, (--) no visible particles under any observation condition.

			Level				
Excipient Cycle	**Excipient**	**Concentration units**	**Absence**	**Low**	**Medium**	**High**	**Alternative Excipient**
Amino acids	Arginine	mM	++	+	-	-	-
	Histidine (pH)	mM	NA	NA	-	-	-
Surfactants	PS80	% w/v	++	++	+	--	+
Sugar	Trehalose	%w/v	++	+	-	-	+

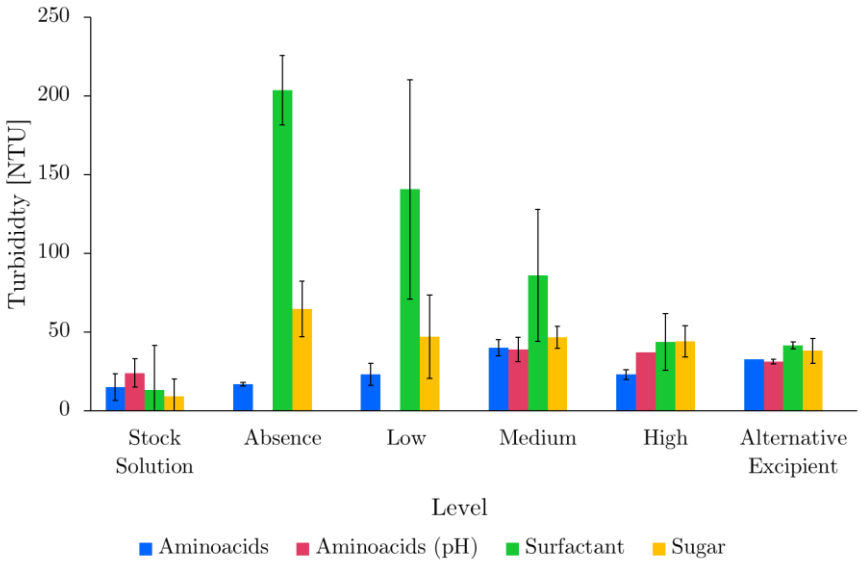

Figure 5.2. Turbidity of FB at different levels of excipients (measured by UV-Visible spectroscopy), with a mAb-A concentration of 73 ±1.8 mg/ml. All formulations had a pH=5.7-6.35 after reconstitution (n=3).

Table 5.4. Z-average values (d.nm) as indicator of aggregation for the different excipients at their corresponding level.

	Type of Excipient			
	Amino acids (Arginine)	**Amino acid (pH) (Histidine)**	**Surfactant (PS80)**	**Sugar (Trehalose)**
Level	**Z-Average [d.nm]**	**Z-Average [d.nm]**	**Z-Average [d.nm]**	**Z-Average [d.nm]**
High	19	15	9	15
Medium	14	24	10	13
Low	31	NA	45	18
Absence	27	NA	63	10
Alternative Excipient	L-Lysine	Sodium Citrate	Poloxamer-188	Sucrose
	14	17	9	16
Stock Solution	8	10	9	9

5.3.2.1 Amino-acids

Different amino acids can be used to stabilize mAb formulations during spray-drying, such as leucine, arginine, histidine, lysine and glycine (Ajmera, 2014; Batens *et al.*, 2018; Dani *et al.*, 2007; Pinto *et al.*, 2021). Studies have already shown that the lack of amino acids in the formulation increases protein aggregation after spray-drying (Ajmera, 2014; Batens *et al.*, 2018). Positively charged amino acids, such as lysine, arginine, and histidine, seem to be able to prevent electrostatic interactions between mAbs in solution, thus avoiding the aggregation phenomenon due to protein crowding (Batens *et al.*, 2018). They also have been suggested to directly form electrostatic and hydrophobic bonds with the protein to stabilize its structure (Massant *et al.*, 2020; Mensink *et al.*, 2017). Moreover, their small size also allows a higher diffusion rate to the droplet surface during drying, which could protect the proteins from interfacial stresses (Bowen *et al.*, 2013; Massant *et al.*, 2020).

Our results revealed that the levels of turbidity were not directly proportional to the arginine concentration within the range tested (Figure 5.2) and for the aggregation levels (Table 5.4) demonstrated that the presence of arginine at medium and high levels improved the stability compared to the low and absence levels. More, at same concentration, both arginine and lysine generate similar levels of turbidity and aggregation (Figure 5.2- Table 5.4).

The presence of histidine in a protein formulation can enhance protein stability and reduce the extent of conformational changes (Baek *et al.*, 2017), and at the same time, it helps attain the desired pH that provides a stable environment for the protein. As the presence of histidine has shown to be necessary, to ensure the correct pH, therefore in this study two levels were selected: Medium (5 mM) and High (10 mM), which only modified the pH in the expected ranges (pH= 5.8 - 6.4) in the formulation before spray-drying, while allowing the measurement of the impact of its stabilization through protein interactions at different concentrations. As shown in Figure 5.2 the turbidity levels do not seem to be impacted by the change in histidine concentration. On the other hand, the Z-average (Table 5.4) values seem to be reduced when increasing the concentration of histidine.

Citrate was proposed as an alternative to histidine, given that it is also a small molecule that can help stabilize mAbs (Kalonia *et al.* 2016; Zheng *et al.*, 2017) and stabilize the pH. Our results also showed that citrate generated a similar level of turbidity to histidine (Figure 5.2), but a lower aggregation level (Table 5.4). Kalonia *et al.* (2016) performed solubility measurements of IgG1 mAb, showing that the histidine buffer provided better stability against aggregation than citrate, at pH values between 4.5 and 6.5.

5.3.2.2 Sugars

Among the stabilization provided by the sugars, there is the vitrification theory that takes place when a glassy matrix is formed during drying, thus immobilizing the protein. Sugars are required to have a high glass transition temperature (Tg) to avoid any damage caused by further crystallization after spray-drying (Kanojia *et al.*, 2018; Pinto *et al.*, 2021). It has been reported as well that sugars are able to

stabilize proteins by replacing the hydrogen bonds present in the liquid state, which is known as the water replacement theory in the drying process (Alhajj *et al.*, 2021). In consequence, sugars are mainly effective against thermal/dehydration stresses. As previously mentioned, sugars like trehalose are known to have preferential exclusion towards mAbs in solution, meaning that the sugar molecules are excluded from the surface of the mAb, creating a repulsion effect and therefore avoid the interaction between the mAbs (Sudrik *et al.*, 2017).

As observed in Figure 5.2 there was not a considerable change in turbidity at the different level concentrations of trehalose. However, when it was not included in the formulation there was an observed increase in turbidity.

Interestingly, the presence of trehalose leads to an increase in the size of the Z-average (Table 5.4). It should be expected that some of the excipients may introduce a small increase or decrease in hydrodynamic diameter (Z-average), such as trehalose. This excipient has normally about 1-2 nm in diameter which should bring the Z-average down, but it has been reported that for some sugars, for example, excipient or impurities thereof can form clusters of about 100-200 nm, consistently found in sugar-containing formulations, and shift the Z-Average of protein formulations up (Arora *et al.*, 2015; Baek *et al.*, 2017; Weinbuch *et al.*, 2015). Therefore, the increase of Z-average could be due to the presence of impurities in the reconstituted solution, as indicated in the study of Weinbuch *et al.* (2015) (Weinbuch *et al.*, 2015).

Trehalose, and other sugars, are known to protect the protein from thermal stresses and their presence during spray-drying conditions is desired. Maury *et al.* (2004) reported a progressive reduction of the amount of aggregates after spray-drying and reconstitution, for formulations with a mass ratio higher than 0.25:1 (trehalose:protein), which at our lowest level was about of 0.53:1 (trehalose:protein) (Maury *et al.*, 2005).

Both trehalose and sucrose showed similar results, at the same concentration, on the protein stability (aggregation levels and turbidity) (Figure 5.2 and Table 5.4). The choice of trehalose over sucrose is linked to the higher glass transition temperature (Tg) of trehalose (≈ 120°C), against the Tg of sucrose (≈ 75°C) (Lerbret *et al.*, 2005). Having a higher Tg can increase the sugars stability by maintaining its physical and chemical properties during processing and storage. The superiority of trehalose in protein stability when drying has been proven in other studies, given its higher propensity of forming intermolecular hydrogen bonds compared to sucrose (Batens *et al.*, 2018).

5.3.2.3 Surfactants

Surfactants are known to protect the protein at the liquid-air interfaces by the competitive adsorption theory. It is proposed as well that some surfactants may stabilize proteins due to the formation of reversible complexes, through hydrophobic binding, depending on the binding affinity and the protein (H. J. Lee *et al.*, 2011). However, the most prevalent mechanism is the one linked to the prevention of the interfacial stresses (Pinto *et al.*, 2021).

In the present study, a direct correlation between the concentration of PS80 and the reduction in turbidity of the reconstituted solution was observed (Figure 5.2) . Other studies have shown a decrease in turbidity when increasing the concentration of surfactant in spray-dried protein formulations (Batens *et al.*, 2018; Faghihi *et al.*, 2017). This result demonstrates the importance of the incorporation of this excipient in the formulation of mAb-A to assure the stability of the spray-dried protein. Regarding the alternative surfactant tested, Pol-188, it provided a lower turbidity than PS80 at same concentration. A possible explanation for this behavior might come from the interaction mechanism of the protein-surfactant as suggested by Khan et al. (2015) This suggests that the type of surfactant could as well impact the stability, therefore it would be interesting to compare different types of surfactants in an optimized formulation.

In this study, the surfactant is found to be the most effective excipient for protein stabilization at higher concentrations. This could be further explained by the competitive adsorption theory, consequently the higher surface of surfactant available, the higher the protection level. In this case the size of the micelles was considered as the available surface, which was absorbed at the droplet surface. By calculation of the size of the sprayed droplets and their surface and the surfactant surface, it was possible to approximate the covered surface by surfactant during the spraying step, the calculation is developed right here after (Section 5.3.2.3(a)).

(a) Surfactant droplet surface coverage

Taking into consideration that the surfactants are expected to cover the surface of the drying droplets by a monolayer, and then avoid the protein concentration in the liquid/air interface during spray-drying (Khan *et al.*, 2015), calculating the size of the droplets generated during the spraying step of spray-drying is important in order to know the available droplet surface covered. This is achieved by performing a mass balance on the droplet generated into a powder particle (Figure 4.6) in Chapter 4 Section 4.3.3. as shown below on Equations 5.1 to 5.5. Then a calculation of the total surface offered by the surfactant micelles can gives us an approximate idea of the percentage of surface available to cover the available droplet surface. For the calculations both systems (sprayed droplets of formulation FB and surfactant micelles) were considered as spheres and were in non-polydisperse conditions.

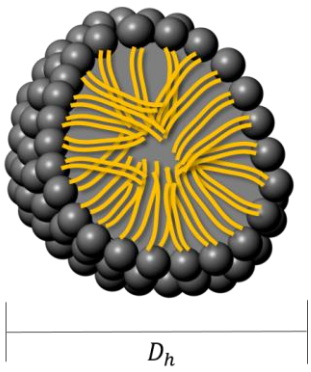

Figure 5.3. Representation of a micelle and its corresponding hydrodynamic radius (Dh).

Assuming that we have a volume of liquid feed (V_{at}) of 15 ml for all the formulations during spray-drying an approximative value of the total number of droplets (N_{dr}) during atomization can be calculated (Equation 5.1) by dividing the total atomization volume (V_{at}) by the volume of one single droplet (V_{dr}) (Equation 5.2)

$$N_{dr} = \frac{V_{at}}{V_{dr}} \quad (5.1)$$

$$V_{dr}[ml] = \frac{4}{3}\pi\left(\frac{D50_{dr}}{2\times10^{12}}\right)^3 \quad (5.2)$$

The surface of one droplet (S_{dr}) is calculated as indicated in Equation 5.3, while the total surface of sprayed droplets (S_{Tdr}) was obtained by the product of Equation 5.4.

$$S_{dr} = 4 \times \pi\left(\frac{D50_{dr}}{2\times10^{6}}\right)^2 \quad (5.3)$$

$$S_{Tdr} = S_{dr} \times N_{dr} \quad (5.4)$$

Once the droplet surface is calculated, the available surface of surfactant to cover it was approximated. The micelle diameter was known as the Hydrodynamic diameter (Dh), Tomlinson *et al.* (2020) measured PS80 micelles by DLS and found the Dh to be approximatively in a range of 9.0-9.4 nm.

The volume of surfactant (V_s) is calculated using its respective concentration at a volume of 15 ml of solution. The approximated micelles surface ($S_{micelle}$) was calculated using Equation 5.5, while the approximated number of micelles ($N_{micelle}$) present in the formulation FB is calculated using Equation 5.6. Finally, the total surface of surfactant available ($S_{Tmicelle}$) in the formulation solution was calculated using Equation 5.7. With all this information it is possible to do an approximation of the droplet surface covered by the micelles as noted in Table 5.5.

$$S_{micelle} = 4 \times \pi\left(\frac{D_h}{2\times10^{9}}\right)^2 \quad (5.5)$$

$$N_{micelle} = \frac{V_s}{V_{micelle}} \quad (5.6)$$

$$S_{Tmicelle} = S_{micelle} \times N_{micelle} \quad (5.7)$$

Table 5.5. Data for the calculation of the surface coverage of sprayed droplets with surfactant PS80 (ρ= 1.02 g/cm3) at different PS80 concentrations. The values for the concentration at 200 ppm corresponded to formulation F1.100 of Chapter 4, Section 4.3.4, at 750 ppm and 1500 pm corresponds to formulation FB in this chapter Section 5.3.

Concentration [ppm]	$D50_{dr}$ [µm]	S_{Tdr} [m2]	D_h [m]	$S_{micelle}$ [m2]	$V_{micelle}$ [m3]	$V_{micelle}$ [ml]	V_s in 15 ml [ml]	$N_{micelle}$	$S_{Tmicelle}$ [m2]	Surface coverage [%]
at 200	30.5	3.0	9E-09	3E-16	4E-25	4E-19	3E-03	7E+15	2	65
at 750	31.3	2.9	9E-09	3E-16	4E-25	4E-19	1E-02	3E+16	7	250
at 1500	33.3	2.7	9E-09	3E-16	4E-25	4E-19	2E-02	5E+16	14	532

The sprayed droplet surface coverage provided by the surfactant, in this case PS80, increased around 284% when passing from a concentration of 200 ppm to 750, and 718% when increasing from 200 ppm

to 1500 ppm. Theoretically, when passing 100% of coverage it was possible that the PS80 molecules were generating more than one layer at the droplet surface, which possibly avoids the mAb presence at the air/liquid interface.

5.3.3 Synthesis of Part 2 of Chapter 5

The concentration of mAb-A plays an important role in aggregation during spray-drying. By reducing the concentration from 100 mg/ml to 75 mg/ml a considerable reduction in turbidity and aggregation was observed. Nevertheless, the formulation continues to be considered as relatively high-concentration, in terms of subcutaneous delivery.

The results indicated that the presence of the excipients was important in the protein stabilization. As previously reported in literature, the sugars and surfactants could mainly avoid irreversible intermolecular contacts (Dani *et al.*, 2007). Using alternative excipients at the same ratios yielded similar results in terms of turbidity and stability. In this study, the excipient that showed a higher impact on protein stability by reducing the turbidity (NTU) and aggregation (Z-average) was the surfactant.

The goal of using alternative excipients was to identify if any given effect observed was specific to the excipient tested or the class of excipients it belongs to. In general, for the alternative excipients, excluding the surfactant, the turbidity response was similar to the one obtained at the medium and high levels of those of the initial excipients (Figure 3.2). Therefore, the study was continued with the same excipients used so far as sugars and amino acids, while increasing their concentrations. On the other hand, we targeted the surfactants as the excipient of major relevance for the decrease of turbidity and aggregation, and it was decided to test different molecules in Part 3 of the study.

5.4 PART 3

Proposition of an optimized formulation for mAb-A

5.4.1 Materials and Methods

5.4.1.1 Materials

Formulation FC

Formulation FC was prepared as well from the initial solution of mAb-A with a protein target concentration of 75 mg/ml.

Four different formulations were produced by adding the excipients to achieve the excipient concentrations given in Table 5.6.

Table 5.6. Composition of formulation FC.

Component Concentration	FA.75	FC.1	FC.2	FC.3
Arginine-HCl [mM]	53	100	100	100
Trehalose [%]	8.6	10	10	10
Histidine [mM]	5	10	10	10
*Surfactant [% w/v] (*PS80, **PS20, ***Pol-188)*	0.075*	0.150*	0.150**	0.400***
Solid content	0.174	0.199	0.199	0.202

*Polysorbate-80, **Polysorbate-20,***Poloxamer-188

5.4.1.2 Methods

The same conditions used for spray-drying of FA (Section 5.2) and FB (Section 5.3) were used now with FC. For both, spray-dried powder and reconstituted solution, the characterization tests employed were those presented in Part 5.1, with additional characterizations, which helped to have a more in depth appreciation of the aggregation populations.

Powder characterization

(a)Scanning Electron Microscopy

Powder samples were previously coated with two layers of platinum using the Sputter Coater Polaron SC7640, using argon gas, a current of 19 mA and a vacuum of $(8 - 6)10^{-2}$ mbar. The coated powder images were then captured using a SEM Nova NanoSEM 450 from ThermoFisher (FEI). It is a high-resolution SEM with FEG tip with field emission. Samples were observed with a resolution of ×5000.

Reconstituted solution from powder

(a)Accelerated stability test

After spray-drying, the powder samples were stored at 4°C in sealed vials until the reconstitution protocol was performed. After reconstitution the solutions were stored at 40°C for one month immediately and sampling was performed right before the stability test (T0) and at week two (T2W) and four (T4W). They were then placed at 4°C before the following characterization analysis.

(b)Protein concentration

Concentration was measured at 280 nm using in a quartz cell, using an extinction coefficient of 1.55 $ml.\ mg^{-1}cm^{-1}$, using a spectrophotometer (Agilent Cary 8454). The blank used was mili-Q water.

(c)Osmolality

Osmolarity measurements were performed on a 20 µL sample volume using a freezing-point osmometer 210 Micro-Sample from Fiske.

(d)Solution density

The solution density before spray-drying and after reconstitution was measured with a Mettler Toledo DM-40 densimeter, at 20°C. Use of 3 ml of a water standard with a density of 0.99 g/cm^3 at 20°C was used. The operating principle was based on the oscillation of a U-shaped borosilicate glass tube (volume = 1 mL) whose resulting frequency was directly proportional to the density of the liquid or gas injected. It has an integrated electronically controlled thermostat. The density is the physical quantity that characterizes the mass of a body per unit of volume. It was expressed in g/cm^3 in the international system.

(e)Viscosity

The viscosity was measured using a Brookfield AMETEK Low-Range Viscometer, 100 to 240 VAC at a temperature of 22°C in a range of 50 to 100 rpm, using a volume of solution of 60 ml.

Aggregates analysis of reconstituted solution FC

The overall properties and stability of protein solutions depend on the presence, within tolerance, or absence of particle populations. So far, in the previous chapters (3 and 4), and in Part 1 and 2 (Sections 5.2 and 5.3) of this chapter, the analysis of protein stability was focused on the detection of the presence of aggregation using the Dynamic Light Scattering technique, and the turbidity measurements as an indirect indicator of the presence of aggregates. In this Section, the different particle populations of aggregates were characterized using the following techniques.

(a)Dynamic Light Scattering (DLS)

The DLS principle was previously discussed on Chapter 3, Section 1.2.4. DLS analyses were performed in a Zetasizer Nano (Malvern, Herrenberg Germany) as follows: 60 μl of the mAb-A solutions were analysed in plastic cuvettes at 25°C using the automatic mode for identifying the best number of sub-runs and measurement time (n=3). The z-average diameter was calculated from the correlation function using the Dispersion Technology Software version 6.01 (Malvern, Herrenberg, Germany).

(b)Nanoparticle Tracking Analysis (NTA)

NTA technique allows simultaneously visualization of the size and count nanoparticles in liquid suspensions. The NTA uses both microscopic imaging and particle light interactions, based on the Brownian motion principle, to obtain the particle size distribution of suspensions (Figure 5.4) (Filipe *et al.*, 2010a; Gross-Rother *et al.*, 2020).

The measurement was realized when the solution was injected into the sample cell where a laser beam passes obliquely through, and then the particles in suspension scatter the light that was detected by a charge-coupled device on a microscope, and created a record of each particle in movement (Gross *et al.*, 2016; Patois *et al.*, 2012). Then, the software analysis of the pathway data calculate the diffusion coefficient D, using the Stokes-Einstein equation 5.8 for each registered particle. If the temperature and viscosity of the suspension were known, it was possible to calculate the hydrodynamic diameter d_H of each particle. Since each scattering center is recorded separately, the resulting estimate of the particle size distribution was a direct count, and not an intensity-weighted, z-average distribution (Gross-Rother *et al.*, 2020).

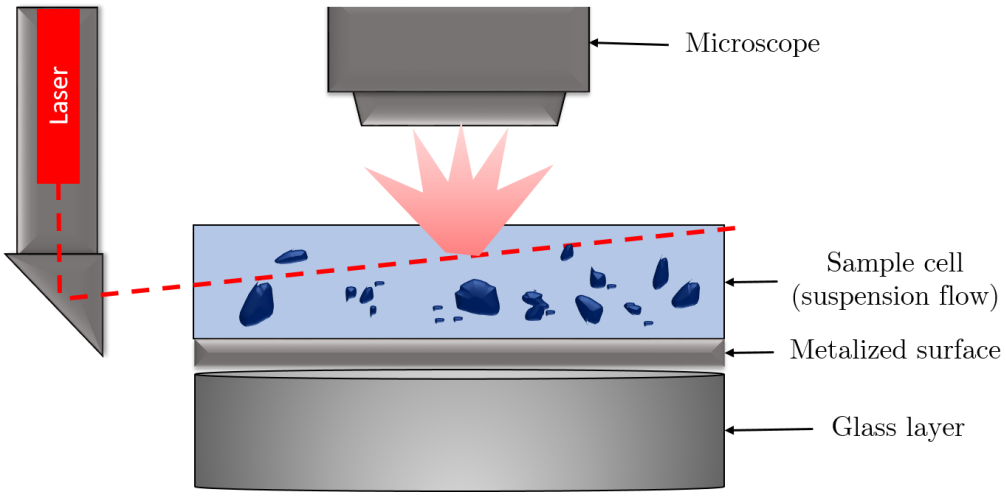

Figure 5.4. Nano Tracking Analysis measurement principle and configuration. (adapted from (Gross-Rother et al., 2020)).

$$D = \frac{T\kappa_B}{3\pi\eta d_h} \quad (5.8)$$

Where D : diffusion coefficient, η : viscosity, T:absolute temperature, d_H :spherical-equivalent hydrodynamic diameter, κ_B: Boltzmann´s constant

Nanoparticle tracking analysis (NTA) was performed in a NS300 equipped with a 407 nm laser. A volume of 1 mL (sample diluted in water at 1 mg/mL) was used for each measurement using a syringe pump at speed 50. The results were averaged from three videos of 60 seconds at a temperature of 25°C. The shutter and gain were manually adjusted and fixed at the same value for all measurements, to optimize the visualization of all individual aggregates with a minimum background noise. The detection threshold was also adjusted manually, ensuring that all particles in the video are correctly tracked and visual noise was ignored. Particles smaller than 50 nm are considered as visual noise and are excluded from the result.

(c)Differential Scanning Fluorimetry (DSF)

The DSF is an accessible biophysical technique to monitor both protein unfolding and thermal stability. The technique measures protein unfolding by tracking changes in fluorescence as a function of temperature, in a controlled environment. DSF uses a hydrophobic fluorescent dye that binds to proteins when unfolding or it can measure the changes in intrinsic protein fluorescence as the proteins unfold, due to the presence of tryptophan, which is the method used in the present study. An example of the a general DSF thermogram is shown in Figure 5.5.

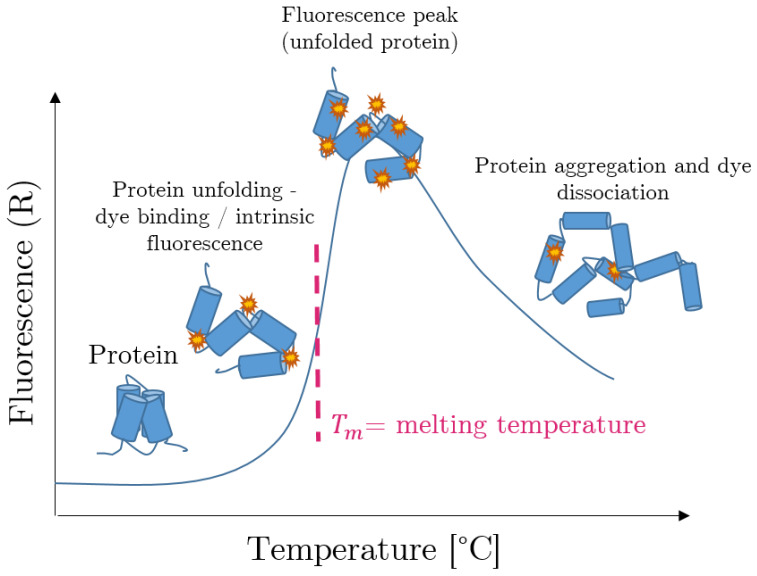

Figure 5.5. Example of the melting curve showing fluorescence as function of temperature, for protein stability analysis, using Differential Scanning Fluorimetry. The inflection point of the melting curve, corresponding to the point of 50% of folded state, is the melting temperature (T_m) (adapted from Samuel et al., 2021)

Given that proteins are molecules in a thermodynamic equilibrium between folded and unfolded states any change in the energy of their surroundings (i.e., change of temperature, pH, ionic strength, presence of specific anions or cations) can lean the protein on to the unfolded state (Bowling *et al.*, 2016). When quantified, this phenomenon allows for the determination of the melting temperature (T_m), known as the temperature at which 50% of a protein is in the folded state (Samuel *et al.*, 2021). By changing the conditions or adding excipients to the protein solution it is possible to stabilize the protein through a reduction of the Gibbs free energy, resulting from new molecular interactions (hydrogen bonds, van der Waals interactions, etc.) or conformational reordering of the target protein (K. Gao *et al.*, 2020; Wen *et al.*, 2020). By increasing the Gibbs free energy an increase in thermal stability is achieved and thereby an increase in T_m (K. Gao *et al.*, 2020; S. H. Kim *et al.*, 2022). As changes in protein conformation, through complex formation even of weakly binding ligands affect the thermal stability, this technique has proven effective to assess the impact of different stabilizers in formulation (S. H. Kim *et al.*, 2022).

DSF measurements were performed in the UNCLE (Unchained Labs) unit, with a range from 10°C to 90°C with a heating rate of 1°C/min. The solutions were analyzed at 75 g/L. 2 or 3 measurements were performed for each sample. The Tm1 using BCM mode and Tonset using derivate BCM mode were recorded.

(d)UHPLC Size Exclusion Chromatography (SEC)

Size exclusion chromatography is a well-established method for characterizing protein solutions based on their molecular weight and/or molecular weight distribution. One of the main applications of the SEC

is the measurement of levels of reversible self-associated or aggregated (non-reversible) soluble high molecular-weight (HWM) biomolecule forms that may impact the final formulation safety and efficacy (Bouvier *et al.*, 2014; Brusotti *et al.*, 2018). The technique consists of separation by a gel containing spherical beads that have pores with a specific size distribution (Giridhar *et al.*, 2017). The sample is injected into the column, that contains a rigid porous particle column packing, and is mobilized by a solvent (mobile phase) through the column. As small molecules diffuse through the pores of the matrix, the bigger molecules that do not fit into the pores will be eluted first, as indicated in Figure 5.6.

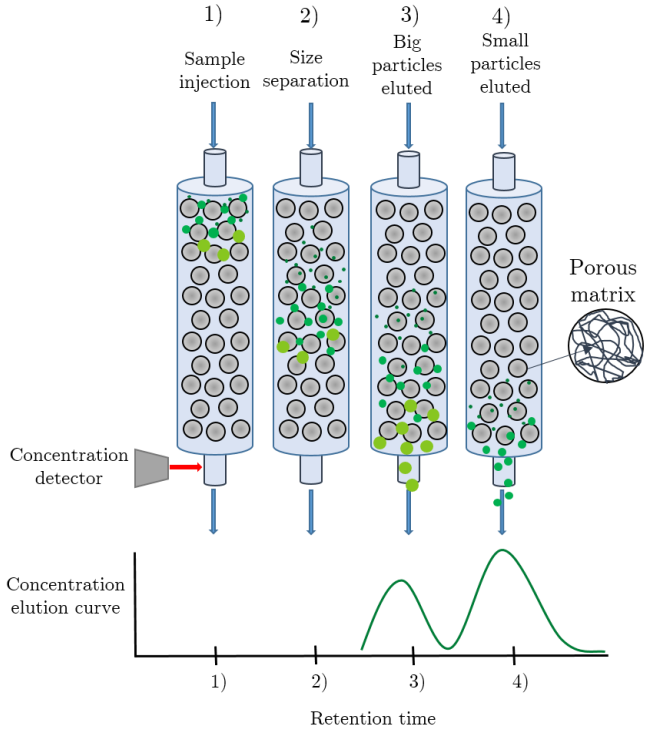

Figure 5.6. Mechanism of size exclusion chromatography (SEC), adapted from (Giridhar et al., 2017).

Size exclusion chromatography (SEC) was used to characterize the High Molecular Weight (HMW) aggregates present in the reconstituted sample of the spray dried mAb-A. The column used was a Waters Acquity UPLC BEH200 (Waters, ref. 186005226). The mobile phase comprised 50 mM sodium phosphate, 300 mM sodium perchlorate, (pH 7.0) at a flow rate of 0.3 mL/min. mAb-A was diluted to 5 mg/ml using milli-Q water. The injection volume was 2 µL to achieve the 10 µg protein load. Samples were prepared either directly from the liquid feed or by dissolving an appropriate amount of a spraydried powder in a small volume of the mobile phase. Detection was performed at lZ280 nm. Each chromatogram was integrated using the commercial Dionex Chromeleon™ or Waters Empower or Agilent OpenLAB™ software.

(e)Capillary electrophoresis sodium dodecyl sulfate (CE-SDS)

CE-SDS apart for being used to estimate the apparent molecular weight of proteins, is also used to confirm the consistency of manufactured biologics, i.e., chemical or physical instabilities during production, transportation and storage. The principle of this technique is the separation of molecules

with different molecular weights (MW) and charge densities through a sieving polymer network (Figure 5.7) (H. Gao *et al.*, 2022; Sänger–van de Griend, 2019). Proteins are denatured using an excess of sodium dodecyl sulphate (SDS), forming protein–SDS complexes that have the same mass-to-charge ratio and allow separation based on their hydrodynamic radius and the proteins are separated in increasing size order (H. Gao *et al.*, 2022; Scheller *et al.*, 2021).

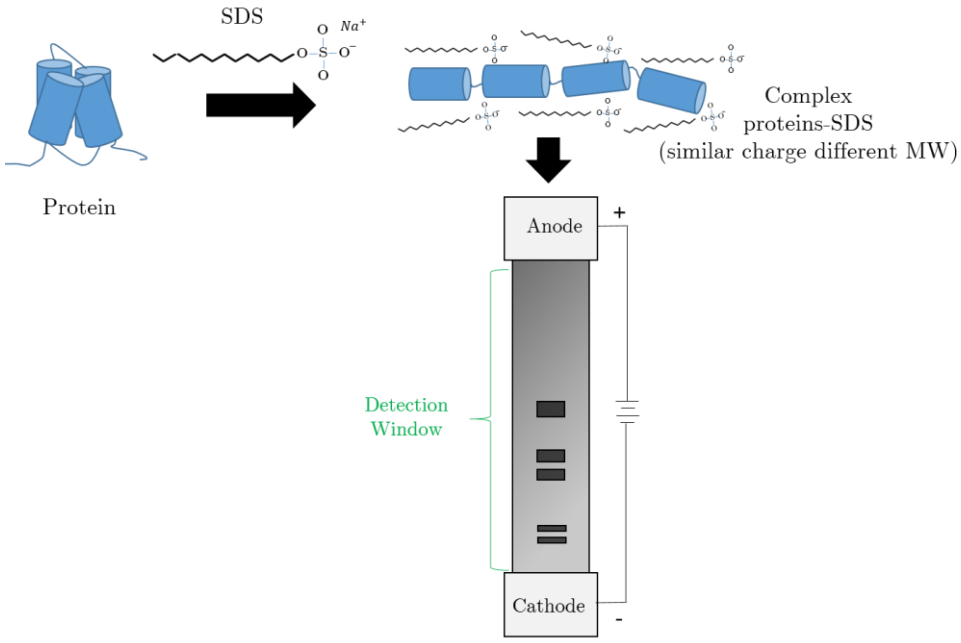

Figure 5.7. Diagram of the process of CE-SDS.

The Low Molecular Weight (LMW) aggregates were assessed in a Protein Simple Maurice (ProteinSimple Bioscience and Technology). The sample was diluted to 2 mg/ml with mili-Q water and pre-heatead at 65°C for 10 min followed by an ice bath and then a centrifugation step. The capillary dimensions were 17 cm total length, 15 cm effective length, and 50 μm internal diameter. The injection occurred at 4.6 kV for 20 s. The separation occurred at 5.75 kV for 35 min. The sample chamber temperature was 15°C and the protein signal was detected by UV at 220 nm. The capillary rinsing and gel filling between sample injections were automatically performed by the instrument.

(f)Imaged Capillary Isoelectric Focusing (icIEF)

The icIEF technique relies on charged proteins attributes to make them migrate through a gel in response to an electric field. Proteins separation when migrating will be based on their pI at a certain pH, and a gradient inside a gel is established by ampholyte mixtures. When the protein encounters the pH corresponding to its pI it will stop migrating, at this value the protein has zero charge (Figure 5.8) (Kahle *et al.*, 2019). The UV-adorption allows a continous measurement of the migration (Kahle *et al.*, 2019; Suba *et al.*, 2015).

During mAb production (drying, purification, transport) and storage the protein may suffer from diverse physico-chemical stresses, resulting in the formation of charge variants like oxidation of tryptophan or deamidation of asparagine. These modifications affect the full charge profile of the mAb (Suba *et al.*, 2015). The purpose of this analytical procedure was to determine charge heterogeneity and isoelectric point (pI) of the mAb-A isoforms by a Maurice Combo System (ProteinSimple Bioscience and Technology) equipped with a Imaging Capillary Electrophoresis with a CCD camera.

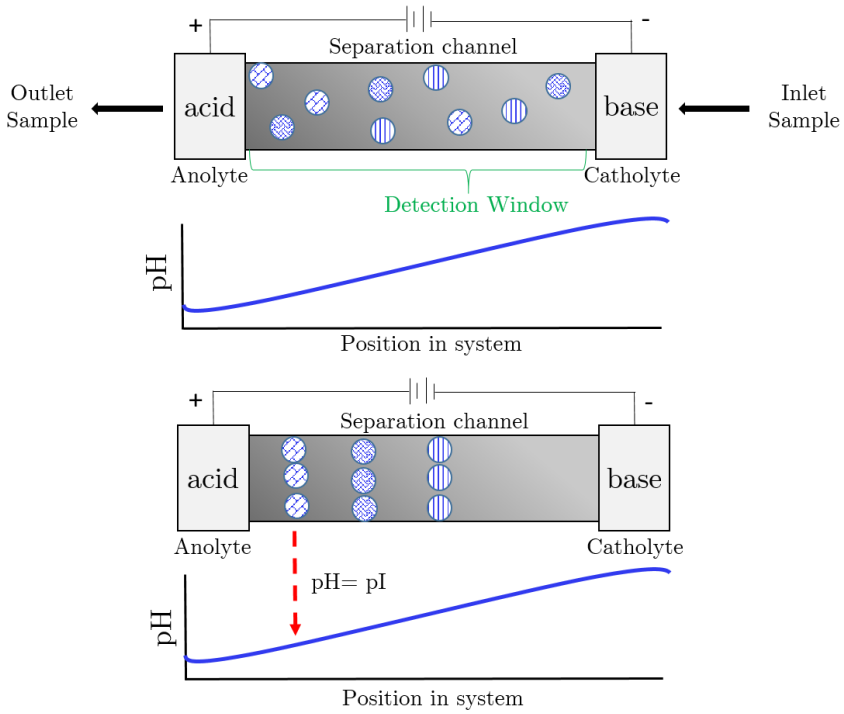

Figure 5.8. Schema of icIEF separation, (top) The entire capillar is filled with a solution of ampholytes (represented by the gray color gradient) that create a pH gradient. The protein samples, represented by circles with different patterns, are distributed throughout. (Bottom) When the axial electric field is applied the proteins migrate electrophoretically along the column up to the position where the local pH equals the pI of the protein. (Adapted from Herr et al., 2000).

The solution of mAb-A was first diluted with water to a concentration of 2 mg/mL. The dilution was subsequently mixed with a solution containing methyl-cellulose 1% (to reduce protein interactions), the broad-range ampholytes pH 3–10, two pI markers (7.05 and 9.22) and mili-Q water. Samples are loaded and the system encompasses an autosampler and a Charge Coupled Device (CCD) camera to capture the UV absorption image from the UV detector operating at 280 nm.

5.4.2 **Results and discussion**

The second series (formulation FB) gave insightful information about the impact of each excipient on the protein stability. This leads to formulation FC, where the concentration of excipients (Table 3.5) were modified to assure a higher protection of the mAb during the spray-drying process and reconstitution from the spray dried powder, departing from the previous results (Section 5.3.2). In this last series of formulations (FC), an extended set of characterization tests were performed on the spray-

dried powder and the reconstituted formulation which was subjected to an accelerated stability study. The latter allowed evaluation of the robustness of the selected formulation by characterizing the general physico-chemical characteristics and the aggregation population.

5.4.2.1 Physical characterization of the spray-dried powder of FC

One of the advantages of SD is the particle engineering capacity, and besides from the process operating conditions, some of the powder characteristics are influenced by the formulation composition and concentration. Some of these powder characteristics are density, particle size distribution, morphology and moisture content. For example, a higher solid composition will yield higher particle sizes which increases the reconstitution times (Batens *et al.*, 2018), the morphology of which will impact the powder cohesiveness making it easier or harder to handle during transportation (Ziaee *et al.*, 2019), among others. The particle size and density also allows the calculation of the initial droplet size during spray-drying, as shown in Section 2.3.3, calculations of which was performed as well in this section.

The particle size distributions achieved using a nozzle of 0.7 mm for different versions of formulation FC (Table 5.6) are shown in Table 5.7, in comparison to formulation FA.75. The sizes (D50= 8.7-12.2 μ) in the range 1 μm to 28 μm are consistent with the values observed in the MEB images (Figure 5.9) showing a characteristic spherical and torus morphology of spray dried mAbs (Batens *et al.*, 2018; Faghihi *et al.*, 2017). The particle sizes are consistent with a lab-scale SD process, as reported by other authors (Bowen *et al.*, 2013; Gikanga *et al.*, 2015)

Table 5.7. Particle Size Distribution of the control formulation (FA.75) and the optimized formulations (FC.1, FC.2, FC.3).

	Particle Size Distribution [m]			
Formulation	*D10*	*D50*	*D90*	*D3;2*
FA.75	1.7	8.7	16.8	4.3
FC.1	1.3	8.9	17.2	4
FC.2	1.3	8.7	20.2	3.9
FC.3	2.6	12.2	28.4	5.6

5.4.2.2 Accelerated stability and extended characterization of optimized formulation

The excipient variation studies in Part 1 (Section 5.3) demonstrated that surfactants are the excipients with the highest impact on protein stability. Therefore, to study more in depth the effect of this excipient in the formulation, in addition to PS80 and Pol-188, the surfactant PS20 was added to the study, given that it is one of the most-commonly used non-anionic surfactant for mAb stabilization (H. J. Lee *et al.*, 2011).

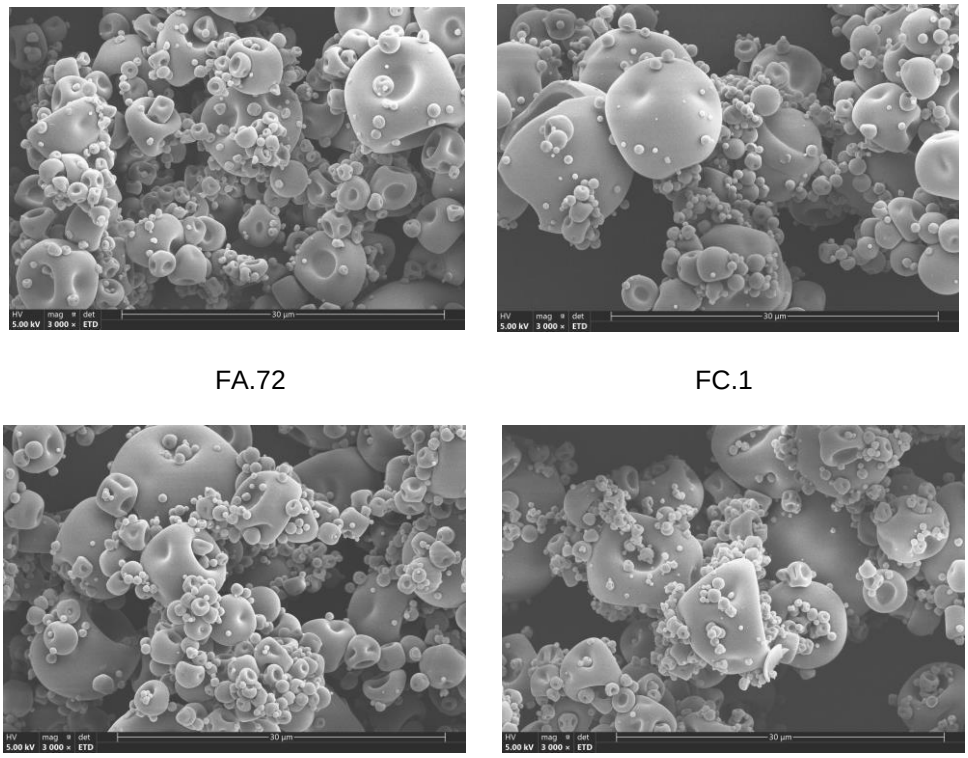

Figure 5.9. SEM images of spray-dried mAb formulations (FA.75 and different versions of FC.).

Given that a general increase in the excipients concentration in the solution showed an improvement in protein stability during the spray-drying process in Section 5.3, three different formulations, with a general increment of the concentration of excipients (arginine, histidine, trehalose and surfactants) were proposed.

Formulation FA.75 was selected as the control formulation given its relative presence of aggregates, compared to the formulations used in Chapter 4 (F1.100, F2.100). Its composition was the following: mAb-A 75 mg/ml, arginine 53 mM, histidine 5 mM, PS80 750 ppm.

All three optimized formulations were at a mAb-A concentration of 75 mg/ml but had an increased concentration of excipients: arginine 100 mM, histidine 10 mM, and the concentration and type of surfactant varied according to the formulation: PC.1 (PS80 at 1500 ppm), PC.2 (PS20 at 1500 ppm), PC.3 (Pol-188 at 4000 ppm).

To better understand the physico-chemical stability of the reconstituted formulation after the spray-drying process, an accelerated stability test was carried out at 40°C. Samples were analysed at the time of reconstitution T0, at two weeks (T2W) and four weeks (T4W). The results of the characterization were divided into two main segments, the first one introduces a general characterization of the reconstituted solution FC. Whereas, the second segment shows results of the aggregation characterization analysis.

As previously mentioned, the formulation has to achieve certain general characteristics such as, pH, viscosity and osmolality. The pH values obtained for FA.75 and all FC formulations were in the range that was stable for mAb-A (Table 5.8)

Table 5.8. Osmolality and pH measurements of formulations FA.75 and FC after reconstitution.

	Osmolarity [mOsm/kg]			**pH**		
Formulation	*T0*	*T2W*	*T4W*	*T0*	*T2W*	*T4W*
FA.75	NA	453	479	6.5	4.8	4.6
FC.1	503	496	489	6.8	6.4	6.4
FC.2	473	491	495	6.1	6.1	6.1
FC.3	489	483	488	6.2	6.2	6.3

The suggested osmolality for subcutaneous injection solutions, to avoid any discomfort and pain on the patient, is around 300 mOsm/kg. Maximum reported osmolality tolerated by patiens is around 600 mOsm/kg, when applying volumes of 0.5 ml (Taghizadeh *et al.*, 2022). The osmolality is a characteristic of the solution that is influenced mainly by the concentration of the components of the formulation. The values of osmolality obtained here can still be lowered by further manipulation of the formulation (Table 5.8).

5.4.2.3 Aggregates analysis of reconstituted solution FC

A first approach to determine if the formulations have any possible aggregation was the optical inspection. It can shed light on which formulations present a major problem by the opalescence present, measured by turbidity. The opalescence in formulations FC.1, FC.2, FC.3 seems to be lower when compared to formulation FA.75 (Figure 5.10), with no visible particles observed as indicated in Table 5.9.

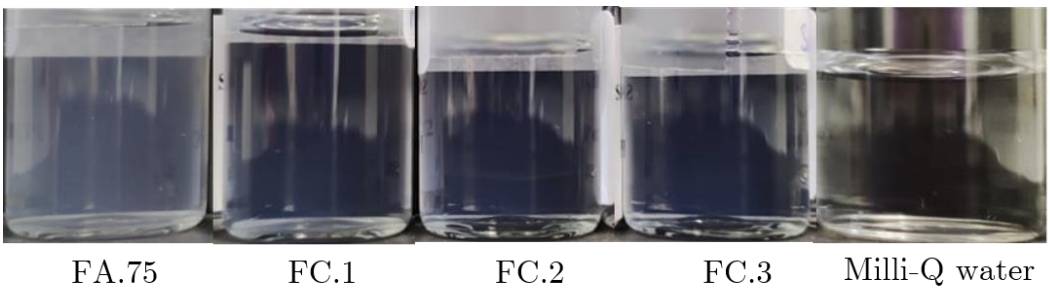

Figure 5.10. Reconstituted solution from spray dried powder for the control formulation (FA.75), the optimized formulations (FC.1, FC.2 and FC.31.), and Milli-Q water at T0.

Table 5.9 Optical Inspection of FC, where the values of present particles are represented as follows: (++) more than 5 particles visible to the naked eye, (+) 1-5 particles visible to the naked eye, (-) particles only visible when inspecting under light, (- -) no visible particles in any observation condition.

Formulation	Visual Inspection
FA.75	+
FC.1	-
FC.2	--
FC.3	--

For a better evaluation of the aggregation after the stability test of the reconstituted spray dried powder, for the optimized formulations, orthogonal techniques were used. They allowed the detection of the different aggregates sizes, in the visible (Vs), subvisible (SbV), submicron (Sm) and oligomer size ranges.

According to Narhi *et al.* (2012) oligomers or high-molecular weight species (HMWs) detected by SEC are in the 0.1 μm size range, particles with diameters of 0.1 -1 μm are considered as Sm, from 1 to 100 μm are SbV, and higher than 100 μm are considered as Vs (Joubert *et al.*, 2011). The recommended detection technique will vary according to the size of the aggregate. The HMWs were measured by UHPLC-SEC, Sm by DLS and NTA, and Vs by optical inspection. Fragments or Low Molecular Weight species (LMWs) were measured by CGE.

The values obtained of HMWs% (Figure 5.11a) and LMWs% (Figure 5.11b), respectively measured by UHPLC-SEC and CE-SDS techniques, showed very similar results at the start of the stability test (T0), at two- weeks (T2W) and at four-weeks (T4W). The HMWs% of all formulations increased over time at 40°C, but there was no significant difference between the control (FA.75) and the optimized formulations. This could indicate that the presence of the different surfactants and the increase ifn general excipients concentration bring the same protection against the formation of HMWs.

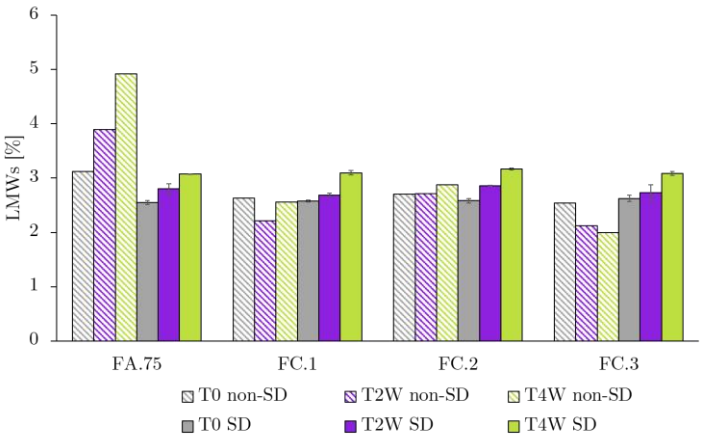

(a)

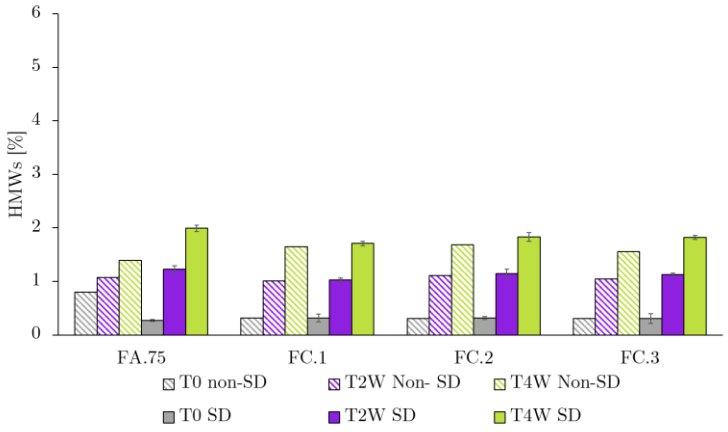

(b)

Figure 5.11. a) HMWs and b) LMWs aggregates of FA.75 and FC formulations. Obtained by UHPLC-SEC and CE-SDS respectively (n=3).

On the other hand, the small increase of LMWs% over time at 40°C, on variations of FC seems to be negligible, in particular when compared to the formulation that was not spray-dried (non-SD). The causes behind the higher values of LMWs% observed for the non-SD FA.75 are not fully understood at this point; however, it can be confirmed that the SD process does not induce a problem of LMWs formation.

It has previously been reported that high concentrations of Arginine suppresses apparent oligomerization on mAbs which increase the HWM%, through initial binding of arginine to the mAb surface (Scherer *et al.*, 2010). The increase in concentration of Arginine from 53 mM (FA.75) to 100 mM (FC.1, FC.2, FC.3) showed a slight decrease on the HWM%.

Considering the sensitivity and the range of measurement of the DLS (1-1000 nm) it would be difficult to evaluate the difference in the impact of the impurities and the excipients on protein stability (Xu, 2015). However, it is still a useful technique to analyse the evolution of aggregation over time and its sensitivity to larger aggregates makes it a good complement to turbidity measurements.

Formulation FC.3 showed Z-average values close to the reconstituted spray-dried powder (SD) and the stock solution (non-SD) (Table 5.10). The detection of Sm by NTA is able to count particles from 30 nm - 1 µm. Compared to DLS, NTA gives better peak resolution and less interference of larger particles, and gives approximate particle counts (Filipe *et al.*, 2010b). The formulation using PS80 (FC.1) showed the lowest particle count among all the formulations, followed by FC.3 which uses Pol-188.

Table 5.10. Analysis of sub-visible and sub-micron particles by DLS (Z-average) and NTA (Concentration of particles)

	Z-Average [d.nm]			Concentration [particles/ml] (10^8)		
Formulation	T0	T2W	T4W	T0	T2W	T4W
FA.75 (non-SD)	8±0.1	15±5	17±2	0.9	3.6	7.2
FC.1 (Non-SD)	10±0.1	10±0	10±0.1	NA	NA	NA
FC.2 (Non-SD)	10±0	10±0.1	12±0.2	NA	NA	NA
FC.3 (Non-SD)	11±0.6	10±0.2	12±0.9	NA	NA	NA
FA.75 (SD)	11±0.1	11±0.0	11±0.2	1.8	2.7	2.7
FC.1 (SD)	10±0.3	10±0.3	10±0.3	0.7	0.7	0.9
FC.2 (SD)	10±0.2	11±0.3	13±1	1.2	1.4	2
FC.3 (SD)	10±0.1	11±0.5	11±0.2	0.6	0.8	1.6

On the other hand, the highest particle count was attributed to the formulation FA.75, which contains the lower dose of excipients present in the formulation compared to formulations FC. What can be extracted from these results was that with higher concentrations of excipients it was possible to achieve a better stabilization of the protein during a process with different stress sources such as SD.

Techniques used to directly analyse the protein chemical and conformational stability after the spray-drying process were the cIEF and DSF. The cIEF is a high-resolution analytical technique that allows the separation of protein/peptide mixtures, protein glycoforms and other charge variants, based on their isoelectric point (pI)) (Lin *et al.*, 2011). The increase of acidic species is normally due to different modifications of the mAb, among which we can find deamidation, aggregation, mismatched disulphide bond, etc. (Du *et al.*, 2012; Lin *et al.*, 2011). Stressed mAb samples are prone to generate higher levels of acidic or basic species. Among the basic species one of the causes are protein fragments formation and the aggregation phenomena (Du *et al.*, 2012). cIEF was used to analyse the charge variants in the mAbA spray-dried powder formulation. Through all formulations the percentage values of acid and basic species are very similar, indicating no major impact of the excipients between the control sample (FA.75) and the optimized formulation (FC.1, FC.2, FC.3) (Table 5.11).

DSF is a biophysical technique that allows the tracking of the protein folding state and its thermal stability, by measuring the changes of an extrinsic fluorescent dye or the intrinsic fluorescence oftryptophan, present in the mAb, upon exposure to increasing temperature (K. Gao *et al.*, 2020; Simeonov, 2013).

Table 5.11. cIEF results: calculated percentage of charge variant ratio for each mAb sample (FA.75, FC.1, FC.2, FC.3) FC.2 (SD).

icIEF

	Acid Species [%]			Basic Species [%]		
	T0	T2W	T4W	T0	T2W	T4W
FA.75 (non-SD)	18	32	53	13	15	15
FC.1 (non-SD)	18	25	33	14	13	12
FC.2 (non-SD)	18	26	34	13	13	12
FC.3 (non-SD)	19	23	31	14	14	12
FA.75 5 (SD)	19	25	33	14	14	11
FC.1 (SD)	19	25	32	13	13	12
FC.2 (SD)	18	24	34	13	13	12
FC.3 (SD)	19	24	32	13	13	12

For this study, DSF was used to assess the protein thermal stability after the spray-drying process by determining the melting temperature (T_{m}). The value of T_{m} indicates when 50% of a protein or a certain moiety is unfolded, and in the case of mAbs the first T_{m} (T_{m1}) normally corresponds to the $CH2$ domain unfolding (Simeonov, 2013). A decrease in the melting temperature might indicate that some of the molecular interactions of the protein have been altered due to an instability caused by the stresses generated during the spray-drying process. In Figure 5.12, we observed no meaningful difference between the stock solution (non-SD) and the reconstituted solution (SD) T_{m} values for the FC variant formulations. It means that the possible conformational changes affecting the T_{m} do not differ among them. Meanwhile, the control formulation (F1.75) showed a slightly higher difference between the non-SD and the SD values of T_{m}. It can be concluded that the spray-drying process does not have a major impact on the mAb-A conformational structure when the excipients concentration is increased

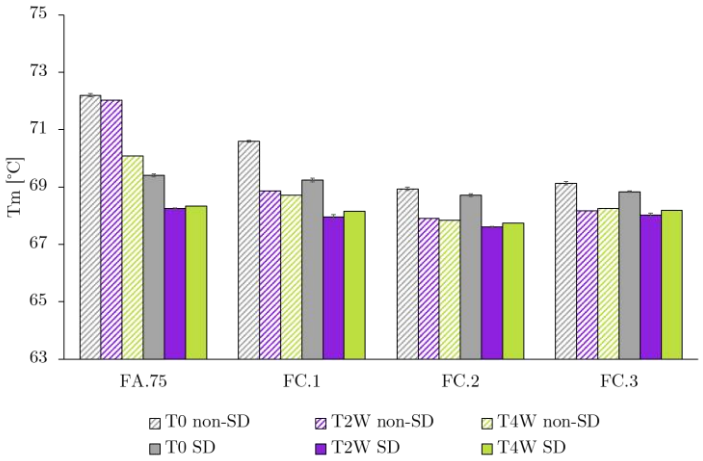

Figure 5.12. Melting temperature obtained during the DSF technique for the stock solution (non-SD) and the spray-dried (SD) formulations FC.1, FC.2, FC.3 and FA.75 (n=3).

The turbidity of the formulations changed during the stability test at 40°C: for formulations FC.2 (PS20 - 1500 ppm) and FC.3 (Pol-188 - 4000 ppm), there was an increase in turbidity over time for both non-SD and SD, but without a substantial change in turbidity between them. This corresponds to the

previously described optical inspection results (Table 5.1) and the Z-average values (Table 5.4). On the other hand, the T0 values of FA.75 (PS80-750 ppm) and FC.1 (PS80 - 1500 ppm) were slightly higher compared to FC.2 and FC.3, which diminish at T2W and T4W. This phenomenon is still not fully understood and will require further investigation. The optical inspection shows a slightly higher opalescence for SD FA.75 at T0, which is not noticeable on SD FC.1. The values of non-SD for FC.1 are slightly higher (Figure 5.13), the source of which has not been yet identified, therefore this phenomenon should be studied further.

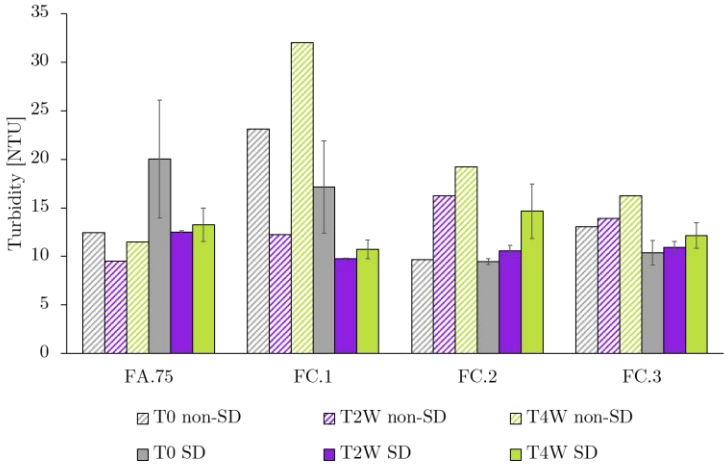

Figure 5.13. Turbidity results from the stability test performed on the optimized formulation (FC.1, FC.2, FC.3) and the control formulation (FA.75) after spray-drying and its corresponding stock solution (non-SD) (n=3).

Therapeutic protein formulations usually contain polysorbates (20 and 80) in the range of 0.003% to 0.8% w/v (SINGH *et al.*, 2017). The critical micelle concentration (CMC) is an important factor when using polysorbates in a protein formulation, given that they are proposed to build a monolayer around the droplet generated in the spraying step of SD, when at the CMC value (Khan *et al.*, 2015). The approximate values of CMC of polysorbates, given that they can be affected by the presence of the protein and other excipients, are considerably low (Khan *et al.*, 2015). The CMC, at 25°C, for PS80 is 0.0017 % w/v and for PS20 is 0.0067% w/v (Kerwin, 2008; Singh *et al.*, 2017; Tian *et al.*, 2010). It has been proven, as well, that some surfactants can be effective in protein stabilization even at values lower than their CMC (S. Wang *et al.*, 2018).

Similar mAb formulations to FA (Part 1) produced by SANOFI (data not shown) were found to be stable during the spray-freeze drying process at a concentration of PS80 of 0.02 % w/v, although it was not the case for the mAb-A powder produced from spray-drying, at which an increase greater than 0.075 % w/v was required for an improvement in overall mAb-A stability.

On the other hand, CMC of Pol-188 has a higher fluctuation depending on temperature, concentration and excipients present in the formulation (H. L. Kim *et al.*, 2014; S. H. Lee *et al.*, 2011). The protective

mechanism of this surfactant is less correlated with its CMC value and other mechanisms of protection have been suggested in literature, such as the formation of protein-surfactant complexes (H. L. Kim *et al.*, 2014; Lefebvre *et al.*, 2021) .

The formulations FC.1 and FC.2 contain PS20 and PS80 at 0.15 % w/v whereas FC.3 contains Pol188 at 0.4 %w/v. According to the literature (Grapentin *et al.*, 2020), poloxamers are considered more chemically stable than polysorbates. As mentioned before, even if the surfactant seems to have a better impact at higher concentrations, there is a limit before it becomes a denaturalizing agent during storage.

Batens *et al.* (2018) and Baek & Zydney. (2017) reported a reduction in viscosity on IgG formulations attributed to the shielding of electrostatic interactions between proteins provided by the presence of amino acids (L-Histidine and L-Arginine among others). The improved formulation showed a decrease in viscosity compared to formulations F1 and F2. When considering a subcutaneous delivery, the viscosity of highly concentrated protein solutions is recommended to be under 20 cP to enable easy administration through a thin-needle. Higher viscosities would require the use of larger gauge needles and/or a higher force to inject the drug product. At a molar ratio of (0.3:1 of trehalose:mAb) it is possible to observe a lower solution viscosity upon reconstitution (Gikanga *et al.*, 2015).

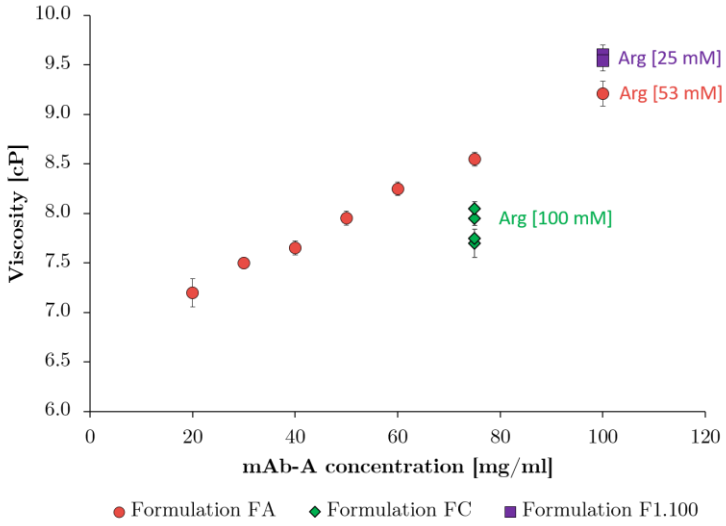

Figure 5.14. Comparison of the mAb-A and arginine concentration effect on the formulation viscosity for FA, FC from this chapter, and F1.100 used in chapter 4.

5.4.3 **Synthesis Chapter 5**

The stability of the mAb-A measured by orthogonal analytical techniques for the different types of aggregates present in a reconstituted solution from spray-dried powders produced from different conditions showed small differences for the three different surfactants (PS20, PS80 and Pol-188) at the same concentration.

Our spray-drying experiments showed that when the mAb-A is well protected through a robust formulation the impact of the process operating conditions was minor, and it was able to produce a final formulation that was adequate for reconstitution with lower turbidity and aggregates families present.

Conclusions and Perspectives

CONCLUSIONS

This thesis focused on the spray-drying of biopharmaceuticals, particularly proteins.

The growing interest in biopharmaceuticals, particularly proteins, has been on the rise due to their specific activity and effectiveness in treating various chronic diseases. However, producing protein-based formulations presents a significant challenge due to the high intrinsic instability of proteins. One solution to this issue is to convert liquid formulations into solid forms through drying processes. Various drying techniques, such as spray-freeze drying, freeze-drying, spray-drying, and electrospray-drying, are currently used, but each comes with unique stresses that can lead to protein denaturation or aggregation and a loss of activity.

Spray-drying has gained popularity as a method for producing dried protein-based biopharmaceuticals because of its faster drying cycle, ability to control particle engineering and its lower energy consumption compared to other drying technologies, such as freeze-drying. However, spray-drying also comes with certain stresses, including thermal/dehydration stress, shear stress, and interfacial stress. Therefore, protecting the proteins against these stresses during the transition from liquid to solid state using this process is still a challenge.

One of the challenges when spray-drying biopharmaceutical proteins is to select the appropriate operating parameters that will ensure a minimum level of protein aggregation, while also meeting the requirements for pharmaceutical use (moisture content, particle size, easy reconstitution in water, physical and chemical stability).

Another challenge is selecting the appropriate stabilizers (excipients) that can provide sufficient protection against one or more types of stress. While a certain combination of concentrations and types of excipients may protect the protein under certain spray-drying conditions, its effect may be limited if the experimental conditions are drastically changed. However, it is important to keep in mind that the selection of a stabilizer will be as a result of the function of the protection mechanism that it offers.

The current study employed a dual methodology to investigate the compatibility of a protein formulation with the spray-drying process:

1. The first approach examined the impact of various stress factors created during spray-drying on the stability of a protein, specifically focusing on Bovine Serum Albumin (BSA) as a model pure protein and then on a monoclonal antibody (mAb). The shear stress was replicated under the same conditions as the spray-drying process, while the thermal stress was simulated under harsher conditions to assess the impact of thermal stress at different protein concentrations in extreme environments.

2. In a given combination of excipients, it may be interesting to modify the mass proportion of each excipient to better investigate the contribution of each to the protection provided to the protein by the whole formulation. The second approach was then centred on the formulation, investigating how variations in the formulation composition and concentration of protein and excipients can affect the mAb stability during the transition from a liquid to a dry form, using a spray-drying process. In this study, the stability of the generated spray-dried powders and their reconstituted solutions was evaluated by measuring the aggregation levels and turbidity using various techniques, such as dynamic light scattering, UV-Visible spectroscopy, HPLC-SEC, and nanoparticle tracking analysis, among others.

The main conclusions drawn in this thesis include:

- **From the drying study of a pure model protein, BSA**

For the formulations with two different BSA concentrations (100 and 200 mg/ml) without excipients, the shear stress generated in the lab-scale spray-dryer, in the order of 10^3 corresponding to shear rates in the order of 10^5 [s^{-1}], did not lead to high levels of aggregation of BSA.

These values of shear rate/shear stresses are commonly found in studies of protein aggregation during spray-drying. When the BSA was exposed to severe thermal stresses, which was not typically seen in a spray-drying process for this type of proteins, it resulted in similarly high levels of aggregation for both protein concentrations. These results align with previous research which has identified high temperatures and the absence of excipients as factors contributing to increased protein aggregation.

When comparing the aggregation levels generated by the decoupled stresses to the spray-drying ones, we found that the difference between the shear stress test and the spray-drying was small. The thermal stress generated the highest aggregation values. but we must keep in mind that whilst the wet bulb temperature is similar between the spray-drying process and the droplet drying, the exposure timeof the protein to the drying air in the latter is longer. Even though, the drying conditions between spray-drying and the thermal/dehydration stress test were not the same, they allowed us to understand the relevance of the study of the decoupled stresses for this kind of processes.

It is relevant to mention that we did a previous screening study of the spray-drying parameters (nozzle diameter, inlet temperature, liquid feed flow rate) on BSA. There was no clear correlation between those input parameters and the protein aggregation. Nevertheless, we chose the values that reported a good compromise between the mentioned output parameters results.

Using a model protein such as BSA was beneficial for us because it is a well-characterized protein with known properties, making it easier to study and understand the effects of different stresses on protein stability. As well, it can serve as a starting point for understanding the behaviour of other proteins and could also be used as a control in comparison to the other proteins being studied, in this case the mAb. However, it is important to keep in mind that the data is not completely directly transferable between the two proteins.

- **From the drying study of a mAb solution**

After observing the effect of the decoupled stresses in a protein formulation (BSA) that did not contain any excipients, we wanted to observe the effect of the same conditions on a formulated protein solution (mAb). This new formulation contained a mAb at a concentration of 100 mg/ml, containing different types of excipients: sugars (trehalose), amino acids (arginine and histidine) and surfactants (polysorbate-80).

Initially the same stress-cutting approach developed for the previous study with BSA was applied to the mAb. The results of the shear stress test demonstrated once again that the shear forces generated in our operating conditions are not high enough to destabilize the molecule, even less for a protected molecule like is the case of our mAb formulation containing excipients. From the thermal stress results, contrary to the ones obtained for the BSA, the mAb aggregation was low. This effect is most likely linked to presence of excipients in the mAb formulation.

In the case of the mAb formulation at 100 mg/ml the highest aggregation levels were found when the stresses were coupled in the spray-drying process. This led us to investigate the possible parameters that were affecting the protein stability by varying the drying temperature (70-120 °C) and the liquid feed flow rate (3 and 6 ml/min), as well as the concentrations of the proteins and excipients in the formulation, i.e, reducing the protein concentration from 100 to 75 mg/ml while also increasing the excipient concentration. This study was able to provide us with relevant information, showing that a change in the formulation composition was more effective in improving the formulation stability than the process parameters of spray-drying. This finding opened the possibility to explore the impact that the protein concentration had on the stability and the level of protection that every excipient offers to mAb-A.

Thus, the study which followed varying the protein concentration from 10 to 100 mg/ml, showed that working below concentrations of 75 mg/ml did not introduce drastic changes to the aggregation levels, therefore we continued with this concentration for the evaluation of the excipients concentration. Each excipient was analyzed individually by changing its concentration in the formulation while all the others remained at a fixed level. This allowed us to observe the impact each one had on protein stability. The results indicated that a general increase in the excipients concentration reduced the levels of aggregation. The surfactant was the excipient with the highest effect on reduction of protein aggregation and turbidity in solution. As previously explained the spray-drying process generates a large air-liquid surface that creates a lot of contact points of stress for the proteins in the droplets, thus it is expected that an excipient whose action mechanism is to prevent the protein reaching the droplet air-liquid interface area.

The formulations for the last spray-drying experiments were prepared considering all the previous findings. Therefore, the protein concentration was targeted at 75 mg/ml, and all excipients concentrations were increased again. With these new characteristics, three different final formulations were produced, each one with a different type of surfactant (polysorbate-80, polysorbate-20 and poloxamer-188).

The stability of the mAb-A was measured by orthogonal analytical techniques for the different types of aggregates present in a reconstituted solution from spray-dried powders. These powders produced from different conditions, showed small differences for the three different surfactants (PS20, PS80 and Pol-188) at the same concentration.

The question posed at the beginning of this thesis concerned a problem identified in an industry case where a mAb formulation dried by three different techniques, including spray-drying, did not provide the same level of protection as mAb in dry powder. The spray-dried powder was the worst of the three. The question was whether it would be possible to obtain a mAb spray-dried powder with good quality (minimal degradation due to the drying technology). This thesis was able to demonstrate with our spray-drying experiments, albeit on a bench scale, that when the mAb is well protected through a robust formulation the impact of the process operating conditions is minor, and it can produce a final formulation that is adequate for reconstitution with lower turbidity while maintaining all other quality attributes.

PROSPECTS FOR FUTURE STUDIES

Despite the progress obtained, the study could be deepened to allow a better understanding of the interplay of the protection mechanisms of stabilizers due to their combined use in the formulations.

Different study topics could be pursued, concerning the formulation and/or the process, such as:

- **ON THE PROCESS**

Decoupling of stresses

Increase the range of operating parameters values for both shear and thermal stress tests, to have a more accurate vision of the protein behaviour. Also to verify if there is a stress threshold after which the formulation does not provide any protection to the protein.

As well, another important step will be to homogenize the drying conditions between the thermal/dehydration stress test and the spray-drying process. For example, with a similar drying kinetics, final moisture content and size of the droplets. A higher size of droplets during spray-drying will allow a better comparison between both techniques by creating similar singular systems for study.

On-line follow-up of the protein aggregation in the thermal stress test

An in real-time observation of the protein aggregation phenomena during the thermal stress test, using a suspended droplet, will be a very interesting way to explore the exact moment of the first appearance of the aggregation populations due to thermal/dehydration stresses.

- **ON THE FORMULATION**

Monoclonal Antibody formulation without excipients

The study of the monoclonal antibody without excipients will be interesting to create a more refined idea of the impact of the aggregation of excipients to a formulation.

Type of monoclonal antibody

To try the excipients type and concentration in another type of antibody during a spray-drying process to observe if the extent of protection is really linked to this specific antibody used in this thesis.

General formulation

With the purpose of comparison, to observe the effect of the formulation on the aggregation levels of the mAb when using other drying technologies, which could be of interest to the industry.

- **CHARACTERIZATION**

Advanced characterization of the powder after spray-drying

Exploring the physical characteristics of the spray-dried powder in more depth will bring a new understanding onto the different mechanisms of protection that were involved in the formation of the mAb dry form. For example, by investigating the potential of characterization methods, such as Raman spectroscopy, for the study of excipients in the surface, or mass spectrometry, to better understand the protein structure and stability during spray-drying.

Using techniques such as circular dichroism or nuclear magnetic resonance spectroscopy to study the effect of excipients on the conformation of the protein, which will give insight into the mechanisms of protection provided by different excipients.

Study of the powder physical characteristics such as wettability, dispersibility to have a wider picture of what is happening at the powder level right after spray-drying.

Résumé étendu en français

Chapitre I. Introduction et objectifs

Les biopharmaceutiques, ou médicaments biologiques, sont toutes des molécules obtenues par des techniques biotechnologiques. Elles comprennent les acides nucléiques, cellules vivantes, tissus et protéines. Elles sont utilisées dans de nombreux domaines de la médecine et sont devenues les traitements cliniques les plus efficaces pour diverses maladies, notamment les cancers et les troubles métaboliques (Kesik-Brodacka, 2018 ; Yeh et al., 2018). Du point de vue de la fabrication, de la formulation et du contrôle qualité, les protéines thérapeutiques posent de nombreux défis par rapport aux molécules de faible poids moléculaire en raison de leur complexité (Staub et al., 2011).

L'intérêt pour certains biopharmaceutiques protéiques, tels que les anticorps monoclonaux, a récemment augmenté en raison de leurs propriétés de ciblage hautement spécifiques approuvées pour le traitement de diverses maladies chroniques (Castelli et al., 2019 ; Ramezani et al., 2014). Les anticorps monoclonaux constituent le groupe le plus important de protéines recombinantes utilisées à la fois pour la thérapie humaine et pour l'imagerie *in vivo* de différents types de maladies (Kunert et al., 2016). Il existe plusieurs classes d'anticorps monoclonaux, parmi lesquelles les IgG sont les seules actuellement utilisées en clinique en raison de leur demi-vie circulante prolongée et de leur relative facilitée de production (Kaplon et al., 2022 ; Ramezani et al., 2014).

Pendant l'année 2021, 11 anticorps monoclonaux différents ont obtenu des premières approbations soit aux États-Unis, soit en Europe, et au niveau mondial, 27 nouvelles thérapies par anticorps font l'objet d'un examen par les organismes de réglementation. Cela témoigne d'une croissance de 30 % du pipeline clinique commercial de stades avancés pour les thérapies par anticorps monoclonaux (Kaplon et al., 2022). L'un des principaux défis dans le développement des anticorps monoclonaux est leur instabilité inhérente et la nécessité de développer des formulations stables. La plupart des formulations commerciales d'anticorps monoclonaux sont disponibles sous forme de formes posologiques liquides qui offrent des options d'administration pratiques pour les patients, l'administration sous-cutanée étant la plus courante selon de nombreux auteurs (Batens et al., 2018 ; Jackisch et al., 2014 ; Le Basle et al., 2020 ; Viola et al., 2018). Cependant, une formulation liquide présente plusieurs défis du point de vue de la stabilité (Ramezani et al., 2014 ; SINGH et al., 2017 ; Walters et al., 2014).

Par rapport à d'autres formes posologiques, les formulations liquides d'anticorps monoclonaux favorisent les interactions monomère-monomère et plusieurs changements chimiques, ce qui peut avoir un impact sur plusieurs attributs de qualité critiques (CQAs), tels que l'agrégation, la fragmentation et la perte d'activité biologique (Le Basle et al., 2020). L'élimination de l'eau confère à la formulation différents avantages, tels qu'une réduction des coûts de transport, une facilité de manipulation et de stockage, et surtout une plus grande stabilité moléculaire (Ramezani et al., 2014). Elle peut également éliminer les inconvénients liés à l'étape de congélation de la solution des protéines avant sa conversion en produit pharmaceutique, tels que la dénaturation des protéines causée par la cryoconcentration et

les variations de pH, ainsi que l'hétérogénéité de la vitesse de congélation, qui peut entraîner des changements substantiels dans la composition de la solution congelée (Langford et al., 2020). Les avantages de l'élimination de l'eau peuvent être obtenus grâce à la production d'une formulation en poudre à partir d'un procédé de séchage tel que la lyophilisation, le séchage par congélation ou le séchage par atomisation.

Le procédé de séchage par atomisation implique la nébulisation, à travers une buse, d'une formulation liquide dans une phase gazeuse chauffée où le solvant s'évapore. La formation de gouttelettes et l'évaporation ultérieure du solvant se produisent à une vitesse très rapide (< 2s depuis la formation des gouttelettes jusqu'aux particules séchées) (Bögelein et al., 2010 ; Bowen et al., 2013 ; Ousset et al., 2018 ; Schaefer et al., 2015 ; Ziaee et al., 2019). Les avantages du séchage par atomisation en tant que procédé de fabrication de poudre comprennent la scalabilité du procédé et la capacité de design (ingénierie) des caractéristiques des particules.

Au cours des 15 dernières années, certains produits pharmaceutiques protéiques ont été séchés par atomisation avec succès (Ajmera, 2014 ; Devahastin et al., 2020 ; Emami et al., 2018 ; Pinto et al., 2021). Néanmoins, le séchage par atomisation d'une solution contenant des protéines pures suscite de vives inquiétudes quant à la dégradation et à l'inactivation, en raison de l'endommagement de sa structure. (Ajmera, 2014 ; Emami et al., 2018 ; Keshani et al., 2015). Les facteurs de stress possibles auxquels la protéine est soumise pendant le séchage par atomisation surviennent à l'étape d'atomisation, où la protéine, sensible à l'interface air-eau, est soumise à des contraintes de cisaillement exercées par le dispositif (buse) d'atomisation. Une autre source de stress est présente lors de la déshydratation ou conversion de la protéine en un état solide et sec (Ajmera, 2014 ; Grasmeijer et al., 2019 ; Mensink et al., 2017). Toute perte d'activité pendant le séchage par atomisation entraîne une réduction de la qualité du produit final.

L'impact du procédé sur la structure de la protéine pendant la production d'une la forme sèche (poudre) et lors de son stockage peut être réduit ou minimisé par l'action d'excipients. Les excipients sont d'une grande aide pour stabiliser les protéines pharmaceutiques, telles que les anticorps monoclonaux, contre les contraintes générées par le procédé de séchage par atomisation, étant donné qu'ils fournissent différents mécanismes protecteurs (remplacement de l'eau, vitrification et adsorption compétitive, et exclusion préférentielle) contre la dénaturation (Grasmeijer et al., 2013 ; Chiu et al., 2011 ; Mensink et al., 2017 ; Sudrik et al., 2017).

Un autre point critique est que la réponse de la stabilité de la formulation au séchage par atomisation peut varier d'un équipement à l'autre et selon les conditions opératoires du procédé. L'analyse des paramètres opératoires et de formulation sur l'intégrité des protéines est une tâche complexe car les différentes contraintes sont présentes (mécaniques, thermiques, déshydratation...) au cours de ce procédé de séchage très rapide. Comprendre les effets individuels de certaines de ces contraintes sur la dénaturation des protéines pharmaceutiques s'avère être une stratégie intéressante pour aider au criblage des conditions du procédé de séchage, ainsi qu'aux excipients de stabilisation. Néanmoins, cette stratégie de criblage et de compréhension des effets des paramètres opératoires et de formulation

ne remplace pas l'étude du procédé de séchage par atomisation qui doit enfin être réalisée pour l'optimisation des conditions opératoires et de formulation (type et niveau d'excipients, concentration en protéines) afin d'obtenir une composition finale de poudre séchée par atomisation de haute qualité pour la reconstitution.

Thesis objectives

Cette thèse vise à fournir une meilleure compréhension des facteurs affectant la stabilité d'une poudre séchée par atomisation contenant un anticorps spécifique, par :

- Le découplage de certaines sources de stress (mécaniques, thermiques/déshydratation) auxquelles une protéine pharmaceutique est soumise lors d'un procédé de séchage par atomisation, en utilisant différentes configurations expérimentales. Cette approche méthodologique a été appliquée à différentes protéines : une protéine modèle non formulée (BSA) et une solution formulée de mAb (mAb-A).
- Le séchage par atomisation sur la formulation de mAb-A, avec l'étude de l'effet des paramètres du procédé et de la composition de la formulation (concentration en protéines, excipients) sur l'intégrité (niveau d'agrégation) de la protéine après reconstitution.

Chapitre 2. Etat de l'art.

Ce chapitre introduit d'abord les protéines biopharmaceutiques et les problèmes qu'elles rencontrent dans la formulation liquide et se termine avec un focus sur les anticorps monoclonaux. La stabilisation des protéines en formulation liquide représente un défi auquel l'industrie pharmaceutique est confrontée de nos jours. Une des solutions proposées pour y remédier est de passer d'une formulation liquide à une formulation solide grâce à un procédé de séchage. Il existe différents types de procédé de séchage (spray-freeze drying, lyophilisation, séchage par atomisation, etc.), chacun avec un ensemble différent de paramètres de procédé qui généreront différents types de contraintes. Une technique telle que la lyophilisation présente des contraintes interfaciales solide-liquide, des contraintes de déshydratation et des changements de pH, entre autres. La technique de spray-freeze drying présente des changements de formulation (pH, concentration des composants), des contraintes de cisaillement et des contraintes de déshydratation.

Le procédé de séchage par atomisation est une des techniques de séchage qui gagne en importance dans la fabrication de produits biopharmaceutiques à base de protéines. Cependant, cette technique présente également certaines contraintes, les trois principales étant les contraintes thermiques et de déshydratation, les contraintes de cisaillement et les contraintes interfaciales. Pour réduire l'impact des contraintes lors du séchage par atomisation, la sélection des bons paramètres du procédé est essentielle. Dans un mode de pulvérisation avec une buse de type bi-fluide (où un gaz est utilisé comme fluide auxiliaire de la désintégration du liquide), le ratio massique entre le débit du gaz d'atomisation et le débit d'alimentation de la solution protéique joue un rôle important sur les propriétés de la poudre obtenue et sur la stabilité de la protéine lors de la reconstitution de cette poudre dans l'eau. La

température d'entrée déterminera la stabilité de la protéine en contrôlant les contraintes thermiques exercées pendant le séchage et la teneur en humidité finale de la poudre.

Outre les conditions opératoires du procédé de séchage par atomisation, la formulation est un autre facteur critique dans la stabilisation des produits biopharmaceutiques à base de protéines. Différents stabilisants peuvent être ajoutés à la formulation pour éviter ou réduire l'impact des contraintes présentes dans le procédé de séchage par atomisation. Cependant, il est important de garder à l'esprit que la sélection du stabilisant dépendra du mécanisme de protection qu'il offre.

Cette thèse porte sur la génération de formes stables et sèches d'anticorps monoclonaux (mAbs) par le procédé de séchage par atomisation. Dans les chapitres suivants, nous explorons l'impact de ce procédé de séchage et de la formulation sur la stabilité d'une formulation à base de protéines, à travers la caractérisation des poudres obtenues et des solutions reconstituées à partir de celles-ci.

Chapitre 3. BSA : modèle pour l'étude du séchage par atomisation de protéines

Le chapitre 3 présente la première partie de notre étude, consacrée à une investigation rationnelle sur la résistance d'une protéine modèle aux différentes contraintes auxquelles elle sera soumise par le procédé de séchage par atomisation, sans aucun facteur de formulation protecteur contre la dénaturation (agrégation).

Différentes protéines ont été utilisées comme modèles pour étudier la résistance des protéines aux contraintes inhérentes aux techniques de séchage. Les modèles les plus courants sont des enzymes telles que l'alcool déshydrogénase (Shiga et al. 2014), la déshydrogénase lactique (Grasmeijer et al. 2019), le lysozyme (Ajmera 2014), ou une famille de protéines globulaires (albumines) comme la gammaglobuline bovine BGG (Heng & Yeates, 2018), l'ovoalbumine OVA (Ajmera 2014), et l'albumine de sérum bovin BSA (Hackl et al, 2018.I, Hackl et al, 2018.II). Les poids moléculaires de ces protéines modèles les plus courantes sont compris entre 14 et 240 kDa.

La BSA est la protéine modèle de choix dans la phase initiale de notre étude, en raison de ses caractéristiques telles que la pureté, la solubilité dans l'eau, son coût accessible et sa disponibilité en tant que produit commercial. De nombreuses études ont été menées avec la BSA et différents excipients en utilisant le séchage par atomisation comme procédé choisi (Jalalipour et al. 2007, Rajagopal et al. 2013, Constantino et al. 2000, Prinn et al. 2001, Grasmeijer et al. 2016, Wilson et al. 2020). L'état de l'art qui suit dans cette section se concentre sur la collecte des principales informations trouvées dans la littérature à partir de ces études.

À partir des résultats obtenus dans ce chapitre, nous avons observé que la contrainte de cisaillement générée dans les conditions d'un sécheur par atomisation à l'échelle du laboratoire ne crée pas de niveaux élevés d'agrégation sur la BSA. De plus, la formulation de BSA ne contenait aucun stabilisant, ce qui signifie que même sans aucune protection, la contrainte de cisaillement semble ne pas avoir d'effet sur la dénaturation de la protéine.

Lorsque la BSA a été soumise à une contrainte thermique (72°C pendant 1 h)), elle a montré un état d'agrégation élevé similaire pour les deux concentrations de BSA (100 mg/ml et 200 mg/ml).

Les résultats de cette étude ont confirmé que les températures élevées et l'absence d'excipients étaient responsables d'une augmentation de l'agrégation de la BSA en solution reconstituée. D'après la revue de littérature, il semble que l'ajout de certains stabilisants permettrait un meilleur contrôle (réduction) du niveau d'agrégation de la protéine dans les conditions utilisées dans un sécheur par atomisation à l'échelle du laboratoire. Les études suivantes partiront de formulations contenant des excipients pour mieux protéger la protéine qui nous intéresse (les anticorps monoclonaux) des contraintes couplées rencontrées dans le procédé de séchage par atomisation.

Chapitre 4. Séchage par atomisation d'anticorps monoclonaux : impact de différents facteurs de stress rencontrés par une formulation protéique au cours du séchage par atomisation

Parmi les différentes études menées sur le séchage par atomisation de protéines biopharmaceutiques, celles portant sur les anticorps monoclonaux (mAbs) ont gagné en popularité ces dernières années (Batens et al., 2018 ; Bowen et al., 2013 ; Gikanga et al., 2015 ; Maury et al., 2005 ; Ramezani et al., 2014). Le séchage par atomisation des anticorps monoclonaux correspond aux sujets traités dans les chapitres 4 et 5 de cette thèse.

Comme déjà indiqué dans les chapitres précédents, le séchage par atomisation réunit différents stress pour les protéines, tels que le cisaillement/interfaciale et thermique/déshydratation, qui dépendent des paramètres d'opération et du type d'équipement utilisé. On sait déjà que certains niveaux de contrainte de cisaillement peuvent induire des réarrangements moléculaires sur la protéine, la conduisant à un état d'instabilité qui peut la rendre plus sensible à d'autres contraintes (Morgan et al., 2020). Des études sur l'isolation de la contrainte de cisaillement à l'aide d'homogénéisateurs à haute pression, de la capillarité et de buses de pulvérisation ont été rapportées sur différentes protéines, telles que l'hormone de croissance humaine, le caséinate, la lactoferrine et les mAbs (IgG) (Dao et al., 2022 ; Duerkop et al., 2018 ; Maa et al., 1998b ; Wang et al., 2019). Néanmoins, à notre connaissance, l'étude de la contrainte de cisaillement sur les mAbs n'a pas été rapportée sur une configuration de buse de pulvérisation.

Par ailleurs, on considère que la contribution la plus importante à l'instabilité des biomolécules pendant le séchage par atomisation se produit principalement lors de l'étape de séchage en raison des contraintes thermiques et de déshydratation, qui affecteront principalement les structures secondaires et tertiaires (Bhambhani et al., 2020 ; Ghandi et al., 2012). Différentes techniques expérimentales ont été utilisées pour évaluer le stress thermique des protéines en chauffant des solutions contenant des protéines dans des bains d'eau ou des environnements de four (Alsaddique et al., 2016 ; Hawe et al., 2009). Une technique de séchage de gouttelettes uniques en suspension, qui a été principalement utilisée pour étudier la cinétique du séchage (Boel et al., 2020 ; Sadek et al., 2015 ; Souza Lima et al., 2020) pourrait être intéressante pour étudier l'impact thermique/déshydratation d'une opération de séchage sur une gouttelette unique contenant la protéine, comme l'ont démontré Haque et al. (2013), avec l'isolat de protéines de lactosérum (Haque et al., 2013).

Dans ce chapitre, l'étude réalisée sur une solution de mAb (mAb-A) est déclinée en trois parties :

1. Une première étude dans laquelle les contraintes de cisaillement dues à l'étape d'atomisation et les contraintes thermiques/déshydratation lors de l'étape de séchage ont été découplées, comme cela a été fait précédemment dans le chapitre 3 avec une protéine modèle, la BSA. Aucune étude de découplage des contraintes mécaniques et thermiques/déshydratation comme celle réalisée sur la BSA ne semble avoir été réalisée sur des formulations de mAbs. L'impact du découplage de ces sources de contraintes a été comparé à celui observé sur le niveau d'agrégation de mAb-A dans une solution de mAb-A (F1) reconstituée à partir d'une poudre produite par séchage par atomisation.

2. Une deuxième étude de séchage par atomisation dans des conditions variables de débit d'alimentation en liquide et de température d'entrée a été réalisée dans mAb-A (F1).

3. Une dernière étude a été réalisée sur le séchage par atomisation de solutions de mAb-A (F1, F2), où le paramètre d'étude était la composition de mAb-A.

Les résultats ont montré que les contraintes découplées (thermiques/déshydratation et cisaillement) ne sont pas aussi néfastes pour la formulation mAb-A F1.100 que lorsqu'elles sont couplées dans le procédé de séchage par atomisation.

De plus, la composition de la formulation (concentration de protéines et d'excipients) a montré avoir un impact plus important sur la stabilisation de la mAb-A que les conditions opératoires du procédé, comme en témoigne la réduction de la concentration de protéines (100 mg/ml à 75 mg/ml) et l'augmentation de la concentration d'excipients.

Nous avons pu observer que le changement de la composition de la formulation était plus efficace pour améliorer la stabilité de la formulation que les paramètres du procédé de séchage par atomisation. Cette découverte a ouvert la possibilité d'explorer le niveau de protection offert par chaque excipient au mAb-A, ce qui a été réalisé dans l'étude suivante présentée dans le chapitre 5.

Chapitre 5. Séchage par atomisation de mAbs : études de formulation de mAb-A

Ce chapitre est structuré en trois parties, chacune étant consacrée à un paramètre de formulation spécifique :

- La partie 1 est dédiée à la variation de la concentration de mAb-A dans la formulation à sécher (formulation FA);
- La partie 2 est consacrée à la variation de la concentration des excipients individuels (formulation FB) ;
- La partie 3 rassemble les informations récupérées des parties I et II pour générer une formulation améliorée pour le mAb-A qui sera séchée par atomisation et caractérisé plus en profondeur afin de mieux comprendre le phénomène d'agrégation (Formulation FC).

Dans la partie 1, nous avons étudié la concentration seuil de mAb-A pour préparer des solutions de protéines à concentration relativement élevée pour le séchage par atomisation, conduisant à des solutions reconstituées avec peu ou pas d'agrégats.

Une fois la concentration seuil en protéines identifiée, la partie 2 a consisté à étudier l'impact des excipients, à ladite concentration en mAb-A, sur l'agrégation de la solution reconstituée à partir de la poudre séchée par atomisation. Comme indiqué au chapitre 2, une large gamme d'excipients peut être ajoutée aux solutions protéiques pour assurer une stabilité globale et une protection contre différents types de stress (Chiu et al., 2011 ; Emami et al., 2018 ; Grasmeijer et al., 2013 ; Maury et al., 2005 ; Mensink et al., 2017 ; Pinto et al., 2021 ; Sudrik et al., 2017). Les sucres, les surfactants et les acides aminés font partie des excipients sélectionnés pour cette étude : tréhalose, saccharose, arginine, lysine, histidine, citrate, polysorbate-80 (PS80), polysorbate-20 (PS20) et poloxamère-188 (Pol-188).

Quatre cycles de séchage différents ont été effectués, chacun correspondant à un excipient, qui a été étudié à différents niveaux de concentration, tandis que les autres sont restés constants. L'analyse de chaque excipient individuel a permis d'avoir une meilleure perspective des mécanismes de protection possibles qui ont lieu pendant le processus de séchage par atomisation.

Enfin, à partir de la sélection d'une concentration plus appropriée de mAb-A et d'excipients, une nouvelle formulation de mAb-A est proposée et la poudre séchée par atomisation qui en résulte fait l'objet d'une étude de caractérisation plus poussée, à l'aide de techniques orthogonales, qui sont détaillées dans la partie 3 de ce chapitre.

CONCLUSION

Le séchage par atomisation gagne en popularité en tant que méthode de production de biomédicaments à base de protéines séchées en raison de son cycle de séchage plus rapide, de sa capacité à contrôler l'ingénierie des particules et de sa consommation d'énergie plus faible par rapport à d'autres technologies de séchage, telles que la lyophilisation. Cependant, le séchage par atomisation présente également certaines contraintes, notamment le stress thermique/déshydratation, le stress de cisaillement et le stress interfacial. Par conséquent, protéger les protéines contre ces contraintes lors de la transition de l'état liquide à l'état solide à l'aide de ce procédé reste un défi.

Cette thèse a utilisé une approche multi-méthodologique pour étudier la compatibilité d'une formulation de protéine avec le procédé de séchage par atomisation :

1. La première approche a examiné l'impact de divers facteurs de contrainte créés lors séchage par atomisation sur la stabilité d'une protéine, en se concentrant spécifiquement sur l'albumine de sérum bovin (BSA) en tant que modèle de protéine pure, puis sur un anticorps monoclonal (mAb). Les stresses ont été séparés (dans deux différentes dispositifs expérimentaux) par stress thermique/déshydratation et stress dû au cisaillement lors de la pulvérisation en gouttelettes. Les résultats sur l'agrégation des protéines ont été alors comparés à ceux dû aux stresses couplés dans le procédé de séchage par atomisation. Le stress de cisaillement a été reproduit dans les mêmes conditions que le procédé de séchage par atomisation, tandis que le stress thermique a été simulé dans des conditions plus sévères pour évaluer l'impact du stress thermique à différentes concentrations de protéines dans des environnements extrêmes.

2. Dans une combinaison donnée d'excipients, nous avons modifié la proportion massique de chaque excipient afin d'étudier plus précisément la contribution de chacun à la protection offerte à la protéine par la formulation globale. La deuxième approche s'est donc concentrée sur la formulation, en investiguant comment les variations de la composition de la formulation et de la concentration de la protéine et des excipients peuvent affecter la stabilité du mAb lors de la transition d'une forme liquide à une forme sèche, en utilisant un procédé de séchage par atomisation. Dans cette étude, la stabilité des poudres générées et de leurs solutions reconstituées a été évaluée en mesurant les niveaux d'agrégation et la turbidité à l'aide de diverses techniques, telles que la diffusion de la lumière dynamique, la spectroscopie UV, la CLHP-SEC et l'analyse de suivi de nanoparticules, entre autres.

Les principales conclusions de cette thèse concernent :

- L'étude de séchage d'une protéine modèle pure, la BSA.

Pour les formulations avec deux concentrations différentes de BSA (100 et 200 mg/ml) sans excipients, le stress de cisaillement généré dans un pulvérisateur à l'échelle du laboratoire, de l'ordre de 10^3 et correspondant à des taux de cisaillement de l'ordre de 10^5 [s-1], n'a pas entraîné de niveaux élevés d'agrégation de la BSA.

Ces valeurs de taux de cisaillement/stress de cisaillement sont couramment observées dans les études sur l'agrégation des protéines lors du séchage par atomisation. Lorsque la BSA a été soumise à un stress thermique sévère, qui n'est pas typiquement observé dans un procédé de séchage par atomisation pour ce type de protéines, cela a entraîné des niveaux élevés d'agrégation similaires pour les deux concentrations de protéines. Ces résultats concordent avec des recherches antérieures qui ont identifié des températures élevées et l'absence d'excipients comme des facteurs contribuant à une augmentation de l'agrégation des protéines.

En comparant les niveaux d'agrégation générés par les contraintes découplées avec ceux du séchage par atomisation, nous avons constaté que la différence entre le test de stress de cisaillement et le séchage par atomisation était faible. Bien que le stress thermique ait généré les valeurs d'agrégation les plus élevées, il est important de garder à l'esprit que nous avons effectué le séchage dans des conditions difficiles. Aient une exposition directe plus longue aux stress thermique, comparé au séchage par atomisation qui a un temps de séjour plus réduit (< 2 s) ou la proteine est en contacte avec l'air de séchage (Ousset *et al.*, 2018). Il est important de souligner que nous avons réalisé une étude préliminaire des paramètres de séchage par atomisation (diamètre de la buse, température d'entrée, débit d'alimentation liquide) sur la BSA. Il n'y avait pas de corrélation claire entre ces paramètres d'entrée et les paramètres de sortie suivants : agrégation des protéines, teneur en humidité de la poudre pulvérisée ou rendement du procédé. Néanmoins, nous avons choisi les valeurs qui présentaient un bon compromis entre les résultats des paramètres de sortie mentionnés.

L'utilisation d'une protéine modèle telle que la BSA était judicieuse car il s'agit d'une protéine bien caractérisée aux propriétés connues, ce qui facilite l'étude et la compréhension des effets des différents stress sur la stabilité des protéines. De plus, elle peut servir de point de départ pour comprendre le

comportement d'autres protéines et peut également être utilisée comme témoin comparatif par rapport aux autres protéines étudiées, comme les mAbs. Cependant, il est important de garder à l'esprit que les données ne sont pas complètement transférables directement d'une protéine à une autre.

- À partir de l'étude de séchage d'une solution de mAb

Après avoir observé l'effet des contraintes découplées dans une formulation de protéine (BSA) ne contenant aucun excipient, nous avons souhaité observer l'effet des mêmes conditions sur une solution de protéine formulée (mAb). Cette nouvelle formulation contenait mAb à une concentration de 100 mg/ml, comprenant différents types d'excipients : des sucres (tréhalose), des acides aminés (arginine et histidine) et des tensioactifs (polysorbate-80).

Initialement, la même approche de réduction des contraintes développée pour l'étude précédente avec la BSA a été appliquée au mAb. Les résultats du test de stress de cisaillement ont une fois de plus démontré que les forces de cisaillement générées dans nos conditions opératoires ne sont pas suffisamment élevées pour déstabiliser la molécule, encore moins pour une molécule protégée comme c'est le cas de notre formulation de mAb contenant des excipients. En ce qui concerne les résultats du stress thermique, contrairement à ceux obtenus pour la BSA, l'agrégation du mAb était faible. Cet effet est très probablement lié à la présence d'excipients dans la formulation de mAb.

Dans le cas de la formulation de mAb à 100 mg/ml, les niveaux d'agrégation les plus élevés ont été observés lorsque les contraintes étaient couplées dans le procédé de séchage par atomisation. Cela nous a conduit à étudier les paramètres possibles qui affectaient la stabilité de la protéine en variant la température de séchage (70-120 °C) et le débit d'alimentation en liquide (3 et 6 ml/min), ainsi que les concentrations des protéines et des excipients dans la formulation, c'est-à-dire en réduisant la concentration de protéines de 100 à 75 mg/ml et en augmentant la concentration d'excipients. Cette étude nous a fourni des informations pertinentes, montrant qu'un changement dans la composition de la formulation était plus efficace pour améliorer la stabilité de la formulation que les paramètres du procédé de séchage par atomisation. Ainsi, l'étude qui a suivi en faisant varier la concentration de protéines de 10 à 100 mg/ml a montré que travailler en dessous de concentrations de 75 mg/ml n'introduisait pas de changements drastiques au niveau des niveaux d'agrégation, nous avons donc poursuivi avec cette concentration pour l'évaluation de la concentration des excipients. Chaque excipient a été analysé individuellement en modifiant son niveau de concentration dans la formulation tandis que tous les autres restaient à un niveau fixe. Cela nous a permis d'observer l'impact de chacun sur la stabilité de la protéine. Les résultats ont indiqué qu'une augmentation générale de la concentration des excipients réduisait les niveaux d'agrégation. Le tensioactif était l'excipient ayant l'effet le plus important sur la réduction de l'agrégation des protéines et de la turbidité en solution. Comme expliqué précédemment, le procédé de séchage par atomisation génère une grande surface air-liquide qui crée de nombreux points de contact de stress pour les protéines dans les gouttelettes, il est donc attendu qu'un excipient dont le mécanisme d'action est d'empêcher la protéine d'atteindre la zone d'interface air-liquide de la gouttelette.

Les formulations pour les dernières expériences de séchage par atomisation ont été préparées en tenant compte de toutes les découvertes précédentes. Par conséquent, la concentration de protéines était ciblée à 75 mg/ml et toutes les concentrations d'excipients étaient à nouveau augmentées. Avec ces nouvelles caractéristiques, trois formulations finales différentes ont été produites, chacune avec un type différent de tensioactif (polysorbate-80, polysorbate-20 et poloxamère-188). La stabilité du mAb-A a été mesurée par des techniques analytiques orthogonales pour les différents types d'agrégats présents dans une solution reconstituée à partir de poudres séchées par atomisation. Ces poudres produites dans différentes conditions ont montré de petites différences pour les trois tensioactifs différents (PS20, PS80 et Pol-188) à même concentration.

La question posée au début de cette thèse concernait un problème identifié dans un cas industriel où une formulation de mAb séchée par trois techniques différentes, dont le séchage par atomisation, posse plus de stress sur la formulation du mAb. La question était de savoir s'il serait possible d'obtenir une poudre séchée par atomisation de mAb de bonne qualité (dégradation minimale due à la technologie de séchage). Cette thèse a pu démontrer, avec nos expériences de séchage par atomisation, bien que à l'échelle du laboratoire, que lorsque le mAb est bien protégé par une formulation robuste, l'impact des conditions de fonctionnement du procédé est mineur, et il peut produire une formulation finale adaptée à la reconstitution avec une turbidité réduite et maintenir toutes les autres caractéristiques

Perspectives futures

Malgré les progrès réalisés, l'étude pourrait être approfondie afin de mieux comprendre l'interaction des mécanismes de protection des stabilisants en raison de leur utilisation combinée dans les formulations. Différents sujets d'étude pourraient être explorés :

- **SUR LE PROCÉDÉ**

Découplage des contraintes : Élargir la plage de valeurs des paramètres de fonctionnement pour les tests de contraintes de cisaillement et thermiques, afin d'avoir une vision plus précise du comportement de la protéine. Vérifier également s'il existe un seuil de contrainte au-delà duquel la formulation ne fournit aucune protection à la protéine.

Suivi en ligne de l'agrégation des protéines lors du test de contrainte thermique : Une observation en temps réel des phénomènes d'agrégation des protéines pendant le test de contrainte thermique, en utilisant une gouttelette suspendue, serait une manière très intéressante d'explorer le moment exact de la première apparition des populations d'agrégats dus aux contraintes thermiques et de déshydratation.

- **SUR LA FORMULATION**

Formulation d'anticorps monoclonal sans excipients : L'étude de l'anticorps monoclonal sans excipients permettra de mieux comprendre l'impact de l'agrégation des excipients sur une formulation.

Type d'anticorps monoclonal : Essayer le type et la concentration d'excipients sur un autre type d'anticorps lors d'un procédé de séchage par atomisation pour observer si l'étendue de la protection est réellement liée à cet anticorps spécifique utilisé dans cette thèse.

Formulation générale : Dans le but de comparaison, observer l'effet de la formulation sur les niveaux d'agrégation du mAb lors de l'utilisation d'autres technologies de séchage, ce qui pourrait intéresser l'industrie.

- **CARACTÉRISATION**

Caractérisation avancée de la poudre après le séchage par atomisation :

Approfondir l'étude des caractéristiques physiques de la poudre obtenue par atomisation permettra d'apporter un nouvel éclairage sur les différents mécanismes de protection impliqués dans la formation de la forme sèche du Mab. Par exemple, en explorant le potentiel de méthodes de caractérisation telles que la spectroscopie Raman pour l'étude des excipients en surface, ou la spectrométrie de masse pour mieux comprendre la structure et la stabilité de la protéine pendant le séchage par atomisation.

Utilisation de techniques telles que le dichroïsme circulaire ou la spectroscopie par résonance magnétique nucléaire pour étudier l'effet des excipients sur la conformation de la protéine, ce qui permettra d'obtenir des informations sur les mécanismes de protection offerts par différents excipients.

Bibliography

(Adler *et al.*, 2000) M. Adler, M. Unger, and G. Lee. “Surface Composition of Spray-Dried Particles of Bovine Serum Albumin/Trehalose/Surfactant”. In: Pharmaceutical Research. 17.(7) (July 2000), pp. 863–870. Doi: 10.1023/A:1007568511399

(Agyei *et al.*, 2017) D. Agyei, I. Ahmed, Z. Akram, H. M. N. Iqbal, and M. K. Danquah. “Protein and Peptide Biopharmaceuticals: An Overview”. In: Protein and Peptide Letters. 24(2) (2017), pp. 94–101. Doi: 10.2174/0929866523666161222150444

(Ajmera, 2014) A. Ajmera. “Stable spray dried protein formulation and implementation in vaccine development”. [Doctoral Dissertation, Christian Albrecht University]. Open Access Repository of Kiel University. (2014).

(Akhtar *et al.*, 2018) K. Akhtar, S. A. Khan, S. B. Khan, and A. M. Asiri. “Scanning Electron Microscopy: Principle and Applications in Nanomaterials Characterization”. In: Handbook of Materials Characterization. Ed. by S. K. Sharma. Cham: Springer International Publishing, (2018), pp. 113–145. Doi: 10.1007/978-3-319-92955-2_4

(Alhajj *et al.*, 2021) N. Alhajj, N. J. O’Reilly, and H. Cathcart. “Designing enhanced spray dried particles for inhalation: A review of the impact of excipients and processing parameters on particle properties”. In: Powder Technology. 384 (May 2021), pp. 313–331. Doi: 10.1016/j.powtec.2021.02.031

(Alsaddique *et al.*, 2016) J. A. Alsaddique, R. M. Pabari, and Z. Ramtoola. “Effect of Thermal and Shear Stressors on the Physical Properties, Structural Integrity and Biological Activity of the Anti-TNF-alpha Monoclonal Antibody, Infliximab”. In: Current Pharmaceutical Biotechnology. 17(10) (2016), pp. 905–914. Doi: 10.2174/1389201017666160519111815

(Ameri *et al.*, 2006) M. Ameri and Y.-F. Maa. “Spray-drying of Biopharmaceuticals: Stability and Process Considerations”. In: Drying Technology. 24(6) (July 2006), pp. 763–768 (cit. on pp. 44, 80). Doi: 10.1080/03602550600685275

(Amin *et al.*, 2014) S. Amin, G. V. Barnett, J. A. Pathak, C. J. Roberts, and P. S. Sarangapani. “Protein aggregation, particle formation, characterization & rheology”. In: Current Opinion in Colloid & Interface Science. 19(5) (Oct. 2014), pp. 438–449. Doi: 10.1016/j.cocis.2014.10.002

(Anandharamakrishnan & Ishiwarya, 2015) Anandharamakrishnan, C. and Ishwarya, S.P. Introduction to spray-drying. In Spray-drying Techniques for Food Ingredient Encapsulation. Ed. by C. Anandharamakrishnan and S.P. Ishwarya). John Wiley & Sons. (2015). Doi: 10.1002/9781118863985.ch1

(Antony *et al.*, 2022) J.V.Antony, R. Koya, P.N. Pournami, G.G. Nair, J.P. Balakrishnan. Protein secondary structure assignment using residual networks. J Mol Model 28, 269 (2022). https://doi-org.gorgone.univ-toulouse.fr/10.1007/s00894-022-05271-z

(Aro *et al.*, 2020) R. Aro, M. W. Ben Ayoub, I. Leito, and É. Georgin. “Moisture in Solids: Comparison Between Evolved Water Vapor and Vaporization Coulometric Karl Fischer Methods”. In: International Journal of Thermophysics. 41(8) (June 2020), p. 41-113. Doi: 10.1007/s10765-020-02697-6

(Arora *et al.*, 2015) J. Arora, J. M. Hickey, R. Majumdar, R. Esfandiary, S. M. Bishop, H. S. Samra, C. R. Middaugh, D. D. Weis, and D. B. Volkin. “Hydrogen exchange mass spectrometry reveals protein interfaces and distant dynamic coupling effects during the reversible self-association of an IgG1 monoclonal antibody”. In: mAbs. 7(3) (May 2015). pp. 525–539. Doi: 10.1080/19420862.2015.1029217

(Arsiccio *et al.*, 2020) A. Arsiccio, P. Giorsello, L. Marenco, and R. Pisano. “Considerations on Protein Stability During Freezing and Its Impact on the Freeze-Drying Cycle: A Design Space Approach”. In: Journal of Pharmaceutical Sciences. 109(1) (Jan. 2020), pp. 464– 475. Doi: 10.1016/j.xphs.2019.10.022

(Baek *et al.*, 2017) Y. Baek, N. Singh, A. Arunkumar, and A. L. Zydney. “Effects of Histidine and Sucrose on the Biophysical Properties of a Monoclonal Antibody”. In: Pharmaceutical Research. 34(3) (Mar. 2017), pp. 629–639. Doi: 10.1007/s11095-016-2092-0

(Baek & Zydney) Youngbin Baek, Andrew L Zydney. “Intermolecular interactions in highly concentrated formulations of recombinant therapeutic proteins”. In: Current Opinion in Biotechnology. 53 (2018), pp.59-64. Doi: 10.1016/j.copbio.2017.12.016.

(Bansal *et al.*, 2019) R. Bansal, S. Gupta, and A. S. Rathore. “Analytical Platform for Monitoring Aggregation of Monoclonal Antibody Therapeutics”. In: Pharmaceutical Research. 36(11) (Aug. 2019), p. 152. Doi: 10.1007/s11095-019-2690-8

(Barros *et al.*, 2021) M. Barros, X. Zhang, S. Kenrick, and J. J. Valente. “Opalescence Measurements: Improvements in Fundamental Knowledge, Identifying Sources of Analytical Biases, and Advanced Applications for the Development of Therapeutic Proteins”. In: Journal of Pharmaceutical Sciences.110(11) (Nov. 2021), pp. 3550–3557. Doi: 10.1016/j.xphs.2021.06.013

(Batens *et al.*, 2018) M. Batens, J. Massant, B. Teodorescu, and G. Van den Mooter. “Formulating monoclonal antibodies as powders for reconstitution at high concentration using spray-drying: Models and pitfalls”. In: European Journal of Pharmaceutics and Biopharmaceutics. 127 (June 2018), pp. 407–422. Doi: 10.1016/j.ejpb.2018.02.002

(Bee *et al.*, 2009) J. S. Bee, J. L. Stevenson, B. Mehta, J. Svitel, J. Pollastrini, R. Platz, E. Freund, J. F. Carpenter, and T. W. Randolph. “Response of a concentrated monoclonal antibody formulation to high shear”. In: Biotechnology and Bioengineering.103(5) (Aug. 2009), pp. 936–943. Doi: 10.1002/bit.22336

(Bhambhani *et al.*, 2020) A. Bhambhani and V. Antochshuk. “Vaccines and Microorganisms”. In: Drying Technologies for Biotechnology and Pharmaceutical Applications. Section: 5. John Wiley & Sons, Ltd, (2020), pp. 121–136. Doi: 10.1002/9783527802104.ch5

(Bhambhani *et al.*, 2021) A. Bhambhani, J. Stanbro, D. Roth, E. Sullivan, M. Jones, R. Evans, and J. Blue. “Evaluation of Microwave Vacuum Drying as an Alternative to Freeze-Drying of Biologics and

Vaccines: the Power of Simple Modeling to Identify a Mechanism for Faster Drying Times Achieved with Microwave". In: AAPS PharmSciTech. 22(1) (Jan. 2021), p. 52. Doi: 10.1208/s12249-020-01912-9

(B. Bhatnagar *et al.*, 2020) B. Bhatnagar and S. Tchessalov. "Advances in Freeze Drying of Bio- logics and Future Challenges and Opportunities". In: Drying Technologies for Biotechnology and Pharmaceutical Applications. Section: 6. John Wiley & Sons, Ltd, 2020, pp. 137–177. Doi: 10.1002/97835278

(B. S. Bhatnagar *et al.*, 2007) B. S. Bhatnagar, R. H. Bogner, and M. J. Pikal. "Protein stability during freezing: separation of stresses and mechanisms of protein stabilization". In: Pharmaceutical Development and Technology. 12(5) (2007), pp. 505–523. Doi: 10.1080/10837450701481157

(Boel *et al.*, 2020) E. Boel, R. Koekoekx, S. Dedroog, I. Babkin, M. R. Vetrano, C. Clasen, and G. Van den Mooter. "Unraveling Particle Formation: From Single Droplet Drying to Spray-drying and Electrospraying". In: Pharmaceutics. 12(7) (July 2020). p. 625. Doi: 10.3390/pharmaceutics12070625

(Bogahawaththa *et al.*, 2022) D. Bogahawaththa and T. Vasiljevic. "Shear-induced structural changes and denaturation of bovine immunoglobulin G and serum albumin at different temperatures". In: Food Hydrocolloids. 124 (Mar. 2022), p. 107283. Doi: 10.1016/j.foodhyd.2021.107283

(Bögelein *et al.*, 2010) J. Bögelein and G. Lee. "Cyclone selection influences protein damage during drying in a mini spray-dryer". In: International Journal of Pharmaceutics. 401(1) (Nov. 2010), pp. 68–71. Doi: 10.1016/j.ijpharm.2010.09.023

(Bohr *et al.*, 2023) A. Bohr, J. P. Boetker, T. Rades, J. Rantanen, and M. Yang. "Application of Spray-drying and Electrospraying/Electospinning for Poorly Watersoluble Drugs: A Particle Engineering Approach". In: Current Pharmaceutical. Design. 20(3) (2014), pp. 325– 348. Doi:10.2174/13816128113199990399

(Borzova *et al.*, 2016) V. A. Borzova, K. A. Markossian, N. A. Chebotareva, S. Y. Kleymenov, N. B. Poliansky, K. O. Muranov, V. A. Stein-Margolina, V. V. Shubin, D. I. Markov, and B. I. Kurganov. "Kinetics of Thermal Denaturation and Aggregation of Bovine Serum Albumin". In: PLOS ONE. 11(4) (2016). Doi: 10.1371/journal.pone.0153495

(Both *et al.*, 2018) E. M. Both, M. Nuzzo, A. Millqvist-Fureby, R. M. Boom, and M. A. I. Schutyser. "Morphology development during single droplet drying of mixed component formulations and milk". In: Food Research International. 109 (July 2018), pp. 448–454. Doi: 10.1016/j.foodres.2018.04.043

(Bouvier *et al.*, 2014) E. S. P. Bouvier and S. M. Koza. "Advances in size-exclusion separations of proteins and polymers by UHPLC". In: TrAC Trends in Analytical Chemistry. 63 (Dec. 2014), pp. 85–94. Doi: 10.1016/j.trac.2014.08.002

(Bowen *et al.*, 2013) M. Bowen, R. Turok, and Y.-F. Maa. "Spray-drying of Monoclonal Antibodies: Investigating Powder-Based Biologic Drug Substance Bulk Storage". In: Drying Technology. 31(13-14) (Oct. 2013) pp. 1441-1450. Doi: 10.1080/07373937.2013.796968

(Bowling *et al.*, 2016) J. J. Bowling, W. R. Shadrick, E. C. G. a. R. E. Lee, J. J. Bowling, W. R. Shadrick, and E. C. G. a. R. E. Lee. Going Small: Using Biophysical Screening to Implement Fragment Based Drug Discovery. Publication Title: Special Topics in Drug Discovery. IntechOpen, (Nov. 2016). Doi: 10.5772/66423

(Bumbrah & Sharma, 2016) G.S. Bumbrah, R.M. Sharma. “Raman spectroscopy – Basic principle, instrumentation and selected applications for the characterization of drugs of abuse”. In: Egyptian Journal of Forensic Sciences. 6(3) (2016) pp. 209-215. Doi: 10.1016/j.ejfs.2015.06.001.

(Brusotti *et al.*, 2018) G. Brusotti, E. Calleri, R. Colombo, G. Massolini, F. Rinaldi, and C. Temporini. “Advances on Size Exclusion Chromatography and Applications on the Analysis of Protein Biopharmaceuticals and Protein Aggregates: A Mini Review”. In: Chromatographia. 81(1) (Jan. 2018), pp. 3–23. Doi: 10.1007/s10337-017-3380-5

(Cabral-Marques *et al.*, 2009) H. Cabral-Marques and R. Almeida. “Optimisation of spray-drying process variables for dry powder inhalation (DPI) formulations of corticosteroid/cyclodextrin inclusion complexes”. In: European Journal of Pharmaceutics and Biopharmaceutics. 73(1) (Sept. 2009), pp. 121–129. Doi: 10.1016/j.ejpb.2009.05.002

(Castelli *et al.*, 2019) M. S. Castelli, P. McGonigle, and P. J. Hornby. “The pharmacology and therapeutic applications of monoclonal antibodies”. In: Pharmacology Research & Perspectives. 7(6) (2019). Doi: 10.1002/prp2.535

(Chan *et al.*, 2009) C. E. Z. Chan, A. H. Y. Chan, B. J. Hanson, and E. E. Ooi. “The use of antibodies in the treatment of infectious diseases”. In: Singapore Medical Journal. 50(7) (July 2009), 663–672.

(Chiu *et al.*, 2011) P.-L. Chiu, D. F. Kelly, and T. Walz. “The use of trehalose in the preparation of specimens for molecular electron microscopy”. In: Micron. 42(8) (Dec. 2011). pp. 762–772. Doi:10.1016/j.micron.2011.06.005

(Conner *et al.*, 2014) J. Conner, D. Wuchterl, M. Lopez, B. Minshall, R. Prusti, D. Boclair, J. Peterson, and C. Allen. “Chapter 26 - The Biomanufacturing of Biotechnology Products”. In: Biotechnology Entrepreneurship. Ed. by C. Shimasaki. Boston: Academic Press, (Jan. 2014), pp. 351–385. Doi:10.1016/B978-0-12-404730-3.00026-9

(Costantino *et al.*, 2000) H. R. Costantino, L. Firouzabadian, K. Hogeland, C. Wu, C. Beganski, K. G. Carrasquillo, M. Córdova, K. Griebenow, S. E. Zale, and M. A. Tracy. “Protein Spray-Freeze Drying. Effect of Atomization Conditions on Particle Size and Stability”. In: Pharmaceutical Research. 17(11) (Nov. 2000), pp. 1374–1382. Doi: 10.1023/A:1007570030368

(Dalmoro *et al.*, 2013) A. Dalmoro, M. d’Amore, and A. A. Barba. “Droplet size prediction in the production of drug delivery microsystems by ultrasonic atomization”. In: Translational Medicine. UniSa 7 (2013), pp. 6–11.

(Dani *et al.*, 2007) B. Dani, R. Platz, and S. T. Tzannis. “High concentration formulation feasibility of human immunoglubulin G for subcutaneous administration”. In: Journal of Pharmaceutical Sciences. 96(6) (2007), pp. 1504–1517. Doi: 10.1002/jps.20508

(Dao *et al.*, 2022) H. M. Dao, S. Sahakijpijarn, R. R. Chrostowski, C. Moon, F. Mangolini, Z. Cui, and R. O. Williams. “Aggregation of Lactoferrin Caused by Droplet Atomization Process via a Two-Fluid Nozzle: The Detrimental Effect of Air–Water Interfaces”. In: Molecular Pharmaceutics. 19(7) (July 2022) pp. 2662– 2675. Doi: 10.1021/acs.molpharmaceut.2c00358

(Das *et al.*, 2020) T. K. Das, L. O. Narhi, A. Sreedhara, T. Menzen, C. Grapentin, D. K. Chou, V. Antochshuk, and V. Filipe. “Stress Factors in mAb Drug Substance Production Processes: Critical Assessment of Impact on Product Quality and Control Strategy”. In: Journal of Pharmaceutical Sciences. 109(1) (Jan. 2020), pp. 116–133. Doi: 10.1016/j.xphs.2019.09.023

(De Maria *et al.*, 2016) S. De Maria, G. Ferrari, and P. Maresca. “Effects of high hydrostatic pressure on the conformational structure and the functional properties of bovine serum albumin”. In: Innovative Food Science & Emerging Technologies. 33 (Feb. 2016), pp. 67– 75. Doi: 10.1016/j.ifset.2015.11.025

(Deller *et al.*, 2016) M. C. Deller, L. Kong, and B. Rupp. “Protein stability: a crystallographer’s perspective”. In: Acta Crystallographica. Section F, Structural Biology Communications. 72(Pt 2) (Jan. 2016), pp. 72–95. Doi: 10.1107/S2053230X15024619

(Deng *et al.*, 2014) S.-P. Deng and D.-S. Huang. “SFAPS: An R package for structure/function analysis of protein sequences based on informational spectrum method”. In: Methods. Recent development in bioinformatics for utilizing omics data. 69(3) (Oct. 2014), pp. 207–212. Doi:10.1016/j.ymeth.2014.08.004

(Depreter *et al.*, 2013) F. Depreter, G. Pilcer, and K. Amighi. “Inhaled proteins: challenges and perspectives”. In: International Journal of Pharmaceutics. 447(1-2) (Apr. 2013), pp. 251–280. Doi: 10.1016/j.ijpharm.2013.02.031

(Devahastin *et al.*, 2020) S. Devahastin and M. Jinorose. “A Concise History of Drying”. en. In: Drying Technologies for Biotechnology and Pharmaceutical Applications. Section: 2. John Wiley & Sons, Ltd, 2020, pp. 9–2. Doi: 10.1002/9783527802104.ch2

(Du *et al.*, 2012) Y. Du, A. Walsh, R. Ehrick, W. Xu, K. May, and H. Liu. “Chromatographic analysis of the acidic and basic species of recombinant monoclonal antibodies”. In: mAbs. 4(5) (Sept. 2012). Publisher: Taylor & Francis, p. 578. Doi: 10.4161/mabs.21328

(Duerkop *et al.*, 2018) M. Duerkop, E. Berger, A. Dürauer, and A. Jungbauer. “Impact of Cavitation, High Shear Stress and Air/Liquid Interfaces on Protein Aggregation”. In: Biotechnology Journal. 13(7) (July 2018). Doi: 10.1002/biot.201800062

(Dutta *et al.*, 2018) S. Dutta, J. A. Moses, and C. Anandharamakrishnan. “Modern frontiers and applications of spray-freeze-drying in design of food and biological supplements”. In: Journal of Food Process Engineering. 41(8) (2018). Doi: 10.1111/jfpe.128 e12881

Eibl *et al.*, 2019) R. Eibl and D. Eibl. Single-Use Technology in Biopharmaceutical Manu- facture. John Wiley & Sons, Aug. 2019. Doi: 10.1002/9781119477891

(Eijkelboom *et al.*, 2023) N. M. Eijkelboom, A. P. van Boven, I. Siemons, P. F. C. Wilms, R. M. Boom, R. Kohlus, and M. A. I. Schutyser. “Particle structure development during spray-drying from a single droplet to pilot-scale perspective”. In: Journal of Food Engineering. 337 (Jan. 2023), p. 111222. Doi: 10.1016/j.jfoodeng.2022.111222

(Emami *et al.*, 2018) F. Emami, A. Vatanara, E. J. Park, and D. H. Na. “Drying Technologies for the Stability and Bioavailability of Biopharmaceuticals”. In: Pharmaceutics. 10(3) (Aug. 2018), p. 131. Doi:10.3390/pharmaceutics10030131

(Faghihi *et al.*, 2017) H. Faghihi, A. R. Najafabadi, and A. Vatanara. “Optimization and characterization of spray-dried IgG formulations: a design of experiment approach”. In: DARU Journal of Pharmaceutical Sciences. 25(1) (Oct. 2017), p. 22. Doi: 10.1186/s40199-017-0187-8

(Filipe *et al.*, 2010a) V. Filipe, A. Hawe, and W. Jiskoot. “Critical Evaluation of Nanoparticle Tracking Analysis (NTA) by NanoSight for the Measurement of Nanoparticles and Protein Aggregates”. In: Pharmaceutical Research. 27(5) (2010), pp. 796–810. Doi: 10.1007/s11095-010-0073-2

Fournaise *et al.*, 2020) T. Fournaise, J. Burgain, C. Perroud, J. Scher, C. Gaiani, and J. Petit. “Impact of formulation on reconstitution and flowability of spray-dried milk powders”. In: Powder Technology. 372 (July 2020), pp. 107–116. Doi: 10.1016/j.powtec.2020.05.085

(H. Gao *et al.*, 2022) H. Gao, S.-T. Wang, F. Hu, B.-B. Shen, M.-F. Sun, H. Wang, L. Li, and W.-J. Fang. “Investigation of an Uncommon Artifact during Reducing Capillary Electrophoresis-Sodium Dodecyl Sulfate Analysis of a Monoclonal Antibody with Dynamic Light Scattering and Reversed Phase High-Performance Liquid Chromatography”. In: Pharmaceutical Research. 39(8) (Aug. 2022), pp. 1959–1968. Doi: 10.1007/s11095-022-03303-0

(K. Gao *et al.*, 2020) K. Gao, R. Oerlemans, and M. R. Groves. “Theory and applications of differential scanning fluorimetry in early-stage drug discovery”. In: Biophysical Reviews. 12(1) (Feb. 2020), pp. 85–104. Doi: 10.1007/s12551-020-00619-2

(Garidel *et al.*, 2017) P. Garidel, A. B. Kuhn, L. V. Schäfer, A. R. Karow-Zwick, and M. Blech. “High-concentration protein formulations: How high is high?” In: European Journal of Pharmaceutics and Biopharmaceutics. 119 (Oct. 2017), pp. 353–360. Doi: 10.1016/j.ejpb.2017.06.029

(Ghandi *et al.*, 2012) A. Ghandi, I. B. Powell, T. Howes, X. D. Chen, and B. Adhikari. “Effect of shear rate and oxygen stresses on the survival of Lactococcus lactis during the atomization and drying stages of spray-drying: A laboratory and pilot scale study”. In: Journal of Food Engineering. 113(2) (Nov. 2012), pp. 194–200. Doi: 10.1016/j.jfoodeng.2012.06.005

(Giancola *et al.*, 1997) C. Giancola, C. De Sena, D. Fessas, G. Graziano, and G. Barone. “DSC studies on bovine serum albumin denaturation. Effects of ionic strength and SDS concentration”. In:

International Journal of Biological Macromolecules. 20(3) (June 1997), pp. 193–204. Doi: 10.1016/s0141-8130(97)01159-8

(Gikanga *et al.*, 2015) B. Gikanga, R. Turok, A. Hui, M. Bowen, O. B. Stauch, and Y.-F. Maa. “Manufacturing of High-Concentration Monoclonal Antibody Formulations via Spray-drying-the Road to Manufacturing Scale”. In: PDA journal of pharmaceutical science and technology. 69(1) (Feb. 2015), pp. 59–73. Doi: 10.5731/pdajpst.2015.01003

(Giridhar *et al.*, 2017) G. Giridhar, R. K. N. R. Manepalli, and G. Apparao. “Chapter 3 - Size-Exclusion Chromatography”. In: Thermal and Rheological Measurement Techniques for Nanomaterials Characterization. Ed. by S. Thomas, R. Thomas, A. K. Zachariah, and R. K. Mishra. Micro and Nano Technologies. Elsevier, Jan. 2017, pp. 51–65. Doi: 10.1016/B978-0-323-46139-9.00003-7

Giroux *et al.*, 2010) H. J. Giroux, J. Houde, and M. Britten. “Preparation of nanoparticles from denatured whey protein by pH-cycling treatment”. In: Food Hydrocolloids. 24(4) (June 2010), pp. 341–346. Doi: 10.1016/j.foodhyd.2009.10.013

(Grapentin *et al.*, 2020) C. Grapentin, C. Müller, R. S. K. Kishore, M. Adler, I. ElBialy, W. Friess, J. Huwyler, and T. A. Khan. “Protein-Polydimethylsiloxane Particles in Liquid Vial Monoclonal Antibody Formulations Containing Poloxamer 188”. In: Journal of Pharmaceutical Sciences. 109(8) (2020), pp. 2393–2404. Doi: 10.1016/j.xphs.2020.03.010

(Grasmeijer *et al.*, 2013) N. Grasmeijer, M. Stankovic, H. de Waard, H. W. Frijlink, and W. L. J. Hinrichs. “Unraveling protein stabilization mechanisms: Vitrification and water replacement in a glass transition temperature controlled system”. In: Biochimica et Biophysica Acta (BBA) - Proteins and Proteomics. 1834(4) (Apr. 2013), pp. 763–769. Doi: 10.1016/j.bbapap.2013.01.020

(Grasmeijer *et al.*, 2019) N. Grasmeijer, V. Tiraboschi, H. J. Woerdenbag, H. W. Frijlink, and W. L. J. Hinrichs. “Identifying critical process steps to protein stability during spray-drying using a vibrating mesh or a two-fluid nozzle”. In: European Journal of Pharmaceutical Sciences. 128 (Feb. 2019), pp. 152–157. Doi: 10.1016/j.ejps.2018.11.027

(Gross *et al.*, 2016) J. Gross, S. Sayle, A. R. Karow, U. Bakowsky, and P. Garidel. “Nanoparticle tracking analysis of particle size and concentration detection in suspensions of polymer and protein samples: Influence of experimental and data evaluation parameters”. In: European Journal of Pharmaceutics and Biopharmaceutics. 104 (July 2016), pp. 30–4. Doi: 10.1016/j.ejpb.2016.04.013

(Gross-Rother *et al.*, 2020) J. Gross-Rother, M. Blech, E. Preis, U. Bakowsky, and P. Garidel. “Particle Detection and Characterization for Biopharmaceutical Applications: Current Principles of Established and Alternative Techniques”. In: Pharmaceutics. 12(11) (Nov. 2020), p. 1112. Doi: 10.3390/pharmaceutics12111112

(Hackl *et al.*, 2018a) E. Hackl, J. Darkwah, G. Smith, and I. Ermolina. “Effect of Arginine on the Aggregation of Protein in Freeze-Dried Formulations Containing Sugars and Polyol: 1-Formulation

Development”. In: AAPS PharmSciTech. 19(2) (Feb. 2018), pp. 896–911. Doi: 10.1208/s12249-017-0884-0

(Hackl *et al.*, 2018b) E. Hackl, J. Darkwah, G. Smith, and I. Ermolina. “Effect of Arginine on the Aggregation of Protein in Freeze-Dried Formulations Containing Sugars and Polyol: II. BSA Reconstitution and Aggregation”. In: AAPS PharmSciTech. 19(7) (Oct. 2018), pp. 2934–2947. Doi:10.1208/s12249-018-1114-0

(Haque *et al.*, 2015) M. A. Haque, J. Chen, P. Aldred, and B. Adhikari. “Denaturation and Physical Characteristics of Spray-Dried Whey Protein Isolate Powders Produced in the Presence and Absence of Lactose, Trehalose, and Polysorbate-80”. In: Drying Technology. 33(10) (July 2015), pp. 1243–1254. Doi:10.1080/07373937.2015.1023311

(Hawe *et al.*, 2009) A. Hawe, J. C. Kasper, W. Friess, and W. Jiskoot. “Structural properties of monoclonal antibody aggregates induced by freeze–thawing and thermal stress”. In: European Journal of Pharmaceutical Sciences. 38(2) (Sept. 2009), pp. 79–87. Doi: 10.1016/j.ejps.2009.06.001

(Hede *et al.*, 2008) P. D. Hede, P. Bach, and A. D. Jensen. “Two-fluid spray atomisation and pneumatic nozzles for fluid bed coating/agglomeration purposes: A review”. In: Chemical Engineering Science. 63(14) (July 2008), pp. 3821–3842. Doi: 10.1016/j.ces.2008.04.014

(Herr *et al.*, 2000) A. E. Herr, J. I. Molho, J. G. Santiago, T. W. Kenny, D. A. Borkholder, G. J. Kintz, P. Belgrader, and M. A. Northrup. “Miniaturized Capillary Isoelectric Focusing (cIEF): Towards a Portable High-Speed Separation Method”. In: Micro Total Analysis Systems 2000. Ed. by A. van den Berg, W. Olthuis, and P. Bergveld. Dordrecht: Springer Netherlands, 2000, pp. 367–370. Doi: 10.1007/978-94-017-2264-3_85

(Horn *et al.*, 2020) J. Horn, H.-C. Mahler, and W. Friess. “Drying for Stabilization of Protein Formulations”. In: Drying Technologies for Biotechnology and Pharmaceutical Applications. Section: 4. John Wiley & Sons, Ltd, 2020, pp. 91–119. Doi: 10.1002/9783527802104.ch4

(Huppertz *et al.*, 2019) T. Huppertz, T. Vasiljevic, B. Zisu, and H. Deeth. “Chapter 8 - Novel Processing Technologies: Effects on Whey Protein Structure and Functionality”. In: Whey Proteins. Ed. by H. C. Deeth and N. Bansal. Academic Press, Jan. 2019, pp. 281–334. Doi:

(Jackisch *et al.*, 2014) C. Jackisch, V. Müller, C. Maintz, S. Hell, and B. Ataseven. “Subcutaneous Administration of Monoclonal Antibodies in Oncology”. In: Geburtshilfe und Frauenheilkunde. 74(4) (Apr. 2014), pp. 343–349. Doi: 10.1055/s-0034-1368173

(Jalalipour *et al.*, 2007) M. Jalalipour, A. Rouholamini Najafabadi, H. Tajerzadeh, K. Gilani, and M. Barghi. “The effect of protein stabilizers on the physical state and aerosol performance of spray-dried albumin microparticles”. In: Journal of Drug Delivery Science and Technology. 17(2) (Jan. 2007), pp. 149–153. Doi: 10.1016/S1773-2247(07)50023-7

(Jaspe *et al.*, 2006) J. Jaspe and S. J. Hagen. “Do Protein Molecules Unfold in a Simple Shear Flow?” In: Biophysical Journal. 91(9) (Nov. 2006), pp. 3415–3424. Doi: 10.1529/biophysj.106.089367

(Jones *et al.*, 2019) R. R. Jones, D. C. Hooper, L. Zhang, D. Wolverson, and V. K. Valev. “Raman Techniques: Fundamentals and Frontiers”. In: Nanoscale Research Letters. 14(1) (July 2019), p. 23. Doi: 10.1186/s11671-019-3039-2

(Jordan *et al.*, 1994) G. M. Jordan, S. Yoshioka, and T. Terao. “The Aggregation of Bovine Serum Albumin in Solution and in the Solid State”. In: Journal of Pharmacy and Pharmacology. 46(3) (1994), pp. 182–185. Doi: 10.1111/j.2042-7158.1994.tb03774.x

(Joubert *et al.*, 2011) M. K. Joubert, Q. Luo, Y. Nashed-Samuel, J. Wypych, and L. O. Narhi. “Classification and characterization of therapeutic antibody aggregates”. In: The Journal of Biological Chemistry. 286(28) (July 2011), pp. 25118–25133. Doi: 10.1074/jbc.M110.160457

(Kahle *et al.*, 2019) J. Kahle, M. Stein, and H. Wätzig. “Design of experiments as a valu- able tool for biopharmaceutical analysis with (imaged) capillary isoelectric focusing”. In: ELECTROPHORESIS. 40(18-19) (2019), pp. 2382–2389. Doi:10.1002/elps.201900162

(Kalonia *et al.*, 2016) C. Kalonia, V. Toprani, R. Toth, N. Wahome, I. Gabel, C. R. Middaugh, and D. B. Volkin. “Effects of Protein Conformation, Apparent Solubility, and Protein–Protein Interactions on the Rates and Mechanisms of Aggregation for an IgG1Monoclonal Antibody”. In: The Journal of Physical Chemistry B. 120(29) (July 2016), pp. 7062–7075. Doi: 10.1021/acs.jpcb.6b03878

(Kannan *et al.*, 2019) A. Kannan, I. C. Shieh, and G. G. Fuller. “Linking aggregation and interfacial properties in monoclonal antibody-surfactant formulations”. In: Journal of Colloid and Interface Science. 550 (Aug. 2019), pp. 128–138. Doi: 10.1016/j.jcis.2019.04.060

(Kanojia *et al.*, 2018) G. Kanojia, R. ten Have, D. Brugmans, P. C. Soema, H. W. Frijlink, J.-P. Amorij, and G. Kersten. “The effect of formulation on spray dried Sabin inactivated polio vaccine”. In: European Journal of Pharmaceutics and Biopharmaceutics. 129 (Aug. 2018), pp. 21–29. Doi: 10.1016/j.ejpb.2018.05.021

(Kaplon *et al.*, 2022) H. Kaplon, A. Chenoweth, S. Crescioli, and J. M. Reichert. “Antibodies to watch in 2022”. In: mAbs. 14(1) (Dec. 2022), p. 2014296. Doi: 10.1080/19420862.2021.2014296

(Kawasaki *et al.*, 2019) H. Kawasaki, T. Shimanouchi, Y. Kimura. “Recent development of optimization of lyophilisation process”. In: Journal of Chemistry. 2019 (May 2019). Doi: 10.1155/2019/9502856

(Kendrick *et al.*, 1997) B. S. Kendrick, B. S. Chang, T. Arakawa, B. Peterson, T. W. Randolph, M. C. Manning, and J. F. Carpenter. “Preferential exclusion of sucrose from recombinant interleukin-1 receptor antagonist: Role in restricted conformational mobility and compaction of native state”. In: Proceedings of the National Academy of Sciences. 94(22) (Oct. 1997), pp. 11917–11922. Doi: 10.1073/pnas.94.22.11917

(Kerwin, 2008) B. Kerwin. “Polysorbates 20 and 80 Used in the Formulation of Protein Biotherapeutics: Structure and Degradation Pathways”. In: Journal of pharmaceutical sciences.97 (Aug. 2008), pp. 2924–2935. Doi: 10.1002/jps.21190

(Keshani *et al.*, 2015) S. Keshani, W. R. W. Daud, M. M. Nourouzi, F. Namvar, and M. Ghasemi. “Spray-drying: An overview on wall deposition, process and modeling”. In: Journal of Food Engineering. 146 (Feb. 2015), pp. 152–162. Doi: 10.1016/j.jfoodeng.2014.09.004

(Kesik-Brodacka, 2018) M. Kesik-Brodacka. “Progress in biopharmaceutical development”. In: Biotechnology and Applied Biochemistry. 65(3) (2018), pp. 306–322. Doi: 10.1002/bab.1617

(Khan *et al.*, 2015) T. A. Khan, H.-C. Mahler, and R. S. K. Kishore. “Key interactions of surfactants in therapeutic protein formulations: A review”. In: European Journal of Pharmaceutics and Biopharmaceutics. 97 (Nov. 2015), pp. 60–67. Doi: 10.1016/j.ejpb.2015.09.016

(H. L. Kim *et al.*, 2014) H. L. Kim, A. McAuley, B. Livesay, W. D. Gray, and J. McGuire. “Modulation of protein adsorption by poloxamer 188 in relation to polysorbates 80 and 20 at solid surfaces”. In: Journal of Pharmaceutical Sciences. 103(4) (Apr. 2014), pp. 1043–1049. Doi: 10.1002/jps.23907

(S. H. Kim *et al.*, 2022) S. H. Kim, H. J. Yoo, E. J. Park, and D. H. Na. “Nano Differential Scanning Fluorimetry-Based Thermal Stability Screening and Optimal Buffer Selection for Immunoglobulin G”. en. In: Pharmaceuticals. 15(1) (Jan. 2022), p. 29. Doi: 10.3390/ph15010029

(Kunert *et al.*, 2016) R. Kunert and D. Reinhart. “Advances in recombinant antibody manufacturing”. In: Applied Microbiology and Biotechnology. 100(8) (Apr. 2016), pp. 3451– 3461. Doi: 10.1007/s00253-016-7388-9

(Langford *et al.*, 2018) A. Langford, B. Bhatnagar, R. Walters, S. Tchessalov, and S. Ohtake. “Drying technologies for biopharmaceutical applications: Recent developments and future direction”. In: Drying Technology. 36(6) (Apr. 2018), pp. 677–684. Doi: 10.1080/07373937.2017.1355318

(Langford *et al.*, 2020) A. Langford, S. Ohtake, D. Lechuga-Ballesteros, and K.-i. Izutsu. “Introduction”. In: Drying Technologies for Biotechnology and Pharmaceutical Applications. John Wiley & Sons, Ltd, 2020, pp. 1–7. Doi: 10.1002/9783527802104.ch1

(Lasheras *et al.*, 2000) J. C. Lasheras and E. J. Hopfinger. “Liquid Jet Instability and Atomization in a Coaxial Gas Stream”. In: Annual Review of Fluid Mechanics. 32(1) (2000), pp. 275–308. Doi: 10.1146/annurev.fluid.32.1.275

(Le Basle *et al.*, 2020) Y. Le Basle, P. Chennell, N. Tokhadze, A. Astier, and V. Sautou. “Physicochemical Stability of Monoclonal Antibodies: A Review.” In: Journal of Pharmaceutical Sciences. 109(1) (Jan. 2020), pp: 169-190. Doi: 10.1016/j.xphs.2019.08.009

(H. S. Lee *et al.*, 2019) H. S. Lee and K.-H. Liu. Drug Metabolism, Pharmacokinetics and Bioanalysis. In: Pharmaceutics. (June 2019). Doi: 10.3390/books978-3-03897-917-3

(H. J. Lee *et al.*, 2011) H. J. Lee, A. McAuley, K. F. Schilke, and J. McGuire. “Molecular origins of surfactant-mediated stabilization of protein drugs”. In: Advanced Drug Delivery Reviews. 63(13) (Oct. 2011), pp. 1160–1171. Doi:10.1016/j.addr.2011.06.015

(S. H. Lee *et al.*, 2011) S. H. Lee, D. Heng, W. K. Ng, H.-K. Chan, and R. B. H. Tan. “Nano spray-drying: A novel method for preparing protein nanoparticles for protein therapy”. In: International Journal of Pharmaceutics. 403(1) (Jan. 2011), pp. 192–200. Doi: 10.1016/j.ijpharm.2010.10.012

(Lefebvre *et al.*, 2021) G. Lefebvre, A. Maze, R. Alvarez-Palencia Jimenez, F. Bruckert, V. Filipe, S. Huille, and M. Weidenhaupt. “Surfactant Protection Efficacy at Surfaces Varies with the Nature of Hydrophobic Materials”. In: Pharmaceutical Research. 38(12) (Dec. 2021), pp. 2157–2166. Doi: 10.1007/s11095-021-03133-6

Lerbret *et al.*, 2005) A. Lerbret, P. Bordat, F. Affouard, M. Descamps, and F. Migliardo. “How Homogeneous Are the Trehalose, Maltose, and Sucrose Water Solutions? An Insight from Molecular Dynamics Simulations”. In: The Journal of Physical Chemistry B. 109(21) (June 2005), pp. 11046–11057. Doi: 10.1021/jp0468657

(Li *et al.*, 2019) J. Li, M. E. Krause, X. Chen, Y. Cheng, W. Dai, J. J. Hill, M. Huang, S. Jordan, D. LaCasse, L. Narhi, E. Shalaev, I. C. Shieh, J. C. Thomas, R. Tu, S. Zheng, and L. Zhu. “Interfacial Stress in the Development of Biologics: Fundamental Understanding, Current Practice, and Future Perspective”. In: The AAPS Journal. 21(3) (Mar. 2019), pp. 44. Doi: 10.1208/s12248-019-0312-3

(H. Li *et al.*, 2019) H. Li, J. Li, J. Bodycomb, G.S. Patience. “Experimental Methods in Chemical Engineering: Particle Size Distribution by Laser Diffraction—PSD”. In: The Canadian Journal of Chemical Engineering. 97 (2019) pp. 1974-1981. Doi: 10.1002/cjce.23480

(Lin *et al.*, 2011) J. Lin, Q. Tan, and S. Wang. “A high-resolution capillary isoelectric focusing method for the determination of therapeutic recombinant monoclonal antibody”. In: Journal of Separation Science. 34(14) (July 2011), pp. 1696–1702. Doi: 10.1002/jssc.201100067

(Lipiäinen, 2018a) T. Lipiäinen. “Stability and analysis of solid-state forms in pharmaceutical powders”. [Doctoral dissertation, University of Helsinki]. Helsingin yliopisto. May 2018

(J. K. Liu, 2014) J. K. Liu. “The history of monoclonal antibody development – Progress, remaining challenges and future innovations”. In: Annals of Medicine and Surgery. 3(4) (Sept. 2014), pp. 113–116. Doi: 10.1016/j.amsu.2014.09.001

(L. Liu *et al.*, 2015) L. Liu, X. Cai, J. Zhang, and C. Xu. “Particle-size Measurements in a Micro-channel with Image Dynamic Light Scattering Method”. In: Procedia Engineering. 102 (2015), pp. 904–910. Doi: 10.1016/j.proeng.2015.01.211

(R.-M. Lu *et al.*, 2020) R.-M. Lu, Y.-C. Hwang, I.-J. Liu, C.-C. Lee, H.-Z. Tsai, H.-J. Li, and H.-C. Wu. “Development of therapeutic antibodies for the treatment of diseases”. In: Journal of Biomedical Science.27(1) (Jan. 2020), p. 1. Doi: 10.1186/s12929-019-0592-z

(X. Lu *et al.*, 2018) X. Lu and R. M. Murphy. “Nanoparticle Tracking for Protein Aggregation Research”. In: Methods in molecular biology (Clifton, N.J.) 1777 (2018), pp. 145–158. Doi: 10.1007/978-1-4939-7811-3_7

(Maa *et al.*, 1998a) Y.-F. Maa and C. C. Hsu. “Investigation on Fouling Mechanisms for Recombinant Human Growth Hormone Sterile Filtration”. English. In: Journal of Pharmaceutical Sciences. 87(7) (July 1998), pp. 808–812. Doi: 10.1021/js980114x

(Maguire *et al.*, 2018) C. M. Maguire, M. Rösslein, P. Wick, and A. Prina-Mello. “Characterisation of particles in solution – a perspective on light scattering and comparative technologies”. In: Science and Technology of Advanced Materials. 19(1) (Dec. 2018), pp. 732–745. Doi:10.1080/14686996.2018.1517587

(Majorek *et al.*, 2012) K. A. Majorek, P. J. Porebski, M. Chruszcz, S. C. Almo, W. Minor, W. “Structural and immunologic characterization of bovine, horse, and rabbit serum albumins”. In: Molecular Immunology. 52(3–4) (2012), pp. 174-182. Doi: 10.1016/j.molimm.2012.05.011.

(Manning *et al.*, 1989) M. C. Manning, K. Patel, and R. T. Borchardt. “Stability of protein pharmaceuticals”. In: Pharmaceutical Research. 6(11) (Nov. 1989), pp. 903–918. Doi: 10.1023/a:1015929109894

(Mason *et al.*, 2012) B. D. Mason, C. Schöneich, and B. A. Kerwin. “Effect of pH and Light on Aggregation and Conformation of an IgG1 mAb”. In: Molecular Pharmaceutics. 9(4) (Apr. 2012), pp. 774–790. Doi: 10.1021/mp2004719

(Massant *et al.*, 2020) J. Massant, S. Fleurime, M. Batens, H. Vanhaerents, and G. Van den Mooter. “Formulating monoclonal antibodies as powders for reconstitution at high concentration using spray-drying: Trehalose/amino acid combinations as reconstitution time reducing and stability improving formulations”. In: European Journal of Pharmaceutics and Biopharmaceutics.156 (Nov. 2020), pp. 131–142. Doi: 10.1016/j.ejpb.2020.08.019

(Matsarskaia *et al.*, 2020) O. Matsarskaia, L. Bühl, C. Beck, M. Grimaldo, R. Schweins, F. Zhang, T. Seydel, F. Schreiber, and F. Roosen-Runge. “Evolution of the structure and dynamics of bovine serum albumin induced by thermal denaturation”. In: Physical Chemistry Chemical Physics. 22(33) (2020). Publisher: Royal Society of Chemistry, pp. 18507– 18517. Doi: 10.1039/D0CP01857K

(Maury *et al.*, 2005) M. Maury, K. Murphy, S. Kumar, A. Mauerer, and G. Lee. “Spray-drying of proteins: effects of sorbitol and trehalose on aggregation and FT-IR amide I spectrum of an immunoglobulin G”. en. In: European Journal of Pharmaceutics and Biopharmaceutics. 59(2) (Feb. 2005), pp. 251–261. Doi: 10.1016/j.ejpb.2004.07.010

(McKechnie *et al.*, 2018) W. S. McKechnie, N. Tugcu, and S. Kandula. “Accurate and Rapid Protein Concentration Measurement of In-Process, High Concentration Protein Pools”. In: Biotechnology Progress. 34(5) (2018), pp. 1234–1241. Doi: 10.1002/btpr.2695mcke

(Mensink *et al.*, 2017) M. A. Mensink, H. W. Frijlink, K. van der Voort Maarschalk, and W. L. J. Hinrichs. “How sugars protect proteins in the solid state and during drying (review): Mechanisms of stabilization in relation to stress conditions” In: European Journal of Pharmaceutics and Biopharmaceutics. 114 (May 2017), pp. 288–295. Doi: 10.1016/j.ejpb.2017.01.024

(Mezhericher *et al.*, 2008) M. Mezhericher, A. Levy, and I. Borde. “Heat and mass transfer of single droplet/wet particle drying”. In: Chemical Engineering Science. 63(1) (Jan. 2008), pp. 12–23. Doi: 10.1016/j.ces.2007.08.052

(Moorthy *et al.*, 2015) B. S. Moorthy, B. Xie, E. M. Moussa, L. K. Iyer, S. Chandrasekhar, J. P. Panchal, and E. M. Topp. “Structure of Monoclonal Antibodies”. In: Biobetters: Protein Engineering to Approach the Curative. Ed. by A. Rosenberg and B. Demeule. AAPS Advances in the Pharmaceutical Sciences Series. New York, NY: Springer, 2015, pp. 81–89. DOI: 10.1007/978-1-4939-2543-8_6

(Morgan *et al.*, 2020) B. A. Morgan, M. Manser, M. Jeyanathan, Z. Xing, E. D. Cranston, and M. R. Thompson. “Effect of Shear Stresses on Adenovirus Activity and Aggregation during Atomization To Produce Thermally Stable Vaccines by Spray-drying”. en. In: ACS Biomaterials Science & Engineering. 6(7) (July 2020), pp. 4304–4313. Doi: 10.1021/acsbiomaterials.0c00317

(Mutukuri *et al.*, 2021) T. T. Mutukuri, Y.-F. Maa, B. Gikanga, R. Sakhnovsky, and Q. T. Zhou. “Electrostatic spray-drying for monoclonal antibody formulation”. In: International Journal of Pharmaceutics. 607 (Sept. 2021), p. 120942. Doi: 10.1016/j.ijpharm.2021.120942

(Narhi *et al.*, 2009) L. O. Narhi, Y. Jiang, S. Cao, K. Benedek, and D. Shnek. “A critical review of analytical methods for subvisible and visible particles”. eng. In: Current Pharmaceutical Biotechnology 10.4 (June 2009), pp. 373–381.

(Ndoye *et al.*, 2013) F. T. Ndoye, N. Erabit, D. Flick, and G. Alvarez. “In-line characterization of a whey protein aggregation process: Aggregates size and rheological measurements”. In: Journal of Food Engineering. 115(1) (Mar. 2013), pp. 73–82. Doi: 10.1016/j.jfoodeng.2012.09.021

(Noble, 2014) J. E. Noble. “Quantification of protein concentration using UV absorbance and Coomassie dyes”. In: Methods in Enzymology. 536 (2014), pp. 17–26. Doi: 10.1016/B978-0-12-420070-8.00002-7

(Ohtake *et al.*, 2013) S. Ohtake and W. Wang. “Protein and Peptide Formulation Development”. In: Pharmaceutical Sciences Encyclopedia. Section: 1, (2013), pp. 1–44. Doi: 10.1002/9780470571224.pse510

(Olsson *et al.*, 2016) C. Olsson, H. Jansson, and J. Swenson. “The Role of Trehalose for the Stabilization of Proteins”. In: The Journal of Physical Chemistry B. 120(20) (May 2016), pp. 4723–4731. Doi: 10.1021/acs.jpcb.6b02517

(Ortega-Rivas *et al.*, 2006) E. Ortega-Rivas, P. Juliano, and H. Yan. Food Powders: Physical Properties, Processing, and Functionality. Springer Science & Business Media, (Apr. 2006)

(Ousset *et al.*, 2018) A. Ousset, J. Meeus, F. Robin, M. A. Schubert, P. Somville, and K. Dodou. “Comparison of a Novel Miniaturized Screening Device with Büchi B290 Mini Spray-Dryer for the Development of Spray-Dried Solid Dispersions (SDSDs)”. In: Processes. 6(8) (Aug. 2018), p. 129. Doi: 10.3390/pr6080129

(Pal *et al.*, 2020) A. Pal, A. Gope, A. Athair, and G. Iannacchione. “A comparative study of the drying evolution and dried morphology of two globular proteins in de- ionized water solutions”. In: RSC Advances. 10 (Apr. 2020), pp. 16906-16916. Doi: 10.1039/D0RA01748E

(Patois *et al.*, 2012) E. Patois, M. A. H. Capelle, C. Palais, R. Gurny, and T. Arvinte. “Evaluation of nanoparticle tracking analysis (NTA) in the characterization of therapeutic antibodies and seasonal influenza vaccines: pros and cons”. In: Journal of Drug Delivery Science and Technology. 22(5) (Jan. 2012), pp. 427–433. Doi: 10.1016/S1773-2247(12)50069-9

(Pinto *et al.*, 2021) J. T. Pinto, E. Faulhammer, J. Dieplinger, M. Dekner, C. Makert, M. Nieder, and A. Paudel. “Progress in spray-drying of protein pharmaceuticals: Literature analysis of trends in formulation and process attributes”. In: Drying Technology. 39 (Apr. 2021), pp. 1425–1446. Doi: 10.1080/07373937.2021.1903032

(Popescu *et al.*, 2020) G. Popescu, I. Radulov, O. A. Iordănescu, M. D. Orboi, L. Rădulescu, M. Drugă, G. S. Bujancă, I. David, D. I. Hădărugă, C. A. L. (Banciu), N. G. Hădărugă, and M. Riviş. “Karl Fischer Water Titration—Principal Component Analysis Approach on Bread Products”. en. In: Applied Sciences. 10(18) (Jan. 2020), p. 6518. Doi: 10.3390/app10186518

(Preston *et al.*, 2021) K. B. Preston and T. W. Randolph. “Stability of lyophilized and spray dried vaccine formulations”. In: Advanced Drug Delivery Reviews. 171 (Apr. 2021), pp. 50–61. Doi: 10.1016/j.addr.2021.01.016

(Prigent *et al.*, 2022) S. L. Prigent and C. Bailly. “From shear stress to wall pressure spectra: a semi-analytical approach to account for mean pressure gradients in turbulent boundary layers” In: Acta Acustica. 6 (2022), p. 43. Doi: 10.1051/aacus/2022034

(Prinn *et al.*, 2002) K. B. Prinn, H. R. Costantino, and M. Tracy. “Statistical Modeling of protein spray-drying at the lab scale”. en. In: AAPS Pharmaceutical Science Technologies. 3(1) (Mar. 2002), pp. 32–39. Doi: 10.1208/pt030104

(Quevedo *et al.*, 2021) M. Quevedo, H. P. Karbstein, and M. A. Emin. “Influence of thermo- mechanical treatment and pH on the denaturation kinetics of highly concentrated whey protein isolate”. In: Journal of Food Engineering. 9(9) (Mar. 2021), p. 1196. Doi: 10.3390/foods9091196

(Raimundo da Silva *et al.*, 2017) C. Raimundo da Silva, E. Martins, A. Caldas Pereira Silveira, M. Simeão, A. L. MENDES, I. TULER PERRONE, P. Schuck, and A. F. De Carvahlo. “Thermodynamic characterization of single-stage spray dryers: Mass and energy balances for milk drying”. In: Drying Technology. 35(15). (2017): Doi: 10.1080/07373937.2016.1275675

(Ramezani *et al.*, 2014) V. Ramezani, A. Vatanara, A. R. Najafabadi, M. A. Shokrgozar, A. Khabiri, and M. Seyedabadi. “A comparative study on the physicochemical and biological stability of IgG1 and monoclonal antibodies during spray-drying process”. In: DARU Journal of Pharmaceutical Sciences. 22(1) (Mar. 2014), p. 31. Doi: 10.1186/2008-2231-22-31

(Reslan *et al.*, 2017) M. Reslan, Y. K. Demir, B. L. Trout, H.-K. Chan, and V. Kayser. “Lack of a synergistic effect of arginine–glutamic acid on the physical stability of spray-dried bovine serum albumin”. In: Pharmaceutical Development and Technology. 22(6) (Aug. 2017), pp. 785–791 Doi: 10.1080/10837450.2016.1185116

(Sadek *et al.*, 2015) C. Sadek, P. Schuck, Y. Fallourd, N. Pradeau, C. Le Floch-Fouéré, and R. Jeantet. “Drying of a single droplet to investigate process–structure– function relationships: a review”. In: Dairy Science & Technology. 95(6) (2015). Doi: 10.1007/s13594-014-0186-1

(Šafarič, 2019) L. Šafarič. “Anaerobic Digester Fluid Rheology and Process Efficiency : Interactions of Substrate Composition, Trace Element Availability, and Microbial Activity”. [Doctoral dissertation, Linköping University]. Publisher: Linköping University Electronic Press. 2019

(Samuel *et al.*, 2021) E. L. G. Samuel, S. L. Holmes, and D. W. Young. “Processing binding data using an open-source workflow”. In: Journal of Cheminformatics. 13(1) (Dec. 2021), p. 99. Doi: 10.1186/s13321-021-00577-1

(Sänger–van de Griend, 2019) C. E. Sänger–van de Griend. “CE-SDS method development, validation, and best practice—An overview”. In: ELECTROPHORESIS. 40(18-19) (2019). Doi:10.1002/elps.201900094, pp. 2361–2374

(Santos *et al.*, 2017) D. Santos, A. C. Maurício, V. Sencadas, J. D. Santos, M. H. Fernandes, and P. S. Gomes. “Spray-drying: An Overview”. In: Biomaterials - Physics and Chemistry - New Edition (Dec. 2017). Doi: 10.5772/intechopen.72247

(Schaefer *et al.*, 2015) J. Schaefer and G. Lee. “Arrhenius activation energy of damage to catalase during spray-drying”. In: International Journal of Pharmaceutics. 489(1) (July 2015), pp. 124–130. Doi: 10.1016/j.ijpharm.2015.04.078

(Scheller *et al.*, 2021) C. Scheller, F. Krebs, R. Wiesner, H. Wätzig, and I. Oltmann-Norden. “A comparative study of CE-SDS, SDS-PAGE, and Simple Western—Precision, repeatability, and apparent molecular mass shifts by glycosylation”. In: ELECTROPHORESIS .42(14-15) (2021), pp. 1521–1531. Doi:10.1002/elps.202100068

(Scherer *et al.*, 2010) T. Scherer, J. Liu, S. Shire, and A. Minton. “Intermolecular Interactions of IgG1 Monoclonal Antibodies at High Concentrations Characterized by Light Scattering”. In: The journal of physical chemistry. B. 114 (Oct. 2010), pp. 12948–12957. Doi: 10.1021/jp1028646

(Schmitz-Schug *et al.*, 2013) I. Schmitz-Schug, P. Foerst, and U. Kulozik. “Impact of the spray-drying conditions and residence time distribution on lysine loss in spray dried infant formula”. en. In: Dairy Science & Technology. 93(4) (July 2013), pp. 443–462. Doi: 10.1007/s13594-013-0115-8

(Schutyser *et al.*, 2019) M. A. I. Schutyser, E. M. Both, I. Siemons, E. M. J. Vaessen, and L. Zhang. “Gaining insight on spray-drying behavior of foods via single droplet drying analyses”. In: Drying Technology. 37(5) (Apr. 2019), pp. 525–534. Doi:10.1080/07373937.2018.1482908

(Sharma *et al.*, 2021) A. Sharma, D. Khamar, S. Cullen, A. Hayden, and H. Hughes. “Innovative Drying Technologies for Biopharmaceuticals”. In: International Journal of Pharmaceutics. 609 (Nov. 2021), p. 121115. Doi: 10.1016/j.ijpharm.2021.121115

(Shiga *et al.*, 2014) H. Shiga, H. Joreau, T. L. Neoh, T. Furuta, H. Yoshii. “Encapsulation of Alcohol Dehydrogenase in Mannitol by Spray Drying”. Pharmaceutics, 6(1) (2014), pp. 185–194. Doi: 10.3390/pharmaceutics6010185

(Simeonov, 2013) A. Simeonov. “Recent Developments in the Use of Differential Scanning Fluorometry in Protein and Small Molecule Discovery and Characterization”. In: Expert opinion on drug discovery. 8(9) (Sept. 2013), pp. 1071–1082. Doi: 10.1517/17460441.2013.806479

(Singh & Van den Mooter, 2016) A. Singh and G. Van den Mooter. “Spray-drying formulation of amorphous solid dispersions”. In: Advanced Drug Delivery Reviews. Amorphous pharmaceutical solids. 100 (May 2016), pp. 27–50. Doi: 10.1016/j.addr.2015.12.010

(Singh *et al.*, 2017) S. M. Singh, S. Bandi, D. N. M. Jones, and K. M. G. Mallela. “Effect of Polysorbate 20 and Polysorbate 80 on the Higher Order Structure of a Monoclonal Antibody and its Fab and Fc Fragments Probed Using 2D NMR Spectroscopy”. In: Journal of pharmaceutical sciences. 106(12) (Dec. 2017), pp. 3486–3498

(Souza Lima *et al.*, 2020) R. de Souza Lima, M.-I. Ré, and P. Arlabosse. “Drying droplet as a template for solid formation: A review”. In: Powder Technology. 359 (Jan. 2020), pp. 161–171. Doi: 10.1016/j.powtec.2019.09.052

(Staub *et al.*, 2011) A. Staub, D. Guillarme, J. Schappler, J.-L. Veuthey, and S. Rudaz. “Intact protein analysis in the biopharmaceutical field”. In: Journal of Pharmaceutical and Biomedical Analysis. 55(4) (June 2011), pp. 810–822. Doi:

(Suba *et al.*, 2015) D. Suba, Z. Urbányi, and A. Salgó. “Capillary isoelectric focusing method development and validation for investigation of recombinant therapeutic monoclonal antibody”. In: Journal of Pharmaceutical and Biomedical Analysis. 55(4) (Oct. 2015), pp. 53–61. Doi: 10.1016/j.jpba.2011.01.031

(Sudrik *et al.*, 2017) C. Sudrik, T. Cloutier, P. Pham, H. S. Samra, and B. L. Trout. “Preferential interactions of trehalose, L-arginine.HCl and sodium chloride with therapeutically relevant IgG1 monoclonal antibodies”. In: mAbs. 9(7) (Oct. 2017) , pp. 1155–1168. Doi:10.1080/19420862.2017.1358328

(Sung *et al.*, 2015) J. J. Sung, N. N. Pardeshi, A. M. Mulder, S. K. Mulligan, J. Quispe, K. On, B. Carragher, C. S. Potter, J. F. Carpenter, and A. Schneemann. “Transmission electron microscopy as an orthogonal method to characterize protein aggregates”. In: Journal of Pharmaceutical Sciences. 104(2) (Feb. 2015), pp. 750–759. Doi: 10.1002/jps.24157

(Taghizadeh *et al.*, 2022) B. Taghizadeh, M. R. Jaafari, and N. Zarghami. “New insight into the importance of formulation variables on parenteral growth hormone preparations: potential effect on the injection-site pain”. In: Frontiers in Endocrinology. 13 (2022). Doi: 10.3389/fendo.2022.963336

(Tian *et al.*, 2010) J.-L. Tian, Y.-Z. Zhao, Z. Jin, C.-T. Lu, Q.-Q. Tang, Q. Xiang, C.-Z. Sun, L. Zhang, Y.-Y. Xu, H.-S. Gao, Z.-C. Zhou, X.-K. Li, and Y. Zhang. “Synthesis and characterization of Poloxamer 188-grafted heparin copolymer”. In: Drug Development and Industrial Pharmacy. 36(7) (July 2010) , pp. 832–838. Doi: 10.3109/03639040903520983

(Timasheff, 2002) S. N. Timasheff. “Protein-solvent preferential interactions, protein hydration, and the modulation of biochemical reactions by solvent components”. In: Proceedings of the National Academy of Sciences of the United States of America. 99(15) (July 2002), pp. 9721–9726. Doi: 10.1073/pnas.122225399

(Tomar *et al.*, 2016) D. S. Tomar, S. Kumar, S. K. Singh, S. Goswami, and L. Li. “Molecular basis of high viscosity in concentrated antibody solutions: Strategies for high concentration drug product development”. In: mAbs. 8(2) (Jan. 2016), pp. 216–228. Doi: 10.1080/19420862.2015.1128606

(Tomlinson *et al.*, 2020) A. Tomlinson, I. E. Zarraga, and B. Demeule. “Characterization of Polysorbate Ester Fractions and Implications in Protein Drug Product Stability”. In: Molecular Pharmaceutics. 17(7) (July 2020), pp. 2345–2353. Doi: 10.1021/acs.molpharmaceut.0c00093

(Tscheliessnig *et al.*, 2012) R. Tscheliessnig, M. Zörnig, E. M. Herzig, K. Lückerath, J. Altrichter, K. Kemter, A. Paunel-Görgülü, T. Lögters, J. Windolf, S. Pabisch, J. Cinatl, H. F. Rabenau, A. Jungbauer, P. Müller-Buschbaum, M. Scholz, J. Koch. “Nano-coating protects biofunctional materials”. In: Materials Today. 15(9) (2012), pp. 394-404. Doi: 10.1016/S1369-7021(12)70166-9.

(Uskoković, 2012) V. Uskoković. “Dynamic Light Scattering Based Microelectrophoresis: Main Prospects and Limitations”. In: Journal of Dispersion Science and Technology. 33(12) (Nov. 2012), pp. 1762–1786. Doi:10.1080/01932691.2011.625523

(Vasconcelos *et al.*, 2016) T. Vasconcelos, S. Marques, J. das Neves, and B. Sarmento. “Amorphous solid dispersions: Rational selection of a manufacturing process”. In: Advanced Drug Delivery Reviews. 100 (May 2016), pp. 85–101. Doi: 10.1016/j.addr.2016.01.012

(Viola *et al.*, 2018) M. Viola, J. Sequeira, R. Seiça, F. Veiga, J. Serra, A. C. Santos, and A. J. Ribeiro. “Subcutaneous delivery of monoclonal antibodies: How do we get there?”. In: Journal of Controlled Release. 286 (Sept. 2018), pp. 301–314. Doi: 10.1016/j.jconrel.2018.08.001

(Walters *et al.*, 2014) R. H. Walters, B. Bhatnagar, S. Tchessalov, K.-I. Izutsu, K. Tsumoto, and S. Ohtake. “Next Generation Drying Technologies for Pharmaceutical Applications.” In: Journal of Pharmaceutical Sciences. 103(9) (2014), pp. 2673–2695. Doi: 10.1002/jps.23998

(J. Wang *et al.*, 2019) J. Wang, F. Maoulida, C. Ben Amara, S. Ghnimi, N.-E. Chihib, E. Dumas, and A. Gharsallaoui. “Spray-drying of protein/polysaccharide complexes: Dissociation of the effects of shearing and heating”. In: Food Chemistry. 297 (Nov. 2019), p. 124943. Doi: 10.1016/j.foodchem.2019.06.010

(S. Wang *et al.*, 2018) S. Wang, A. P. Liu, Y. Yan, T. J. Daly, and N. Li. “Characterization of product-related low molecular weight impurities in therapeutic monoclonal antibodies using hydrophilic interaction chromatography coupled with mass spectrometry”. In: Journal of Pharmaceutical and Biomedical Analysis. 154 (May 2018), pp. 468–475. Doi: 10.1016/j.jpba.2018.03.034

(Wanning *et al.*, 2015) S. Wanning, R. Süverkrüp, and A. Lamprecht. “Pharmaceutical spray freeze drying”. In: International Journal of Pharmaceutics. 488(1) (July 2015), pp. 136–153. Doi: 10.1016/j.ijpharm.2015.04.053

(Weinbuch *et al.*, 2015) D. Weinbuch, J. K. Cheung, J. Ketelaars, V. Filipe, A. Hawe, J. den Engelsman, and W. Jiskoot. “Nanoparticulate Impurities in Pharmaceutical-Grade Sugars and their Interference with Light Scattering-Based Analysis of Protein Formulations”. eng. In: Pharmaceutical Research. 32(7) (July 2015), pp. 2419–2427. Doi: 10.1007/s11095-015-1634-1

(Wen *et al.*, 2020) J. Wen, H. Lord, N. Knutson, and M. Wikström. “Nano differential scanning fluorimetry for comparability studies of therapeutic proteins”. In: Analytical Biochemistry. 593 (Mar. 2020), p. 113581. Doi: 10.1016/j.ab.2020.113581

(White, 2011) F. M. White, “Fluid Mechanics,” 7th Edition, McGraw- Hill, New York, 2011.

(Wilson *et al.*, 2020) N. E. Wilson, T. T. Mutukuri, D. Y. Zemlyanov, L. S. Taylor, E. M. Topp, and Q. T. Zhou. “Surface Composition and Formulation Heterogeneity of Protein Solids Produced by Spray-drying”. In: Pharmaceutical Research. 37(1) (Jan. 2020), p. 14. Doi: 10.1007/s11095-019-2738-9

(Wisniewski, 2015) R. Wisniewski. “Spray-drying Technology Review”. Publisher: 45th International Conference on Environmental Systems. (July 2015)

(Xu, 2015) R. Xu. “Light scattering: A review of particle characterization applications”. In: Particuology. 18 (Feb. 2015), pp. 11–21. Doi: 10.1016/j.partic.2014.05.002

(Yeh *et al.*, 2018) M.-K. Yeh and Y.-C. Chen. (Eds.).Biopharmaceuticals. (2018) doi: 10.5772/intechopen.72960

(Zheng *et al.*, 2017) S. Zheng, D. Qiu, M. Adams, J. Li, R. V. Mantri, and R. Gandhi. “Investigating the Degradation Behaviors of a Therapeutic Monoclonal Antibody Associated with pH and Buffer Species”. In: AAPS PharmSciTech. 18(1) (Jan. 2017), pp. 42–48. Doi: 10.1208/s12249-015-0403-0

(Zhou *et al.*, 2015) C. Zhou, W. Qi, E. Neil Lewis, and J. F. Carpenter. “Concomitant Raman spectroscopy and dynamic light scattering for characterization of therapeutic proteins at high concentrations”. In: Analytical Biochemistry. 472 (Mar. 2015), pp. 7–20. Doi: 10.1016/j.ab.2014.11.016

(Ziaee *et al.*, 2019) A. Ziaee, A. B. Albadarin, L. Padrela, T. Femmer, E. O’Reilly, and G. Walker. “Spray-drying of pharmaceuticals and biopharmaceuticals: Critical parameters and experimental process optimization approaches”.In: European Journal of Pharmaceutical Sciences. 127 (Jan. 2019), pp. 300–318. Doi: 10.1016/j.ejps.2018.10.026

List of figures

List of tables

Séchage par atomisation de produits biopharmaceutiques

L'obtention des produits biopharmaceutiques sous une forme sèche présente différents avantages pour la prolongation de la stabilité des formulations. Néanmoins, les procédés de séchage imposent aux protéines différentes sources de stress. Pour ce qui est du procédé de séchage par atomisation utilisé dans le cadre de cette thèse, les produits biopharmaceutiques sont exposés au stress thermique et aux forces de cisaillement et d'adsorption à l'interface liquide/air lors de l'atomisation. L'intensité du stress doit être contrôlée et maîtrisée lors du séchage pour éviter des changements structuraux des produits biopharmaceutiques. Les conditions d'opération lors de l'atomisation et la formulation vont conditionner fortement les propriétés d'usage de la biomolécule (masse volumique, granulométrie et propriétés cohésives en plus des propriétés fonctionnelles) ainsi comme sa stabilité. Cette thèse cherche à représenter les interactions entre les différents paramètres du séchage par atomisation ainsi comme l'effet des différents excipients sur lesquels on peut agir pour contrôler la stabilité de la protéine, la fonctionnalité et l'intégrité des particules solides obtenues.

MOTS CLES : Séchage par atomisation, Biopharmaceutiques, Proteins, Agrégation, Contrainte de cisaillement, Contrainte thermique, Contrainte de déshydratation.

Spray-drying of biopharmaceutical drug products

Obtaining biopharmaceutical products in dry form has various advantages for prolonging the stability of formulations. However, drying processes impose various sources of stress on proteins. Regarding the spray-drying process used in this thesis, biopharmaceutical products are exposed to thermal stress and shear and adsorption forces at the liquid/air interface during atomization. The intensity of stress must be controlled and mastered during drying to avoid structural changes of biopharmaceutical products. The operating conditions during atomization and the formulation strongly condition the usage properties of the biomolecule (bulk density, particle size distribution, and cohesive properties in addition to functional properties) as well as its stability. This thesis aims to represent the interactions between the various parameters of spray-drying as well as the effect of different excipients that can be used to control protein stability and the functionality and integrity of the obtained solid particles.

KEYWORDS: Spray-drying, Biopharmaceutics, Proteins, Aggregation, Shear stress, Thermal stress, Dehydration stress.